The Role of WNK1 in B Cell Biology

Darryl Antony Hayward

University College London (UCL)

and

The Francis Crick Institute

PhD Supervisor: Victor Tybulewicz

A thesis submitted for the degree of

Doctor of Philosophy

University College London (UCL)

May 2019

Declaration

I, Darryl Antony Hayward confirm that the work presented in this thesis is my own. Where information has been derived from other sources, I confirm that this has been indicated in the thesis.

Abstract

WNK1 is a kinase that has been implicated in ion homeostasis in cells through the activation of the kinases OXSR1 and STK39, which in turn phosphorylate the NKCC- and KCC-families of ion cotransporters leading to their activation and inhibition respectively. Mutations in the human *WNK1* gene that cause overexpression of *WNK1* result in pseudohypoaldosteronism type II, a condition where individuals present with hypertension and high concentrations of potassium in their blood. WNK1 has been implicated in migration and cell division in cancer cells. Work in $CD4^+$ T cells has shown that WNK1 is a negative regulator of adhesion and a positive regulator of migration, but the function of WNK1 in other immune cells remains unknown. The work presented in this thesis describes the function of WNK1 in B cells. I have used inducible deletion of WNK1 in both naïve and activated B cells, as well as an inhibitor of WNK1, to assess the role of WNK1 in mature B cell biology. I have shown that WNK1 is a crucial kinase for several aspects of B cell biology in mice, since loss of *Wnk1* expression caused dysregulation of B cell survival, adhesion, migration and development. WNK1 is required in B cells during an immune response as it positively regulates proliferation after activation. Furthermore, WNK1-deficient B cells display defects in antigen presentation to $CD4^+$ T cells as well as defective responses to stimulation with CD40L, highlighting a role for WNK1 in the regulation of crosstalk between B and $CD4^+$ T cells. WNK1-deficient B cells are not able to mount a T-dependent antibody response nor differentiate into germinal centre B cells. Taken together this work indicates that WNK1 is absolutely required for multiple aspects of B cell function.

Impact Statement

B cells are key mediators of the immune response to infection. During an immune response, antigen-specific B cells form a germinal centre with other cell types, where editing and isotype switching of the immunoglobulin genes occurs. The outputs of the germinal centre are memory B cells and long-lived plasma cells. After infection, these cells provide long-lasting protective immunity from reinfection by either quicker responses in the case of memory B cells or circulating antibodies in blood secreted by long-lived plasma cells. Circulating antibodies can neutralise pathogens, lead to pathogen killing through activation of the complement cascade and formation of the membrane attack complex, or target pathogens for phagocytosis and subsequent killing.

Vaccines use the phenomenon of immunological memory to protect individuals and populations through herd immunity from potentially fatal infections. A hallmark of a successful vaccination is increased levels of antibodies circulating in the blood. B cells are critical to provide protection mediated by vaccination, thus an understanding of how B cells function is required so that vaccines can be designed to provide an optimal antibody response and protection from infection. Additionally, the dysregulation of B cells is implicated in autoimmune diseases such as systemic lupus erythematosus and rheumatoid arthritis. This further highlights how an understanding of B cells and mechanisms involved in their activation will have beneficial impacts on human health.

The work in this thesis focussed on the role of the kinase WNK1 in B cell biology, which has previously not been described in the scientific literature. This work has shown that WNK1 is required in B cells for their survival, migration, and ability to generate T-dependent antigen-specific antibodies, thus furthering the understanding of molecular mechanisms that control these processes in B cells. This work will be published in a scientific journal for dissemination of information to the wider scientific community. This knowledge along with other work may lead to improved vaccine design or therapeutics for autoimmune disorders.

Acknowledgements

I would like to take the time to acknowledge the people that have made this project possible and for supporting me along this journey. Firstly, I want to thank Victor Tybulewicz for giving me the opportunity to work on this project and for his support and guidance during the last four and a half years. Over the years as a group leader, Victor has built a fantastic team of scientists and with whom it has been a pleasure to work with. Within the group, I want to mention people who deserve my thanks, especially the other “WNKers”. Robert Köchl, who first discovered the role of WNK1 in the immune system, was instrumental to initial set up of the project and for his guidance and assistance during the project. Lesley Vanes, who taught me everything I know about immunoblotting and intravenous injections, as well as always up for a laugh in the lab. Harry Hartweger who took me under his wing and introduced me to the social life at NIMR. Leon de Boer and Josh Biggs O’May, who have been great to bounce ideas off of. Finally, from the group, I have to thank Edina Schweighoffer and Jennifer Müller as they have been incredibly patient with me while I asked them questions and have given me great advice. Outside of the lab, I want to thank my thesis committee, Pavel Tolar, George Kassiotis and Ben Seddon, for your support and great discussions about this project. I would also like to thanks Sujana Sivapatham and Jens Stein, who we collaborated with to look at *in vivo* migration of WNK1-deficient B cells and without whom we would not have been able to do this work.

During my time doing my PhD, I have met some fantastic people who have formed fantastic support networks. Bethan Wallbank, Jo Segal, Sophie Roper and Sarah Caswell, you have all been great friends to me and your unwavering support means the world to me, I will truly miss our Friday morning breakfasts together. Thank you Sissy Wamaitha, Joe Wright and Ola Lubojemska for truly accepting me for the ridiculous human I am and for enabling me to continue to make questionable life decisions. Lastly, thank you Tom Watson for being a more than patient housemate, a great friend and someone I could always have great conversations with.

Many people have supported me outside of the Crick and the PhD programme. Chris Armstrong, who has always been one of the greatest friends I have had, thank

you for your support and encouragement, both in science and feats of physical endurance that I didn't know I was capable of. Louise Bonner and Caitlin Chenery (née Donovan), thank you for always standing by me and providing animal therapy, as well as great friendship and understanding. The Magic Six (Lucy Banes, Liz Davis, Faye Johnson, Hazel McDonough and Samantha Phoenix) is a special group of people who allow each other be the truest versions of themselves and for that I will forever be grateful. Sarah Aldous is one of the purest humans I have met and she will always hold a special place in my heart. Thank you for being an amazing housemate, supportive, kind, caring, and most importantly for sharing my obsession with cats.

My amazing boyfriend Fábio Ribeiro Rodrigues, your unwavering and unending support means the world to me. You have made my life better in ways that cannot be put into words. During our time together, you have helped me through some of the darkest times in my life and for that I am eternally grateful. Continue to be the truest version of yourself, because to me you are the greatest person in the world.

Last but not least, I want to thank my family. Especially, to my parents, Karen and Dave Hayward, without you and your unconditional love and support, I don't know how I would have completed this project. You truly are the best parents that anyone could ever ask for and a source of daily inspiration.

These words do not do justice for how much I appreciate everyone mentioned, so I will close with: Thank you very much and I love you all.

Table of Contents

Table of Figures

List of Tables

Abbreviations

AB IMDM	Air buffered Iscove's modified Dulbecco's medium
ACK	Ammonium-chloride-potassium
AID	Activation-induced cytidine deaminase
AKT	RAC-alpha serine/threonine-protein kinase/Protein kinase B
APC	Antigen-presenting cell
APE1	Apurinic/apyrimidinic endonuclease 1
ARP	Actin-related protein
ATF2	Activating transcription factor 2
ATP	Adenosine triphosphate
AVD	Apoptotic volume decrease
BAFF	B cell activating factor of the tumour necrosis factor family
BAFFR	BAFF receptor
BAK	Bcl-2 homologous antagonist killer
BAX	Bcl-2-associated X protein
BCL-X_L	Bcl-2-like protein 1
BCL	B cell lymphoma
BCR	B cell antigen receptor
BLIMP1	B lymphocyte-induced maturation protein 1
BLNK	B cell linker
BSA	Bovine serum albumin
BTK	Bruton's tyrosine kinase
C	Complement component
c-Cbl	Casitas B-lineage lymphoma
CaM	Calmodulin
CaN	Calcineurin
CARD11	Caspase recruitment domain-containing protein 11
Cbl-b	Casitas B-lineage lymphoma b
CBM	CARD11-BCL10-MALT1 complex
CCL	Chemokine (C-C motif) ligand
CCR	Chemokine (C-C motif) receptor
CD40L	CD40 ligand
cDNA	Complementary DNA

cGAS	Cyclic GMP-AMP synthase
CGG	Chicken gamma globulin
cIAP	Cellular inhibitor of apoptosis protein
CLIP	Class II-associated invariant chain peptide
CLP	Common lymphoid progenitor
CLR	C-type lectin receptor
CMFDA	5-chloromethylfluorescein diacetate
CR	Complement receptor
CSR	Class switch recombination
CTLA4	Cytotoxic T-lymphocyte-associated protein 4
CTV	CellTrace Violet
CXCL	C-X-C motif chemokine ligand
CXCR	C-X-C motif chemokine receptor
DAG	Diacyl glycerol
DAMP	Damage-associated molecular pattern
DMSO	Dimethyl sulphoxide
DNA	Deoxyribonucleic acid
DNGR1	Dendritic cell natural killer lectin group receptor 1
DOK3	Docking protein 3
DTT	Dithiothreitol
DYRK2	Dual specificity tyrosine-phosphorylation-regulated kinase 2
E2A	Transcription factor E2-alpha
EBF1	Early B cell factor 1
EDCI	*N*-(3-dimethylaminopropyl)-*N*′-ethylcarbodiimide
EDTA	Ethylenediaminetetraacetic acid
ELISA	Enzyme-linked immunosorbent assay
ELK1	ETS domain-containing protein 1
ENaC	Epithelial sodium channel
ERK	Extracellular signal-regulated kinase
FACS	Fluorescence-activated cell sorting
FCS	Foetal calf serum
FLT3	FMS-like tyrosine kinase 3
FOB	Follicular B

FOXO1	Forkhead box protein O1
FOXP3	Forkhead box protein P3
$GABA_AR$	Gamma-aminobutyric acid A receptor
GC	Germinal centre
GEF	Guanine nucleotide exchange factor
GPCR	G-protein coupled receptor
HBSS	Hank's buffered saline solution
HEL	Hen egg lysozyme
HEV	High endothelial venule
HOIL-1	Haem-oxidised IRP2 ubiquitin ligase 1 homologue
HOIP	HOIL-1-interacting protein
HPRT	Hypoxanthine-guanine phosphoribosyltransferase
HSAN2	Hereditary sensory and autonomic neuropathy type II
HSC	Haematopoietic stem cell
HSN2	Hereditary sensory neuropathy type II
ICAM-1	Intercellular adhesion molecule 1
ICOS	Inducible costimulator
ICOSL	ICOS ligand
IDO	Indoleamine 2,3-dioxygenase
Ig	Immunoglobulin
iGC	*In vitro* germinal centre
IκB	Inhibitor of NF-κB
IKK	Inhibitor of NF-κB kinase
IL	Interleukin
ILC	Innate lymphoid cell
IP_3	Inositol-1,4,5-trisphosphate
IRES	Internal ribosomal entry site
JNK	c-Jun N-terminal kinase
KCC	Potassium-chloride cotransporter
LFA-1	Lymphocyte function-associated antigen 1
LPS	Lipopolysaccharide
LUBAC	Linear ubiquitin chain assembly complex
MAC	Membrane attack complex

MACS	Magnetic-activated cell sorting
MALT1	Mucosa-associated lymphoid tissue lymphoma translocation protein 1
MAP2K	MAPK kinase
MAP3K	MAP2K kinase
MAPK	Mitogen-activated protein kinase
MASP	Mannose-binding lectin-associated serine protease
MAX	MYC-associated factor X
MEK	MAP/ERK kinases
MHC	Major histocompatibility complex
MO25α	Calcium-binding protein 39/Mouse protein 25 alpha
MTOC	Microtubule organising centre
mTORC1	Mammalian target of rapamycin complex 1
MYC	Myelocytoatosis oncogene
MZB	Marginal zone B
NCC	Sodium-chloride cotransporter
NEDD4L	E3 ubiquitin-protein ligase NEDD4-like
NEMO	NF-κB essential modulator
NFAT	Nuclear factor of activated T cells
NFκB	Nuclear factor kappa-light-chain-enhancer of activated B cells
NFKB2	Nuclear factor NF-κB p100 subunit
NHEJ	Non-homologous end joining
NIK	NF-κB-inducing kinase
NK	Natural killer
NKCC	Sodium-potassium-chloride cotransporter
NP	4-hydroxy-3-nitrophenylacetyl
ODN1826	Class B CpG oligonucleotide – murine TLR9 ligand
OVA	Ovalbumin
OXSR1	Oxidative stress-responsive 1
PALS	Periarteriolar lymphoid sheath
PAMP	Pathogen-associated molecular pattern
PAX5	Paired box protein 5

PBS	Phosphate buffered saline
PDK	Phosphoinositide-dependent kinase
PFA	Paraformaldehyde
PHAII	Pseudohypoaldosteronism type II
PI3K	Phosphoinositide 3-kinase
PIP_2	Phosphatidylinositol-4,5-bisphosphate
PKC	Protein kinase C
PLC	Phospholipase C
PMA	Phorbol-12-myristate-13-acetate
PNAd	Peripheral lymph node addressin
PRAS40	Proline-rich AKT substrate of 40 kDa
PRR	Pattern recognition receptor
qPCR	Quantitative polymerase chain reaction
RAC	RAS-related C3 botulinum substrate
RAF1	v-raf-leukaemia viral oncogene 1
RAG	Recombination activating gene
RAP	RAS-related protein
RAS	Resistance to audiogenic seizures
RASGRP1	RAS guanyl-releasing protein
RCE	*Rosa26*^{CreERT2}
RIAM	RAP1-GTP-interacting adapter molecule
RLR	Retinoic acid-inducible gene 1-like receptors
RNA	Ribonucleic acid
RNASeq	RNA sequencing
ROMK	Renal outer medullary potassium channel
RSS	Recombination signal sequences
S1K	Schedule 1 killing
S1P	Sphingosine-1-phosphate
S1PR	S1P receptor
SAP	SLAM-associated protein
SD	Standard deviation
SDS	Sodium dodecyl sulphate
SDS-PAGE	SDS-polyacrylamide gel electrophoresis

SEM	Standard error of mean
SGK1	Serum and gluticorticord-induced protein kinase
SHARPIN	Shank-associated RH domain-interacting protein
SHM	Somatic hypermutation
SLAM	Signalling lymphocyte activation molecule
SLC12A	Solute carrier family 12
SMAD2	Mothers against decapentaplegic homologue 2
SMUG1	Single-strand selective monofunctional uracil DNA glycosylase
SOS1	Son of sevenless homologue 1
SRBC	Sheep red blood cells
STIM	Stromal interaction molecule
STK39	Serine/threonine-protein kinase 39
SYK	Spleen tyrosine kinase
TCR	T cell antigen receptor
T_{FH}	Follicular helper T
T_{FR}	Follicular regulatory T
TGF	Transforming growth factor
TGS	Tris-glycine-SDS
T_H	Helper T cell
TNF	Tumour necrosis factor
TPM	Transcripts per million
TRAF	TNF receptor-associated factor
ULK1	Unc-51-like kinase 1
UNG	Uracil DNA glycosylase
UVRAG	UV radiation resistance-associated gene
VCAM-1	Vascular cell adhesion molecule 1
VEGF-A	Vascular endothelial growth factor A
VLA-4	Very late antigen 4
WAS	Wiskott-Aldrich syndrome protein
WAVE	WAS family verprolin-homologous protein
WNK	With no lysine
ZAP70	Zeta-chain associated protein kinase 70

Chapter 1. Introduction

1.1 Overview of the Immune System

Ever since the beginning of life on Earth, organisms have had to defend themselves from attack by either viruses or other organisms. Thus, immunity is a very old concept as cell intrinsic defence has existed in one form or another and has driven evolution in a form of an arms race. With the advent of multicellularity, cells with specialised functions arose, which gave birth to another form of innate immunity: cells whose sole function was to protect the larger organism from “other”. As evolutionary time progressed, more and more of these cells arose with different functions within the organism, which led to functions other than responding to infection, such as: surveillance in protecting from tumours and wound healing. Eventually, in vertebrates, two major branches arose: the innate immune system and the adaptive immune system. I will give an overview of how these two systems work together in mammals to protect from pathogenic organisms.

1.1.1 Innate Immunity

The innate immune system has the ability to protect an organism from pathogens by using generic responses hardwired into the genome. The response is unique for different classes of pathogens, e.g. the response to extracellular gram-negative bacteria is different to the response to a virus. Innate immunity is generally the first line of defence against invading pathogens and can be found in many organisms, including unicellular organisms such as bacteria and fungi. For example, bacteria can express restriction endonucleases that will cut invading DNA that can be differentiated from “self” as it is not methylated, thereby protecting themselves from infection by DNA bacteriophages (Tock and Dryden, 2005). In mammals, the innate immune system is generally considered to consist of 4 main areas: barriers, complement, inflammation and myeloid cells.

Barriers such as the skin and the epithelium in the gastrointestinal tract are the first line of defence as they physically prevent entry of pathogens into the organism. Maintenance of barriers is very important as many commensal microorganisms live at barrier sites, and if the barrier becomes compromised, they can become opportunistic pathogens. Complement is a cascade of protein-protein interactions

and cleavages that ultimately leads to clearance of pathogens. It can be activated by three pathways: classical by binding to immunoglobulins, alternative basal constitutive activation and by binding to mannose-binding lectins. This highlights the interplay between the innate and adaptive branches, as immunoglobulins from the adaptive response can activate the complement cascade. Complement components (C) can lead to clearance by opsonising pathogens for phagocytosis, driving inflammation or formation of the membrane attack complex (MAC) in cell membranes, which leads to lysis of bacteria and enveloped viruses (Figure 1.1) (Gialeli *et al.*, 2018). Inflammation can occur in response to infection and is characterised by redness, swelling, pain, heat and loss of function. The primary purpose of inflammation is to allow the infiltration of phagocytes to a site of infection in order to control numbers of pathogens. There are various drivers of inflammation including lipids and cytokines (Iqbal *et al.*, 2016).

The major mediators of the immune response to an infection are the myeloid cells. These are white blood cells that carry out specialised functions within the immune system but have generic responses for any given class of pathogen. Examples of myeloid cells include: dendritic cells, macrophages, eosinophils and neutrophils. These cells have the ability to detect infection in two main ways: “self vs non-self” and “danger”. Myeloid cells express pattern recognition receptors (PRRs) that bind either pathogen-associated molecular patterns (PAMPs) or damage-associated molecular patterns (DAMPs) (Takeuchi and Akira, 2010, Vénéreau *et al.*, 2015). Examples of PRRs that recognise PAMPs include Toll-like receptors (TLRs), retinoic acid-inducible gene 1-like receptors (RLRs), cyclic GMP-AMP synthase (cGAS) and C-type lectin receptors (CLRs). TLRs are found both at the plasma membrane and in the cytoplasm, and can detect a range of non-self-antigens such as lipopolysaccharide (LPS), peptidoglycan and double stranded RNA through their leucine-rich repeats (Takeuchi and Akira, 2010). RLRs are cytosolic and bind to double-stranded RNA or uncapped 5’ end of RNA, which indicate the RNA is not host derived (Ori *et al.*, 2017). cGAS is found in the cytoplasm and binds B-form double-stranded DNA, a hallmark of infection or mitochondrial damage (Ori *et al.*, 2017). CLRs are found on the plasma membrane, where they detect bacterial and fungal species and can cooperate with TLRs to lead to activation of the myeloid cell (Del Fresno *et al.*, 2018). Examples of PRRs that bind DAMPs include P2X7 and Dendritic cell natural killer lectin group receptor 1 (DNGR1), which bind ATP and actin released

from dying cells respectively (Vénéreau *et al.*, 2015). Signals from PRRs lead to activation and a tailored response from the myeloid cells towards the particular threat, as well as tailoring of the adaptive immune system through secretion of particular cytokines (Takeuchi and Akira, 2010).

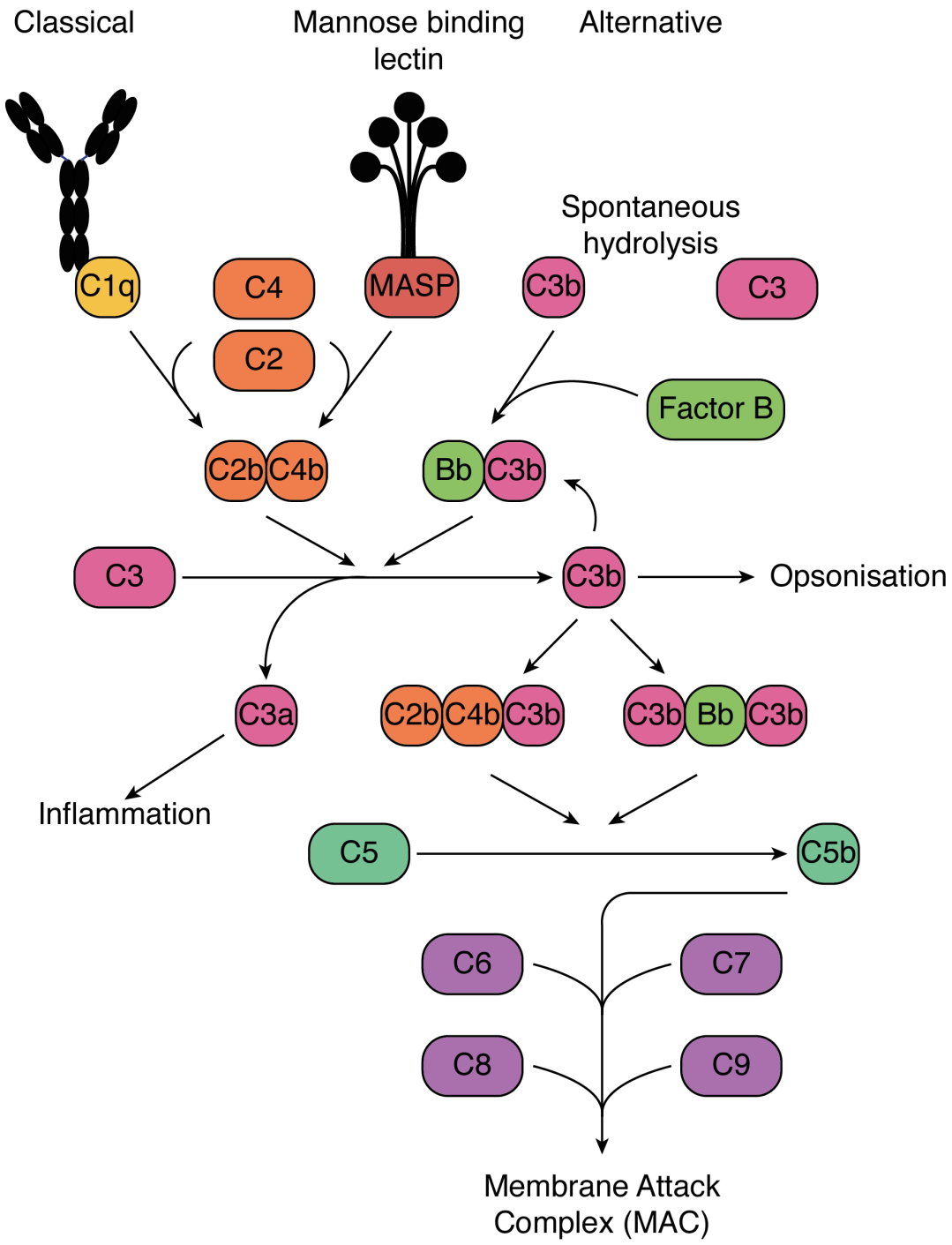

Figure 1.1 Overview of Complement Cascade

Schematic of the complement cascade. The complement cascade can be activated by either antibodies, mannose binding lectins or spontaneous hydrolysis of C3. C1q binding to antibodies and mannose-binding lectin-associated serine protease (MASP) binding to mannose binding lectin leads to the cleavage of C2 and C4. C3 is cleaved to C3a and C3b by C3 convertase made up of either C2bC4b or C3bBb. C3a leads to inflammation and C3b opsonises pathogens for phagocytes. C3b is a subunit of C5 convertase leading to the generation of C5b from C5, which leads to the formation of the membrane attack complex through recruitment of C6, C7, C8 and C9.

1.1.2 Adaptive Immunity

The adaptive immune system by contrast uses genetic recombination to generate diversity of immunoglobulin domain-containing receptors that are specific for one type of antigen. In jawed vertebrates there are three major cell types: $CD4^+$ T cells, $CD8^+$ T cells and B cells. T cells arise from the thymus, where their progenitors undergo genetic rearrangements at the T cell antigen receptor (TCR) alpha and beta loci, and selection to produce either $CD4^+$ or $CD8^+$ T cells. These T cells recognise peptides bound to major histocompatibility (MHC) molecules, $CD8^+$ T cells are restricted to MHC class I whereas $CD4^+$ T cells are restricted to MHC class II (Gascoigne *et al.*, 2016). B cells arise from the bone marrow and are discussed in further detail in Section 1.2.

$CD4^+$ T cells are activated by cells known as antigen-presenting cells (APCs) such as dendritic cells. These cells sample the environment and degrade proteins to display peptides on MHC class II, allowing $CD4^+$ T cells to become activated if they encounter their cognate antigen. $CD4^+$ T cells are known as helper T cells (T_H) as upon their activation they can secrete a distinct set of cytokines which aid in the resolution of an infection by directing other cells, including innate cells, to carry out particular functions. The set of cytokines released is dependent on the environment established by innate cells. For example, interleukin (IL)-12 secreted by dendritic cells will lead to differentiation into T_H1 cells that secrete interferon-γ but IL-4 drives differentiation into T_H2 cells, which secrete IL-4, IL-5 and IL-13 (Zhu, 2018).

$CD8^+$ T cells are also known as cytotoxic T cells as they possess the ability to kill infected or transformed host cells. Cytotoxic T cells are activated by dendritic cells in a process called cross-presentation, where internalised antigens are loaded on MHC class I rather than MHC class II (Embgenbroich and Burgdorf, 2018). Conventional presentation of peptides on MHC class I occurs in nucleated cells during proteasomal degradation of proteins. Peptides generated by proteasomal degradation are then loaded onto MHC class I and then transported to the cell surface. This system provides a snapshot of the proteins being made inside the cell for surveillance by $CD8^+$ T cells. If a cell is infected with a virus, viral peptides will be presented on MHC class I and thus a primed $CD8^+$ T cells can detect an infected cell (Van De Weijer *et al.*, 2015). When this occurs, the cytotoxic T cell induces apoptosis in the target cell, thereby restricting infection (Halle *et al.*, 2017).

1.2 B Cells

As previously mentioned, B cells belong to the adaptive branch of the immune system. In this section I will describe in detail their development, survival, trafficking around the body, activation and immune responses.

1.2.1 B Cell Development and Selection

Like all haematopoietic cells, B cells derive from multipotent haematopoietic stem cells (HSC) found in the bone marrow (Tamma and Ribatti, 2017). More specifically, B cells develop from an oligopotent progenitor known as the common lymphoid progenitor (CLP), which retains the ability to differentiate into B cells, T cells or innate lymphoid cells (ILCs) (Constantinides *et al.*, 2014, Kondo *et al.*, 1997, Yang *et al.*, 2011). CLPs express both FMS-like tyrosine kinase 3 (FLT3) and IL-7 receptor, which both promote both survival and proliferation (Sitnicka *et al.*, 2003, Sitnicka *et al.*, 2002). Figure 1.2 shows an overview of B cell development in the bone marrow post CLP.

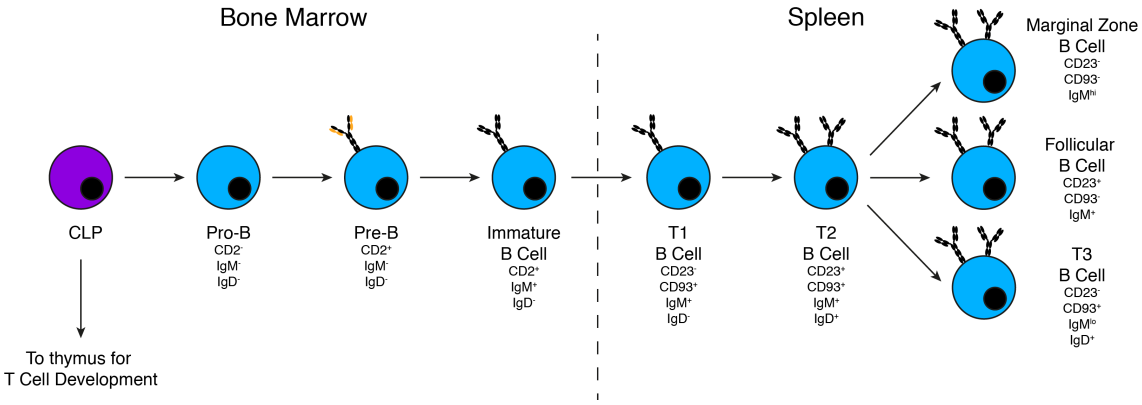

Figure 1.2 Overview of B Cell Development and Maturation

Schematic showing the development and maturation of B cells, and cell surface markers used to identify them. B cells arise from common lymphoid progenitors (CLP) in the bone marrow that develop into pro-B cells. B cell progenitors undergo genetic rearrangements at the *Igh* and *Igl* loci to produce unique BCR on the surface of immature B cells. Black domains indicate rearranged Ig chains, and yellow domains indicate λ5 and VpreB1. Immature B cells migrate to the spleen where they undergo maturation from T1 to T2 cells. T2 cells are able to complete maturation by becoming either a marginal zone B cell or a follicular B cell. T3 cells are anergic and the product of failed maturation.

Commitment to the B cell lineage is driven through upregulation of several different transcription factors, which is in part instructed by high concentrations of IL-7 (Dias *et al.*, 2005). Transcription factor E2-alpha (E2A) activates the expression of forkhead box protein O1 (FOXO1). FOXO1 and E2A together induce expression of early B cell factor 1 (EBF1), which may be the critical factor for CLPs to differentiate into the B cell lineage (Lin *et al.*, 2010, Zandi *et al.*, 2008). EBF1 is necessary for the expression of the transcription factor paired box protein 5 (PAX5) (O'Riordan and Grosschedl, 1999). PAX5 is known as the master regulator of the B cell lineage and is activated at the pro-B cell stage. Together with EBF1, PAX5 suppresses expression of genes required for differentiation into other lymphoid lineages (Nechanitzky *et al.*, 2013, Schebesta *et al.*, 2007).

In order to generate diverse antigen receptors, both B and T cell progenitors undergo V(D)J recombination, which requires both recombination activating gene 1 and 2 (RAG1 and RAG2). V(D)J recombination is necessary for both B and T cell development, as shown by *Rag1*$^{-/-}$ mice lacking both B and T cells (Mombaerts *et al.*, 1992, Shinkai *et al.*, 1992). Upregulation of RAG1 and RAG2 occurs early during B cell development at the pro-B cell stage, and is dependent on FOXO1 (Amin and Schlissel, 2008). V(D)J recombination occurs at the immunoglobulin (Ig) heavy and light chain gene loci for the B cell antigen receptor (BCR) and at the gene loci of the alpha and beta subunits of the TCR. The variable regions of the heavy chain gene loci (*Igh*) are arranged into variable (V), diversity (D) and joining (J) segments, whereas in the light chain gene loci (*Igl*) variable regions contain only V and J segments. These segments are flanked by recombination signal sequences (RSSs), which contain a palindromic heptamer and an A-T rich nonamer that are separated by either 12 or 23 base pairs (12-RSS and 23-RSS respectively) (Bassing *et al.*, 2002). The complex of RAG1 and RAG2 only binds to one 12-RSS and one 23-RSS and induces a nick specifically at the site between the gene segment and the RSS (McBlane *et al.*, 1995). Further processing leads to the generation of blunt ends and proteins involved in non-homologous end joining (NHEJ) are recruited to the RAG complex leading to the re-joining of the DNA segments (Rooney *et al.*, 2004). At the heavy chain gene loci, first D and J segments are joined and then a V segment is joined to the DJ segment to generate a completely rearranged VDJ segment (Bassing *et al.*, 2002).

After successful genetic rearrangement at the heavy chain locus, the Ig heavy chain protein is produced and trafficked to the plasma membrane with surrogate light chain molecules known as λ5 and VpreB1 (Karasuyama *et al.*, 1990, Tsubata and Reth, 1990). This complex is known as the pre-BCR and its expression is the defining feature of the transition from a pro-B cell to a pre-B cell. The pre-BCR associates with an Igα and Igβ (CD79a and CD79b) dimer as the cytoplasmic portion of the pre-BCR does not possess the ability to signal alone. This association is required since mice that lack either the transmembrane portion of the heavy chain ($\mu MT^{-/-}$ mice) or lack CD79A do not have mature B cells and are blocked at the pro-B cell stage (Kitamura *et al.*, 1991, Pelanda *et al.*, 2002). Galectin-1 and heparan sulphate on stromal cells have been implicated as ligands for the pre-BCR (Bradl *et al.*, 2003, Gauthier *et al.*, 2002, Vettermann *et al.*, 2008). Signalling downstream of the pre-BCR results in up to 6 cell divisions and downregulation of *Rag1* and *Rag2* due to phosphoinositide 3-kinase (PI3K) signalling inhibiting FOXO1 (Amin and Schlissel, 2008). If the first allele is successfully rearranged, allelic exclusion occurs to ensure only one heavy chain allele is expressed, thus guaranteeing that the B cells are not bi-specific. Allelic exclusion is dependent on signalling of the pre-BCR through spleen tyrosine kinase (SYK) and zeta-chain associated protein kinase 70 (ZAP70) (Schweighoffer *et al.*, 2003).

After successive rounds of division, pre-B cells arrest in the G_1 phase of the cell cycle (Kurosaki *et al.*, 2010), which induces reactivation of the RAG complex that now facilitates recombination of the V and J segments of the light chain loci. There are two loci that encode for immunoglobulin light chains: Igκ and Igλ. In mice, Igκ is the preferred locus for VJ recombination to occur. After successful light chain rearrangements, the BCR can be fully assembled and is now expressed on the surface. The BCR consists of 2 heavy chain molecules, 2 light chain molecules, 1 Igα molecule and 1 Igβ molecule. B cells that now express IgM alone on their surface are termed immature B cells.

The combination of rearranged heavy and light chain genes can lead to 10^{12} theoretical BCRs (Mårtensson *et al.*, 2010). This broad range of BCRs and therefore specificities is advantageous to protect animals from a wide range of pathogens. However, there is large potential for generating B cells with BCRs that bind self-antigens. To prevent these cells from entering the periphery and producing

antibodies against “self”, they undergo negative selection. If an immature B cell encounters self-antigen for which it has specificity and there is sustained signalling through the BCR, it can lead to cell death thereby removing the cell from the pool of cells that enter the periphery. However, BCR signalling can also lead to a phenomenon known as receptor editing, whereby upon encounter of self-antigen the RAG complex can be reactivated. This allows other light chain alleles to be rearranged to generate a new BCR that may no longer be self-reactive (Nemazee, 2017).

Immature B cells leave the bone marrow and home to the spleen to complete their development, at which point they are termed transitional (T) B cells. There are three different subsets of transitional B cells, which can be differentiated based on cell surface markers: T1 ($CD93^+$ $CD23^-$ IgM^{hi}), T2 ($CD93^+$ $CD23^+$ IgM^{hi}) and T3 ($CD93^+$ $CD23^+$ IgM^{lo}) (Allman *et al.*, 2001). T1 cells are able to become T2 cells within 48 hours by upregulating IgD and CD23 on their surface (Loder *et al.*, 1999). At the T2 stage of development, B cells undergo both negative and positive selection and upregulate IgD on their surface. Here they can encounter additional self-antigens, which can induce anergy or cell death thus removing these cells from the B cell repertoire. It is thought that T3 B cells are this anergic cell type and not a stage of B cell development to generate mature B cells (Teague *et al.*, 2007). In contrast, if cells receive insufficient signals through the BCR or fail to receive survival signals, they are also removed from the repertoire. If a T2 cell passes this round of selection they become mature B cells.

In the spleen, there are two distinct subsets of mature B cells: follicular B cells (FOB; $CD93^-$ $CD23^+$ IgM^+) and marginal zone B cells (MZB; $CD93^-$ $CD23^-$ IgM^{hi}). FOB cells constitute the majority of mature B cells and are found in the white pulp of the spleen adjacent to the periarteriolar lymphoid sheath (PALS), where T cells reside (Mebius and Kraal, 2005). This localisation allows for B and T cells to interact and thus form a germinal centre (GC). FOB cells are recirculating and can change location repeatedly between lymph nodes, bone marrow and spleen. MZB cells are found in the marginal sinuses at the border of the red and white pulp allowing them to respond quickly to blood-borne antigens and T-independent antigens (Mebius and Kraal, 2005, Martin *et al.*, 2001). MZB cells are retained at the marginal sinus by sphingosine-1-phosphate (S1P) binding to S1P receptor (S1PR) 1 (Cinamon *et al.*, 2004). MZB retention is mediated by the integrins lymphocyte function-associated

antigen 1 (LFA-1) and very late antigen 4 (VLA-4) on MZB cells binding to intercellular adhesion molecule 1 (ICAM-1) and vascular cell adhesion molecule 1 (VCAM-1) respectively, which are expressed in the marginal zone (Lu and Cyster, 2002). MZB cells can sample antigens in the blood, due to their close proximity to the red pulp, and transport the antigen to the follicle in a C-X-C chemokine receptor type (CXCR) 5-, S1PR1- and S1PR3-dependent manner to allow FOB to survey for their cognate antigen (Cinamon *et al.*, 2008, Arnon *et al.*, 2013).

1.2.2 Naïve B Cell Survival

Though generation of a diverse repertoire of BCRs is important, maintenance of the cells is of equal importance. FOB cells have been shown to have a half-life of four and a half months when bone marrow output is ablated by conditional deletion of *Rag2* (Hao and Rajewsky, 2001), showing that there are mechanisms supporting long-lived survival of B cells. B cell survival is mediated by both cell-intrinsic mechanisms driven by the BCR, and secretion of the B cell activating factor of the tumour necrosis factor-family (BAFF).

To establish the requirement for BCR in B cell survival, mice were genetically engineered to knock in a pre-rearranged VDJ region of the heavy chain flanked by LoxP sites into the *IgH* locus. This allowed for inducible deletion of the BCR upon Cre expression. After Cre induction, there was rapid loss of surface levels of IgM that accompanied cell death (Lam *et al.*, 1997). A similar approach showed that the signalling portion of the BCR, Igα and Igβ, are required for B cell survival (Kraus *et al.*, 2004). This highlights that signalling through the BCR is needed for survival. Importantly, B cells with a fixed BCR specificity can survive in the absence of cognate antigen, suggesting that antigen-independent, named tonic, signalling mediates survival of B cells (Lam *et al.*, 1997).

BAFF is a member of the tumour necrosis factor (TNF)-family and is able to bind to three distinct receptors that have differential expression in B cell populations: BAFF receptor (BAFFR), transmembrane activator and calcium-modulator and cyclophilin ligand interactor (TACI), and B cell maturation antigen (BCMA). BAFF is closely related to another TNF-family member called a proliferation-inducing ligand (APRIL), which is only able to bind TACI and BCMA. BAFF has been shown to regulate both development of B cells and survival since BAFF-deficient mice have B

cells that are blocked at the T1 stage of splenic development (Schiemann *et al.*, 2001) and antibody-mediated blocking of BAFF *in vivo* leads to a reduction in mature B cell numbers in the B2 compartment only (Gross *et al.*, 2001). The important role of BAFF in B cell survival is further illustrated by studies in which overexpression of BAFF in transgenic mice led to B cell hyperplasia, suggesting that levels of BAFF production limit the size of the B cell compartment (Mackay *et al.*, 1999). In contrast to BAFF-deficient mice, APRIL-deficient mice do not display a reduction in mature B cell populations, but have a reduction of the innate-like B1 cells in the peritoneal cavity (Sindhava *et al.*, 2014, Varfolomeev *et al.*, 2004).

BCMA is only expressed in plasma cells and is required for the generation and maintenance of plasma cells by binding of both BAFF and APRIL as only neutralisation of both leads to loss of plasma cells (Benson *et al.*, 2008, O'Connor *et al.*, 2004). All mature B cells express TACI, with MZB cells expressing it at higher levels than FOB cells. Deletion of TACI has revealed its role as a negative regulator of B cell survival (Seshasayee *et al.*, 2003, von Bülow *et al.*, 2001), which has been shown to be achieved via its cleavage from the cell surface by a disintegrin and metalloprotease 10 (ADAM10) thereby acting as a soluble decoy receptor for BAFF (Hoffmann *et al.*, 2015).

Analysis of the A/WySnJ mouse strain revealed that an insertion of a transposable element in the gene encoding BAFFR, *Tnfrsf13c*, was the cause for the B cell hypoplasia associated with this mouse strain (Thompson *et al.*, 2001, Yan *et al.*, 2001). Mice lacking expression of *Tnfrsf13c* phenocopy the BAFF-deficient and A/WySnJ mice with a block at the T1 stage of B cell maturation (Lentz *et al.*, 1996, Sasaki *et al.*, 2004, Schiemann *et al.*, 2001). Further work using anti-BAFFR antibodies to block BAFF binding in mice caused a loss of mature B cells, indicating that BAFF binding to BAFFR is responsible for the survival and maturation of B cells (Rauch *et al.*, 2009). BAFF is produced by various cell types including: T cells, monocyte-derived dendritic cells, neutrophils and macrophages (Nardelli *et al.*, 2001, Puga *et al.*, 2011, Schneider *et al.*, 1999). However, evidence suggests that only BAFF production by follicular reticular cells is required for naïve B cell survival (Cremasco *et al.*, 2014).

BAFF binding to BAFFR induces a network of signalling cascades that lead to survival of B cells (summarised in Figure 1.3). The non-canonical nuclear factor kappa-light-chain-enhancer of activated B cells (NF-κB) pathway is activated upon

BAFF binding; TNF receptor-associated factor (TRAF) 3 is recruited to the cytoplasmic tail of BAFFR (Morrison *et al.*, 2005) along with TRAF2 and either cellular inhibitor of apoptosis protein (cIAP) 1 or cIAP2. This leads to a change of target for cIAP1 and cIAP2 E3 ubiquitin ligase activity. Instead of ubiquitinating and degrading NF-κB-inducing kinase (NIK), cIAP1 and cIAP2 now ubiquitinate TRAF3 leading to its degradation (Liao *et al.*, 2004). This in turn results in stabilisation of NIK (Liao *et al.*, 2004) and thus allows phosphorylation and activation of inhibitor of NF-κB kinase (IKK) 1 (Ling *et al.*, 1998). Processing of nuclear factor NF-κB p100 subunit (NFKB2) induced by IKK1 phosphorylation generates p52 (Senftleben *et al.*, 2001), a transcription factor that associates with RELB and regulates transcription of genes (Saccani *et al.*, 2003). There is also evidence that NIK may directly phosphorylate NFBK2, which can lead to its processing to p52 (Xiao *et al.*, 2001). Constitutive deficiency of NIK and IKK1 leads to a reduction in mature B cells, either mediated by defects maturation or survival (Hahn *et al.*, 2016, Kaisho *et al.*, 2001, Senftleben *et al.*, 2001). When *Map3k14* (gene encoding NIK) expression is lost in an inducible manner, there is a partial reduction in numbers of mature B cells (Brightbill *et al.*, 2015). In contrast when mature B cells lose expression of *Chuk* (gene encoding IKK1), there is no effect on the numbers of B cells, suggesting, surprisingly, that IKK1 is dispensable for BAFF-mediated survival of B cells (Jellusova *et al.*, 2013).

BAFF stimulation of B cells induces additional cascades of signalling, which appear to be dependent on the BCR and the BCR coreceptor CD19. Inducible deletion of *Syk* leads to a large reduction in mature B cell numbers, implicating its role in survival of B cells. BAFF stimulation of B cells has been shown to induce phosphorylation of both Igα and SYK, showing that the BCR is co-opted during BAFF-induced signalling. In addition, phosphorylation of RAC-alpha serine/threonine-protein kinase (AKT, also known as protein kinase B) and phosphorylation of extracellular signal-regulated kinase (ERK) 1 and 2 are dependent on *Syk* expression (Schweighoffer *et al.*, 2013). CD19 recruitment of PI3K to the BCR leads to phosphorylation of AKT and indeed CD19 has been implicated in B cell survival in the absence of *Syk* expression (Hobeika *et al.*, 2015). Despite the phosphorylation of ERK1 and 2 downstream of BAFF stimulation, their activation is not required for B cell survival, instead ERK5 has been implicated in survival of B cells (Jacque *et al.*, 2015).

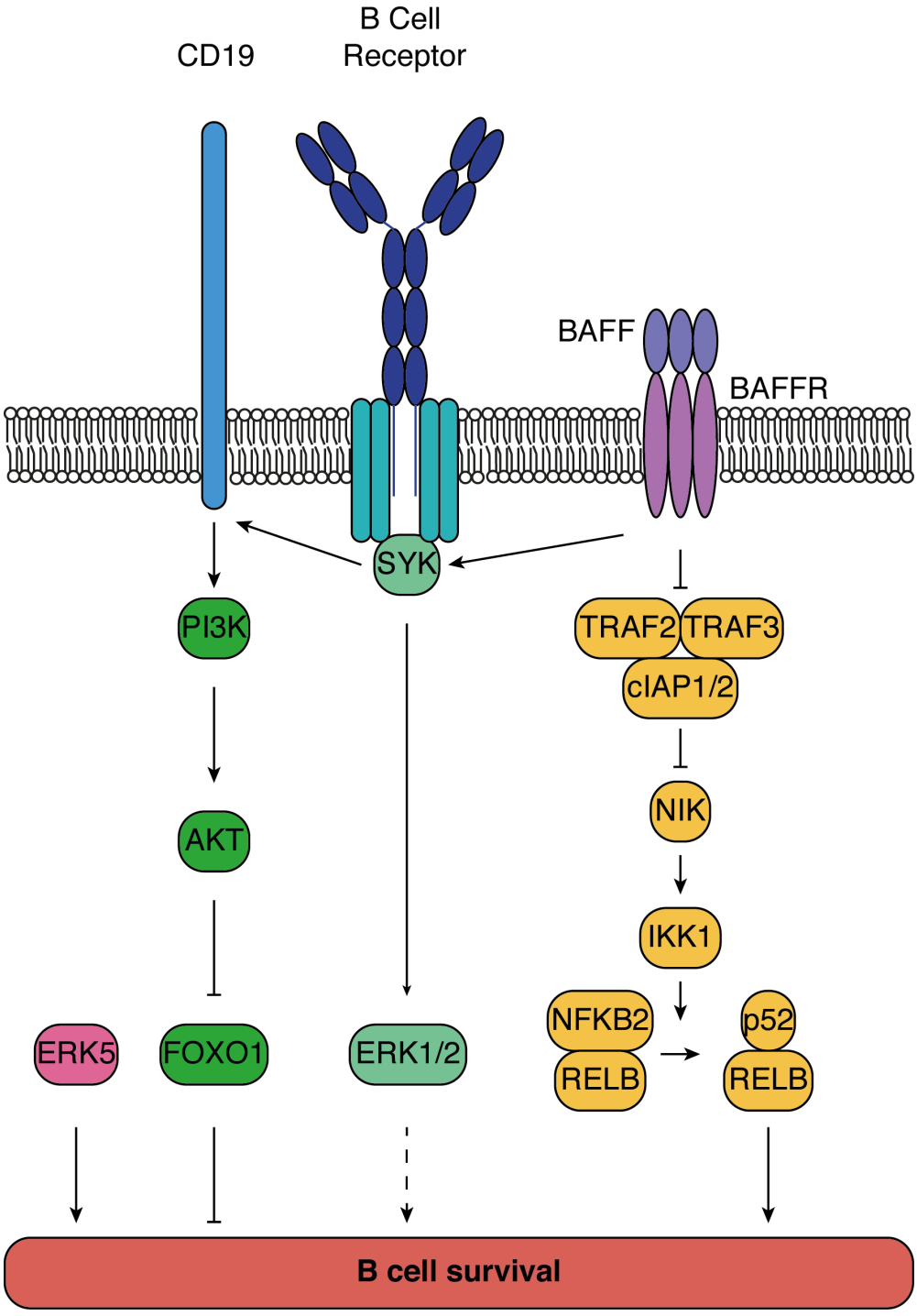

Figure 1.3 Signalling Pathways Involved in B Cell Survival

Schematic of signalling pathways controlling B cell survival. BAFFR signals through TRAF2, TRAF3 and cIAP1 and cIAP2 lead to TRAF3 degradation, thus relieving inhibition of NIK and activating non-canonical NF-κB signalling. This leads to the processing of NFKB2 to p52, which translocates to the nucleus with RELB to activate transcription of pro-survival genes. BAFFR also signals through SYK and CD19 via the BCR leading to the activation of PI3K and ERK1/2. PI3K activates AKT causing the inhibition of FOXO1, a negative regulator of B cell survival. Additionally, ERK5 activation promotes B cell survival. Figure was adapted from (Schweighoffer and Tybulewicz, 2018)

BAFF-induced signalling promotes B cell survival through regulation of apoptosis. Apoptosis is one way in which cells undergo programmed cell death through cysteine-aspartic proteases (caspases). Growth factor depletion or stress causes the release of cytochrome C from mitochondria, which leads to activation of caspases, inducing apoptosis by degradation of cellular components. Cytochrome C release from mitochondria is regulated by the apoptotic regulators known as the B cell lymphoma (BCL) 2-family. BCL2-family proteins can regulate apoptosis through being either pro-apoptotic or anti-apoptotic. For example, Bcl-2-associated X protein (BAX) and Bcl-2 homologous antagonist killer (BAK) are required for permeabilisation of the outer mitochondrial membrane, which facilitates cytochrome C release (Youle and Strasser, 2008). In contrast, BCL-X_L, encoded by *Bcl2l1*, prevents apoptosis by inhibiting VDAC1-mediated transport of calcium (Ca^{2+}) into mitochondria, which drives apoptosis (Monaco *et al.*, 2015). BAFF has been shown to regulate apoptosis by inducing upregulation of anti-apoptotic genes including, *Bcl2l1* and *Mcl1* (Hsu *et al.*, 2002, Woodland *et al.*, 2008), and restricting upregulation of BIM, a pro-apoptotic protein, induced by BCR signalling (Craxton *et al.*, 2005).

1.2.3 Adhesion and Migration in Naïve B Cell Homing to Secondary Lymphoid Organs

In order to survey the body for infection, B cells travel the secondary lymphoid organs, the spleen and lymph nodes (LNs), via the circulatory and lymphatic systems. An overview of lymphocyte entry and exit into and from LNs can be seen in Figure 1.4. In order to gain entry to LN, lymphocytes initially tether and then roll along the endothelium of high endothelial venules (HEV) mediated by L-selectin (CD62L) (Warnock *et al.*, 1998). CD62L binds a complex of proteins known as peripheral lymph node addressin (PNAd), which includes the sialomucins CD34 and glycosylation-dependent cell adhesion molecule 1 (GLYCAM-1) in mice (Rosen, 2004). If this interaction is disrupted then lymphocytes are unable to tether to HEV endothelial cells and thus do not enter LN (Von Andrian, 1996, Warnock *et al.*, 1998).

After rolling along the endothelium, lymphocytes adhere tightly to the endothelial cells which is mediated by LFA-1 ($\alpha_L\beta_2$) (Warnock *et al.*, 1998, Andrew *et al.*, 1998), although there is work suggesting that VLA-4 also contributes (Berlin-

Rufenach *et al.*, 1999). B cell adhesion to HEV endothelial cells is induced by either chemokine (C-C motif) ligand (CCL) 21, C-X-C motif chemokine ligand (CXCL) CXCL12 or CXCL13 (Okada *et al.*, 2002, Ebisuno *et al.*, 2003), which is tethered to the surface of endothelial cells by heparan sulphate (Bao *et al.*, 2010, Girard *et al.*, 2012). Binding of CCL21, CXCL12 and CXCL13 to CC chemokine receptor (CCR) 7, CXCR4 and CXCR5 respectively leads to activation of LFA-1 and tight binding to the endothelium via ICAM-1 and ICAM-2 (Figure 1.4A).

All chemokine receptors are G-protein-coupled receptors (GPCRs). Upon binding ligand, the chemokine receptor transduces signals to activate phospholipase C (PLC), which leads to the hydrolysis of phosphatidylinositol-4,5-bisphosphate (PIP_2) to diacyl glycerol (DAG) and inositol-1,4,5-trisphosphate (IP_3). Both IP_3 and DAG lead to the activation of RAS guanyl-releasing protein (RASGRP) 2, which acts as a guanine nucleotide exchange factor (GEF) for RAS-related protein (RAP) 1 leading to its activation (Ghandour *et al.*, 2007). Activated RAP1 regulates integrin affinity through activation of TALIN-1 via interaction with RAP1-GTP-interacting adapter molecule (RIAM) (Han *et al.*, 2006). Activation of TALIN-1 leads to anchorage of the integrins to the actin cytoskeleton and switches them to a high affinity state (Tadokoro *et al.*, 2003). RAP1 also regulates avidity of LFA-1 through the recruitment of regulator for cell adhesion and polarisation enriched in lymphoid tissues (RAPL) to α_L, leading to LFA-1 clustering (Katagiri *et al.*, 2003).

The molecular mechanisms behind transmigration through the endothelium into the parenchyma of the LN are poorly understood (Girard *et al.*, 2012). However, it is known that tight adhesion to the endothelial layer, along with shear flow (Cinamon *et al.*, 2001) and endothelial production of autotaxin to produce lysophosphatidic acid (Bai *et al.*, 2013) are required for lymphocyte transmigration.

After arrival in the parenchyma of the LN, B cells migrate towards follicles by following a chemotactic gradient of CXCL13 (Gunn *et al.*, 1998, Okada *et al.*, 2002). CXCL13 is produced by follicular dendritic cells (FDCs), which reside in LN follicles thus establishing the chemotactic gradient (Vissers *et al.*, 2001). Dissemination of CXCL13 occurs through the conduit system, allowing migration along the conduits (Roozendaal *et al.*, 2009). In the follicle, naïve B cells migrate via random walk at a velocity of 6 μm/min (Okada *et al.*, 2005) to survey for their cognate antigen (Figure 1.4B).

If a B cell fails to encounter cognate antigen, their egress from the LN is promoted so they can home to a different LN or spleen. Egress is mediated by S1P and S1PR1 signalling, leading to entry of B cells into lymphatic vessels (Matioubian *et al.*, 2004, Park *et al.*, 2012, Sinha *et al.*, 2009). S1P is generated by lymphatic endothelial cells, thus providing a gradient of S1P to induce chemotaxis to the lymphatic vessels (Pham *et al.*, 2010). S1P stimulation leads to downregulation of S1PR1 and thus desensitisation, this allows B cells to be retained in the LN after entry due to the high concentration of S1P in the blood (Girard *et al.*, 2012, Park *et al.*, 2012). Once in the lymphatic vessels, B cells leave the LN and return to the circulation via the thoracic ducts (Figure 1.4B).

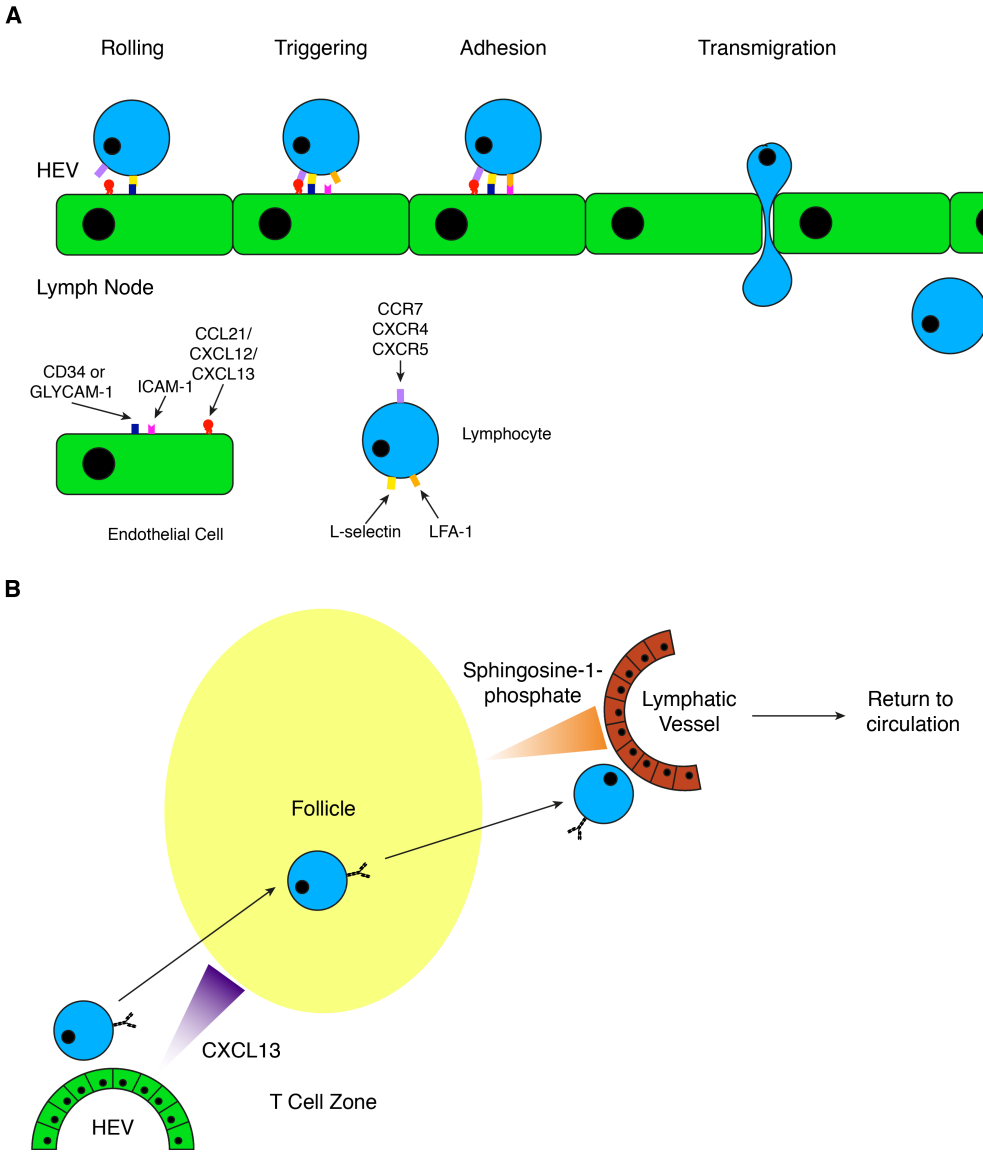

Figure 1.4 Entry and Exit of B Cells in Lymph Nodes

(**A**) Rolling of B cells along high endothelial venules (HEV) is mediated by L-selectin binding to CD34 or GLYCAM-1. Binding of either CCL21 or CXCL12 to CCR7 or CXCR4 respectively leads to triggering of the B cells and affinity increase in LFA-1, allowing tight adhesion to ICAM-1 on HEV. This tight adhesion allows the B cell to transmigrate through the endothelial layer into the parenchyma of the lymph node. (**B**) Once inside the lymph node, the B cell migrates to the follicle in a CXCL13-dependent manner. In the follicle the B cell can survey for cognate antigen leading to its activation. If no cognate antigen is present, B cells leave by migrating to the efferent lymphatic vessels by binding of sphingosine-1-phosphate. The B cells using the lymphatic vessels to return to the circulation where they can enter another lymph node or the spleen.

1.2.4 Early Events in B Cell Activation

In order for B cells to become activated, they need to encounter their cognate antigen which can occur at a variety of locations inside the LN. Upon entry into the LN, B cells survey dendritic cells in the T cell zone for antigen, which can lead to their activation (Qi *et al.*, 2006). Small soluble antigens of less than 70 kDa in size are able to drain into the conduit system of LNs via afferent lymphatics. These small antigens can be captured by cognate B cells leading to their activation (Roozendaal *et al.*, 2009). Larger antigens coated by C3 can be captured by subcapsular sinus macrophages expressing complement receptor 3 (CR3, CD11b), and the antigen is relayed by the macrophages from the subcapsular sinus to the follicular side. Here the antigen can be captured by B cells in either a cognate or a non-cognate manner. Cognate interaction of antigen by the B cell at the subcapsular sinus proximal region of the follicle leads to B cell activation (Carrasco and Batista, 2007). The non-cognate capture of antigen is mediated by CR2 (CD21) on the B cells. The B cells then migrate back into the follicle core and the antigen is deposited on FDCs mediated by CR1 (CD35) on their surface. This is a rapid process as the majority of antigen is transported to FDCs 8 hours post immunisation (Phan *et al.*, 2007). This is analogous to the shuttling of antigen by MZB from the red pulp to the white pulp previously mentioned. FDCs are an important APC for B cells as they can present antigen for extended periods of time, up to 9 days after immunisation. This allows for activation of cognate B cells that entered the follicle days after initial immunisation or pathogen infection (Suzuki *et al.*, 2009).

Upon binding of cognate antigen through the BCR, a signalling cascade is initiated leading to B cell activation (Figure 1.5). The BCR associates with the Src-family tyrosine kinases LCK, LYN, FYN and BLK (Clark *et al.*, 1992) and stimulation through the BCR leads to their activation (Burkhardt *et al.*, 1991). Upon activation, the ITAM motifs of Igα and Igβ are phosphorylated (Flaswinkel and Reth, 1994). ITAM motifs were first described in 1989 (Cambier, 1995, Reth, 1989) and their phosphorylation allows binding of SYK to Igα and Igβ through its tandem SH2 domains (Rowley *et al.*, 1995). This induces activation of SYK and facilitates autophosphorylation for maximal activation (Rowley *et al.*, 1995). SYK is required for BCR-mediated signalling and directly phosphorylates B cell linker (BLNK), which acts as a scaffold protein recruiting other signalling components such as PLCγ2, VAV1

and growth factor receptor bound protein 2 (GRB2) (Fu *et al.*, 1998, Goitsuka *et al.*, 1998, Wienands *et al.*, 1998, Ishiai *et al.*, 1999).

LYN is able to phosphorylate the BCR coreceptor CD19, which leads to recruitment of PI3K to the BCR signalosome (Fujimoto *et al.*, 2000, Tuveson *et al.*, 1993). PI3K catalyses the phosphorylation of PIP_2 to phosphatidylinositol-3,4,5-trisphosphate (PIP_3). Generation of PIP_3 leads to recruitment of proteins to the plasma membrane through their pleckstrin homology domains. These proteins include Bruton's tyrosine kinase (BTK) (Saito *et al.*, 2001), AKT and phosphoinositide-dependent kinase (PDK) 1. Dual recruitment of AKT and PDK1 leads to phosphorylation and activation of AKT (Alessi *et al.*, 1997, Manning and Toker, 2017, Stokoe *et al.*, 1997). Activation of AKT has pleiotropic effects in cells. It has been shown to regulate proliferation by sequestering FOXO1 in the cytoplasm, leading to decreased expression of genes that negatively regulate survival, growth and proliferation (Brunet *et al.*, 1999, L. *et al.*, 1999, Manning and Toker, 2017). Additional regulation of growth and metabolism occurs through activation of mammalian target of rapamycin complex 1 (mTORC1) by AKT (Kovacina *et al.*, 2003, Manning and Toker, 2017). Activation of BTK is mediated by binding to PIP_3 as well as phosphorylation by LYN (Rawlings *et al.*, 1996, Saito *et al.*, 2001). Phosphorylated BLNK also binds BTK through its SH2 domain, facilitating phosphorylation and activation of PLCγ2 by BTK (Chiu *et al.*, 2002, Hashimoto *et al.*, 1999).

PLCγ2 activation leads to the generation of IP_3 and DAG. IP_3 release from the plasma membrane leads to its binding to receptors on the endoplasmic reticulum (ER), inducing the release of Ca^{2+} from the ER (Sugawara *et al.*, 1997). The depletion of Ca^{2+} from the ER is sensed by stromal interaction molecule (STIM) 1 and STIM2, which then translocate to the ER-plasma membrane interface. Here they facilitate the opening of Ca^{2+} release-activated Ca^{2+} channels, which allows for sustained Ca^{2+} influx into the cytoplasm by allowing Ca^{2+} from the extracellular space to enter the cell (Shaw *et al.*, 2013). Cytoplasmic Ca^{2+} binds to calmodulin (CaM), which then complexes with and activates the phosphatase calcineurin (CaN) (Kurosaki *et al.*, 2010). CaN dephosphorylates nuclear factor of activated T cells (NFAT)-family proteins, which can now translocate from the cytoplasm into the nucleus due to a nuclear localisation sequence being revealed (Beals *et al.*, 1997). Ca^{2+} and DAG together lead to the activation of protein kinase C (PKC), which activates both

canonical and non-canonical NF-κB pathways. Canonical NF-κB signalling is initiated by PKC phosphorylation of caspase recruitment domain-containing protein 11 (CARD11), leading to association with BCL10 and mucosa-associated lymphoid tissue lymphoma translocation protein 1 (MALT1) to form the CBM complex. The CBM complex activates the IKK complex, which consists of IKK1, IKK2 and NF-κB essential modulator (NEMO). Activated IKK complex phosphorylates inhibitor of NF-κB (IκB), resulting in degradation of IκB. This reveals a nuclear localisation sequence on NF-κB dimer of RelA and p50, allowing their translocation to the nucleus (Kurosaki *et al.*, 2010, Perkins, 2007, Shinohara *et al.*, 2005). PKC also phosphorylates IKK1 leading to the activation of non-canonical NF-κB signalling (Dolmetsch *et al.*, 1997, Saijo *et al.*, 2002, Trushin *et al.*, 1999).

DAG is able to activate the small GTPase resistance to audiogenic seizures (RAS) through the GEFs RASGRP1 and RASGRP3 (Coughlin *et al.*, 2005, Taher *et al.*, 2017). RAS is additionally activated by another exchange factor son of sevenless homologue 1 (SOS1), which is recruited to the BCR signalosome by GRB2 binding to BLNK (D'Ambrosio *et al.*, 1996, Nagai *et al.*, 1995). RAS initiates mitogen-activated protein kinase (MAPK) signalling via v-raf-leukaemia viral oncogene 1 (RAF1). Activation of RAF1 leads to the phosphorylation of ERK1/2 via MAPK kinase (MAP2K) 1 and MAP2K2 (Ehrhardt *et al.*, 2004, Nagaoka *et al.*, 2000, Oh-hora *et al.*, 2003, Teixeira *et al.*, 2003, Kurosaki *et al.*, 2010). ERK1/2 phosphorylate and activate the transcription factors myelocytoatosis oncogene (MYC) and ETS domain-containing protein 1 (ELK1) (Dal Porto *et al.*, 2004). MAPK signalling is also mediated by VAV-family proteins recruited to BLNK and RAS-related C3 botulinum substrate (RAC) 1 and RAC2, which lead to the activation of p38 MAPK and c-Jun N-terminal kinase (JNK) (Hashimoto *et al.*, 1998, Ishiai *et al.*, 1999). Activated p38 MAPK and JNK are able to activate the transcription factors c-Jun, activating transcription factor 2 (ATF2) and myc-associated factor X (MAX) (Dal Porto *et al.*, 2004). In addition, VAV-family proteins have been shown to regulate Ca^{2+} flux (Doody *et al.*, 2001, Tedford *et al.*, 2001).

Further to activation of transcription factors that upregulate expression of genes that regulate cell cycle, metabolism and protein synthesis, signalling via the BCR leads to regulation of the cytoskeleton and ultimately internalisation of antigen. Signalling via RAC- and VAV-family proteins leads to the reorganisation of the actin

cytoskeleton via Wiskott-Aldrich syndrome protein (WAS) and WAS-family verprolin-homologous protein (WAVE) complex regulation of actin-related protein (ARP) 2/3 (Tolar, 2017, Tybulewicz and Henderson, 2009). After the formation of the immune synapse, the actin cytoskeleton is able to generate pulling forces to test antigen affinity, mediated by myosin IIa, on BCR clusters (Hoogeboom *et al.*, 2018, Natkanski *et al.*, 2013, Tolar, 2017, Tolar and Spillane, 2014). These pulling forces are able to induce internalisation of antigen into the cell in a clathrin-coated pit-dependent manner (Tolar, 2017, Tolar and Spillane, 2014), along with membranes from APCs (Suzuki *et al.*, 2009).

In addition to actin cytoskeletal regulation, BCR signalling through GRB2 and docking protein 3 (DOK3) leads to the relocalisation of the microtubule organising centre (MTOC) to the immune synapse (Schnyder *et al.*, 2011, Yuseff *et al.*, 2011). This facilitates the arrival of MHC class II containing lysosomes to the immune synapse (Yuseff *et al.*, 2011), allowing for endocytosed antigen to be degraded and peptides loaded onto MHC class II molecules. Peptide loading onto MHC class II is facilitated by H2-M, which removes class II-associated invariant chain peptide (CLIP) from the peptide binding groove of MHC class II allowing binding of other peptides for presentation (Denzin and Cresswell, 1995). B cells also express H2-O which functions to regulate H2-M by binding to the MHC class II binding region on H2-M, thus preventing CLIP removal from MHC class II (Adler *et al.*, 2017, Guce *et al.*, 2013). After CLIP replacement on MHC class II, the MHC class II-containing vesicles are then transported to the plasma membrane along microtubules (Bretou *et al.*, 2016). How fusion occurs is unclear but the actin cytoskeleton is known to be required (Bretou *et al.*, 2014, Bretou *et al.*, 2016).

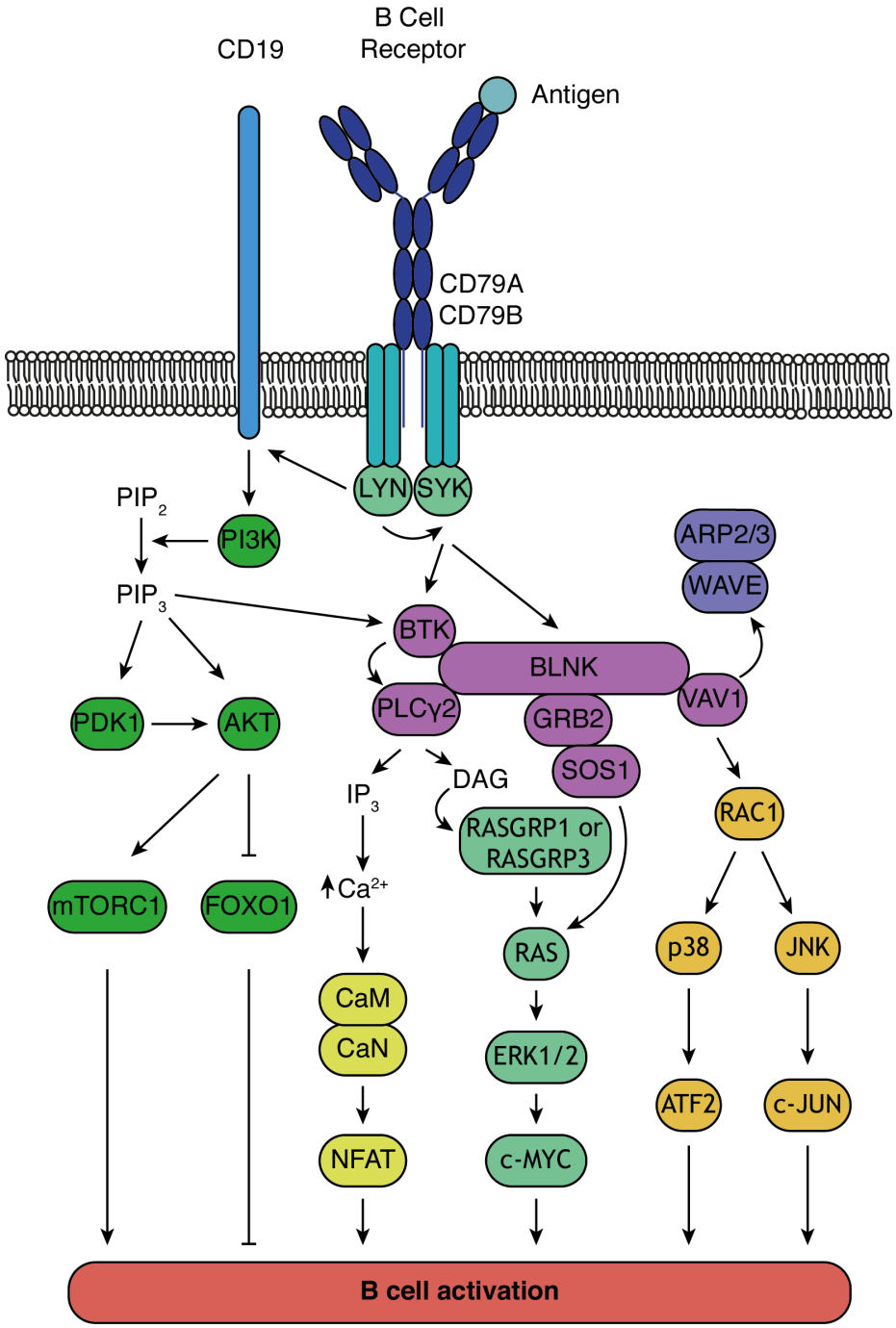

Figure 1.5 Simplified Overview of Signalling Pathways Downstream of BCR

Schematic showing signalling cascades induce by binding of cognate antigen through the BCR. Upon binding cognate antigen, recruitment of LYN leads to phosphorylation of the ITAMs of CD79A and CD79B, and of CD19. Phosphorylation of CD79A and CD79B leads to the recruitment and activation of SYK. Phosphorylation of CD19 leads to the recruitment of PI3K and generation of PIP_3, which recruits and activates PDK1, AKT and BTK. Active AKT inhibits FOXO1 and activates mTORC1. BTK is phosphorylated by SYK, which also phosphorylates the scaffold BLNK. BLNK recruits PLCγ2, GRB2-SOS1 and VAV1. BTK activates PLCγ2, which generates DAG and IP_3 leading to increased intracellular Ca^{2+} and activation of the small GTPase RAS. RAS activation is also mediated by GRB2-SOS1 leading to c-MYC activation by MAPK signalling. Increased intracellular Ca^{2+} activated NFAT by CaM and CaN. VAV1 leads to activation of ATF2 and c-JUN via RAC1, and regulates the actin cytoskeleton through WAVE complex and ARP2/3.

1.2.5 Antigen Presentation to CD4$^+$ T Cells

In order to present antigen to cognate CD4$^+$ T cells and receive “help”, the B cells need to migrate to the border between the follicle and T cell zone (B-T border). To do this they use the chemokine receptor CCR7, which binds CCL19 and CCL21 that is produced by stromal cells in the T cell zone of the lymph node and extends into the T cell zone-proximal region of the follicle (Okada *et al.*, 2005).

Once at the border of the follicle and the T cell zone, B cells have the opportunity to act as APCs to activated CD4$^+$ T cells. During their activation, B cells upregulate a variety of proteins on their surface, which together are termed activation markers. These activation markers include CD69, CD80, CD86 and MHC class II. CD69 upregulation promotes the retention of activated B cells by forming a complex with S1PR1, leading to its internalisation and degradation (Bankovich *et al.*, 2010). CD80, CD86 and MHC class II all enhance the ability of B cells to communicate with T cells in an antigen dependent manner. CD80 and CD86 are ligands for the TCR coreceptor CD28 and are required for complete TCR signalling (Linsley *et al.*, 1991, Linsley *et al.*, 1990). Activated CD4$^+$ T cells express CD154, also known as CD40 ligand (CD40L), on their surface, which upon binding to CD40 initiates signalling that further activates B cells. Disruption in the interaction of CD40 and CD40L leads to an attenuation of the B cell immune response by lack of formation of a germinal centre (Han *et al.*, 1995a). Conjugation of B and T cells is also dependent on signalling lymphocyte activation molecule (SLAM) interactions and SLAM-associated protein (SAP) in T cells (Qi *et al.*, 2008).

CD40 is a member of the TNF receptor-family, and signalling downstream of CD40 is mediated by TRAF proteins. Upon binding of CD40L, CD40 forms a homotrimer leading to the recruitment of TRAF1, TRAF2, TRAF3, TRAF5 and TRAF6 (Haswell *et al.*, 2001, Pullen *et al.*, 1999a, Pullen *et al.*, 1999b, Pullen *et al.*, 1998). Recruitment of the heterodimer of TRAF2 and TRAF3 in complex with cIAP1 and cIAP2 to CD40 further recruits shank-associated RH domain-interacting protein (SHARPIN), haem-oxidised IRP2 ubiquitin ligase 1 homologue (HOIL-1) and HOIL-1-interacting protein (HOIP) (Gerlach *et al.*, 2011). SHARPIN, HOIL-1 and HOIP form the linear ubiquitin chain assembly complex (LUBAC) which is required for activation of the NF-κB and JNK signalling pathways (Gerlach *et al.*, 2011). Binding of TRAF6 to CD40 leads recruitment of PI3K to the plasma membrane

through Casitas B-lineage lymphoma (c-Cbl) and Cbl-b leading to activation of AKT (Arron *et al.*, 2001). TRAF2 recruitment leads to the activation of JNK and p38 MAPK in a MAP3K1 dependent manner (Gallagher *et al.*, 2007).

Stimulation through CD40 leads to the upregulation of inducible costimulator (ICOS) ligand (ICOSL) via NIK and NF-κB signalling (Hu *et al.*, 2011). ICOSL on the B cell binding to ICOS on the T cell is required for T cell differentiation into T follicular helper cells (T_{FH}) and for B cell differentiation into a germinal centre B cell (Hamel *et al.*, 2014, Hu *et al.*, 2011, Liu *et al.*, 2015). After a successful interaction with a cognate $CD4^+$ T cell, B cells start to undergo division at the B-T border and migrate back into the follicle together with the conjugated cognate T cell (Okada *et al.*, 2005).

1.2.6 The Germinal Centre Reaction

The germinal centre is a specialised structure that develops during an immune response, where somatic hypermutation (SHM) and class switch recombination (CSR) takes place to generate high affinity antibodies of different isotypes (Berek *et al.*, 1991, Jacob *et al.*, 1991, Nieuwenhuis and Opstelten, 1984). There are two distinct areas within the germinal centre: the light zone and the dark zone. GC B cells found in the dark zone are termed centroblasts and are more proliferative and larger than the GC B cells found in the light zone, which are named centrocytes (Allen *et al.*, 2007a, Allen *et al.*, 2007b, Hauser *et al.*, 2007, MacLennan, 1994, Schwickert *et al.*, 2007). GC B cells shuttle between the two zones, dividing in the dark zone and then migrating to the light zone (Allen *et al.*, 2007b, Hauser *et al.*, 2007, Schwickert *et al.*, 2007). In general, GC B cells can be identified by the expression of CD95, high binding of the antibody clone GL7 and downregulation of IgD on their surface (Victora and Nussenzweig, 2012). Dark zone centroblasts have been shown to be $CXCR4^{hi}$ $CD83^{lo}$ $CD86^{lo}$ and light zone centrocytes are $CXCR4^{lo}$ $CD83^{hi}$ $CD86^{hi}$ (Victora *et al.*, 2010).

In the dark zone, SHM is used to refine the affinity of the BCR to generate B cells with high affinity receptors for antigens present during the immune response. SHM is mediated by the enzyme activation-induced cytidine deaminase (AID), encoded by the *Aicda* gene, which is upregulated upon activation of B cells (Muramatsu *et al.*, 2000, Revy *et al.*, 2000). AID deaminates deoxycytidine to deoxyuridine on single stranded DNA, which is found during transcription of genes

such as the variable regions of the immunoglobulin genes (Bransteitter *et al.*, 2003, Dickerson *et al.*, 2003, Methot and Di Noia, 2017). This leads to mutations in the variable region DNA sequence. Transition mutations can then arise during DNA replication, where the guanine base is exchanged for adenine. The deoxyuridine can be removed by either uracil DNA glycosylase (UNG) or single-strand selective monofunctional uracil DNA glycosylase (SMUG1), which leaves an abasic site that can be replaced by any of the four bases during DNA replication (Dingler *et al.*, 2014, Rada *et al.*, 2002). Furthermore, the mismatch of deoxyuridine and deoxyguanosine can be recognised by mismatch repair machinery leading to excision of the DNA around the mismatch and repair by the error prone DNA polymerase η (Rogozin *et al.*, 2001, Zeng *et al.*, 2001).

CSR is the process by which the constant region of the heavy gene locus is exchanged for another leading to a switch in immunoglobulin isotype, i.e. IgM to IgG1. In mice, all the constant region genes (μ, δ, γ3, γ1, γ2a, γ2b, ε and α) are preceded by a cytokine inducible promoter, intervening exon, and a switch region, except for the δ locus as this is expressed along with the μ locus through alternative splicing (Moore *et al.*, 1981). In the presence of cytokines, transcription and splicing of the intervening exon, switch region and constant region exons occurs to generate a sterile transcript (also known as a germline transcript) (Stavnezer *et al.*, 1988). For example, IL-4 signalling leads to expression of γ1 and ε transcripts (Lutzker *et al.*, 1988, Rothman *et al.*, 1988) and transforming growth factor (TGF) β leads to expression of α transcripts (Ehrhardt *et al.*, 1992, van Vlasselaer *et al.*, 1992). Transcription leads to RNA-DNA hybrids and formation of an R-loop on the non-template strand, which allows AID to deaminate deoxycytidine (Chaudhuri *et al.*, 2003, Reaban and Griffin, 1990, Shinkura *et al.*, 2003), resulting in the formation of double strand breaks. Double stranded breaks can be generated by a UNG-dependent pathway. UNG creates an abasic site and apurinic/apyrimidinic endonuclease 1 (APE1) introduces nicks on both strands in similar locations creating a staggered double strand break (Bross *et al.*, 2000, Papavasiliou and Schatz, 2000, Rada *et al.*, 2002, Schrader *et al.*, 2009). An alternative mechanism is through the mismatch repair machinery nicking and digesting the mutated DNA to create single-stranded DNA, which can lead to double strand breaks if nicking and resection occurs on both strands in a similar location (Matthews *et al.*, 2014). Double strand

breaks are repaired by the NHEJ pathway that now join the variable region with the new constant region (Matthews *et al.*, 2014). The intervening constant regions are excised creating a loop of DNA named the switch circle (Iwasato *et al.*, 1990, Matsuoka *et al.*, 1990).

Other than centrocytes, FDCs, T_{FH} cells, follicular regulatory T (T_{FR}) cells, and tingible body macrophages can be found in the light zone of the germinal centre. Centrocytes test their new BCR by binding to antigen presented on FDCs and compete for help from T_{FH} cells. GC B cells interact with antigen in a different manner to naïve B cells. Rather than clustering of antigen, antigen is trafficked to the periphery of the interface between the B cell and FDC into many clusters, thereby reducing the avidity. They are also able to generate a stronger pulling force on the BCR and it is possible that affinity is tested in this manner as a strong pulling force can disrupt low affinity interactions (Nowosad *et al.*, 2016). Another mechanism for testing affinity is by higher affinity receptors endocytosing more antigen and then presenting more antigenic peptides on MHC class II to T_{FH} cells (Victora *et al.*, 2010). However, recent evidence has shown that the density of MHC class II does not control selection in the GC but rather the entry into the GC (Yeh *et al.*, 2018). T_{FH} cells and GC B cells rely on each other for the continuation of the GC reaction and their survival, mediated by ICOSL, CD40L and IL-21 (Han *et al.*, 1995b, Linterman *et al.*, 2010). If a GC B cell is unable to bind antigen or fails to receive T cell help they die by neglect (Allen *et al.*, 2007a). Apoptotic cells can be cleared by tingible body macrophages (Nieuwenhuis and Opstelten, 1984).

In the last decade a new player in the GC has been identified: T_{FR} cells. They seem to arise from regulatory T cells that express the transcription factor forkhead box p3 (FOXP3) (Chung *et al.*, 2011, Linterman *et al.*, 2011, Wollenberg *et al.*, 2011) and are recruited to the GC independent of recognition of particular antigen (Maceiras *et al.*, 2017). There is additional work showing that they can also be derived from the naïve $CD4^+$ T cell pool (Aloulou *et al.*, 2016). T_{FR} cells can restrain the size of the germinal centre (Chung *et al.*, 2011, Linterman *et al.*, 2011, Wollenberg *et al.*, 2011) as well as facilitate the generation of high-affinity antibodies (Sage *et al.*, 2014). There are different mechanisms that T_{FR} cells may use to regulate the GC reaction (Fonseca *et al.*, 2019) but one of the main mechanisms is through cytotoxic T-lymphocyte-associated protein 4 (CTLA4). CTLA4 deficient mice have increased T_{FH} and GC B cells in the steady state, and blockade of CTLA4 leads

to generation of T_{FH} and GC B cells (Wang *et al.*, 2015). CTLA4 binds to CD80 and CD86 with a higher affinity than CD28 thus acts cell-extrinsically either by interfering with co-stimulation of other T cells or by restricting availability of ligands for CD28 through binding or trans-endocytosis (Qureshi *et al.*, 2011, Walker and Sansom, 2015). Trans-endocytosis has been suggested to be the dominant mechanism by which CTLA4 regulates T cell activation (Hou *et al.*, 2015). Additionally, regulatory T cells can induce tryptophan starvation through induction of indoleamine 2,3-dioxygenase (IDO), which is an enzyme that is involved in the metabolism of tryptophan to kynurenine, or secretion of TGFβ to regulate other T cell functions and activation (Walker and Sansom, 2011). Studies using *in vitro* cocultures have shown that T_{FR} cells can regulate GC B and restrict their proliferation and antibody secretion (Sage *et al.*, 2016).

1.2.7 B Cell Effector Functions

If a B cell survives selection in the germinal centre, it can differentiate into two cell types: a memory B cell or a terminally differentiated plasma cell. The cues that drive fate decision in the germinal centre are not fully understood, but affinity for antigen plays a role as B cells with lower affinity BCRs for antigen become memory B cells, whereas cells with higher affinity BCRs become plasma cells (Sciammas *et al.*, 2011, Shinnakasu *et al.*, 2016). Immunological memory is a hallmark of the adaptive immune system, although recent studies have shown that innate cells may exhibit properties of immunological memory (Hamon and Quintin, 2016). Immunological memory is the ability of the immune system to “remember” which pathogens have previously infected the organism. All immune memory cells have common features: they have been previously activated, and exhibit faster and tailored responses upon reactivation. In the case of memory B cells, after activation they can rapidly form new germinal centres or differentiate into antibody-secreting plasma cells (Zuccarino-Catania *et al.*, 2014). Memory B cells are a heterogenous population of cells and different subsets can be characterised by expression of different combinations of CD73, CD80 and PD-L2 on their surface as well as having the ability to express a switched isotype of surface immunoglobulin (Tomayko *et al.*, 2010). This heterogeneity is reflected in their responses upon reactivation, as cells that are low for memory markers (CD73, CD80 and PD-L2) are more likely to become

germinal centre B cells whereas cells that have higher levels of memory markers differentiate into plasma cells (Zuccarino-Catania *et al.*, 2014). Memory B cells can recirculate between secondary lymphoid organs or can be found at sites of infection, such as the lung (Allie *et al.*, 2019). This allows for a rapid antigen-specific response locally where previous infections occurred.

Plasma cells are professional antibody-secreting cells and can be identified by surface expression of syndecan-1 (CD138) and by lack of B220 expression. The transcription factor B lymphocyte-induced maturation protein 1 (BLIMP1), encoded by the *Prdm1* gene, is expressed in plasma cells, and is upregulated upon activation in B cells (Turner *et al.*, 1994). Together with IRF4, BLIMP1 coordinates plasma cell differentiation by negative regulation of the transcription factors PAX5 and BCL-6 that regulate B cell and GC B cell identity respectively (Sciammas *et al.*, 2006, Shaffer *et al.*, 2002). However, BLIMP1 is not essential for plasma cell fate as BLIMP-1-deficient B cells can still generate isotype-switched antibodies (Kallies *et al.*, 2007). $CD138^{+}$ cells can be split into plasmablasts and plasma cells, where the plasmablasts express low levels of BLIMP-1 and are still proliferating, and plasma cells are no longer dividing and have high expression of BLIMP1 (Kallies *et al.*, 2004). Pre-plasmablast precursors can be found in the light zone of the germinal centre by $BCL\text{-}6^{lo}CD69^{hi}$ expression as these cells have a high affinity BCR and have downregulated GC-signature genes and upregulated a subset of plasma cell signature genes (Ise *et al.*, 2018). It has been shown that T_{FH} cells and stromal cells that express APRIL, support the differentiation of plasmablasts. These stromal cells also express BAFF, IL-6 and CXCL12 that may also facilitate plasmablast survival and differentiation (Zhang *et al.*, 2018a).

Upon receiving signals to become plasma cells, the progenitors leave the germinal centre through the dark zone (Ise *et al.*, 2018, Kräutler *et al.*, 2017, Zhang *et al.*, 2018a). Plasma cells can home to either the red pulp of the spleen or the bone marrow, where they can become long-lived plasma cells. This migration is dependent on the chemokines S1P and CXCL12, where S1P is required for exit from lymphoid tissue and CXCL12 is required for homing to the bone marrow (Hargreaves *et al.*, 2001, Kabashima *et al.*, 2006). Localisation in the bone marrow and the red pulp of the spleen allows direct secretion of antibody into the circulation to provide protective immunity. In the bone marrow, the plasma cell survival niche is dictated by contact with $CXCL12^{+}$ VCAM-1^{+} stromal cells and eosinophils which produce APRIL and IL-

6 (Chu *et al.*, 2011, Tokoyoda *et al.*, 2004). In the absence of eosinophils, plasma cells can still be found in the bone marrow, meaning that there may be other haematopoietic cells that contribute to plasma cell survival (Chu *et al.*, 2011).

Circulating antibodies have different methods of providing protection from reinfection. These mechanisms include: neutralisation of pathogens by binding and prevent invasion into cells, opsonisation of pathogens through recognition of pathogen-bound antibodies by phagocytes leading to phagocytosis and degradation of the pathogen, activation of the complement cascade, induction of antibody-dependent cellular cytotoxicity through natural killer (NK) cells, and degranulation of granulocytes that drives inflammation (Forthal, 2014). This highlights the interplay with the adaptive and innate branches of the immune system as many of these effector functions require innate cells or pathways.

Further to production of antibodies that provide protection, upon activation B cells are able to regulate the immune response by the secretion of cytokines. These cytokines include: IL-6, IL-10, Lymphotoxin α and β, TNFα and vascular endothelial growth factor A (VEGF-A) which can lead to the enlargement of lymphoid organs, maintenance of T_{FH} cells in the germinal centre, and regulation of homeostasis within the immune system (Angeli *et al.*, 2006, Hartweger *et al.*, 2014, Lund *et al.*, 2005).

1.2.8 T-Independent Immune Response

In addition to the T-dependent response, B cells are able to respond to pathogens in a T-independent manner, as athymic mice are able to mount antibody responses (Gershon and Kondo, 1970). T-independent responses can be split into three classes: type 1, type 2 and type 3. Type 1 responses are initiated by B cell recognition of a pathogen through TLRs as well as through the BCR, thus providing two signals to activate the B cell (Bekeredjian-Ding and Jego, 2009). Type 2 responses are initiated by multivalent antigens that lead to extensive BCR crosslinking and provide a sustained signal leading to activation (Mond *et al.*, 1995). This signalling is dependent on BTK as CBA/N mice, which have a deficiency in BTK, are unable to mount an antibody response to type 2 antigens but can do so to type 1 antigens (Mosier *et al.*, 1977). Type 3 responses are characterised by B cells responding to mucosal or blood-borne antigens, that receive help from bone marrow-derived cells rather than thymic-derived cells (Vinuesa and Chang, 2013). For

example, a subset of neutrophils have been shown to have a helper role by secreting BAFF, APRIL and IL-21 that facilitates MZB cells to perform SHM and CSR (Puga *et al.*, 2011).

1.3 WNK1

Kinases are important enzymes that catalyse the phosphorylation of their substrates and are involved in many signal transduction cascades. The with no lysine (WNK)-family of serine/threonine protein kinases are distinct among the kinase families, due to their unique kinase domain. In this section, I will describe one of the family members, WNK1, and its role in physiology.

1.3.1 Discovery and Structure

WNK1 was first discovered at the turn of the century whilst searching for novel MAP/ERK kinases (MEKs) (Xu *et al.*, 2000). *Wnk1* orthologues exist throughout many clades of eukaryotic life, from humans to plants and fungi (Xu *et al.*, 2000). Originally, WNK1 was found to be missing the conserved catalytic lysine in subdomain II of the kinase domain, hence its name, but later work showed that a lysine in subdomain I is the catalytic lysine in WNK1 (Min *et al.*, 2004, Xu *et al.*, 2000). *Wnk1* is found on mouse chromosome 6 and is arranged into 33 exons. Alternative splicing and multiple promoters lead to the generation of different isoforms of WNK1, including one missing the kinase domain (Delaloy *et al.*, 2003, O'Reilly, 2003). *Wnk1* is expressed in various organs of both adult and foetus, including brain, kidney, spleen and heart (Verissimo and Jordan, 2001, Xu *et al.*, 2000).

WNK1 is a large protein, with most isoforms being over 200 kDa and the canonical isoform being 250 kDa large (www.uniprot.org). It is made up of an N-terminal kinase domain, an autoinhibitory domain, and three coiled-coil domains (Moon *et al.*, 2013, Verissimo and Jordan, 2001, Xu *et al.*, 2002). Furthermore, WNK1 is proline rich and contains many PxxP motifs, suggesting that it may have a role as a scaffold to allow binding of proteins with SH3 domains.

WNK1 is critical for embryonic development as constitutive loss of *Wnk1* in mice leads to death between E10.5 and E13.5. *Wnk1*$^{-/-}$ embryos die due to defects in cardiovascular development, and endothelial-specific expression of *Wnk1* is required for normal cardiovascular development (Xie *et al.*, 2009).

1.3.2 Regulation of Ion Homeostasis and Cell Volume

In humans, deletions in the intron between exons 1 and 2 of *WNK1* lead to overexpression of the gene and are associated with the hereditary disorder called pseudohypoaldosteronism type II (PHAII). Patients with PHAII present with hypertension and hyperkalaemia (high levels of serum K^+) (Wilson *et al.*, 2001). WNK1 can be activated by osmotic stress and acts as a Cl^- sensor as Cl^- can bind to its kinase domain inhibiting its autophosphorylation (Piala *et al.*, 2014, Xu *et al.*, 2000). Further to this, WNK1 can be activated by PI3K through AKT (Cheng and Huang, 2011). In the kidney epithelium, activated WNK1 phosphorylates the oxidative stress-responsive 1 (OXSR1) kinase and the related serine/threonine-protein kinase 39 (STK39) in both their S-loop and T-loop, leading to their activation (Anselmo *et al.*, 2006, Vitari *et al.*, 2005, Moriguchi *et al.*, 2005). OXSR1 and STK39 are further activated by calcium-binding protein 39, also known as MO25α (Filippi *et al.*, 2011). Activated OXSR1 and STK39 are able to phosphorylate the cytoplasmic tail of Na^+-K^+-Cl^- cotransporter (NKCC) 1 and NKCC2, encoded by *Slc12a2* and *Slc12a1* respectively, opening the channels and facilitating entry of Na^+, K^+ and Cl^- ions into the cell (Figure 1.6) (Anselmo *et al.*, 2006, Piechotta *et al.*, 2002, Moriguchi *et al.*, 2005, Richardson *et al.*, 2011). Additionally, OXSR1 and STK39 phosphorylate Na^+-Cl^- cotransporter (NCC), encoded by *Slc12a3*, which inhibits internalisation of NCC from the surface of cells and thereby promotes Na^+ and Cl^- entry into the cell (Moriguchi *et al.*, 2005, Rosenbaek *et al.*, 2014). Thus, in the kidney epithelium of patients with PHAII, there is an increase in Na^+, K^+ and Cl^- uptake from the urine to the blood, thus giving rise to hypertension and hyperkalaemia.

Activation of WNK1 and other WNK-family members can lead to phosphorylation of electroneutral K^+-Cl^- cotransporter (KCC) 1, KCC2, KCC3 and KCC4, encoded by the genes *Slc12a4*, *Slc12a5*, *Slc12a6* and *Slc12a7* respectively (De Los Heros *et al.*, 2014). Rather than activating the transporter activity of the KCCs, phosphorylation by OXSR1 and STK39 leads to the inhibition of KCC activity (Jennings and Al-Rohil, 1990, Shekarabi *et al.*, 2017), leading to a block of K^+ and Cl^- ion export.

Conditionally deleting *Oxsr1* in the endothelium causes embryonic lethality, phenocopying the conditional knockout of *Wnk1*, suggesting that WNK1 signalling through OXSR1 in the endothelium is essential for normal embryonic development

(Xie *et al.*, 2013). Constitutive knockout of *Slc12a2* (NKCC1) does not lead to embryonic death but the mice are deaf, growth retarded, have decreased blood pressure and exhibit repetitive circling behaviours (Flagella *et al.*, 1999). This suggests that NKCC1 is not critical for the phenotype observed in the *Wnk1*$^{-/-}$ embryos, or at least that there may be compensation by other transporters, such as NKCC2.

Further ion regulation is mediated by serum and gluticorticord-induced protein kinase (SGK1), which has been shown to be activated by and also activate WNK1 (Cheng and Huang, 2011, Xu *et al.*, 2005a, Xu *et al.*, 2005b). Activation of SGK1 by WNK1 has been shown to be independent of the kinase function of WNK1 (Xu *et al.*, 2005a, Xu *et al.*, 2005b). Through interactions with SGK1, WNK1 has been shown to positively regulate epithelial Na^+ channel (ENaC) via preventing its ubiquitination and degradation by E3 ubiquitin-protein ligase NEDD4-like (NEDD4L), and to negatively regulate renal outer medullary K^+ channel (ROMK) by promoting its endocytosis (Figure 1.6) (Cheng and Huang, 2011, Xu *et al.*, 2005a, Xu *et al.*, 2005b, Zhou *et al.*, 2007). Taken together, the evidence shows that WNK1 activation leads to import of Na^+ and Cl and to a block of K^+ export (Figure 1.6). This ion movement leads to an increase in tonicity inside the cell, which in turn causes swelling of cells as water moves across the plasma membrane via osmosis to restore cellular tonicity.

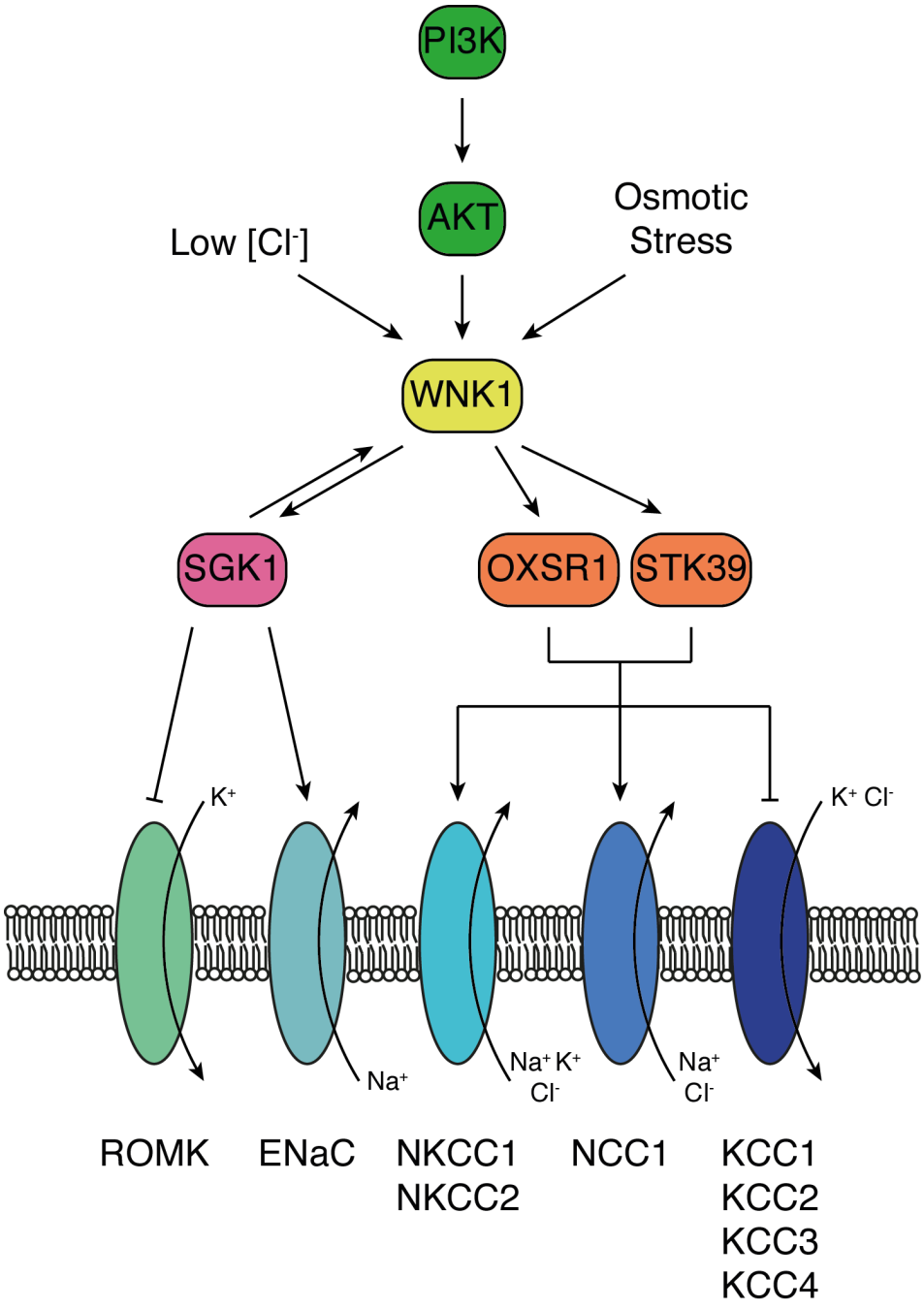

Figure 1.6 WNK1 Regulation of Ion Homeostasis

WNK1 is activated by PI3K/AKT pathway, osmotic stress and low Cl^- concentrations. Activated WNK1 can phosphorylate and activate OXSR1 and STK39, which can phosphorylate ion cotransporters from the SLC12A-family. Phosphorylation of NKCC1 and NCC1 leads to their activation, whereas phosphorylation of KCC1, KCC2, KCC3 and KCC4 leads to their inhibition. WNK1 also activates SGK1, which has also been shown to activate WNK1. Activated SGK1 leads to activation of the ENaC channel, leading to increased Na^+ transport, and inhibition of ROMK via endocytosis, decreasing K^+ transport.

1.3.3 WNK1 in the Central Nervous System

Hereditary sensory and autonomic neuropathy type II (HSAN2), which is an early-onset disorder characterised by loss of pain, touch and heat perception, was found to be caused by mutations in a single-exon open reading frame called hereditary sensory neuropathy type II (*HSN2*) (Lafrenière *et al.*, 2004). It was found that *HSN2* is an exon of *WNK1*, found between exons 8b and 9, and is expressed in a nervous system-specific manner (Shekarabi *et al.*, 2008). This work highlights that WNK1 has roles in the central nervous system.

WNK1 has been shown to regulate Cl^- homeostasis in neurons by phosphorylation of KCC2, a neural-specific KCC-family protein, through forming a physical complex (Friedel *et al.*, 2015, Inoue *et al.*, 2012). The phosphorylation of KCC2 is dependent on STK39 and an unidentified kinase (Friedel *et al.*, 2015). In a model of neuropathic pain, WNK1 has been shown to be activated leading to the phosphorylation of KCC2 (Kahle *et al.*, 2016). Antagonism of gamma-aminobutyric acid A receptor ($GABA_AR$) leads to activation of the WNK1/OXSR1 pathway, suggesting the pathway may be important for adjusting neuronal ion homeostasis (Heubl *et al.*, 2017).

Further to regulation of KCC2, WNK1 has been shown to regulate proliferation and migration in neural progenitors (Sun *et al.*, 2006), suggesting a role for WNK1 during neuronal development. Work using a glioma cell line showed that WNK1/NKCC1 pathway is important for cell migration and for cell volume control (Zhu *et al.*, 2014).

1.3.4 Other Known Functions and Interactors of WNK1

WNK1 has been shown to regulate TGFβ signalling by interacting with mothers against decapentaplegic homologue 2 (SMAD2). It was shown that knockdown of *WNK1* leads to a reduction in the amount of SMAD2 present in the cells through reduced expression of *SMAD2* mRNA. Additionally, knockdown of *WNK1* leads to increased levels of phosphorylated SMAD2 in the nucleus, and increased transcription of SMAD2 target genes, suggesting that WNK1 negatively regulates TGFβ signalling. Taken together, these data show that regulation of TGFβ signalling by WNK1 is multi-faceted as it regulates both levels and activation of SMAD2 (Lee *et al.*, 2007).

Activation of WNK1 is able to activate ERK5 in a manner that is dependent on the MEK5α isoform of MEK5 but not the MEK5β isoform. WNK1 is able to directly phosphorylate MAP3K2 and MAP3K3 *in vitro*, which are upstream of ERK5, but kinase function of WNK1 is not required for their association with WNK1. Furthermore, phosphorylation by WNK1 doesn't directly to activate MAP3K2 and MAP3K3. However, the kinase function of WNK1 seems to be required for complete activation of ERK5 (Xu *et al.*, 2004). This suggests that WNK1 regulates activation of ERK5 by at least two pathways, one that is dependent on kinase function of WNK1 and another that is not.

WNK1 is emerging as a regulator of autophagy as knockdown of WNK1 leads to an increase in the number of LC3 puncta (a marker for autophagosomes), suggesting an increase in the number of autophagosomes. WNK1 positively regulates autophagy by regulating localisation of UV radiation resistance-associated gene (UVRAG), which is a component of class III PI3K that initiates autophagy (Gallolu Kankanamalage *et al.*, 2016, Petiot *et al.*, 2000). Additional regulation is mediated by the negative regulation of unc-51-like kinase 1 (ULK1), which activates the class III PI3K complex (Gallolu Kankanamalage *et al.*, 2016).

In addition to the previously described role for proliferation in neural progenitors, WNK1 has been described to regulate proliferation induced by hypotonic challenge in rat vascular smooth muscle cells through regulation of cyclins, although the mechanism remains unknown (Zhang *et al.*, 2018b). WNK1 has also been implicated in mitosis, since knockdown of when WNK1 in HeLa cells results in a defect in cytokinesis (Tu *et al.*, 2011). This work also showed that WNK1, but not OXSR1, is localised to the microtubule spindles during mitosis (Tu *et al.*, 2011).

1.3.5 WNK1 in the Immune System

Recent work from our laboratory has revealed novel insights into WNK1 biology in the immune system. WNK1 was revealed to be a negative regulator of T cell adhesion in a screen to discover kinases that regulate T cell adhesion to APCs (Köchl *et al.*, 2016). Further work using naïve $CD4^+$ T cells revealed that WNK1 negatively regulates T cell adhesion through LFA-1 by negative regulation of GTP-loading of RAP1 or positive regulation of GTP hydrolysis in RAP1. Furthermore, naïve $CD4^+$ T cells lacking *Wnk1* expression also showed defects in both *in vitro* migration in

response to CCL21 and *in vivo* migration. Thus, WNK1 is a positive regulator of chemokine-induced migration in $CD4^+$ T cells. As a result, the ability of WNK1-deficient $CD4^+$ T cells to home to secondary lymphoid organs was diminished compared to control T cells. Further analysis showed that both CCL21 and anti-CD3 stimulation induced phosphorylation of OXSR1 in a manner that was dependent on WNK1 kinase function as well as PI3K and AKT function. Interestingly, the negative regulation of adhesion through LFA-1 was not dependent on phosphorylation of OXSR1 nor on the expression of *Slc12a2*. However, WNK1 regulation of migration is mediated by phosphorylation of OXSR1 and NKCC1 (Köchl *et al.*, 2016). Unpublished work has also shown that WNK1 is required for the development of T cells, since a knockout of WNK1 during early thymocyte development leads to a block at the double negative 3 stage of development, where cells are undergoing β-selection which is analogous to selection at the pre-B cell stage described previously (unpublished).

Taken together, these studies indicate that WNK1 has pleiotropic roles within cells. WNK1 is important for regulation of autophagy, migration, ion homeostasis, cell volume regulation, control of cell cycle and division, and GABA signalling in neurons. WNK1 has also been implicated in different signalling pathways, including OXSR1 and STK39 activation, ERK5 signalling and regulation of SMAD2 in TGFβ signalling (Figure 1.6 and Figure 1.7).

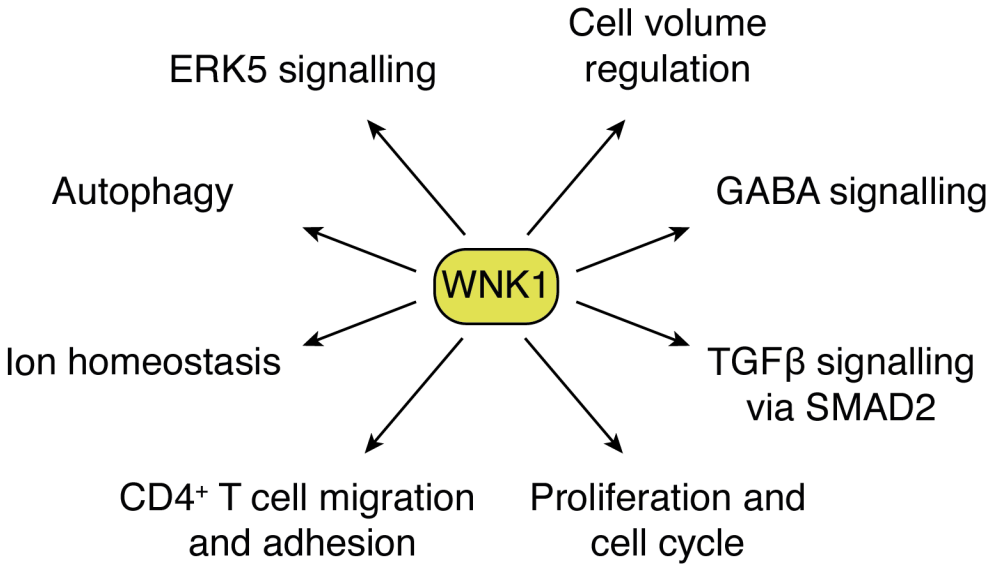

Figure 1.7 WNK1 Regulates Many Cellular Processes and Signalling Pathways

WNK1 has been implicated as a regulator in many cellular processes including: ion homeostasis, cell volume regulation, GABA signalling in neurons, autophagy, proliferation and cell cycle regulation, and migration and adhesion in $CD4^+$ T cells. In addition to the signalling pathway involving OXSR1 and STK39, WNK1 has been implicated in ERK5 signalling, and TGFβ signalling through regulation of SMAD2.

1.4 Aims

The function of WNK1 has been well described in the process of ion homeostasis and regulation in both the kidney and the central nervous system. However, WNK1 is expressed in many cell types including lymphocytes. Little is known about the function of WNK1 in the immune system apart from its role in the regulation of naïve $CD4^+$ T cell adhesion and migration. The main aim of this project was to extend our knowledge of the role of WNK1 in the immune system by investigating its potential function in B cell biology. The project was split into three main questions:

1. Does WNK1 regulate B cell adhesion and migration in naïve B cells?
2. Are B cells able to become activated in the absence of WNK1?
3. Is *Wnk1* expression in B cells required for an antibody response?

In this project, I used inducible deletion of *Wnk1* to answer these questions as well as a knockout of *Slc12a2* to assess the role of NKCC1 in B cell biology. These studies revealed that WNK1 regulates multiple aspects of B cell biology, including adhesion, migration, survival, development, activation, proliferation, antigen presentation to $CD4^+$ T cells and antibody responses to T-dependent antigens.

Chapter 2. Materials & Methods

2.1 Mice

All mice were kept under specific pathogen-free conditions at either the animal facility of the Medical Research Council National Institute for Medical Research (NIMR) or the animal facility of The Francis Crick Institute (Crick). All animal experimentation was conducted according to the project licence, institutional guidelines and UK Home Office regulations. All mice were maintained on the C57BL/6JNimr or C57BL/6Jax background, and genotyped using Transnetyx's genotyping service. C57BL/6J mice were used as wildtype (WT) mice. A list of genetically modified mouse strains used can be found in Table 1. Mice were culled using Schedule 1 (S1K) methods.

2.1.1 Breeding Strategies

Since *Wnk1* and *Rosa26* are 6.8 Mb apart on the same chromosome (Mmu6), we deliberately crossed *Wnk1*$^{fl/+}$ *Rosa26*$^{CreERT2/+}$ mice to C57BL/6J mice to generate mice in which a genetic crossover caused the *Wnk1*^{fl} and *Rosa26*^{CreERT2} alleles to become linked on the same chromosome. Double heterozygous mice were intercrossed to generate *Wnk1*$^{fl/fl}$ *Rosa26*$^{CreERT2/CreERT2}$ homozygous mice. *Wnk1*$^{fl/fl}$ *Rosa26*$^{CreERT2/CreERT2}$ mice were bred *Wnk1*$^{+/-}$ mice so that every offspring was either *Wnk1*$^{fl/+}$ *Rosa26*$^{CreERT2/+}$ or *Wnk1*$^{fl/-}$ *Rosa26*$^{CreERT2/+}$. *Wnk1*$^{fl/fl}$ *Rosa26*$^{CreERT2/CreERT2}$ mice were bred *Wnk1*$^{+/D368A}$ mice so that every offspring was either *Wnk1*$^{fl/+}$ *Rosa26*$^{CreERT2/+}$ or *Wnk1*$^{fl/D368A}$ *Rosa26*$^{CreERT2/+}$. *Eμ-BCL2L1* mice were bred with *Wnk1*$^{+/-}$ mice to generate *Wnk1*$^{+/-}$ *Eμ-BCL2L1* mice. These mice were bred with *Wnk1*$^{fl/fl}$ *Rosa26*$^{CreERT2/CreERT2}$ mice to generate *Wnk1*$^{fl/+}$ *Rosa26*$^{CreERT2/+}$, *Wnk1*$^{fl/-}$ *Rosa26*$^{CreERT2/+}$, *Wnk1*$^{fl/+}$ *Rosa26*$^{CreERT2/+}$ *Eμ-BCL2L1*, and *Wnk1*$^{fl/-}$ *Rosa26*$^{CreERT2/+}$ *Eμ-BCL2L1* offspring. MD4^{+} *Wnk1*$^{+/-}$ mice were bred with *Wnk1*$^{fl/fl}$ *Rosa26*$^{CreERT2/CreERT2}$ mice to generate MD4^{+} *Wnk1*$^{fl/+}$ *Rosa26*$^{CreERT2/+}$ or MD4^{+} *Wnk1*$^{fl/-}$ *Rosa26*$^{CreERT2/+}$ mice. *Wnk1*$^{fl/fl}$ mice were bred to *Aicda*^{Cre}/*Aicda*^{Cre} mice to generate mice which are homozygous for both alleles. *Wnk1*$^{fl/fl}$ *Aicda*^{Cre}/*Aicda*^{Cre} mice were bred to *Wnk1*$^{+/-}$ mice to generate *Wnk1*$^{fl/+}$ *Aicda*^{Cre} and *Wnk1*$^{fl/-}$ *Aicda*^{Cre} mice.

Table 1 List of Genetically Modified Mouse Strains

Allele Common Name	MGI Nomenclature	Description	Reference
μMT^{-}	*Ighm*^{tm1Cgn}	Neomycin resistance gene inserted into exon encoding membrane region of the IgM heavy chain	(Kitamura *et al.*, 1991)
Aicda^{Cre}	Tg$^{(Aicda-cre)9Mbu}$	Random insertion of Cre linked by an IRES to a truncated human CD2 sequence under the control of the Aicda promoter	(Kwon *et al.*, 2008)
Eμ-BCL2L1	Tg$^{(Emu-BCL2L1)87Nnz}$	Random insertion of human *BCL2L1* under regulatory control of the SV40 promoter and the IgH enhancer	(Grillot *et al.*, 1996)
MD4^{+}	Tg$^{(IghelMD4)4Ccg}$	Random insertion of transgene encoding hen egg lysozyme specific IgM and IgD	(Goodnow *et al.*, 1988)
OT-II^{+}	Tg$^{(TcraTcrb)425Cbn}$	Random insertion of transgenes encoding TCRα and TCRβ chains specific for chicken ovalbumin residues 323-339 in the context of MHC class II	(Barnden *et al.*, 1998)
Oxsr1^{T185A}	*Oxsr1*$^{tm1.1Arte}$	Knock-in of allele encoding non-phosphorylatable mutant of OXSR1	(Rafiqi *et al.*, 2010)

Rag1^{-}	*Rag1*^{tm1Mom}	Nuclear localisation sequence and zinc finger motif replaced with neomycin cassette	(Mombaerts *et al.*, 1992)
Rosa26^{CreERT2} (RCE)	*Gt(ROSA)26Sor*$^{tm1(cre/ERT2)Thl}$	Sequence encoding a fusion of Cre recombinase and the oestrogen receptor ligand binding domain inserted into the Rosa26 locus	(de Luca *et al.*, 2005)
Slc12a2^{-}	*Slc12a2*^{tm1Ges}	Knockout allele by insertion of *Neo*^{R} into exon 6	(Flagella *et al.*, 1999)
Wnk1^{-}	*Wnk1*$^{tm1.1Clhu}$	Null allele	(Köchl *et al.*, 2016)
Wnk1^{D368A}	*Wnk1*^{tm1Tyb}	Knock-in of allele encoding kinase-dead mutant of WNK1	(Köchl *et al.*, 2016)
Wnk1^{fl}	Wnk1^{tm1Clhu}	Exon 2 flanked by LoxP sites	(Xie *et al.*, 2009)

2.2 *In vivo* Deletion of Floxed Alleles

Mice were injected via the intraperitoneal route for 3 consecutive days with 2 mg tamoxifen (Sigma-Aldrich; Merck KGaA) dissolved in 100 µl corn oil (Sigma-Aldrich; Merck KGaA). Unless indicated otherwise, mice were sacrificed 7 days after initial tamoxifen injection.

2.3 Bone Marrow and Foetal Liver Chimeras

Bone marrow was harvested from donor mice and either resuspended in ammonium-chloride-potassium (ACK) lysis buffer for two minutes at room temperature to lyse erythrocytes or in a mixture of 90% foetal calf serum (FCS, Biosera) and 10% dimethyl sulphoxide (DMSO, Sigma-Aldrich; Merck KGaA) for freezing using a Mr. Frosty^{TM} Freezing Container (Nalgene; Nalge Nunc International

Corporation). Donor foetal livers were harvested from embryos at E14.5-E16.5 and resuspended in 90% FCS 10% DMSO for freezing. For mixed chimeras, cells were mixed at a 1:4 ratio with cells from μMT mice in order to restrict genomic modifications to the B cell lineage. Cells were intravenously injected into RAG1-deficient mice that were sublethally irradiated with 1 dose of 5 Gy from a ^{37}Cs source. Mice were maintained on 0.02% enrofloxacin (Baytril, Bayer Healthcare) for 4 weeks and the haematopoietic compartment was left to reconstitute for at least 8 weeks prior to performance of any further regulated procedures.

2.4 Preparation of Single Cell Suspensions

Single cell suspensions of spleen, mesenteric lymph nodes and peripheral lymph nodes (axillary, brachial and inguinal) were obtained by pressing the organs through a 70 μm cell strainer. Bone marrow single cell suspensions from the tibia and femur were generated by flushing the bone marrow out of the bone with a syringe filled with Air buffered Iscove's modified Dulbecco's medium (AB IMDM) supplemented with 5% FCS. Blood was collected by puncturing the heart after culling mice. Erythrocytes from spleen and bone marrow were lysed using ACK lysis buffer and incubating at room temperature for two minutes. Erythrocytes from blood were lysed using ACK lysis buffer and incubating at room temperature for five minutes.

2.5 Splenic B Cell Isolation

Splenic single cell suspensions were prepared as described in Section 2.4. Splenocytes were incubated with biotinylated antibodies against CD11c, CD11b, CD43 and Ly-6G for 20 minutes on ice. The labelled cells were incubated with 1.2 to 1.4 x 10^8 streptavidin-Dynabeads (Thermo Fisher Scientific, Inc.) in magnetic-activated cell sorting (MACS) buffer for 20 minutes at 4°C. Tubes were placed on a magnet and the supernatant containing the negative fraction was collected.

2.6 RNA Preparation and Quantitative Real Time Polymerase Chain Reaction (qPCR)

All of the following experiments were performed according to the manufacturer's instructions. RNA was extracted from $5x10^5$ purified splenic B cells using RNeasy Plus Micro Kit (Qiagen). SuperScript™VILO™cDNA Synthesis Kit (Invitrogen; Thermo Fisher Scientific, Inc.) was used to synthesise cDNA from the extracted RNA. Taqman™ Gene Expression Master Mix (Thermo Fisher Scientific, Inc.) and Taqman® Gene Expression Assays (Thermo Fisher Scientific, Inc.) against mouse *Wnk1* (spanning exons 1 and 2 – Mm01184006_m1, spanning exons 5 and 6 – Mm01184014_m1) and *Hprt* (spanning exons 2 and 3 – Mm03024075_m1) were used to perform qPCRs in a QuantStudio3 qPCR machine (Thermo Fisher Scientific, Inc.). The relative expression of *Wnk1* was determined using Microsoft Excel and the following equation:

$$\text{Relative Expression} = \frac{2^{-(\text{Ct gene of interest} - \text{Ct housekeeping gene})}}{\text{mean}\,(2^{-\Delta\text{Ct control group}})}$$

2.7 Stimulation of B Cells

For stimulation with CXCL13, anti-IgM and BAFF, purified splenic B cells were rested in AB IMDM supplemented with 5% FCS for 45 minutes or 3 hours at 37°C. If 0.1% DMSO (Sigma-Aldrich; Merck KGaA), 1 μM PI-103 (BioVision, Inc.), 2 μM MK2206 (Cambridge Bioscience) or WNK463 (MedChem Express) at a range of concentrations were added, this was done 1 hour prior to stimulation. After resting, or purification in the case of B cells stimulated with CD40L and LPS, $2\text{-}4x10^6$ cells were stimulated with either 1 μg/ml recombinant murine CXCL13 (CXCL13, R&D Systems; Biotechne), 10 μg/ml AffiniPure F(ab')$_2$ fragment goat anti-mouse IgM (anti-IgM, Jackson ImmunoResearch Laboratories, Inc.), 200 ng/ml recombinant human BAFF (BAFF, PeproTech), 1 μg/ml recombinant murine CD40L (CD40L, R&D Systems; Biotechne) or 10 μg/ml LPS from Salmonella minnesota R595 (LPS, Enzo Life Sciences, Inc.) for the times indicated. The reaction was stopped using ice cold PBS and the cells were pelleted using centrifugation. The pelleted cells were resuspended in 1x RIPA buffer in order to lyse the cells. The insoluble fraction of the lysate was removed by centrifugation and the soluble fraction was mixed with 5x

sodium dodecyl sulphate (SDS) sample buffer. The samples were then frozen and stored at -20°C.

2.8 Immunoblot

Samples were thawed at room temperature and incubated at 95°C for 5 minutes to denature proteins. Samples were loaded onto either a 4-20% TGX gel (BioRad Laboratories), a 10% TGX gel (BioRad Laboratories) or a 10% SDS-polyacrylamide gel electrophoresis (SDS-PAGE) mini gel. Proteins were separated at 120 V in 1x tris-glycine-SDS (TGS) buffer (BioRad Laboratories) for 1 hour and 30 minutes. Proteins were transferred onto a methanol-activated polyvinylidene fluoride (PVDF) membrane (Merck Millipore) in 3-(cyclohexylamino)-1-propanesulphonic acid (CAPS) buffer at 350 mA for 1 hour and 15 minutes or by using the Trans-Blot® Turbo™ Transfer System (Bio-Rad Laboratories) according to the manufacturer's instructions. Membranes were incubated with Odyssey® Blocking Buffer (LI-COR Biosciences) at room temperature for 1 hour. The membranes were incubated in primary antibody diluted in blocking buffer at 4°C overnight. After washing the membrane 3 times with PBS + 0.05% Tween-20 (Sigma-Aldrich; Merck KGaA), the membranes were incubated with fluorophore-conjugated secondary antibodies at room temperature for 1 hour. A list of antibodies used can be found in Table 2 and Table 3. The Odyssey CLx (LI-COR Biosciences) was used to image the membranes and Image Studio Lite (LI-COR Biosciences) was used to quantify intensities. Microsoft Excel was used to determine relative signals by normalising to loading controls and then to the sum of the signals across multiple experiments (Degasperi *et al.*, 2014).

Table 2 List of Primary Antibodies Used for Immunoblot

Antigen	Clonality (clone)	Species	Supplier	Dilution
α-TUBULIN	Monoclonal (TAT-1)	Mouse	Cell Services STP, Crick	1:15000
ERK2	Monoclonal (D-2)	Rabbit	Santa Cruz Biotechology, Inc.	1:500
MYC	Monoclonal (Y69)	Rabbit	Abcam	1:500
p-AKT (S473)	Monoclonal (193H12)	Rabbit	Cell Signalling Technology, Inc.	1:500
p-PRAS40 (T246)	Monoclonal (C77D7)	Rabbit	Cell Signalling Technology, Inc.	1:500
p-OXSR1	Polyclonal	Sheep	MRC PPU Reagents and Services	1:1000

Table 3 List of Secondary Antibodies Used for Immunoblot

Antigen	Conjugate	Species	Supplier	Dilution
Biotin	Streptavidin Alexa Fluor 680	N/A	Invitrogen; Thermo Fisher Scientific, Inc.	1:4000
Mouse IgG	IRDye® 800CW	Goat	LI-COR Biosciences	1:4000
Rabbit IgG	Alexa Fluor 680	Goat	Invitrogen; Thermo Fisher Scientific, Inc.	1:4000
Rabbit IgG	Alexa Fluor Plus 800	Goat	Invitrogen; Thermo Fisher Scientific, Inc.	1:4000
Sheep IgG	Alexa Fluor 680	Donkey	Invitrogen; Thermo Fisher Scientific, Inc.	1:4000

2.9 Fluorescent Labelling of Cells with Dyes

Single cell suspensions were incubated with either 5 μM CellTrace™ CFSE (CFSE, Thermo Fisher Scientific, Inc.), 5 μM CellTrace Violet (CTV, Thermo Fisher Scientific, Inc.), 1 μM CellTracker™ green CMFDA (CMFDA, Invitrogen; Thermo Fisher Scientific, Inc.) or 10 μM cell proliferation dye eFluor™ 450 (eBioscience; Thermo Fisher Scientific, Inc.) in PBS at 37°C for 10 minutes, unless stated otherwise. Then media supplemented with FCS was added and incubated at 37°C for 7 minutes to soak up excess dye. The cells were pelleted by centrifugation and resuspended in appropriate media for the experiment.

2.10 Flow Cytometry

Single cell suspensions were stained for 20 minutes on ice in PBS containing appropriate antibodies, dyes and live/dead dye. Cells were washed and then resuspended in FACS buffer. Where required samples were labelled with secondary antibodies or streptavidin in PBS after washing out primary antibodies with FACS buffer. For intracellular staining, samples were fixed and permeabilised using BD Cytofix/Cytoperm (BD Biosciences) according to manufacturer's instructions. To determine cell numbers, either a known number of BD Calibrite APC beads (BD Biosciences) were added to each sample or the cells were counted prior to staining using CASY cell counter. Cell populations were analysed using a BD Fortessa X20™ (BD Biosciences) flow cytometer and using FlowJo (TreeStar) software. A list of antibodies and fluorescent probes can be found in Table 4.

Table 4 List of Antibodies, Reagents and Fluorescent Dyes Used for Flow Cytometry and Cell Isolation

Antigen/Dye	Clone	Isotype	Supplier	Dilution
B220	RA3-6B2	Rat IgG2a, κ	BioLegend	1:200
BAFFR	eBio7H22-E16	Rat IgG1, κ	eBioscience; Thermo Fisher Scientific, Inc.	1:100
Biotin (streptavidin)			eBioscience; Thermo Fisher Scientific, Inc.	1:200

CD2 (mouse)	RM2-5	Rat IgG2b, λ	eBioscience; Thermo Fisher Scientific, Inc.	1:400
CD2 (human)	RPA-2.10	Rat IgG1, κ	eBioscience; Thermo Fisher Scientific, Inc.	1:200
CD3ε	145-2C11	Armenian Hamster IgG	BD Biosciences	1:200
CD4	RM4-5	Rat IgG2a, κ	BioLegend	1:200
CD4	GK1.5	Rat IgG2b, κ	eBioscience; Thermo Fisher Scientific, Inc.	1:200
CD11a	M17/4	Rat IgG2a, κ	eBioscience; Thermo Fisher Scientific, Inc.	1:200
CD11b	M1/70	Rat IgG2b, κ	BioLegend	1:200
CD11c	N418	Armenian Hamster IgG	BioLegend	1:200
CD19	6D5	Rat IgG2a, κ	BioLegend	1:200
CD19	1D3	Rat IgG2a, κ	BioLegend	1:200
CD23	B3B4	Rat IgG2a, κ	BioLegend	1:400
CD40	1C10	Rat IgG2a, κ	eBioscience; Thermo Fisher Scientific, Inc.	1:200
CD43	eBioR2/60	Rat IgM	eBioscience; Thermo Fisher Scientific, Inc.	1:200
CD44	1M7	Rat IgG2b, κ	Invitrogen; Therrmo Fisher Scientific, Inc.	1:200
CD45.1	A20	Mouse IgG2a, κ	eBioscience; Thermo Fisher Scientific, Inc.	1:200
CD45.2	104	Mouse IgG2a, κ	eBioscience; Thermo Fisher Scientific, Inc.	1:200

CD69	H1.2F3	Armenian Hamster IgG	BioLegend	1:200
CD71	R17217	Rat IgG2a, κ	eBioscience; Thermo Fisher Scientific, Inc.	1:200
CD80	16-10A1	Armenian Hamster IgG2, κ	BD Biosciences	1:200
CD86	GL1	Rat IgG2a, κ	eBioscience; Thermo Fisher Scientific, Inc.	1:200
CD93	AA4.1	Rat IgG2b, κ	eBioscience; Thermo Fisher Scientific, Inc.	1:100
CD95	Jo2	Armenian Hamster IgG2, λ2	BD Biosciences	1:200
CD138	281-2	Rat IgG2a, κ	BD Biosciences	1:200-300
CmxROS			Invitrogen; Therrmo Fisher Scientific, Inc.	1:50000 (20nM)
CXCR5	L138D7	Rat IgG2b, κ	BioLegend	1:200
$E\alpha_{52-68}$ peptide bound to 1-Ab	eBioY-Ae	Mouse IgG2b	eBioscience; Thermo Fisher Scientific, Inc.	1:200
GR1	RB6-8C5	Rat IgG2b, κ	BioLegend	1:200
ICOSL	HK5.3	Rat IgG2a, κ	Invitrogen; Therrmo Fisher Scientific, Inc.	1:200
IgD	11-26C	Rat IgG2a, κ	eBioscience; Therrmo Fisher Scientific, Inc.	1:200-400
IgG1	X56	Rat IgG1, κ	BD Biosciences	1:200-300
IgG2b	Polyclonal	Goat IgG	Invitrogen; Therrmo Fisher Scientific, Inc.	1:500
IgM	RMM-1	Rat IgG2a, κ	BioLegend	1:200

IgM F(ab)	Polyclonal	Goat IgG	Jackson ImmunoResearch, Inc.	1:300
Ly77	GL7	Rat IgM	eBioscience; Thermo Fisher Scientific, Inc.	1:100
MHC class II (I-A/I-E)	M5/114.15.12	Rat IgG2b, κ	eBioscience; Thermo Fisher Scientific, Inc.	1:200
MitoTracker Green			Invitrogen; Therrmo Fisher Scientific, Inc.	1:50000 (20nM)
Mouse IgG2b	Polyclonal	Goat IgG	Invitrogen; Therrmo Fisher Scientific, Inc.	1:500
Near-IR fluorescent reactive dye			Invitrogen; Therrmo Fisher Scientific, Inc.	1:500
NP			LYNX Rapid Conjugation Kit, Bio-Rad Laboratories	1:400-800
TCRβ	H57-597	Armenian Hamster IgG	BioLegend	1:200
Zombie Aqua™			BioLegend	1:500

2.11 Transwell Assay

Transwell 5 μm pore inserts were coated with 0.5 μg/ml ICAM1 (R&D Systems; Biotechne) overnight at 4°C. After ICAM coating, they were washed with PBS twice and blocked with 2% Bovine serum albumin (BSA, Sigma-Aldrich; Merck KGaA) for an hour at room temperature and then washed with PBS twice. CXCL13 was diluted to 1 μg/ml in RPMI 1640 media (Sigma-Aldrich; Merck KGaA) supplemented with 0.5% BSA. Either medium alone or CXCL13 was added to the Transwell plate. The Transwell insert was then placed into the Transwell plate and 80,000 isolated splenic B cells were added per well. 80,000 splenic B cells were also added to a V-bottom 96-well plate (Corning, Inc.) to determine input cell number. The Transwell plate was placed in an incubator at 37°C for three hours. After removal from the incubator, the

insert was removed and 20 μl of 0.5 M ethylenediaminetetraacetic acid (EDTA) was added to the wells. The migrated cells were transferred to the V-bottom plate and the number of cells migrated and total inputs were determined using flow cytometry.

2.12 *In vitro* Migration

8-well chambered coverglass with non-removable wells (Avantor; VWR) were coated with 3 μg/ml ICAM-1 overnight at 4°C and then washed three times with PBS. Chambers were blocked with 2% BSA for an hour at room temperature and then washed three times. Isolated splenic B cells from each genotype were labelled with either CMFDA or CTV and mixed together at a 1:1 ratio. 1.5 x 10^5 cells were added to each chamber and allowed to settle for 20 minutes in heat chamber of Eclipse Ti2 (Nikon, Inc.) set at 37°C. 10 μg/ml CXCL13 was added to the chamber so that the final concentration was 1 μg/ml. Three videos consisting of 60 frames at a rate of 3 frames/min were generated using Eclipse Ti2 and μManager (https://micro-manager.org) per chamber. Videos were analysed using the TrackMate (Tinevez *et al.*, 2017) plugin in FIJI (Schindelin *et al.*, 2012). Values were filtered for cells that appeared in all frames and had a displacement ≥ 5 μm.

2.13 Intravital Microscopy

This work was carried out by Sujana Sivapatham. B cells were isolated by using mouse B cell isolation kit (STEMCELL Technologies) according to the manufacturer's protocol. B cells from each genotype were labelled either with 5 μM CMTMR or 20 μM CMAC for 20 min at 37°C, 5% CO_2. and mixed at a 1:1 ratio. The mixture was transferred intravenously into sex-matched C57BL/6J mice. 24 hours after transfer, the popliteal LN of recipient mice was surgically exposed for two-photon microscopy as in (Moalli *et al.*, 2014). Immediately prior to imaging, HEVs were labelled by intravenous injection of Alexa Fluor 633-conjugated MECA-79. Two-photon microscopy imaging was performed by using a Trimscope system equipped with an Olympus BX50WI fluorescence microscope and an 20X (NA 0.95, Olympus) or 25X objective (NA 1.10, Nikon), which was controlled by the ImSpector software (LaVision Biotec). A MaiTai Ti: sapphire laser (Spectraphysics) was tuned to 780 nm for excitation of the fluorophores. To perform four – dimensional

analysis of cell behaviour, a 250 x 250 µm field of view with z-steps of 4 µm spacing was recorded every 20 s for 20 - 30 min. Vivofollow software allowed a continuous drift offset correction in real time using fine pattern matching during two-photon microscopy imaging (Vladymyrov *et al.*, 2016). The cell migration analysis was performed by using Imaris 9.1.2 software (Bitplane). Median speeds, meandering index and turning angles (defined as the angle between the two velocity vectors before and after a measurement time point) were calculated from the (x,y,z) coordinates of the transferred B cell centroids. The arrest coefficient was calculated as the percentage per track a cell moved slower than 4 µm/min by using a custom script for Matlab (MathWorks) (Moalli *et al.*, 2014). The motility coefficient was calculated from slope of displacement against time$^{1/2}$.

2.14 Soluble ICAM1 and VCAM1 Complex Binding Assay

Either recombinant murine ICAM1-Fc fusion protein (R&D Systems; Biotechne) or recombinant murine VCAM1-Fc fusion protein (R&D Systems; Biotechne) were mixed with allophycocyanin-AffiniPure goat anti-human IgG (Jackson ImmunoResearch Laboratories, Inc.) in Hank's Balanced Salt Solution (HBSS) supplemented with 0.5% BSA to generate complexes of either ICAM1 or VCAM1 (scICAM1 or scVCAM1). Single cell suspensions of splenocytes were incubated at 37°C for 3 hours in AB IMDM supplemented with 5% FCS. The stimuli were diluted in HBSS + 0.5% BSA so that the final concentrations were: 10 µg/ml anti-IgM, 1 µg/ml CXCL13, and 2.5 mM $MnCl_2$ (Sigma-Aldrich; Merck KGaA). The rested splenocytes were mixed with either scICAM1 or scVCAM1. The mixture of cells and soluble complexes were stimulated at 37°C with each of the stimuli for the indicated time and then fixed with 4% PFA (Alfa Aesar; Thermo Fisher Scientific, Inc.) in PBS. The fixed samples were analysed using flow cytometry.

2.15 *In vivo* Homing Assay

Splenocytes from each genotype were labelled with either CFSE or CTV. The differently dyed splenocytes were then mixed at a 1:1 ratio and injected intravenously into C57BL/6J mice. The mice were sacrificed at the indicated time points and blood, lymph nodes and spleens were harvested. Single cell suspensions were prepared

and flow cytometry was used to determine the ratio of B cells in each organ of each genotype.

2.16 Cell Culture

Single cell suspensions of purified splenic B cells were prepared and cultured in DMEM+ medium at 37°C for the times indicated.

2.16.1 Survival and Activation Assay

Isolated splenic B cells were cultured in flat bottom 48-well plates (Corning, Inc.) at 10^6 cells/well. Cells were stimulated with either 200 ng/ml BAFF, 10 μg/ml anti-IgM, 1 μg/ml CD40L, 1 μg/ml CD40L and 100 ng/ml recombinant murine IL-4 (IL-4, Peprotech), 10 μg/ml LPS, 6 μg/ml class B CpG oligonucleotide – murine TLR9 ligand (ODN1826, InvivoGen), or 50 ng/ml phorbol-12-myristate-13-acetate (PMA, Sigma-Aldrich; Merck KGaA) and 500 ng/ml ionomycin (Sigma-Aldrich; Merck KGaA) at 37°C for 72 hours. The cells were then removed from the 48-well plate and transferred to a V-bottom 96-well plate, where the cells were subjected to centrifugation and the supernatants removed and stored at -80°C for further processing. The number of live cells in the culture was determined using flow cytometry and the HTS function on the cytometers to analyse the same proportion of each sample.

2.16.2 Proliferation Assay

Isolated splenic B cells were first labelled with cell proliferation dye eFluor™ 450 prior to preparation as in Section 0. If required, cells were incubated with either DMSO, 5 μM WNK463 or 10 μM bumetanide for 1 hour at 37°C. Then 0.5-1 x 10^6 cells/well were cultured in flat bottom 48-well plates at 37°C and the indicated stimuli were added. After 72 hours, the cells were removed from culture and the proliferation was assessed by the dilution of cell proliferation dye eFluor™ 450 as measured using flow cytometry.

2.16.3 Cell Surface Activation Marker Upregulation Assay

0.5-1 x 10^6 isolated splenic B cells per well were cultured in flat bottom 48-well plates and cells were stimulated with either anti-IgM or CD40L. The cells were incubated at 37°C for the indicated times, after which the cells were removed from culture. Flow cytometry was used to determine the levels of surface expression of indicated activation markers.

2.16.4 OT-II Antigen Presentation Assay

Splenic B cells were isolated using magnetic negative depletion with Phycoerythrin (PE)-conjugated antibodies against CD11b, CD11c, CD43 and Gr1 and anti-PE microbeads (Miltenyi Biotec) in line with the manufacturer's instructions. Naïve splenic and lymph node $CD4^+$ T cells from OT-II bone marrow chimeras were isolated using PE-conjugated antibodies against B220, CD8, CD11b, CD11c, CD25 and CD44. Biotin-SP AffiniPure $F(ab')_2$ fragment goat anti-mouse IgM (biotinylated anti-IgM, Jackson ImmunoResearch Laboratories, Inc.) was added to the B cells at a concentration of 2.5 mg/ml followed by ovalbumin (OVA) antigen delivery reagent (Miltenyi Biotec) according to manufacturer's instructions. T cells were labelled with CTV. Co-cultures of 2 x 10^5 B cells and 10^5 OT-II $CD4^+$ T cells were set up in 96-well U-bottom plates and incubated at 37°C for 72 hours. Flow cytometry was used to determine T cell proliferation by CTV dilution.

2.16.5 Eα Peptide Antigen Presentation Assay

0.2 μm Dragon Green streptavidin microspheres (Bangs Laboratories, 10 mg/ml) were washed twice with FACS buffer. Washed microspheres were incubated at 37°C for 1 hour with biotinylated anti-IgM at a final concentration of 1.38 μg/10^9 microspheres, and biotin-Eα peptide (Biotin-GSGFAKFASFEAQGALANIAVDKA-COOH, Crick Peptide Chemistry STP) at a range of concentrations: 2.76 μg/10^9 microspheres (high), 1.38 μg/10^9 microspheres (medium), 0.08 μg/10^9 microspheres (low) and No Eα. Conjugated microspheres were washed twice with FACS buffer before resuspending in DMEM+ at a bead concentration of 40 μg/ml. 1.3 x 10^6 isolated splenic B cells were incubated with 4 μg conjugated microspheres for 30 minutes at 37°C. After washing with DMEM+ approximately 0.2 x 10^6 cells were

incubated at 37°C in a U-bottom 96-well plate in duplicate: one for measurement of Eα, one for measurement of total MHC class II. After indicated time points, cells were fixed with 4% formaldehyde (Thermo Fisher Scientific, Inc.) for 40 minutes at room temperature. Eα on MHC class II and total MHC class II was determined using flow cytometry.

2.17 Luminex Cytokine Assay

Supernatants from activation assay from Section 2.16.1 were stored at -80°C until measurement. Procartaplex 4 Plex (Thermo Fisher Scientific, Inc.) was used to measure IL-6, IL-10, TNF-α and VEGF-A using Luminex based technology according to the manufacturer's instructions on Bio-Plex 200 (Bio-Rad Laboratories).

2.18 Antigen Internalisation Assay

Goat F(ab')$_2$ anti-mouse Igκ (Southern Biotech) was biotinylated with 20-fold molar excess of NHS-LC-LC-biotin (Thermo Fisher Scientific, Inc.) and labelled with Cy3 monoreactive dye pack (GE Healthcare) in sodium carbonate buffer (biotinylated anti-κ-Cy3). Excess dye was removed using Zeba 7K MWCO desalting columns (Thermo Fisher Scientific, Inc.). Single cell suspensions of splenocytes were incubated with biotinylated anti-κ-Cy3 for 30 minutes on ice. Samples were split into four and incubated at 37°C for the times indicated before fixation with 2% PFA on ice for 20 minutes. Cells were stained with fluorescently-labelled streptavidin to label antigen on the surface. Flow cytometry was used to determine the internalisation of antigen in B cells at time x using the following equation:

$$= \frac{\mathrm{gMFI(Streptavidin\ at\ 0\ minutes)} - \mathrm{gMFI(Streptavidin\ at\ x\ minutes)}}{\mathrm{gMFI(Streptavidin\ at\ 0\ minutes)}} * 100$$

2.19 Antigen Degradation Assay

Isolated splenic B cells were stimulated with biotinylated anti-IgM as in Section 2.7 for the times indicated. SDS-PAGE and transfer to a PVDF membrane was carried out as in Section 2.8. Membranes were probed with Streptavidin Alexa Fluor 680 conjugate (Thermo Fisher Scientific, Inc.) to detect biotinylated IgH and IgL from F(ab')$_2$ fragment.

2.20 Immunisation with NP-CGG

Mice were injected via the intraperitoneal route with 50 μg of either 4-hydroxy-3-nitrophenylacetyl (NP) – chicken gamma globulin (CGG) (BioSearch Technologies) or CGG (BioSearch Technologies) in 25% Alum (Thermo Fisher Scientific, Inc.) in PBS. The immune response was assessed by either withdrawing blood from superficial veins of the mouse tail or the mice were sacrificed at the required time points and spleens were used for further analysis.

2.21 Transfer of Antigen-Specific B Cells and Immunisation with HEL-SRBCs

Donor cells were isolated from spleens and labelled with CMFDA (Thermo Scientific) and then 10^6 cells were injected intravenously into B6.SJL mice. Hen egg lysozyme (HEL) was conjugated to sheep red blood cells (SRBCs, Patricell Ltd.; TCS Biosciences Ltd) using 521.6 mM *N*-(3-dimethylaminopropyl)-*N′*-ethylcarbodiimide (EDCI, Sigma-Aldrich; Merck KGaA) in conjugation buffer at 4°C for 30 minutes. Mice were injected with either 2 μg of HEL conjugated to 10^9 SRBCs in PBS or just 10^9 SRBCs alone in PBS. Mice were sacrificed at the indicated times.

2.22 ELISAs

2.22.1 Harvesting Serum

Blood harvested from the superficial tail vein was left to clot for at least 30 minutes before centrifugation at 17000 g for 10 minutes at room temperature. The supernatant was transferred to a new tube and centrifuged again at 17000 g for 10 minutes. Finally, the new supernatant was transferred to a new tube and stored at -80°C until the enzyme-linked immunosorbent assay (ELISA) was performed.

2.22.2 NP ELISA

96-well Maxisorp Immunoplates (Nalge Nunc International Corporation) were coated with 5 μg/ml NP_{20}-BSA (Santa Cruz Biotechnology, Inc.) overnight at 4°C and then washed five times with PBS + 0.01% Tween-20. Plates were blocked with 3% BSA in PBS for 2 hours at room temperature and washed twice. Serum was diluted

1:100 for IgM ELISA and 1:1000 for IgG1 ELISA before a serial 1:2 dilution was performed. Diluted sera was added to the coated plates and incubated overnight at 4°C, followed by washing three times. 1.6 μg/ml goat anti-mouse IgM biotin conjugated (CALTAG laboratories; Thermo Fisher Scientific, Inc.) and 4 μg/ml biotin-XX goat anti-mouse IgG1 (Invitrogen; Therrmo Fisher Scientific, Inc.) were added to their respective plates and incubated at room temperature for 2 hours. After washing three times, plates were incubated 1 μg/ml peroxidase labelled streptavidin (Vector Laboratories) for 2 hours at room temperature. Plates were washed five times before incubation with 1x TMB ELISA substrate solution (eBioscience; Thermo Fisher Scientific, Inc.) and the reaction was stopped with 2N H_2SO_4. Signals were quantified using absorption at 450 nm measurement wavelength on SpectraMax 190 (Molecular Devices LLC.). Data was analysed on Microsoft Excel and GraphPad Prism 8 (GraphPad). Only values in the linear portion of the response curve were used to calculate arbitrary values (a.u.) for serum concentrations of NP-specific antibodies.

2.22.3 BAFF ELISA

Serum concentration of BAFF was determined using Mouse BAFF ELISA Kit (Abcam) and was carried out according to manufacturer's specification. Serum was diluted 1:100. Signals were quantified using absorption at 450 nm measurement wavelength on SpectraMax 190. A standard curve was used to determine concentration of BAFF in the serum. Data was analysed on Microsoft Excel and GraphPad Prism 8.

2.23 Statistical Analysis

A Mann-Whitney U-test or a two-way ANOVA were used to determine statistical significance of differences between groups using GraphPad Prism 8. Mann-Whitney U-tests were used compare between different genotypes or conditions, where data had low n values that normality could not be determined or data was shown to not be normally distributed (calculated in GraphPad Prism 8). Two-way ANOVAs were used to compare different conditions over time to determine if there was an effect of genotype over time. Differences with $p < 0.05$ were considered significant.

2.24 Solutions, Buffers and Media

Table 5 List of Solutions, Media and Buffers Used

Solution	Composition
AB IMDM	35.9 mM NaCl, 179 mM Penicillin, 171.9 mM Streptomycin, IMDM powder in dH_2O, adjusted to pH 7.2, sterilised by membrane filtration
ACK lysis buffer	155 mM NH_4Cl, 10 mM $KHCO_3$, 0.1 mM Na_2EDTA
CAPS buffer	3.78 mM CAPS (3-[cyclohexylamino]-1-propanesulphonic acid) in dH_2O, pH 11.0
Conjugation buffer	PBS, 0.35 M mannitol, 0.01 M NaCl
DMEM+	DMEM (Gibco; Thermo Fisher Scientific, Inc.), 100 μM non-essential amino acids (Gibco; Thermo Fisher Scientific, Inc.), 20 mM HEPES buffer (Gibco; Thermo Fisher Scientific, Inc.), 10% FCS, 100 U/ml Penicillin (Sigma-Aldrich; Merck KGaA), 100 μg/ml Streptomycin (Sigma-Aldrich; Merck KGaA), 2 mM L-Glutamine (Sigma-Aldrich; Merck KGaA) and 100 μM 2-mercaptoethanol (Sigma-Aldrich; Merck KGaA).
FACS buffer	PBS, 0.1% NaN_3, 0.5% BSA
MACS buffer	PBS, 2 mM EDTA, 0.5% BSA
PBS	137 mM NaCl, 2.68 mM KCL, 8.10 mM Na_2HPO_4, 1.47 mM KH_2PO_4 in dH_2O
RIPA lysis buffer	50 mM Tris, 150mM NaCl, 50mM NaF, 5mM dithiothreitol (DTT), 2mM EDTA, 2mM $Na_4P_2O_7$, 1mM Na_3VO_4, 1% Triton X100, 0.5% deoxycholate, 0.1% SDS, 1mM PMSF 1x cOmplete EDTA-free protease inhibitor cocktail (Roche), 1x PhoStop (Roche)
SDS sample buffer	0.2 M Tris-HCl, 3% SDS, 10% glycerol, 3% 2-mercaptoethanol, 0.25% bromophenol blue, pH 6.8
Sodium carbonate buffer	15 mM Na_2CO_3, 85 mM $NaHCO_3$, pH 9.3

Chapter 3. Characterising WNK1 Function in Naïve B Cells

Previous work from our laboratory described the function of WNK1 in naïve $CD4^+$ T cells, where it was shown to be a negative regulator of adhesion to ICAM-1 and a positive regulator of migration *in vitro* and *in vivo* (Köchl *et al.*, 2016). No other published work has focussed on WNK1 in the immune system. To expand on this knowledge, I decided to examine the function of WNK1 in B cells. Initially, I investigated whether WNK1 is an active kinase in naïve B cells and if so, what cellular processes it regulates. In order to do this, I used mouse genetics as well as inhibitors of WNK1 and B cell signalling mediators.

3.1 *Wnk1* is Expressed in B cell Subsets

To first identify whether *Wnk1* is expressed in B cells, I used RNASeq data generated by Tiago Brazão from B cell subsets from C57BL/6J (WT) mice that were isolated by fluorescence-activated cell sorting (FACS) (Brazao *et al.*, 2016). The RNASeq data was analysed by Richard Mitter, such that transcript abundance was measured in transcripts per million (TPM). Of interest were the WNK-family members (*Wnk1*, *Wnk2*, *Wnk3* and *Wnk4*), targets of WNK1 (*Oxsr1* and *Stk39*) and members of the solute carrier family 12 (SLC12A) family of ion cotransporters (*Slc12a1*, *Slc12a2*, *Slc12a3*, *Slc12a4*, *Slc12a5*, *Slc12a6* and *Slc12a7*). Figure 3.1 shows that *Wnk1* was the only WNK-family member expressed across all the B cell subsets investigated (Figure 3.1A, B, C and D). In addition, *Oxsr1* was expressed in all B cell subsets, whereas *Stk39* was expressed in B cell populations in the bone marrow but not in B cell subsets in secondary lymphoid organs. This expression of *Stk39* was much lower than that of *Oxsr1* (Figure 3.1E and F). As with the WNK-family members, not all of the SLC12A family members were expressed in B cell subsets. *Slc12a1* and *Slc12a5* were not expressed in any B cell subsets tested (Figure 3.1G and K) and *Slc12a3* was only expressed in pro-B and pre-B cells but not in other B cell populations (Figure 3.1I). *Slc12a2*, *Slc12a4* and *Slc12a7* were expressed across B cell development and in mature B cell populations to a moderate level, with the exception of *Slc12a7* that had no expression in B1a cells (Figure 3.1H, J and M). Of all the members of the SLC12A family, *Slc12a6* was the most highly expressed with

TPM values approximately 10 times more than the other family members (Figure 3.1L).

In summary, *Wnk1* and the downstream effectors *Oxsr1*, *Slc12a2*, *Slc12a4*, *Slc12a6* and *Slc12a7* are expressed in all B cell subsets, including mature naïve B cell subsets in the spleen.

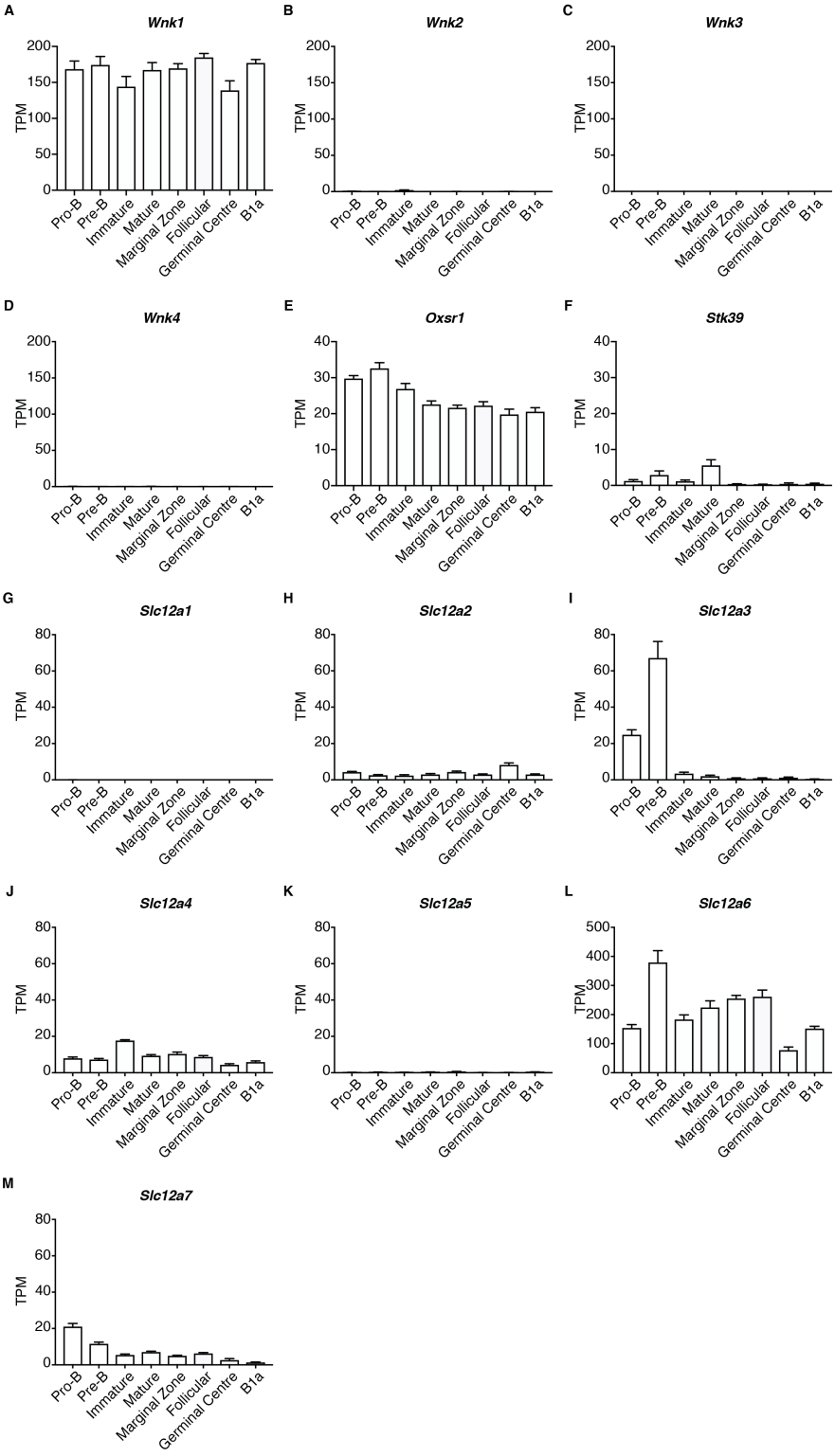

Figure 3.1 Expression of WNK1 and related genes

Bar graphs showing mean ± S.E.M. expression of genes *Wnk1* (**A**), *Wnk2* (**B**), *Wnk3* (**C**), *Wnk4* (**D**), *Oxsr1* (**E**), *Stk39* (**F**), *Slc12a1* (**G**), *Slc12a2* (**H**), *Slc12a3* (**I**), *Slc12a4* (**J**), *Slc12a5* (**K**), *Slc12a6* (**L**), *Slc12a7* (**M**) in different B cell populations. Pro-B, Pre-B, immature and mature B cells were sorted using FACS from bone marrow, marginal zone, follicular and germinal centre B cells from spleen, and B1a cells from the peritoneal cavity. Expression is measured as transcripts per million (TPM) (n=5), (Brazao *et al.*, 2016).

3.2 Analysis of WNK1 Activity in Naïve B Cells Downstream of CXCR5 and BCR

3.2.1 OXSR1 is Phosphorylated in WT B Cells Upon Stimulation Through the BCR and CXCR5

WNK1 is activated downstream of CCR7 and the TCR leading to phosphorylation of OXSR1 (Köchl *et al.*, 2016). Thus, I investigated whether OXSR1 is phosphorylated upon stimulation of CXCR5 and the BCR. I purified B cells from spleens of WT mice by negative depletion. Representative flow cytometry plots of B cells purified in this manner can be seen in Figure 3.2A, showing that the purity of the isolated B cells was high (>90%). The isolated B cells were stimulated with either anti-IgM or CXCL13 and then lysed to measure relative OXSR1 phosphorylation by immunoblot. Both anti-IgM and CXCL13 induced phosphorylation of OXSR1 (Figure 3.2B and C) with CXCL13 being a more potent inducer of OXSR1 phosphorylation (~2.5-fold vs ~1.5-fold). Furthermore, the dynamics of OXSR1 phosphorylation differed between the stimuli, with peak of phosphorylation occurring 10 minutes after anti-IgM stimulation and 1-2 minutes following CXCL13 stimulation.

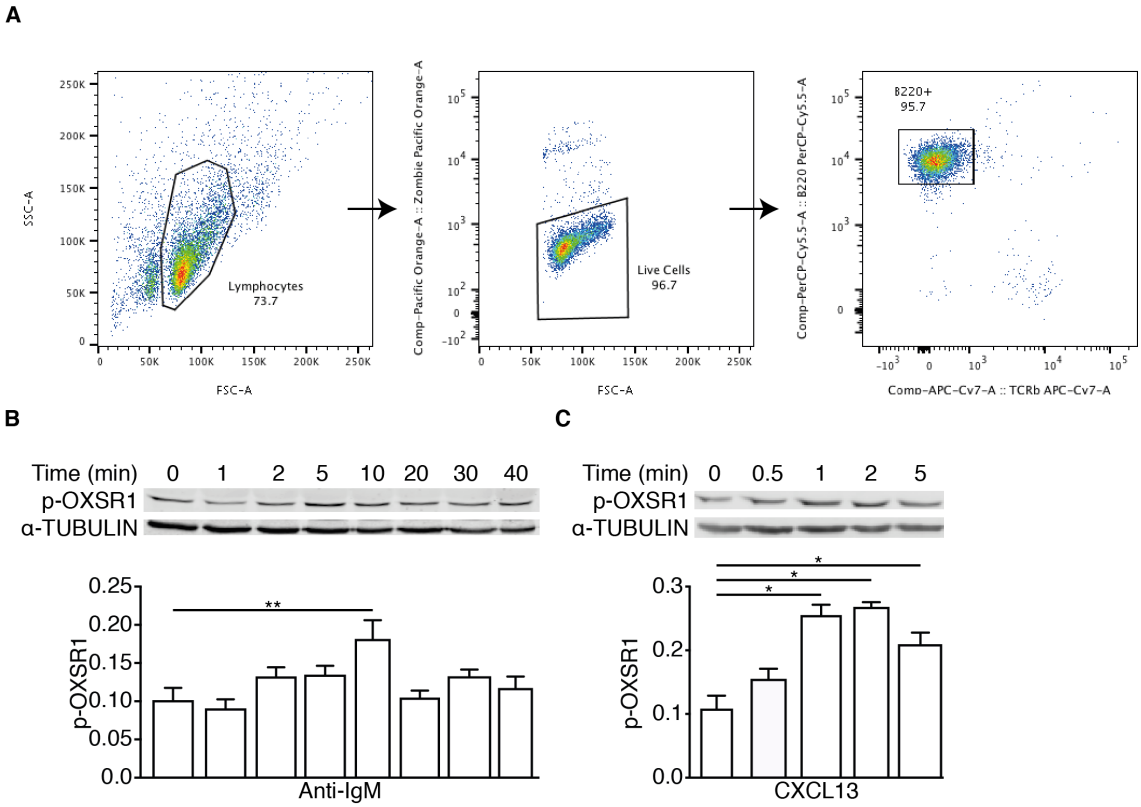

Figure 3.2 OXSR1 is phosphorylated downstream of BCR and CXCR5

(**A**) Representative flow cytometry plots showing purity of B cells after negative depletion from the spleen. Lymphocytes are gated based on forward and side scatter then dead cells are excluded based on low fluorescence of live-dead dye. B cells are identified by gating on $B220^{+}$ $TCR\beta^{-}$ cells. (**B**) Representative immunoblot of WT B cells stimulated with anti-IgM $F(ab)_2$ for the times shown and blotted with antibodies against p-OXSR1 and α-TUBULIN. Below is a bar graph showing the mean ± S.E.M. relative signal of p-OXSR1 at the different time points normalised to α-TUBULIN (n=8). (**C**) Representative immunoblot of WT B cells stimulated with recombinant murine CXCL13 for the times shown and blotted with antibodies against p-OXSR1 and α-TUBULIN. Below is a bar graph showing the mean ± S.E.M. relative signal of p-OXSR1 at the different time points normalised to α-TUBULIN (n=4). Statistical analysis was carried out using a Mann-Whitney U-test; * $p<0.05$, ** $p<0.01$.

3.2.2 Generation of WNK1 Knockout B Cells

Having established that OXSR1 was phosphorylated following BCR and CXCR5 stimulation, I tested whether this is dependent on WNK1. Since the constitutive knockout of *Wnk1* is embryonic lethal, a conditional knockout approach is required. To do this, I utilised the tamoxifen-inducible Cre-LoxP system. The DNA recombinase Cre is fused to a mutated oestrogen receptor that no longer binds oestrogen but retains the ability to bind tamoxifen. Heat shock protein 90 binds to the fusion protein causing retention in the cytoplasm. Upon addition of tamoxifen, heat shock protein 90 is released from the fusion protein allowing translocation of the fusion protein to the nucleus, where it can excise "floxed" regions of DNA. A schematic of the floxed *Wnk1* allele can be seen in Figure 3.3A (Xie *et al.*, 2009). Exon 2 encodes a portion of the kinase domain and its deletion leads to a frameshift from 0 to 2, generating a premature stop codon. To restrict the deletion of *Wnk1* to haematopoietic cells, I generated bone marrow chimeras. Sub-lethally irradiated *Rag1*$^{-/-}$ mice were reconstituted with bone marrow from either *Wnk1*$^{fl/+}$ *Rosa26*^{CreERT2} or *Wnk1*$^{fl/-}$ *Rosa26*^{CreERT2} mice. Henceforth, these chimeric mice are referred to as *Wnk1*$^{fl/+}$ RCE and *Wnk1*$^{fl/-}$ RCE mice respectively. After reconstitution of the haematopoietic system, the chimeras were injected with tamoxifen on 3 consecutive days via the intraperitoneal route. Seven days after initial injection, the mice were culled and organs were harvested for analysis.

To check the efficiency of deletion of exon 2 of *Wnk1*, I isolated B cells from spleens from either *Wnk1*$^{fl/+}$ RCE or *Wnk1*$^{fl/-}$ RCE mice that had been treated with tamoxifen. RNA was extracted from these cells and cDNA was made using a reverse transcription reaction. The cDNA was then used in a qPCR reaction to determine relative expression of the junctions between exon 1 and 2, and exon 5 and 6 of *Wnk1* compared to the expression of *Hprt*. There was efficient deletion of exon 2 of *Wnk1* in *Wnk1*$^{fl/-}$ RCE mice as there was approximately 4% expression when compared to the control *Wnk1*$^{fl/+}$ RCE mice (Figure 3.3B). However, there was not complete loss of *Wnk1* transcripts as there was approximately 55% expression of exons 5 and 6 of *Wnk1* (Figure 3.3C). I was unable to test loss of WNK1 protein as all WNK1 antibodies available for immunoblot were not able to show a clear signal of WNK1 in lymphocytes from WT mice (testing carried out by Robert Köchl, Lesley Vanes and

Harald Hartweger). Thus, this shows that tamoxifen treatment of *Wnk1*$^{fl/-}$ RCE mice gives rise to B cells with little or no expression of WT *Wnk1* mRNA.

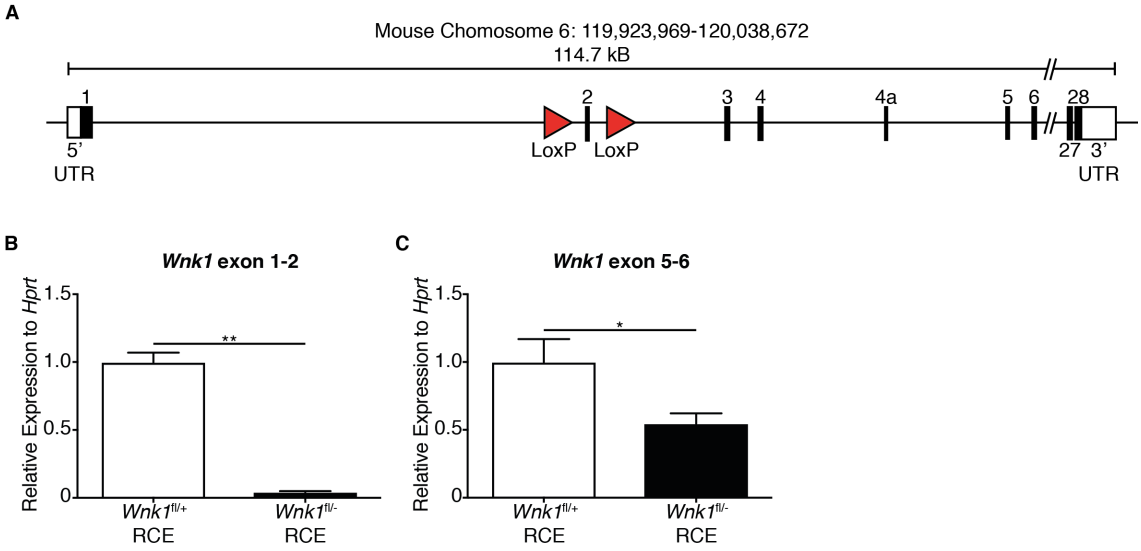

Figure 3.3 Deletion of Exon 2 of *Wnk1* in B Cells

(**A**) Schematic of floxed *Wnk1* allele showing LoxP sites either side of exon 2 of *Wnk1*. (**B**) Bar graph displaying the mean ± S.E.M. relative expression of the junction between exon 1 and exon 2 of *Wnk1* mRNA in B cells normalised to levels of *Hprt* mRNA (n=6). (**C**) Bar graph displaying the mean ± S.E.M. relative expression of the junction between exon 5 and exon 6 of *Wnk1* mRNA in B cells normalised to levels of *Hprt* mRNA (n=6). Statistical analysis was carried out using a Mann-Whitney U-test; * $p<0.05$, ** $p<0.01$.

3.2.3 Generation of B cells expressing Kinase-Dead *Wnk1* Allele

To assess the role of the kinase function of *Wnk1*, I also generated B cells that carry a *Wnk1* allele with a kinase inactivating mutation (D368A) (Köchl *et al.*, 2016). *Wnk1*$^{fl/+}$ *Rosa26*^{CreERT2} and *Wnk1*$^{fl/D368A}$ *Rosa26*^{CreERT2} mice were then used as donors for bone marrow chimeras which are referred from now on as *Wnk1*$^{fl/+}$ RCE and *Wnk1*$^{fl/D368A}$ RCE mice. The chimeras were injected with tamoxifen as before to induce excision of exon 2 in the floxed allele, resulting in the expression of a wild-type or a kinase-dead allele. Seven days after initial tamoxifen injection the mice were culled and organs were harvested.

3.2.4 Phosphorylation of OSXR1 in B Cells is Dependent on WNK1 and its Kinase Activity

To determine whether the phosphorylation of OXSR1 in B cells downstream of the BCR and CXCR5 is dependent on WNK1, I performed immunoblots as before with B cells from *Wnk1*$^{fl/+}$ RCE and *Wnk1*$^{fl/-}$ RCE mice stimulated with anti-IgM or CXCL13. Figure 3.4A and B show that OXSR1 phosphorylation was dependent on WNK1 as the relative phosphorylation was strongly decreased in *Wnk1*$^{fl/-}$ RCE B cells compared to control B cells and did not increase upon stimulation.

To assess whether the kinase activity of WNK1 is required for the phosphorylation of OXSR1, I immunoblotted *Wnk1*$^{fl/+}$ RCE and *Wnk1*$^{fl/D368A}$ RCE B cells after anti-IgM or CXCL13 stimulation. Figure 3.4 C and D show that the phosphorylation of OXSR1 was lower in *Wnk1*$^{fl/D368A}$ RCE B cells compared to the control B cells and again did not increase after stimulation.

In addition to these genetic approaches, I also used an inhibitor of WNK family kinases called WNK463 (Yamada *et al.*, 2016). Due to their unique kinase domains, the WNK463 inhibitor has a high specificity for WNK family members. Based on an *in vitro* kinase activity screen carried out on 140 kinases by the Medical Research Council Protein Phosphorylation and Ubiquitylation Unit (MRC PPU, http://www.kinase-screen.mrc.ac.uk/kinase-inhibitors), the only 2 kinases whose activity was inhibited more than 50% by WNK463, were WNK1 and dual specificity tyrosine-phosphorylation-regulated kinase 2 (DYRK2), with the inhibition of WNK1 being >90% (Figure 3.5A). Thus, WNK463 appears to be very selective with limited off target activity.

I tested the ability of WNK463 to inhibit the phosphorylation of OXSR1 induced by CXCL13 stimulation at different concentrations. Figure 3.5B shows that WNK463 blocked the phosphorylation of OXSR1 at a range of concentrations (1-10μM). Treatment of B cells with WNK463 at 5μM blocked phosphorylation of OXSR1 after stimulation with both anti-IgM (Figure 3.5C) and CXCL13 (Figure 3.5D), consistent with the results in B cells deficient in WNK1 or expressing a kinase inactive WNK1.

Together these data show that WNK1 and WNK1 kinase function is required in B cells to induce phosphorylation of OXSR1 downstream of BCR or CXCR5 stimulation.

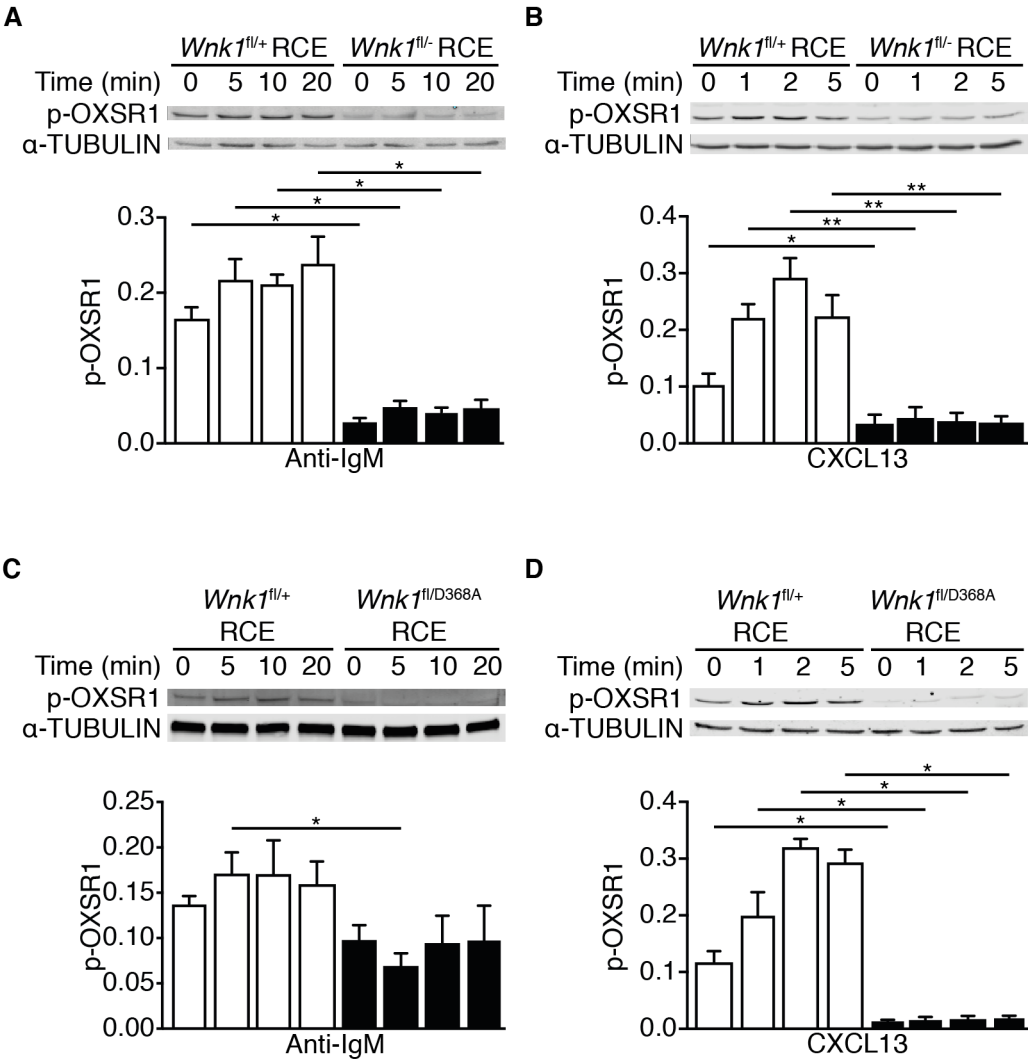

Figure 3.4 Phosphorylation of OXSR1 is Dependent on WNK1 and its Kinase Activity

(**A, B**) Representative immunoblots of B cells from *Wnk1*$^{fl/+}$ RCE and *Wnk1*$^{fl/-}$ RCE mice stimulated with anti-IgM F(ab)$_2$ (A) or recombinant murine CXCL13 (B) for the times shown and blotted with antibodies against p-OXSR1 and α-TUBULIN. Below is a bar graph showing the mean ± S.E.M. relative signal of p-OXSR1 normalised to α-TUBULIN at the different time points (n=4 or 5 for anti-IgM or CXCL13 respectively). (**C, D**) Representative immunoblots of B cells from *Wnk1*$^{fl/+}$ RCE and *Wnk1*$^{fl/D368A}$ RCE mice stimulated with anti-IgM F(ab)$_2$ (C) or recombinant murine CXCL13 (D) for the times shown and blotted with antibodies against p-OXSR1 and α-TUBULIN. Below is a bar graph showing the mean ± S.E.M. relative signal of p-OXSR1 normalised to α-TUBULIN at the different time points (n=5). Statistical analysis was carried out using a Mann-Whitney U-test; * p<0.05, ** p<0.01.

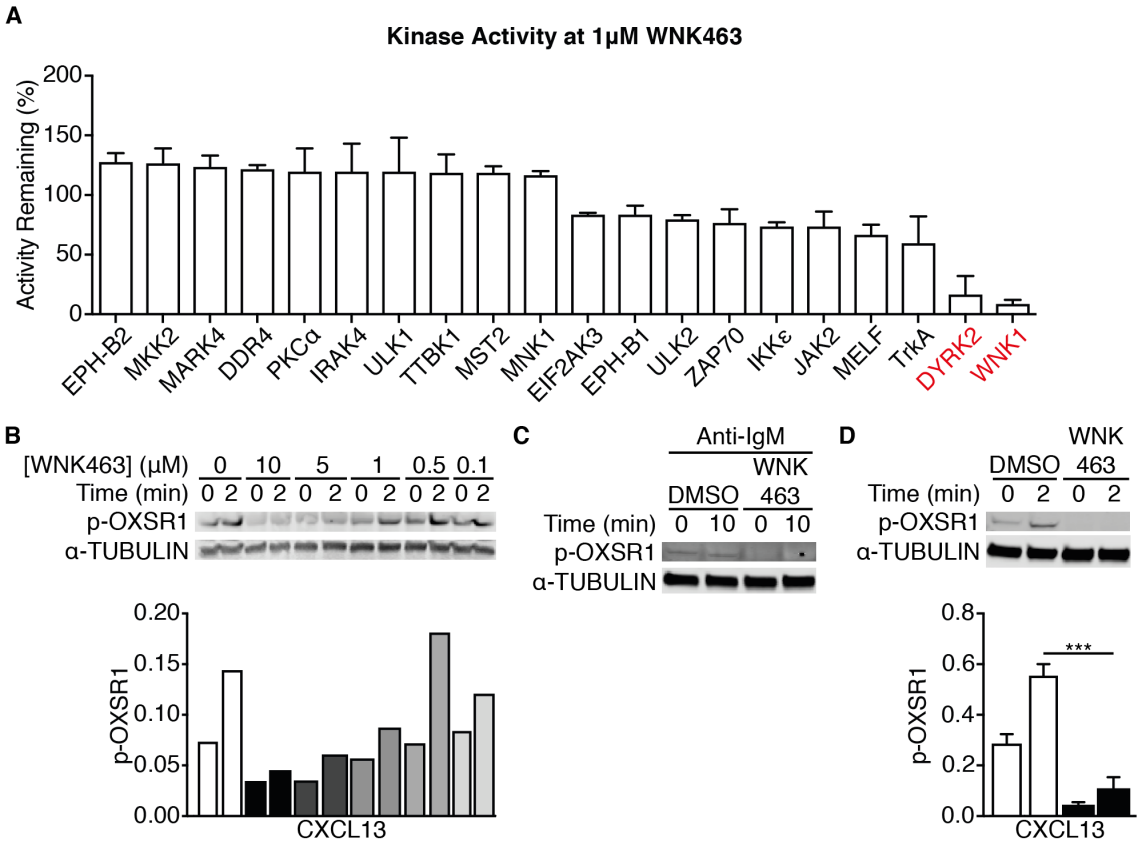

Figure 3.5 Phosphorylation of OXSR1 is inhibited by WNK463

(**A**) Bar graph showing the mean ± S.D. kinase activity of kinases incubated with 1μM WNK463 in an *in vitro* screen carried out by the MRC PPU on 140 kinases (http://www.kinase-screen.mrc.ac.uk/kinase-inhibitors). Only kinases with the highest and lowest activities (10 of each) are displayed. Highlighted in red are kinases whose activity was inhibited by more than 50%. (**B**) Immunoblot of WT B cells incubated with different concentrations of WNK463 and then stimulated with recombinant murine CXCL13 for 2 minutes and blotted with antibodies against p-OXSR1 and α-TUBULIN. Below is a bar graph showing the relative signal of p-OXSR1 normalised to α-TUBULIN for each sample (n=1). (**C**) Representative immunoblot of WT B cells incubated with 5μM WNK463 or vehicle alone (DMSO) and then stimulated with anti-IgM $F(ab)_2$ for 10 minutes and blotted with antibodies against p-OXSR1 and α-TUBULIN (n=7). Quantification of anti-IgM stimulated samples was not possible due to low signal and white background leading to negative values. (**D**) Representative immunoblot of WT B cells incubated with 5μM WNK463 or vehicle alone (DMSO) and then stimulated with recombinant murine CXCL13 for 2 minutes and blotted with antibodies against p-OXSR1 and α-TUBULIN. Below is a bar graph showing mean ± S.E.M. relative signal of p-OXSR1 normalised to α-TUBULIN at the different times (n=7). Statistical analysis was carried out using a Mann-Whitney U-test; *** $p<0.001$.

3.2.5 Phosphorylation of OXSR1 is Dependent on PI3K and AKT Activity

Previous work from our laboratory showed that WNK1 activity is regulated by PI3K and AKT downstream of the TCR and CCR7 (Köchl *et al.*, 2016). To test whether this is the case in B cells after being stimulated through the BCR and CXCR5, I stimulated splenic B cells purified from WT mice with anti-IgM or CXCL13 in the presence of either a PI3K inhibitor (PI-103) or an AKT inhibitor (MK2206). When B cells are stimulated with CXCL13 in the presence of either PI-103 or MK2206, there was a block in the phosphorylation of OXSR1 (Figure 3.6A). However, this block in phosphorylation was not as clear when the B cells are stimulated with anti-IgM. There is a significant decrease in OXSR1 phosphorylation when anti-IgM stimulated cells are incubated with PI-103 and a trend for a decrease when they are incubated with MK2206 (Figure 3.6B). The inhibitors of PI3K and AKT were shown to be working by the decrease in phosphorylation of AKT and proline-rich AKT substrate of 40 kDa (PRAS40) (Figure 3.6A and B).

These data show that in B cells the WNK1-dependent phosphorylation of OXSR1 is also dependent kinase activity of PI3K and AKT, suggesting that PI3K and AKT are intermediate regulators of OXSR1 phosphorylation connecting the BCR or CXCR5 signalling to WNK1.

In summary, I have shown that WNK1 is an active kinase in B cells and that I can efficiently disrupt *Wnk1* to assess its function in B cell biology. Upon stimulation through either the BCR or CXCR5, OXSR1 is phosphorylated, and this is dependent on WNK1 and its kinase activity. In addition, this phosphorylation event is dependent on kinase function of PI3K and AKT.

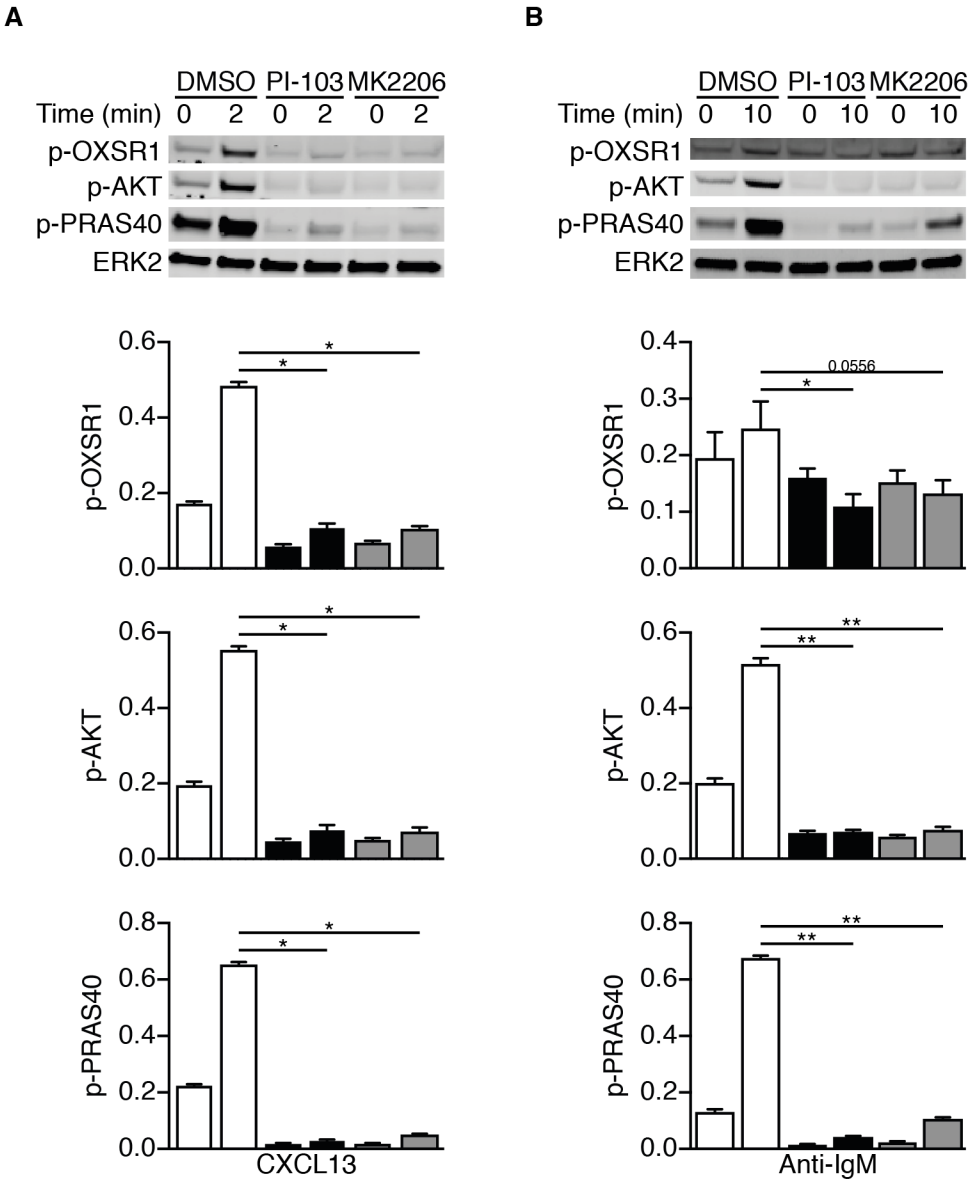

Figure 3.6 OXSR1 Phosphorylation is Regulated by PI3K and AKT

(**A**) Representative immunoblot of WT B cells incubated with either 1μM PI-103 or 2μM MK2206 or vehicle alone (DMSO) and then stimulated with recombinant murine CXCL13 for 2 minutes and blotted with antibodies against p-OXSR1, p-AKT, p-PRAS40 and ERK2. Below are bar graphs showing mean ± S.E.M. relative signal of p-OXSR1, pAKT and pPRAS40 (all normalised to ERK2) from cells incubated with the different inhibitors (n=4). (**B**) Representative immunoblot of WT B cells incubated with either 1μM PI-103 or 2μM MK2206 or vehicle alone (DMSO) and then stimulated with anti-IgM $F(ab)_2$ for 10 minutes and blotted with antibodies against p-OXSR1, p-AKT, p-PRAS40 and ERK2. Below are bar graphs showing mean ± S.E.M. relative signal of p-OXSR1, pAKT and pPRAS40 (all normalised to ERK2) from cells incubated with the different inhibitors (n=5). Statistical analysis was carried out using a Mann-Whitney U-test; * $p<0.05$, ** $p<0.01$.

3.3 Analysis of the Role of the WNK1 Pathway in B Cell Adhesion

3.3.1 WNK1 Regulates LFA-1-Dependent Adhesion Through Its Kinase Activity

Previous work showed that WNK1 is a negative regulator of $CD4^+$ T cell adhesion to ICAM-1 (Köchl *et al.*, 2016). Therefore, it seemed logical to test whether this is also true in B cells, since the signalling pathways regulating LFA-1 are similar in B and T cells. To do this, I investigated the binding of soluble complexes of ICAM-1 (scICAM-1) to B cells stimulated with anti-IgM, CXCL13 and $MnCl_2$ (Figure 3.7A). When the binding of scICAM1 is compared between B cells from *Wnk1*$^{fl/+}$ RCE and *Wnk1*$^{fl/-}$ RCE mice, it is clear that *Wnk1*$^{fl/-}$ RCE B cells bound more scICAM-1 when stimulated through the BCR or CXCR5, or if LFA-1 is switched to a high affinity state by $MnCl_2$ (Figure 3.7B).

To determine whether the kinase function of WNK1 is required for its role as a negative regulator of B cell adhesion to ICAM-1, I repeated the experiment with splenocytes from *Wnk1*$^{fl/D368A}$ RCE mice. Figure 3.7C shows that *Wnk1*$^{fl/D368A}$ RCE B cells displayed the same hyperadhesive phenotype as *Wnk1*$^{fl/-}$ RCE B cells. Of interesting note is that unstimulated *Wnk1*$^{fl/-}$ and *Wnk1*$^{fl/D368A}$ B cells bound more ICAM-1 than their controls. These data suggest that WNK1 is a negative regulator of ICAM-1 binding to B cells, in both stimulated and unstimulated states, and that the kinase activity of WNK1 is required for this function.

The difference in ICAM-1 binding could be due to differences in receptor levels on the surface of naïve B cells when *Wnk1* is deleted. I measured the levels of CXCR5, IgM and CD11a (α_L subunit of LFA-1) using flow cytometry. WNK1 knockout B cells had a little more CD11a, less CXCR5 and no difference in levels of IgM on their surface compared to control B cells (Figure 3.7D). The increase in CD11a on the surface could explain the difference in ICAM-1 binding in unstimulated cells but is insufficient to explain the difference between *Wnk1*$^{fl/+}$ RCE and *Wnk1*$^{fl/-}$ RCE B cells when stimulated with anti-IgM, CXCL13 or $MnCl_2$.

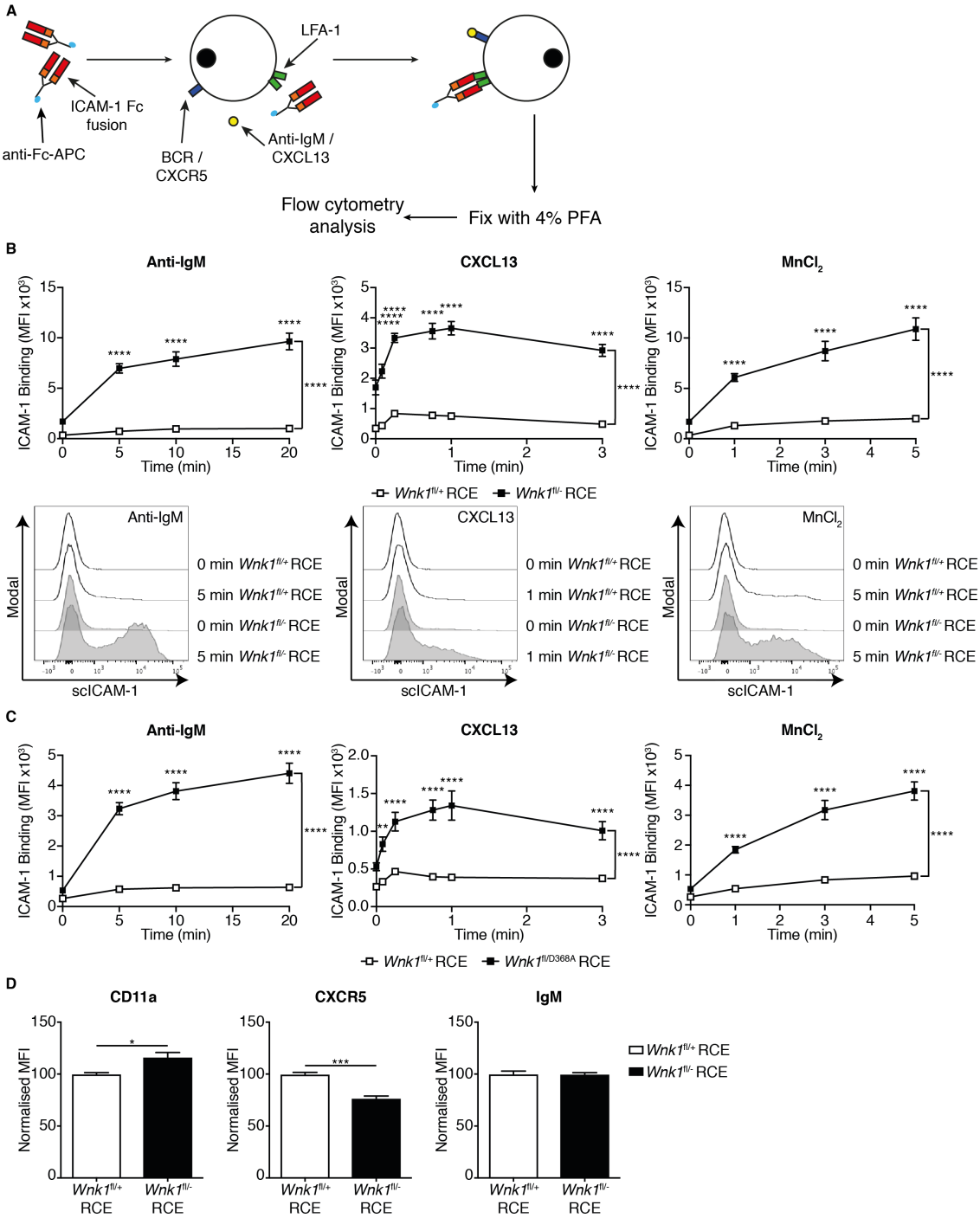

Figure 3.7 WNK1 is a Negative Regulator of ICAM-1 Binding in B cells Through its Kinase Domain

(**A**) Schematic of scICAM-1 binding assay. ICAM-1 Fc fusion proteins were mixed with anti-Fc antibodies labelled with APC to generate scICAM-1. scICAM-1 was mixed with splenocytes that were then stimulated to induce affinity and avidity changes in LFA-1. After given time points the splenocytes were fixed using PFA and ICAM-1 binding was measured on B cells using flow cytometry. (**B**) Line graphs showing mean ± S.E.M. mean fluorescent intensity (MFI) of APC on B220^{+} cells from *Wnk1*$^{fl/+}$ RCE and *Wnk1*$^{fl/-}$ RCE mice after stimulation with anti-IgM, CXCL13 and $MnCl_2$ at the time points shown. Below are overlays of representative histograms of scICAM-1 (APC) in B cells from *Wnk1*$^{fl/+}$ RCE and *Wnk1*$^{fl/-}$ RCE mice after stimulation with anti-IgM, CXCL13 and $MnCl_2$ for the indicated times (n=11). (**C**) Line graphs showing mean ± S.E.M.

MFI of APC on B220^{+} cells from *Wnk1*$^{fl/+}$ RCE and *Wnk1*$^{fl/D368A}$ RCE mice after stimulation with anti-IgM, CXCL13 and $MnCl_2$ at the time points shown (n=6). (**D**) Bar graphs showing mean ± S.E.M. normalised MFI of CD11a, CXCR5 and IgM on the surface of *Wnk1*$^{fl/+}$ RCE and *Wnk1*$^{fl/-}$ RCE B cells. MFI was normalised to the average MFI on *Wnk1*$^{fl/+}$ RCE B cells, which was set to 100 (n=7). Statistical analysis was carried out using a two-way ANOVA with multiple comparisons (B and C) or a Mann-Whitney U-test (D); * $p<0.05$, ** $p<0.01$, *** $p<0.001$, **** $p<0.0001$. Asterisks outside bracket indicate significant differences between genotypes from the two-way ANOVA analysis. Asterisks above points indicate significant differences using multiple comparisons from the two-way ANOVA analysis.

3.3.2 NKCC1 does not Regulate LFA-1-Dependent Adhesion

As WNK1 is known to regulate ion homeostasis through SLC12A family members, I investigated whether ion homoeostasis regulated by the sodium potassium and chloride cotransporter, NKCC1, which is encoded by the gene *Slc12a2*, also regulated LFA-1-dependent adhesion. Although constitutive knockout of *Slc12a2* is not embryonic lethal, knockout mice have to be culled at an early age due to issues with balance and the inner ear. To circumvent this issue, I generated foetal liver chimeras by irradiating *Rag1*$^{-/-}$ mice and reconstituting them with either *Slc12a2*$^{+/+}$ or *Slc12a2*$^{-/-}$ foetal livers harvested from E14.5 embryos.

After reconstitution, I repeated the scICAM-1 binding experiment with B cells from *Slc12a2*$^{+/+}$ and *Slc12a2*$^{-/-}$ chimeras stimulated through the BCR, CXCR5 or treatment with $MnCl_2$. As shown in Figure 3.8, there was no difference in scICAM-1 binding between *Slc12a2*$^{+/+}$ and *Slc12a2*$^{-/-}$ B cells. This suggests that ion homeostasis through NKCC1 alone is not important for the regulation of LFA-1 binding to ICAM-1.

3.3.3 WNK1 Regulates VLA-4-Dependent Adhesion

To determine whether WNK1 regulates other integrins other than LFA-1 ($\alpha_L\beta_2$), I repeated the scICAM1 experiment but replaced ICAM-1-Fc fusion protein with VCAM-1-Fc. This tests the adhesion of B cells through VLA-4 ($\alpha_4\beta_1$) after the cells have been stimulated. As shown in Figure 3.9, WNK1-deficient B cells bound more VCAM-1 than control B cells after stimulation with anti-IgM and CXCL13. This shows that WNK1 is also a negative regulator of B cell adhesion through VLA-4.

In summary, I have revealed that WNK1 is a negative regulator of B cell adhesion to ICAM-1 and VCAM-1, and that the kinase function is required to regulate binding to ICAM-1. This regulation of LFA-1 activity is not mediated through NKCC1, suggesting that ion regulation may not be required for regulating adhesion through WNK1 or that there is compensation from other ion cotransporters. Such a possibility would require further investigation.

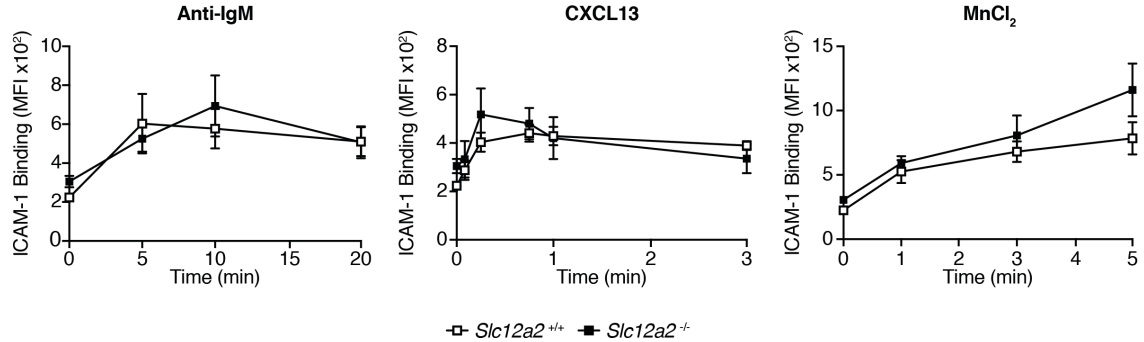

Figure 3.8 B Cell Adhesion to ICAM-1 is not Regulated by NKCC1

Line graphs showing mean ± S.E.M. MFI of APC on B220$^+$ cells from *Slc12a2*$^{+/+}$ and *Slc12a2*$^{-/-}$ foetal liver chimeras after stimulation with anti-IgM, CXCL13 and $MnCl_2$ at the time points shown (n=5-6). Statistical analysis was carried out using a two-way ANOVA with multiple comparisons.

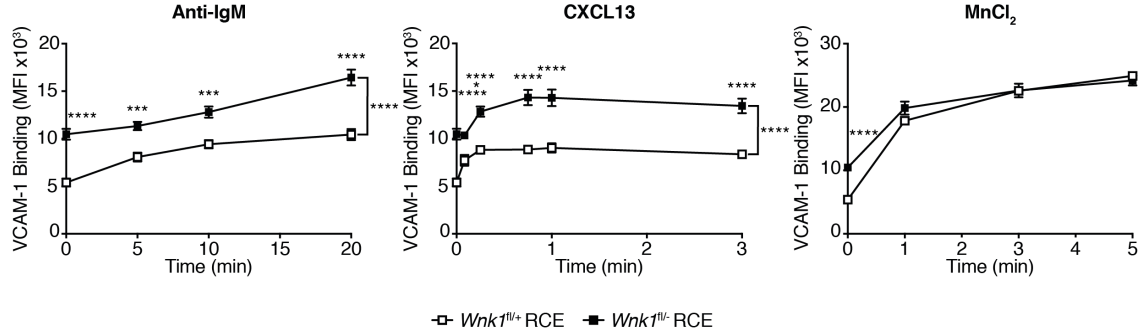

Figure 3.9 WNK1 is a Negative Regulator of B Cell Adhesion to VCAM-1

Line graphs showing mean ± S.E.M. MFI of APC on B220$^+$ cells from *Wnk1*$^{fl/+}$ RCE and *Wnk1*$^{fl/-}$ RCE mice after stimulation with anti-IgM, CXCL13 and $MnCl_2$ at the time points shown (n=6). Statistical analysis was carried out using a two-way ANOVA with multiple comparisons; * $p<0.05$, *** $p<0.001$, **** $p<0.0001$. Asterisks outside bracket indicate significant differences between genotypes from the two-way ANOVA analysis. Asterisks above points indicate significant differences using multiple comparisons from the two-way ANOVA analysis.

3.4 Analysis of the Role of WNK1 in B Cell Migration and Homing

3.4.1 Decreased Migration of WNK1-Deficient B Cells in Response to CXCL13

Since WNK1 has been shown to be a positive regulator of naïve $CD4^+$ T cell migration (Köchl *et al.*, 2016), I investigated whether it is also regulates migration of B cells. To do this, I carried out a Transwell assay with B cells from *Wnk1*$^{fl/+}$ RCE and *Wnk1*$^{fl/-}$ RCE mice in response to CXCL13. Figure 3.10A shows that B cells lacking WNK1 displayed a decreased ability to migrate through a Transwell with 5μm pores. WNK1-deficient B cells did migrate in response to CXCL13 stimulation but to a lesser extent than control B cells.

To measure the speed and displacement of the cells as they are migrating in response to CXCL13, I used microscopy to make videos of the cells migrating in an ICAM-1 coated microscope chamber. Figure 3.10B and C show that there was a reduction in mean speed and displacement in B cells in which *Wnk1* had been knocked out. Together these data demonstrate that WNK1 is a positive regulator of B cell migration after stimulation with CXCL13 *in vitro*.

3.4.2 Impaired Migration of WNK1-Deficient B Cells *in vivo*

To determine whether the *in vitro* migration defect in B cells lacking WNK1 translated to a defect *in vivo*, I collaborated with Sujana Sivapatham in Jens Stein's lab to assess the migration of *Wnk1*$^{fl/+}$ RCE and *Wnk1*$^{fl/-}$ RCE B cells *in vivo*. Intravital imaging of transferred B cells was used to assess the migration of B cells in follicles of lymph nodes. Figure 3.11 shows that WNK1-deficient B cells displayed a defect in migration in lymph node follicles as there is a decrease in mean speed (Figure 3.11A) and track straightness (Figure 3.11B), and an increase in arrest coefficient (Figure 3.11C) and median and lower quartile values of sphericity (Figure 3.11D). Arrest coefficient is the percentage per track a cell moved slower than 4μm/min. Taken together these phenotypes are consistent with WNK1 being a positive regulator of B cell migration *in vivo*.

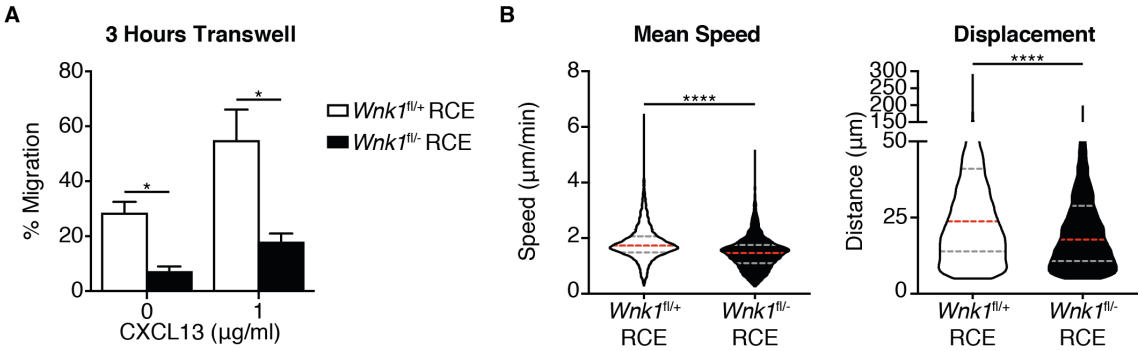

Figure 3.10 WNK1-Deficient B Cells Show Decreased Migration in Response to CXCL13

(**A**) Bar graph showing mean ± S.E.M proportion of *Wnk1*$^{fl/+}$ RCE and *Wnk1*$^{fl/-}$ RCE B cells that migrated through a Transwell membrane with 5µm pores after stimulation with recombinant murine CXCL13 for 3 hours at 37°C. (n=4-5). (**B**) Violin plot of mean speed or displacement with median (red) and upper and lower quartiles (grey) of B cells from *Wnk1*$^{fl/+}$ RCE and *Wnk1*$^{fl/-}$ RCE mice stimulated with 1µg/ml recombinant murine CXCL13 and migrating on the base of ICAM-1 coated chambers. CMFDA- or CTV-labelled cells were imaged using a wide-field microscope. Videos were analysed using TrackMate plugin of FIJI to calculate mean speed and displacement (n=5245-7289). Statistical analysis was carried out using a Mann-Whitney U-test; * p<0.05, **** p<0.0001.

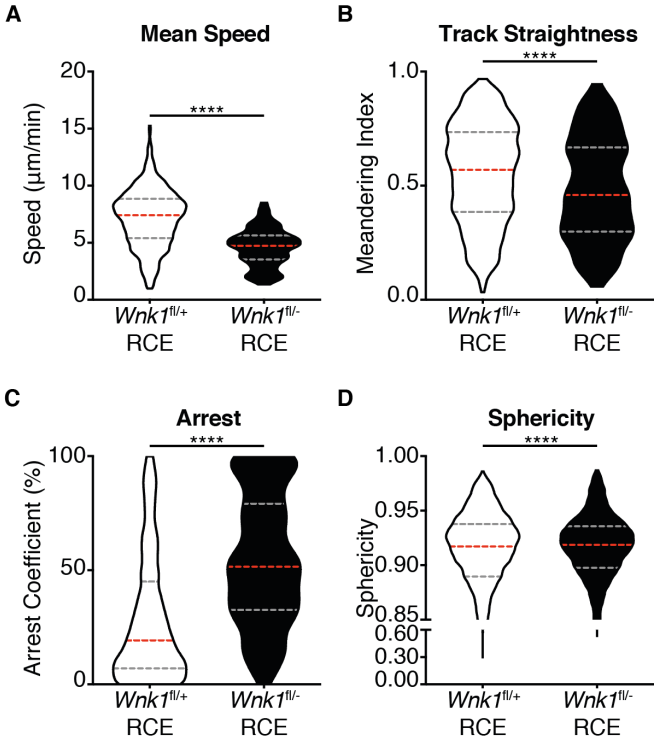

Figure 3.11 WNK1 regulates B Cell Migration *in vivo*

Work done by Sujana Sivapatham. Violin plots showing median (red), lower and upper quartiles (grey) of mean speed (**A**), meandering index (**B**), arrest coefficient (**C**) and sphericity (**D**) of B cells migrating in lymph nodes from intravital videos of labelled *Wnk1*$^{fl/+}$ RCE and *Wnk1*$^{fl/-}$ RCE B cells transferred into WT mice (n=5441-16196). Statistical analysis was carried out using a Mann-Whitney U-test; *** p<0.001, **** p<0.0001.

3.4.3 Decreased Homing of WNK1-Deficient B Cells to Secondary Lymphoid Organs

Since WNK1 has a role in B cell migration and adhesion, I measured the ability of B cells lacking *Wnk1* expression to home to secondary lymphoid organs (Figure 3.12A). 1 hour after transfer, the ratio of *Wnk1*$^{fl/-}$ RCE to *Wnk1*$^{fl/+}$ RCE B cells was reduced in the spleen and lymph nodes and is increased in blood (Figure 3.12B). This shows that there is a reduced ability of WNK1-deficient B cells to home from the blood into secondary lymphoid organs. To determine whether this defect persists over longer time points, I looked 24 hours after transfer of splenocytes. Figure 3.12C shows that there was a reduced ratio of *Wnk1*$^{fl/-}$ RCE to *Wnk1*$^{fl/+}$ RCE B cells in the blood, the spleen and lymph nodes. As there was a decrease in the ratio in all the compartments tested, it could be that WNK1-deficient B cells have a defect in survival or they were stuck in other compartments perhaps due to their increased adhesion.

In summary, I have shown that WNK1 is a positive regulator of B cell migration *in vitro* and *in vivo* as well as B cell homing to secondary lymphoid organs. It remains to be tested whether this is dependent on the kinase function of WNK1 and NKCC1 as has been previously shown in CD4$^+$ T cells (Köchl *et al.*, 2016).

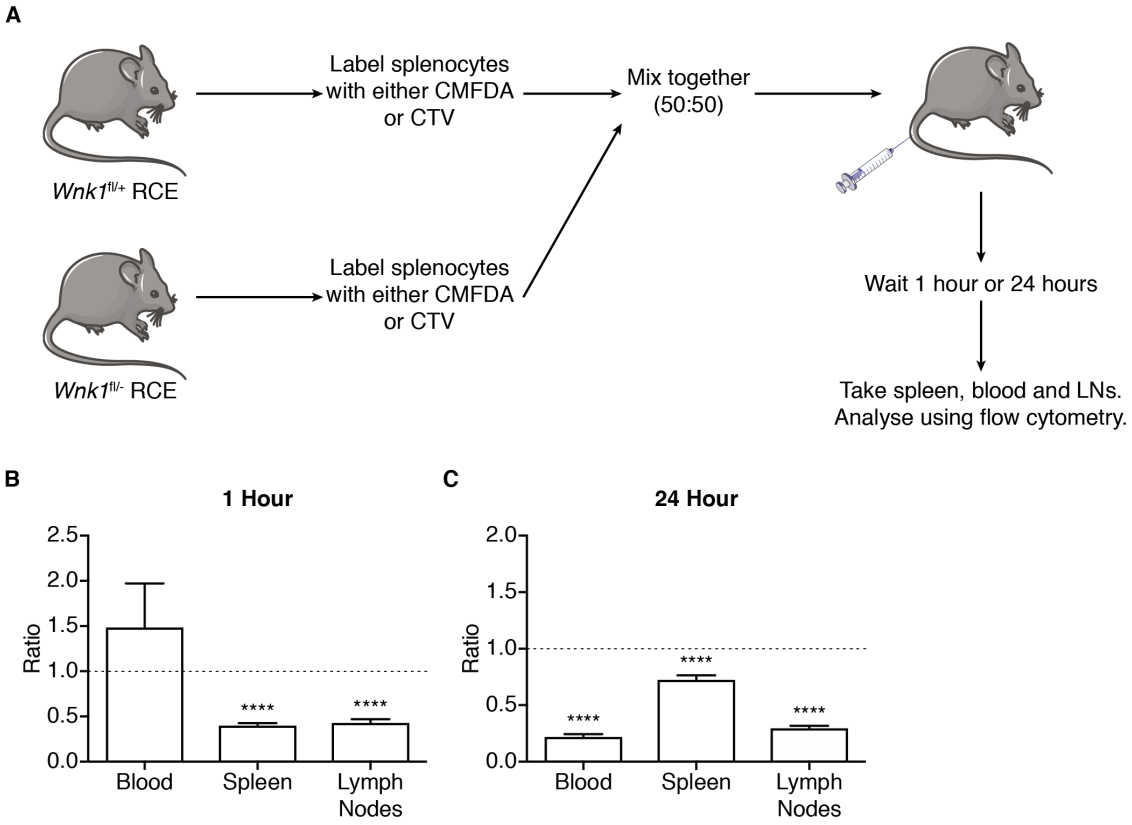

Figure 3.12 WNK1 Regulates B Cell Homing to Secondary Lymphoid Organs

(**A**) Schematic of *in vivo* homing assay. Labelled splenocytes from *Wnk1*$^{fl/+}$ RCE and *Wnk1*$^{fl/-}$ RCE mice were mixed together and intravenously injected into WT mice. After either 1 hour or 24 hours, the mice were culled and flow cytometry was used to determine ratio of *Wnk1*$^{fl/-}$ RCE to *Wnk1*$^{fl/+}$ RCE B cells in blood, spleen and lymph nodes. (**B**) Bar graph showing mean ± S.E.M. ratio of *Wnk1*$^{fl/-}$ RCE to *Wnk1*$^{fl/+}$ RCE B cells found in blood, spleen and lymph nodes from WT mice 1 hour after transfer (n=8). (**C**) Bar graph showing mean ± S.E.M. ratio of *Wnk1*$^{fl/-}$ RCE to *Wnk1*$^{fl/+}$ RCE B cells found in blood, spleen and lymph nodes from WT mice 24 hours after transfer (n=12). Statistical analysis was carried out using a one sample t-test; **** p<0.0001.

3.5 Regulation of B Cell Survival by WNK1

3.5.1 WNK1, WNK1 Kinase Activity and Phosphorylation of OXSR1, but not NKCC1, are Required for Survival and Development of B Cells

When purifying B cells from *Wnk1*$^{fl/+}$ RCE and *Wnk1*$^{fl/-}$ RCE mice, I noticed that there was reduced recovery of B cells from *Wnk1*$^{fl/-}$ RCE mice. To look into this further, I harvested bone marrow, spleen, peripheral lymph nodes and blood from *Wnk1*$^{fl/+}$ RCE and *Wnk1*$^{fl/-}$ RCE chimeras 7 days after initial tamoxifen injection and used flow cytometry to evaluate different B cell populations (Figure 3.13). When *Wnk1* was deleted, there was a rapid loss of B cells in all compartments examined (Figure 3.14A), with the exception of pro-B cells and plasma cells in the bone marrow. This shows that WNK1 regulates B cell survival and may regulate as well as B cell development. As these mice are chimeras made by irradiating *Rag1*$^{-/-}$ mice, I could not determine whether there was a developmental block at the pro-B cell stage or earlier as these cells are partly derived from the host mouse rather than the donor bone marrow. It is possible that the developmental block in *Wnk1*$^{fl/-}$ RCE mice is due to a defect in survival of progenitors such as CLP or HSC but further investigation is required to determine the function of WNK1 during B cell development.

To determine whether the kinase function of WNK1 is required to regulate B cell survival and/or development, Harald Hartweger repeated the experiment by harvesting bone marrow, spleen and lymph nodes from *Wnk1*$^{fl/+}$ RCE and *Wnk1*$^{fl/D368A}$ RCE chimeras 7 days after initial tamoxifen injection. Figure 3.14B shows that there was a trend for a decrease in the number of B cells found in secondary lymphoid organs in *Wnk1*$^{fl/D368A}$ RCE chimeras. There was a similar decrease in the number of developing B cell populations in the bone marrow when only a kinase-dead variant of WNK1 is expressed but not in pro-B and plasma cell numbers.

Harald Hartweger also made radiation foetal liver chimers from either *Oxsr1*$^{+/+}$ or *Oxsr1*$^{T185A/T185A}$ embryos. The *Oxsr1*^{T185A} knock-in allele encodes mutant OXSR1 that can no longer be phosphorylated by WNK1 and thus it cannot be activated in a WNK1-dependent manner. Analysis of B cell populations in these mice showed that there was a loss of B cells in all populations with the exception of pro-B cells (Figure

3.14C). Thus, OXSR1 phosphorylation is critical for generation and/or maintenance of B cell populations.

To investigate whether ion homeostasis regulated by NKCC1 regulates B cell survival and/or development *in vivo*, I repeated the experiment with *Slc12a2*$^{+/+}$ and *Slc12a2*$^{-/-}$ chimeras. As shown in Figure 3.14D, there was no difference in the number of B cells in the bone marrow and the spleen between *Slc12a2*$^{+/+}$ and *Slc12a2*$^{-/-}$ chimeras but an increase of naïve B cells in lymph nodes of *Slc12a2*$^{-/-}$ chimeras. These data indicate that NKCC1 by itself is not required to regulate B cell development or survival in the spleen, but it could act as a negative regulator of B cell survival in lymph nodes or a positive regulator of B cell localisation to lymph nodes.

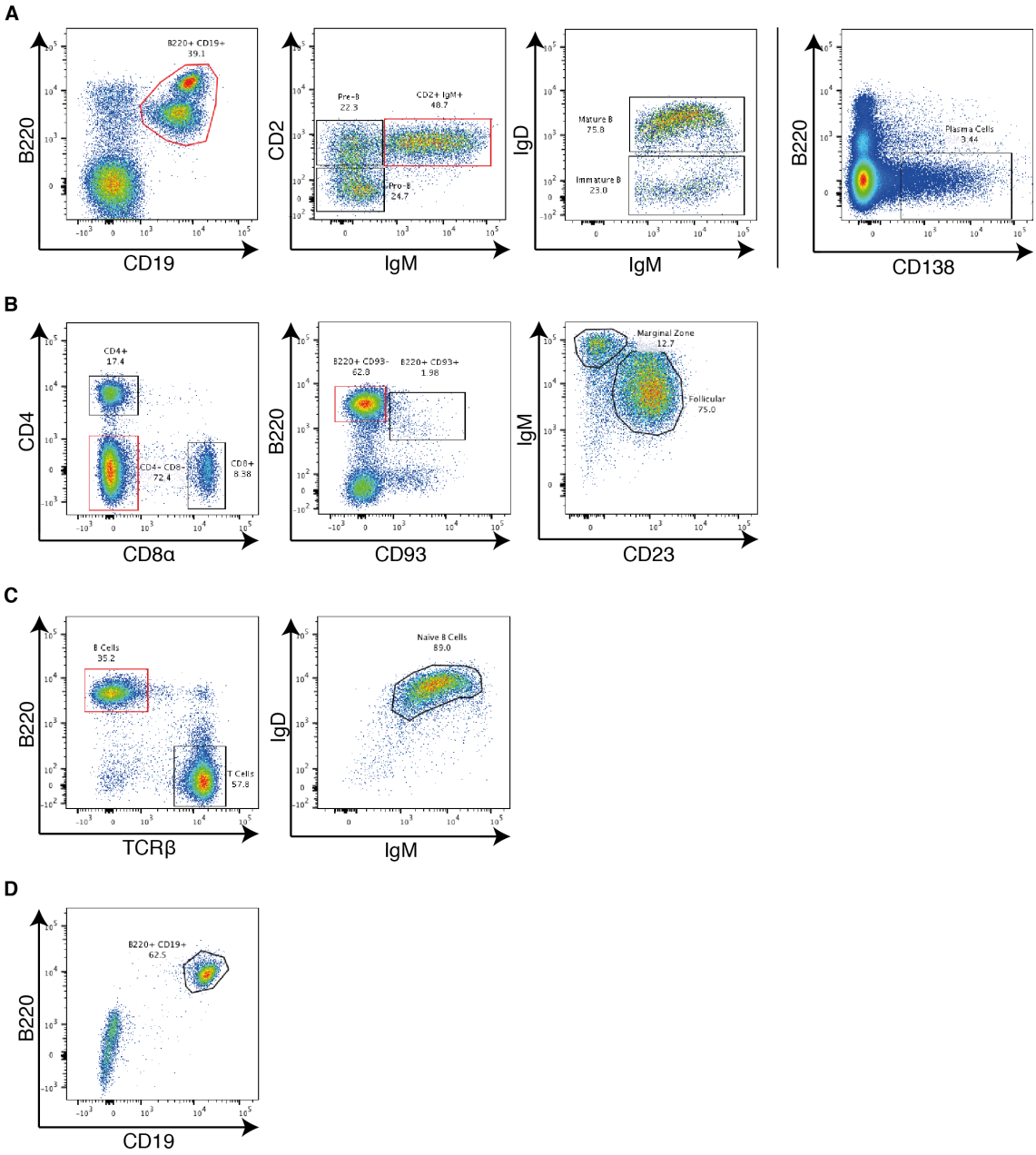

Figure 3.13 Flow Cytometry Gating for B Cell Populations

Representative flow cytometry plots for gating of B cell populations in the bone marrow (**A**), the spleen (**B**), lymph nodes (**C**) and blood (**D**). All samples were initially gated using a lymphocyte gate based on forward and side scatter, singlets and live cells. Red gates indicate populations that were used for gating in the plot to the right, the black line indicates start of new gating from live cells. (**A**) All B cells are defined by $B220^{+}CD19^{+}$, pro-B cells by $CD2^{-}IgM^{-}$, pre-B cells by $CD2^{+}IgM^{-}$, immature B cells by $CD2^{+}IgM^{+}IgD^{-}$, mature B cells by $CD2^{+}IgM^{+}IgD^{+}$, and plasma cells by $B220^{-}CD138^{+}$. (**B**) All mature B cells are defined by $CD4^{-}CD8\alpha^{-}B220^{+}CD93^{-}$ cells, follicular B cells by $CD23^{+}IgM^{med}$ and marginal zone B cells by $CD23^{-}IgM^{hi}$. (**C**) Naïve B cells in lymph nodes are defined by $B220^{+}IgM^{+}IgD^{+}TCR\beta^{-}$. (**D**) B cells in the blood are defined by $B220^{+}CD19^{+}$.

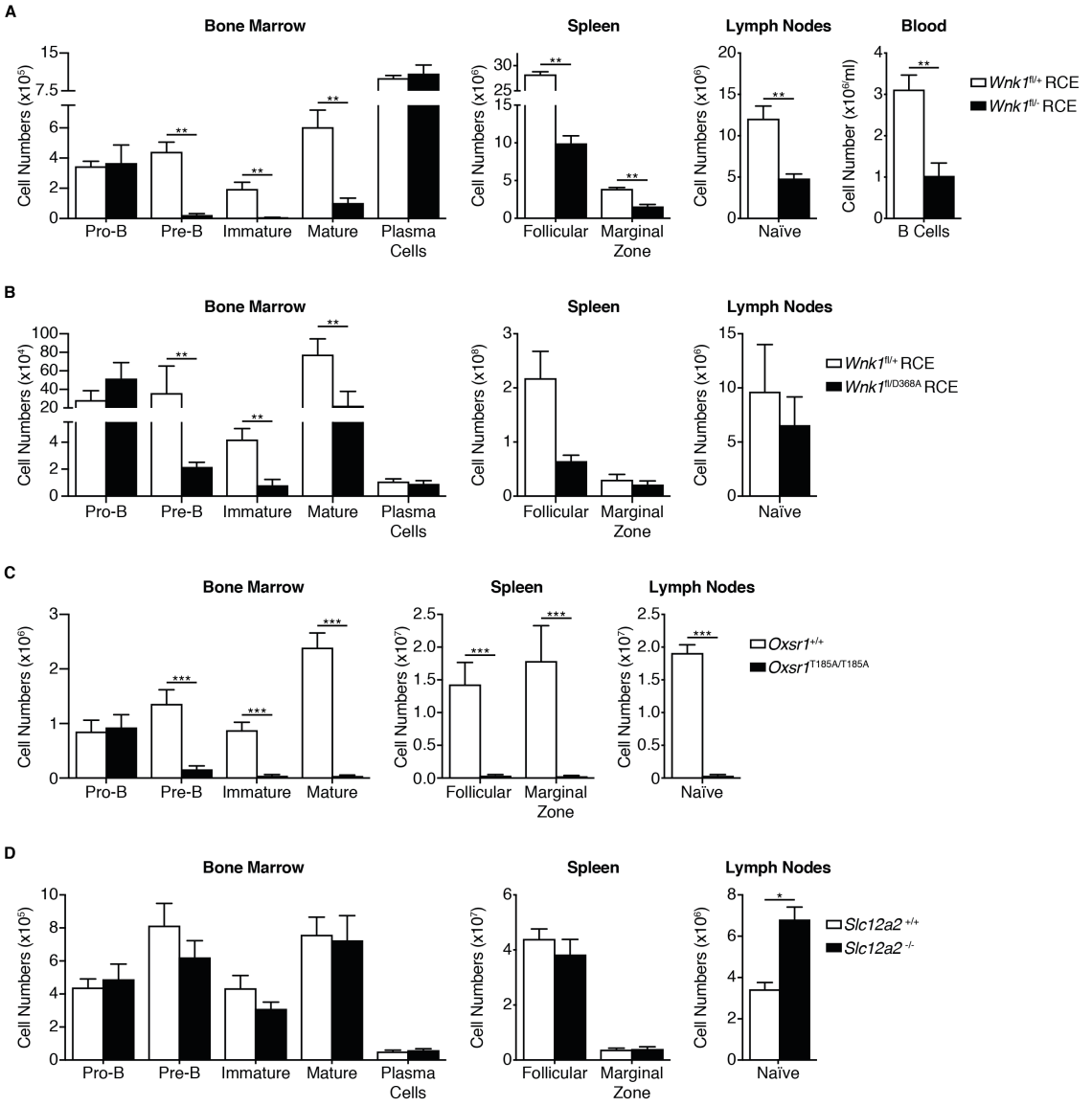

Figure 3.14 WNK1, its Kinase Function and OXSR1 Activation are Required for B Cell Survival but NKCC1 is not Required

(**A**) Bar graphs showing mean ± S.E.M. cell number of B cell populations found in the bone marrow, spleen, lymph nodes and blood in *Wnk1*$^{fl/+}$ RCE and *Wnk1*$^{fl/-}$ RCE mice that were defined using the gating strategy in Figure 3.13 (n=5; blood n=3-5). (**B**) Bar graphs showing mean ± S.E.M. cell number of B cell populations found in the bone marrow, spleen and lymph nodes in *Wnk1*$^{fl/+}$ RCE and *Wnk1*$^{fl/D368A}$ RCE mice that were defined using the gating strategy in Figure 3.13 (n=6). Data generated by Harald Hartweger. (**C**) Bar graphs showing mean ± S.E.M. cell number of B cell populations found in the bone marrow, spleen and lymph nodes in *Oxsr1*$^{+/+}$ and *Oxsr1*$^{T185A/T185A}$ chimeras that were defined using the gating strategy in Figure 3.13 (n=8). Data generated by Harald Hartweger. (**D**) Bar graphs showing mean ± S.E.M. cell number of B cell populations found in the bone marrow, spleen and lymph nodes in *Slc12a2*$^{+/+}$ and *Slc12a2*$^{-/-}$ chimeras that were defined using the gating strategy in Figure 3.13 (n=4-5). Statistical analysis was carried out using a Mann-Whitney U-test; * p<0.05, ** p<0.01, *** p<0.001.

I performed a time course to look at the number of cells in different B cell populations after initial tamoxifen injection to determine whether the loss of B cells is transient. In the bone marrow, there was no recovery of pre-B cells, immature and mature B cells (Figure 3.15B, C and D) up to 8 weeks after initial injection of tamoxifen. The number of pro-B and plasma cells in the bone marrow did not change over this time (Figure 3.15A and E). In secondary lymphoid organs, splenic follicular and marginal zone B cells, and naïve B cells from lymph nodes displayed a reduction in cell number in *Wnk1*$^{fl/-}$ RCE mice that persisted up to 8 weeks post tamoxifen injection (Figure 3.15F, G and H). This shows that the deletion of *Wnk1* leads to a long-lasting decrease in number of mature B cell populations in the spleen, lymph nodes, and developing B cell populations in the bone marrow.

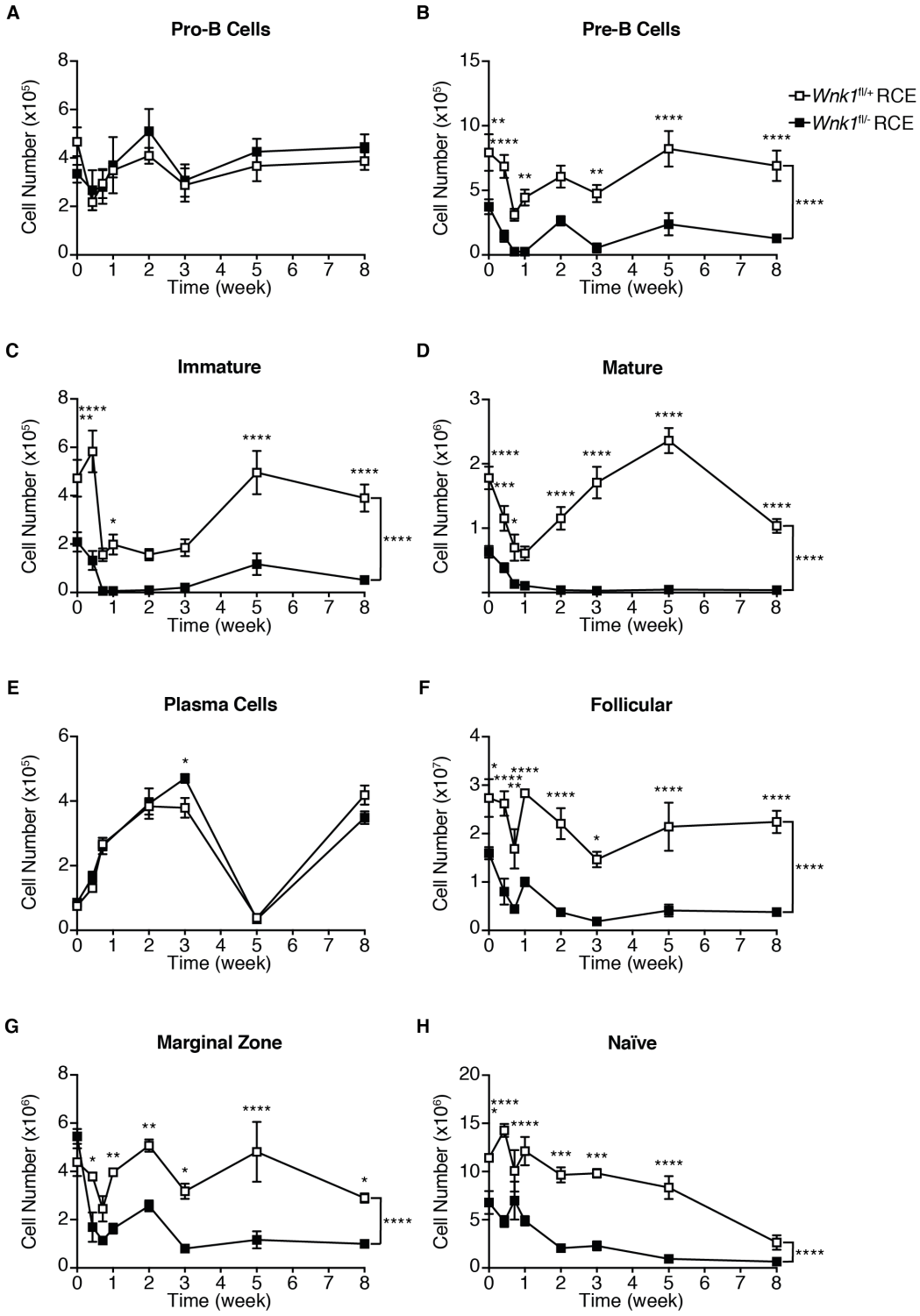

Figure 3.15 Loss of WNK1 Causes a Long-Lasting Reduction in B Cell Number

Line graphs showing mean ± S.E.M. number of cells of pro-B (**A**), pre-B (**B**), immature B cells in the bone marrow (**C**), mature B cells in the bone marrow (**D**), plasma cells in the bone marrow (**E**), follicular B cells in the spleen (**F**), marginal zone B cells in the spleen (**G**) and naïve B cells in lymph nodes (**H**) as defined in Figure 3.13 in *Wnk1*$^{fl/+}$ RCE and *Wnk1*$^{fl/-}$ RCE mice (n=4-5). Statistical analysis was carried out using a two-way ANOVA with multiple comparisons; * p<0.05, ** p<0.01,*** p<0.001, **** p<0.0001. Asterisks outside bracket indicate significant differences

between genotypes from the two-way ANOVA analysis. Asterisks above points indicate significant differences using multiple comparisons from the two-way ANOVA analysis.

3.5.2 WNK1 is Activated by BAFF Signalling and Required for BAFF-Mediated Survival *in vitro*

Since BAFF is a key survival factor for B cells *in vivo*, I assessed the ability of B cells lacking WNK1 to respond to BAFF *in vitro*. B cells from *Wnk1*$^{fl/-}$ RCE mice displayed a decreased response to BAFF *in vitro*, as shown by fewer cells recovered after 3 days of culture with BAFF (Figure 3.16A). There were also fewer *Wnk1*$^{fl/-}$ RCE B cells recovered when cultured with medium alone compared to *Wnk1*$^{fl/+}$ RCE B cells. This suggests that WNK1 is important for *in vitro* survival of B cells both with and without BAFF stimulation.

To determine whether WNK1 is activated after stimulation of BAFFR, I assessed phosphorylation of OXSR1 by immunoblot after BAFF stimulation over a range of time points. Figure 3.16B shows that OXSR1 was phosphorylated after BAFF stimulation in WT B cells, with the peak of phosphorylation occurring at 15 minutes post stimulation. The magnitude of phosphorylation was more similar to that of anti-IgM stimulation than CXCL13 stimulation (1.5- to 2-fold increase). This phosphorylation event was dependent on WNK1 as it was reduced in *Wnk1*$^{fl/-}$ RCE B cells and there was no increase upon BAFF stimulation (Figure 3.16C). Furthermore, it was dependent on kinase activity of WNK1 as when WT B cells were stimulated in the presence of WNK463 there was no phosphorylation of OXSR1 (Figure 3.16D). To test whether the BAFF-induced phosphorylation of OXSR1 is dependent on PI3K and AKT activity, I stimulated WT B cells with BAFF in the presence of PI-103 and MK2206. In this experiment, BAFF stimulation did not induce OXSR1 phosphorylation (Figure 3.16E). However, there was a trend for BAFF-induced phosphorylation of AKT and PRAS40, indicating that the stimulation had induced signalling downstream of BAFFR. Despite the lack of BAFF-induced phosphorylation in these experiments, the level of OXSR1 phosphorylation is decreased in the presence of PI-103 and MK2206, suggesting that the basal phosphorylation of OXSR1 in B cells is mediated by PI3K and AKT.

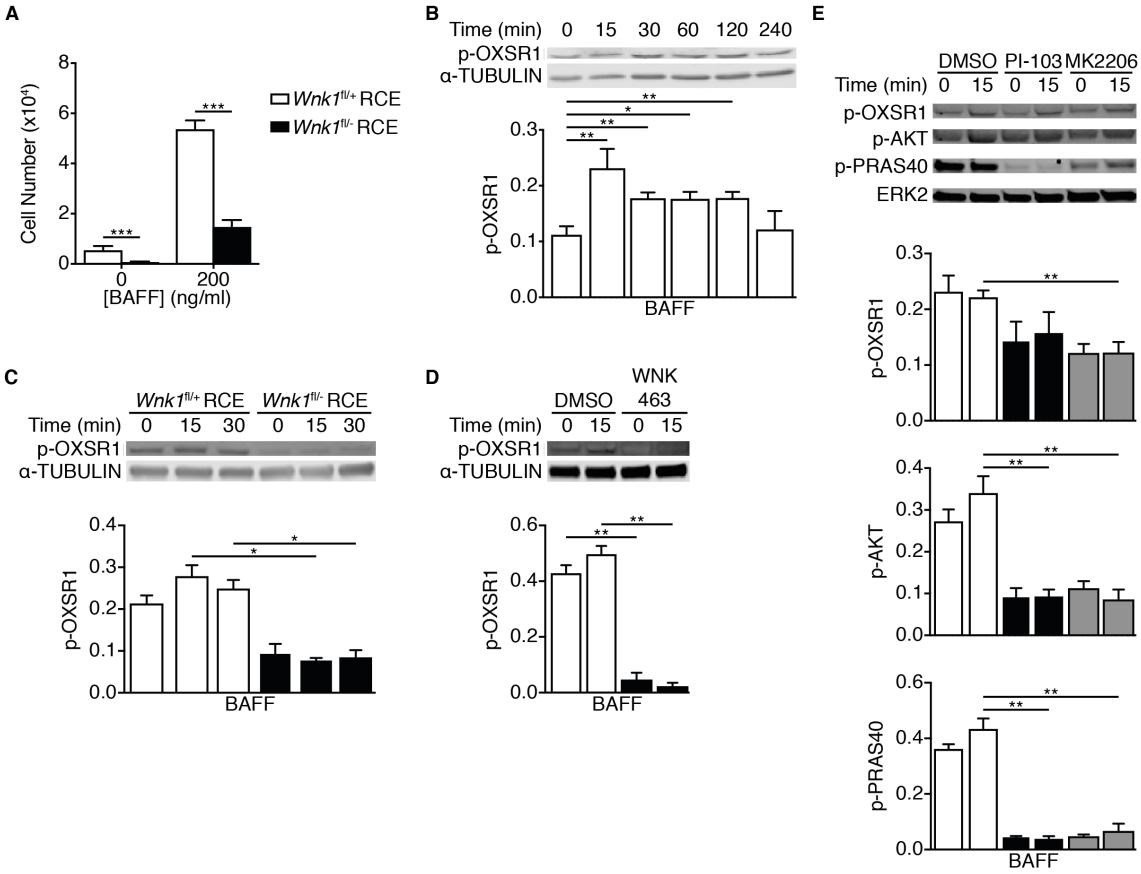

Figure 3.16 WNK1 is Activated by Stimulation with BAFF

(**A**) Bar graph showing mean ± S.E.M. number of *Wnk1*$^{fl/+}$ RCE and *Wnk1*$^{fl/-}$ RCE B cells recovered after 72 hours culture *in vitro* with or without recombinant human BAFF (n=9-15). (**B**) Representative immunoblot of WT B cells stimulated with recombinant human BAFF for the time points shown and blotted with antibodies against p-OXSR1 and α-TUBULIN. Below is a bar graph showing the mean ± S.E.M. relative signal of p-OXSR1 normalised to α-TUBULIN at the different time points (n=7). (**C**) Representative immunoblots of B cells from either *Wnk1*$^{fl/+}$ RCE and *Wnk1*$^{fl/-}$ RCE mice stimulated with recombinant human BAFF for the time points shown and blotted with antibodies against p-OXSR1 and α-TUBULIN. Below is a bar graph showing the mean ± S.E.M. relative signal of p-OXSR1 normalised to α-TUBULIN at the different time points (n=4). (**D**) Representative immunoblot of WT B cells incubated with 5μM WNK463 or vehicle alone (DMSO) and then stimulated with recombinant human BAFF for 15 minutes and blotted with antibodies against p-OXSR1 and α-TUBULIN. Below is a bar graph showing mean ± S.E.M. relative signal of p-OXSR1 normalised to α-TUBULIN at the different time points (n=6). (**E**) Representative immunoblot of WT B cells incubated with either 1μM PI-103 or 2μM MK2206 or vehicle alone (DMSO) and then stimulated with recombinant human BAFF for 15 minutes and blotted with antibodies against p-OXSR1, p-AKT, p-PRAS40 and TUBULIN. Below are bar graphs showing mean ± S.E.M. relative signal of p-OXSR1, pAKT and pPRAS40 (all normalised to ERK2) from cells incubated with the different inhibitors (n=5). Statistical analysis was carried out using a Mann-Whitney U-test; * p<0.05, ** p<0.01, *** p<0.001.

3.5.3 The Loss of B Cells is not Due to a Lack of BAFF Production and WNK1-Deficient B Cells Have Less BAFFR on Their Surface

The evidence provided suggests that WNK1 regulates B cell survival both *in vitro* and *in vivo* by participating in signal transduction from BAFFR. However, the reduced number of B cells in *Wnk1*$^{fl/-}$ RCE mice could be due to less BAFF production as some haematopoietic cells can produce BAFF and potentially loss of WNK1 could lead to reduced BAFF secretion. Alternatively, there could be less BAFFR on the surface of *Wnk1*$^{fl/-}$ RCE B cells compared to control B cells. Thus, I tested both of these hypotheses to determine if either or both contribute to the loss of B cells after deletion of *Wnk1*. To measure BAFF production, I measured serum concentration of BAFF by ELISA from *Wnk1*$^{fl/+}$ RCE and *Wnk1*$^{fl/-}$ RCE mice 7 days after tamoxifen injection. In *Wnk1*$^{fl/-}$ RCE mice there was over three times the concentration of BAFF in the serum compared to *Wnk1*$^{fl/+}$ RCE mice (Figure 3.17). I used flow cytometry to measure surface levels of BAFFR on both *Wnk1*$^{fl/+}$ RCE and *Wnk1*$^{fl/-}$ RCE B cells. Figure 3.17B shows that there was reduced levels of BAFFR on WNK1-deficient B cells compared to control B cells. These data suggest that the decrease in the number of B cells in *Wnk1*$^{fl/-}$ RCE mice is not due to a failure to produce BAFF but may be regulated in part by decreased levels of BAFFR on the surface of *Wnk1*$^{fl/-}$ RCE B cells.

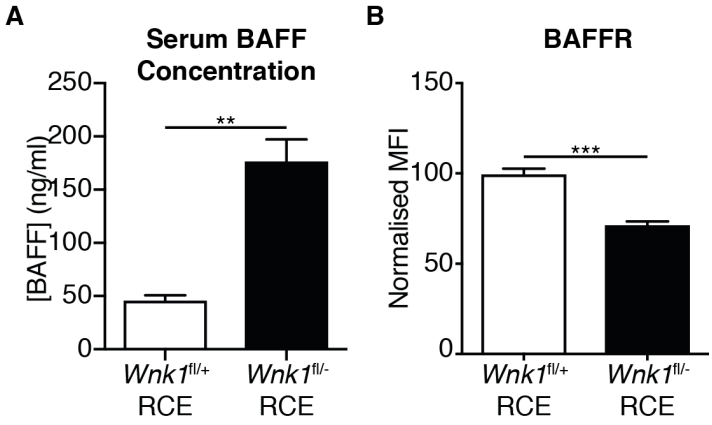

Figure 3.17 Increase in BAFF Serum Levels in *Wnk1*$^{fl/-}$ RCE Mice and a Reduction in BAFFR Surface Expression in WNK1-Deficient B Cells

(**A**) Bar graph showing mean ± S.E.M. of concentration of BAFF in serum of *Wnk1*$^{fl/+}$ RCE and *Wnk1*$^{fl/-}$ RCE mice as measured by ELISA (n=6). (**B**) Bar graph showing mean ± S.E.M. normalised MFI of BAFFR on the surface of *Wnk1*$^{fl/+}$ RCE and *Wnk1*$^{fl/-}$ RCE B cells. MFI was normalised to the average MFI of BAFFR on *Wnk1*$^{fl/+}$ RCE B cells, which was set to 100 (n=7). Statistical analysis was carried out using a Mann-Whitney U-test; ** $p<0.01$, *** $p<0.005$.

3.5.4 Overexpression of an Anti-apoptotic Protein Partially Rescues B Cell Population Numbers in WNK1-Deficient Mice

To determine how WNK1 regulates survival of B cells, I assessed whether B cell-specific overexpression of the anti-apoptotic protein BCL-X_L can rescue the survival defect. *Wnk1*$^{fl/+}$ RCE, *Wnk1*$^{fl/-}$ RCE, *Wnk1*$^{fl/+}$ RCE *Eμ-BCL2L1* and *Wnk1*$^{fl/-}$ RCE *Eμ-BCL2L1* mice were used as donors for bone marrow radiation. Figure 3.18 shows that overexpression of BCL-X_L in WNK1-deficient B cells increased the number of immature and mature B cells in the bone marrow, splenic follicular B cells and naïve B cells in lymph nodes when compared to WNK1-deficient B cells with no BCL-X_L overexpression. Despite this increase, there was still a partial effect of *Wnk1* deletion as there was a trend for a reduction in cell numbers of B cell populations in the spleen and lymph nodes in *Wnk1*$^{fl/-}$ RCE *Eμ-BCL2L1* mice compared to *Wnk1*$^{fl/+}$ RCE *Eμ-BCL2L1* mice. The number of splenic follicular B cells and naïve B cells in lymph nodes in *Wnk1*$^{fl/-}$ RCE *Eμ-BCL2L1* mice was comparable to that from *Wnk1*$^{fl/+}$ RCE mice. However, in the bone marrow the increase in immature and mature cells was smaller and there was no increase in pre-B cells when BCL-X_L is overexpressed.

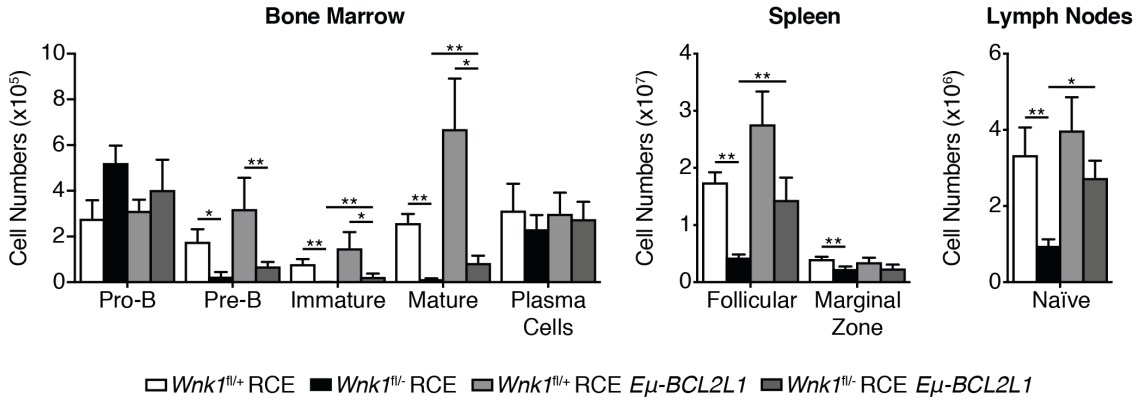

Figure 3.18 Overexpression of BCL-X_L Partially Rescues the Survival Defect in Mature B Cells Lacking *Wnk1* Expression

Bar graphs showing mean ± S.E.M. cell number of B cell populations in the bone marrow, spleen and lymph nodes in *Wnk1*$^{fl/+}$ RCE, *Wnk1*$^{fl/-}$ RCE, *Wnk1*$^{fl/+}$ RCE *Eμ-BCL2L1* and *Wnk1*$^{fl/-}$ RCE *Eμ-BCL2L1* mice that were defined in Figure 3.13 (n=5). Statistical analysis was carried out using a Mann-Whitney U-test; * $p<0.05$, ** $p<0.01$.

3.5.5 WNK1-Deficient B Cells Display no Changes in Mitochondrial Health

BCL-X_L is found in the outer membrane of mitochondria and inhibits VDAC1-mediated transport of Ca^{2+} into mitochondria, a signal that drives apoptosis (Monaco *et al.*, 2015). To assess mitochondrial health in *Wnk1*$^{fl/-}$ RCE B cells, I purified B cells and stained with MitoTracker Green and CmxROS to measure mitochondrial mass and potential respectively. Despite the low number of repeats and thus lack of statistical analysis, Figure 3.19A and B indicates that there was probably no difference in mitochondrial health and levels of apoptosis between *Wnk1*$^{fl/+}$ RCE and *Wnk1*$^{fl/-}$ RCE B cells. In addition, there was no obvious difference in mitochondrial mass or mitochondrial potential (Figure 3.19C).

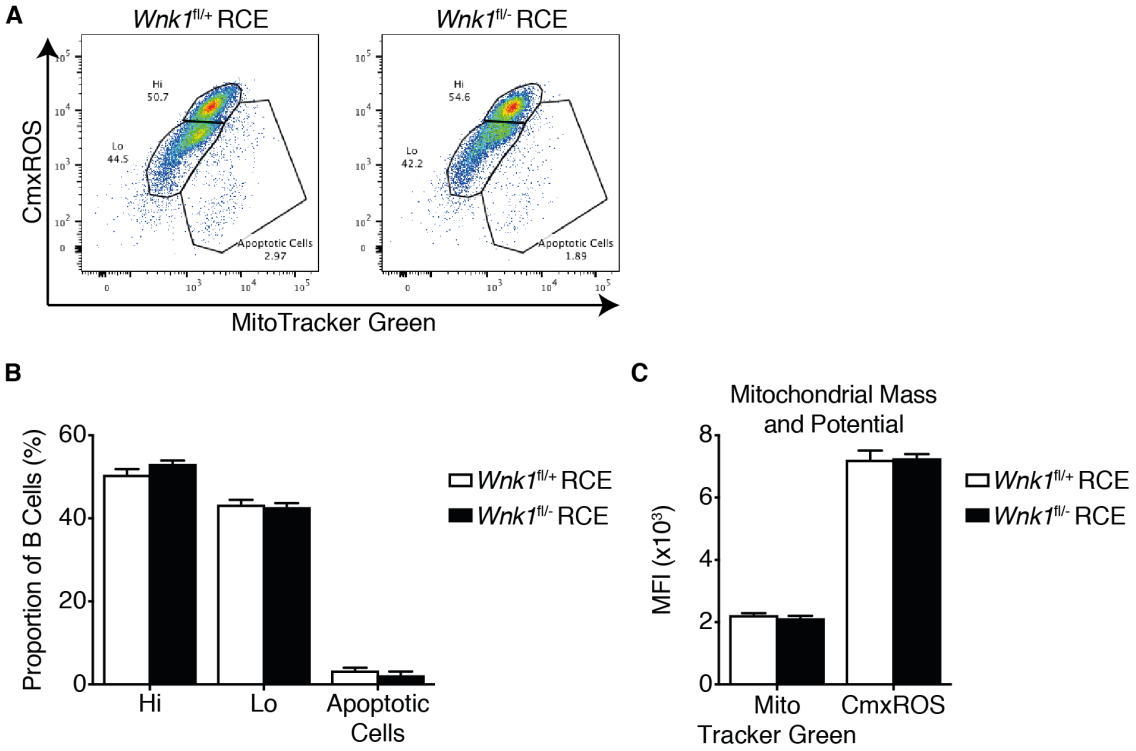

Figure 3.19 Mitochondrial Health is not Altered in B Cells Lacking WNK1 Expression

(**A**) Representative flow cytometry plots of *Wnk1*$^{fl/+}$ RCE and *Wnk1*$^{fl/-}$ RCE B cells showing gating to determine B cells with high mitochondrial potential (Hi), low mitochondrial potential (Lo) and apoptotic cells based on staining with MitoTracker Green and CmxROS. (**B**) Bar graph showing mean ± S.E.M. proportion of B cells in gates shown in flow cytometry plots (n=3). (**C**) Bar graph showing mean ± S.E.M MFI of MitoTracker Green and CmxROS in purified B cells from *Wnk1*$^{fl/+}$ RCE and *Wnk1*$^{fl/-}$ RCE mice (n=3).

In summary, I have shown that deletion of *Wnk1* leads to a reduction of B cells in the mice in the bone marrow, the spleen, lymph nodes and blood and this loss is dependent on the kinase function of WNK1 but not on ion regulation through NKCC1. The loss of B cells is not due to a reduction in the serum levels of BAFF in these mice, as there is a much higher concentration in WNK1 knockout chimeras, which is most likely due to the reduction of B cells so there is less consumption of BAFF. WNK1 is activated downstream of BAFF binding to BAFFR and induces a moderate increase in phosphorylation of OXSR1. WNK1-deficient B cells cannot respond to BAFF to induce B cell survival in an *in vitro* culture setting as well as control B cells. This implies that the survival defect in WNK1-deficient B cells may be through defective signalling downstream of BAFF. There is a partial rescue of the survival defect in mature B cell populations in secondary lymphoid organs when the anti-apoptotic protein BCL-X_L is overexpressed in WNK1-deficient B cells. Furthermore, the mitochondrial health of B cells from *Wnk1*$^{fl/-}$ RCE mice does not seem to be perturbed, indicating that they are not actively undergoing apoptosis.

3.6 Discussion and Outstanding Questions

For the first time, I have shown that WNK1 is an active kinase in B cells and is involved in signalling pathways downstream of the BCR, CXCR5 and BAFFR. In addition, I have shown that WNK1 is activated downstream of PI3K and AKT, since WNK1-dependent phosphorylation of OXSR1 is reduced when B cells are stimulated in the presence of PI-103 and MK2206. It has been suggested that WNK1 is activated by AKT (Cheng and Huang, 2011) and my work is consistent with this proposal as well as similar observations in $CD4^+$ T cells stimulated with anti-CD3 or CCL21 (Köchl *et al.*, 2016).

Furthermore, I have demonstrated that WNK1 plays a role in many different cellular processes in naïve B cells, namely adhesion, migration, survival and development. When B cells lack expression of *Wnk1* they bind more ICAM-1 and VCAM-1 both in an unstimulated state and when stimulated with anti-IgM or CXCL13. This shows that WNK1 is a negative regulator of B cell adhesion through LFA-1 and VLA-4. In the case of ICAM-1 binding through LFA-1, the kinase function of WNK1 is required for its role as a negative regulator of ICAM-1 binding. WNK1-deficient B cells have higher levels of CD11a, the α subunit of LFA-1, which could explain why when they are unstimulated they bind more ICAM-1. However, this is insufficient to explain the difference in ICAM-1 binding between stimulated *Wnk1*$^{fl/+}$ RCE and *Wnk1*$^{fl/-}$ RCE B cells as the magnitude of the difference is too high to be explained by the small increase in surface levels of CD11a.

Despite the known role of WNK1 in ion homeostasis in kidney epithelial cells, I have shown that ion transport through NKCC1 is not required for LFA-1 regulation in B cells. This is consistent with work in $CD4^+$ T cell adhesion to ICAM-1 (Köchl *et al.*, 2016). As WNK1 regulates LFA-1 following treatment with $MnCl_2$, which directly induces an affinity switch of LFA-1, it suggests that WNK1 is not regulating LFA-1 by causing an affinity switch but by another mechanism. This mechanism remains to be discovered in B cells, but in $CD4^+$ T cells WNK1 negatively regulates GTP loading of Rap1, which is the suggested mechanism for regulation of LFA-1-mediated adhesion (Köchl *et al.*, 2016). It is possible that this may also be the case in WNK1-deficient B cells but this remains to be tested. However, there is no difference in VCAM-1 binding after $McCl_2$ treatment between *Wnk1*$^{fl/+}$ RCE and *Wnk1*$^{fl/-}$ RCE B cells. This suggests that regulation of LFA-1 and VLA-4 by WNK1 may differ between the different

integrins. Further investigation is required to understand this difference and the mechanisms underlying the regulation of B cell adhesion by WNK1.

WNK1 is a positive regulator of B cell migration in response to CXCL13 *in vitro* as well as *in vivo* migration in lymph nodes. Again, this is consistent with the phenotype observed in $CD4^+$ T cells (Köchl *et al.*, 2016). The mechanism by which WNK1 regulates B cell migration is unknown. One explanation could be that lower levels of CXCR5 on the surface lead to less responsiveness to CXCL13 and thus reduced migration. In $CD4^+$ T cells, WNK1 regulates migration through phosphorylation of OXSR1 and subsequent ion movement through NKCC1. I have no evidence to suggest that this is the case in B cells but it could be tested using either bumetanide, an inhibitor of ion transport by NKCC1, or using *Slc12a2*$^{-/-}$ B cells. If this were to be true in B cells, the question would still remain how ion movement regulates B cell migration? There is a model of cell migration in confinement called the osmotic engine model (Stroka *et al.*, 2014). In this model, it is posited that water movement into the cell at the leading edge and out of the cell at the rear is enough to cause cell migration. The regulation of this water movement is dependent on polarised ion transport across the cell. As WNK1 regulates activity of ion channels, it is possible that such a process contributes to B cell migration.

Homing of B cells to secondary lymphoid organs relies on both a combination of chemotactic cues and adhesion. It is therefore not a surprise that WNK1-deficient B cells show a defect in homing to spleen and lymph nodes 1 hour after transfer. It appears that this is not a matter of the cells just being slower since there is still a defect 24 hours post transfer. However, the survival defect could be masking the homing phenotype at this point as there are fewer WNK1-deficient B cells found in the blood. An alternative explanation could be that the mutant B cells are “stuck” elsewhere in the recipient mice as they have been shown to be hyperadhesive *in vitro*. This explanation would require further investigation of more compartments in the mouse, especially highly vascularised organs such as the liver and lungs.

I have shown that WNK1 regulates B cell survival both *in vitro* and *in vivo*. This is mostly likely due to a role for WNK1 in transducing BAFFR signals, since BAFF stimulation leads to WNK1-dependent phosphorylation of OXSR1. The survival defect can be partially rescued by overexpression of BCL-X_L but since it is not sufficient for complete rescue, this suggests that tipping the balance in favour of anti-apoptotic mechanisms is not sufficient to rescue all WNK1-deficicent B cells from

dying. The mechanism by which the B cells are dying is not fully understood; their mitochondrial health seems to be similar in both *Wnk1*$^{fl/+}$ RCE and *Wnk1*$^{fl/-}$ RCE B cells suggesting that mitochondrial-induced apoptosis is not regulated by WNK1 or if it is, the window to observe this effect has been missed. It is noteworthy that terminally differentiated plasma cells in the bone marrow no longer depend on WNK1 for their survival even though they express *Wnk1*. Therefore it would be interesting to investigate the role of WNK1 in long-lived plasma cells since there is no confounding survival phenotype.

One explanation for the survival defect could be that the lower levels of BAFFR on WNK1-deficient B cells decrease their ability to survive. This could be true but it could also be a consequence of the higher BAFF serum concentration leading to more internalisation of BAFFR. Additionally, since ERK5 activation has shown to require WNK1 and ERK5 is required for B cell survival, WNK1 could regulate B cell survival through the activation of ERK5. Further investigation is required to determine whether ERK5 is regulated by WNK1 in B cells. An alternative explanation could be that without expression of WNK1, B cells are unable to sense their environment and regulate ion homeostasis. Without correct ion homeostasis regulation, there could be shrinkage of the B cells due to water movement out of the cell. The shrinkage caused by osmotic stress could cause cell death as shown in cardiomyocytes and *S. cerevisiae* (Galvez *et al.*, 2001, Silva *et al.*, 2005) and maybe one of the ways BAFFR induces B cell survival is to maintain the correct cell size through a WNK1-dependent pathway. However, as loss of NKCC1 has no effect on the survival of splenic B cells the regulation of B cell volume leading to survival would have to be mediated by more than just NKCC1 and thus there would be redundancy in ion channels for regulating B cell volume. Further work is required to determine whether WNK1 regulates B cell volume. Harvesting B cells from *Wnk1*$^{fl/+}$ RCE and *Wnk1*$^{fl/-}$ RCE mice may not be a good approach to test this as they may be using other compensatory mechanisms for their survival since they lost expression of *Wnk1* up to 7 days prior to harvesting. Using the inhibitor WNK463 could be a better approach to look at the role of WNK1 kinase activity in regulating cell volume in B cells.

Analysis of B cell populations deficient in WNK1 have revealed that there may be a developmental block since there is a large reduction of pre-B cells in the bone marrow of *Wnk1*$^{fl/-}$ RCE mice following deletion of *Wnk1*. Cell death has not been ruled out as the cause of the developmental block since the deletion of *Wnk1* could

be causing death in HSC, CLP or pro-B cells. Further work is required to determine the cause for the developmental block caused by lack of WNK1. It could be that WNK1 is required to transduce signals from the pre-BCR in order for positive selection to take place, but this would need to be tested using a different driver of Cre expression such as CD2 as CD2 expression occurs early during B cell development. Of interesting note, the numbers of cells in developing B cell populations in *Wnk1*$^{fl/-}$ RCE mice are lower than in *Wnk1*$^{fl/+}$ RCE mice before deletion of *Wnk1* is induced by injection of tamoxifen. This may suggest that *Wnk1* heterozygosity has an impact on reconstitution of the haematopoietic system in radiation chimeras. However, this requires further investigation as only one group of chimeras were used in this experiment so it could be poorer reconstitution due to other causes.

The lack of mature B cell populations in *Oxsr1*$^{T185A/T185A}$ chimeras suggests that phosphorylation and activation of OXSR1 is critical for development or survival of B cells and their precursors. As with WNK1-deficient mice, the pro-B cells that remain could be cells from the *Rag1*$^{-/-}$ hosts so it is impossible to determine if there is a block in B cell development at this stage or an earlier stage of B cell development. No such block in T cell development was seen in *Oxsr1*$^{T185A/T185A}$ chimeras (Köchl *et al.*, 2016). This may be because T cell progenitors express *Stk39* which can compensate for the *Oxsr1* mutation. In contrast, B-lineage progenitors have limited expression of *Stk39*, which may not be able to compensate for the *Oxsr1* mutation. Due to the lack of mature B cells in the spleen and lymph nodes, I was unable to assess whether this OXSR1 mutation caused dysregulation in B cell adhesion, migration, homing and survival similar to the WNK1 mutation. To do this, a conditional deletion of *Oxsr1* would be required to inactivate the *Oxsr1* gene in mature B cells. However, mice with a floxed allele of *Oxsr1* were not available during the time frame of this PhD project.

Chapter 4. WNK1 Function During B Cell Activation

Having shown that WNK1 is activated downstream of the BCR, I next investigated whether activation of B cells is perturbed by the deletion of *Wnk1*. In this chapter, I focus on cellular processes involved in B cell activation measured by *in vitro* assays as well as processing of antigen upon encounter through the BCR.

4.1 Analysis of Activation of WNK1-Deficient B Cells

4.1.1 Reduced Recovery of WNK1-deficient B Cells After Activation

To determine the responsiveness of WNK1-deficient B cells to stimuli that induce activation, I isolated B cells from *Wnk1*$^{fl/+}$ RCE and *Wnk1*$^{fl/-}$ RCE mice, which had been treated with tamoxifen 7 days earlier. I cultured these B cells for 3 days *in vitro*, and stimulated them with either anti-IgM, CD40L, CD40L and IL-4, LPS, ODN1826 or ionomycin and PMA. Figure 4.1 shows that there was less recovery of live B cells after stimulation of *Wnk1*$^{fl/-}$ RCE B cells compared to *Wnk1*$^{fl/+}$ RCE B cells with all stimuli tested. This result could be due to a defect in survival of WNK1-deficient B cells after activation or a defect in proliferation or both.

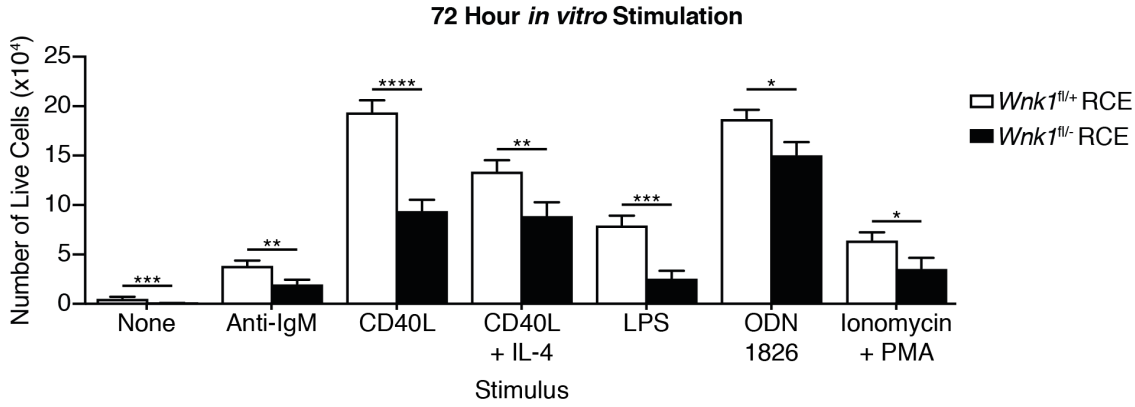

Figure 4.1 Reduced Cell Recovery in WNK1-Deficient B cells After Activation

Bar graph showing mean ± S.E.M. number of *Wnk1*$^{fl/+}$ RCE and *Wnk1*$^{fl/-}$ RCE B cells recovered after 72 hours of stimulation with either medium alone, anti-IgM $F(ab)_2$, recombinant murine CD40L, recombinant murine CD40L and recombinant murine IL-4, LPS, ODN1826 or ionomycin and PMA in an *in vitro* culture (n=9-15). Statistical analysis was carried out using a Mann-Whitney U-test; * $p<0.05$, ** $p<0.01$, *** $p<0.001$, **** $p<0.0001$.

4.1.2 WNK1, Through its Kinase Activity, Regulates Proliferation in Response to Stimulation of the BCR, CD40 and TLR4

As B cells undergo division upon activation with these stimuli, I tested whether the reduced cell recovery is due to a defect in proliferation by stimulating dye-labelled B cells from *Wnk1*$^{fl/+}$ RCE and *Wnk1*$^{fl/-}$ RCE mice with either anti-IgM, CD40L or LPS for 3 days. Upon division the dye is shared equally among the daughter cells, thus allowing measurement of cell division. Flow cytometry and FlowJo software were used to calculate the percentage of cells that enter division and the proliferation index, which is a measure of the average number of divisions carried out by cells that have divided at least once. As shown in Figure 4.2A there was a reduction in the percentage of cells that divided at least once in B cells lacking WNK1 stimulated with anti-IgM and CD40L but not with LPS. In contrast, I observed no difference in the proliferation index although there was a trend for a decrease in this index in *Wnk1*$^{fl/-}$ RCE B cells stimulated with LPS.

I tested whether this dependency on WNK1 for B cell division is dependent on the kinase activity by repeating the experiment with *Wnk1*$^{fl/+}$ RCE and *Wnk1*$^{fl/D368A}$ RCE B cells. Figure 4.2B indicates that kinase function of WNK1 is probably required for the defects in division described above, since *Wnk1*$^{fl/D368A}$ RCE B cells displayed a trend for a similar decrease in percentage of cells that divided at least once. To further test this and to determine whether ion transport through NKCC1 is required, I analysed proliferation in the presence of either WNK463 or bumetanide. Figure 4.2C shows that B cell division was not inhibited by bumetanide but confirms that kinase activity of WNK1 was required as there was a reduction in the number of cells that had divided at least once when cells were stimulated with anti-IgM, CD40L and LPS in the presence of WNK463. I also saw a reduction in the proliferation index when cells were stimulated with LPS.

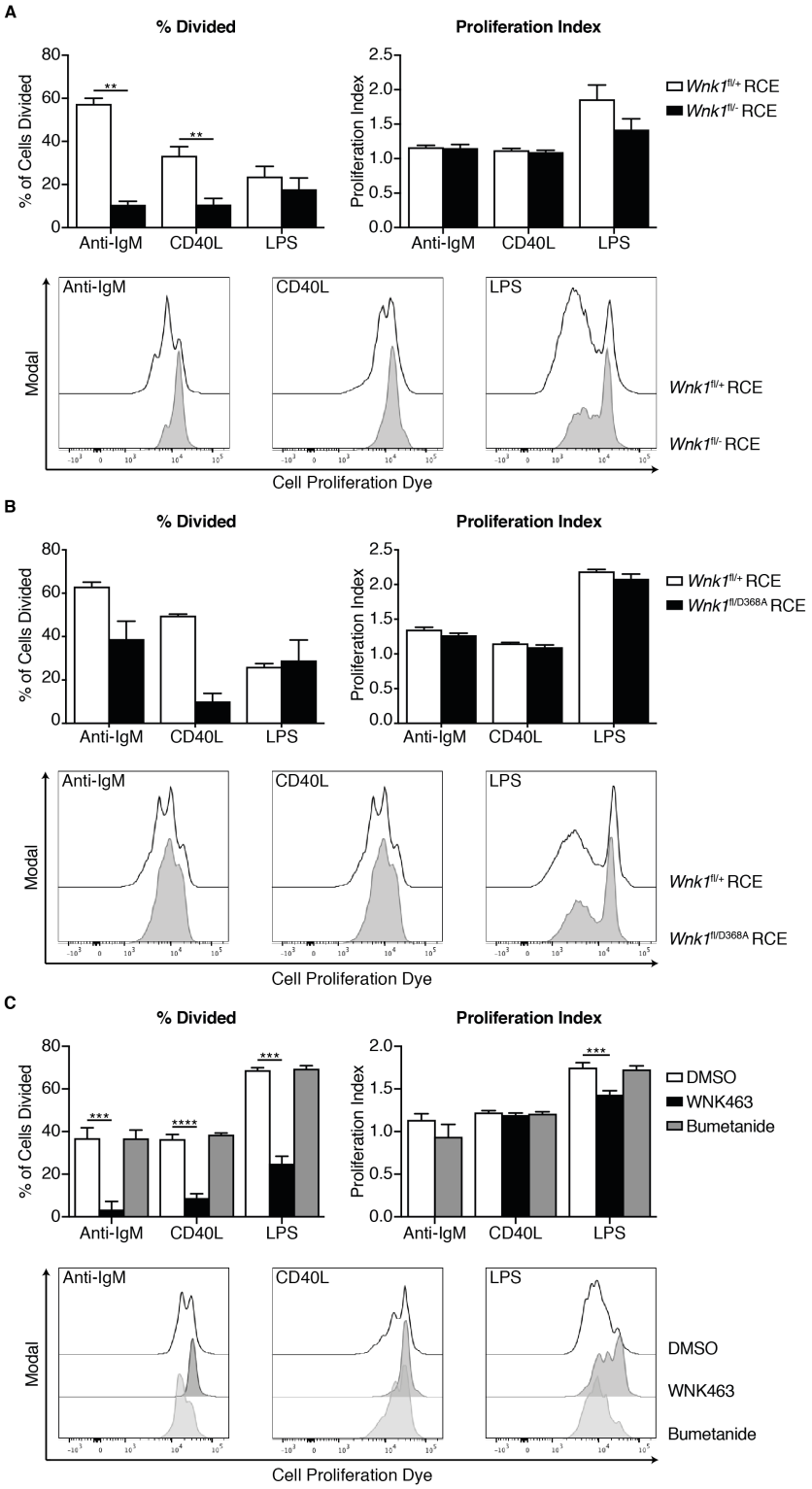

Figure 4.2 WNK1 Kinase Activity is Required for B Cell Proliferation

(**A**) Bar graphs showing mean ± S.E.M. percentage of cells divided (left) and proliferation index (right) of *Wnk1*$^{fl/+}$ RCE and *Wnk1*$^{fl/-}$ RCE B cells stimulated with either anti-IgM F(ab)$_2$, recombinant murine CD40L or LPS. Below are overlays of representative histograms of cell proliferation dye in *Wnk1*$^{fl/+}$ RCE and *Wnk1*$^{fl/-}$ RCE B cells (n=5-6). (**B**) Bar graphs showing mean ± S.E.M. percentage of cells divided (left) and proliferation index (right) of *Wnk1*$^{fl/+}$ RCE and *Wnk1*$^{fl/D368A}$ RCE B cells stimulated with either anti-IgM F(ab)$_2$, recombinant murine CD40L or

LPS. Below are overlays of representative histograms of cell proliferation dye in *Wnk1*$^{fl/+}$ RCE and *Wnk1*$^{fl/D368A}$ RCE B cells (n=3). (**C**) Bar graphs showing mean ± S.E.M. percentage of cells divided (left) and proliferation index (right) of WT B cells stimulated with either anti-IgM $F(ab)_2$, recombinant murine CD40L or LPS in the presence of 5μM WNK463 or 10μM bumetanide or vehicle alone (DMSO). Below are overlays of representative histograms of cell proliferation dye in WT B cells incubated with either μM WNK463 or 10μM bumetanide or vehicle alone (DMSO) (n=8-9). Statistical analysis was carried out using a Mann-Whitney U-test; ** p<0.01, *** p<0.001, **** p<0.0001.

To further understand if survival is a confounding issue in the proliferation defect, I used B cells from *Wnk1*$^{fl/+}$ RCE, *Wnk1*$^{fl/-}$ RCE, *Wnk1*$^{fl/+}$ RCE *Eμ-BCL2L1*, *Wnk1*$^{fl/-}$ RCE *Eμ-BCL2L1* mice and assessed the percentage of cells that had divided at least once and the proliferation index in response to anti-IgM, CD40L and LPS stimulation. Figure 4.3A shows that overexpression of BCL-X_L was not sufficient to rescue the proliferation defect as there was a trend for a reduction in the percentage of cells that had divided at least once in *Wnk1*$^{fl/-}$ RCE *Eμ-BCL2L1* B cells compared to *Wnk1*$^{fl/+}$ RCE *Eμ-BCL2L1* B cells. There was no increase in division when *Wnk1*$^{fl/-}$ RCE and *Wnk1*$^{fl/-}$ RCE *Eμ-BCL2L1* B cells were compared. In addition, I calculated the number of cells that would be alive in the well if there had been no division using the following equation:

$$= \frac{1}{2^0}(\text{no. cells 0 divisions}) + \frac{1}{2^1}(\text{no. cells 1 division}) + \cdots + \frac{1}{2^n}(\text{no. cells n divisions})$$

Figure 4.3B shows that there was a reduction in the number of cells when division is removed from the equation in *Wnk1*$^{fl/-}$ RCE B cells compared to *Wnk1*$^{fl/+}$ RCE B cells, which is rescued by overexpression of BCL-X_L when cells are stimulated with anti-IgM and LPS but not with CD40L. These results suggest that both survival and proliferation contribute to the reduced recovery of WNK1-deficient cells shown in Figure 4.1.

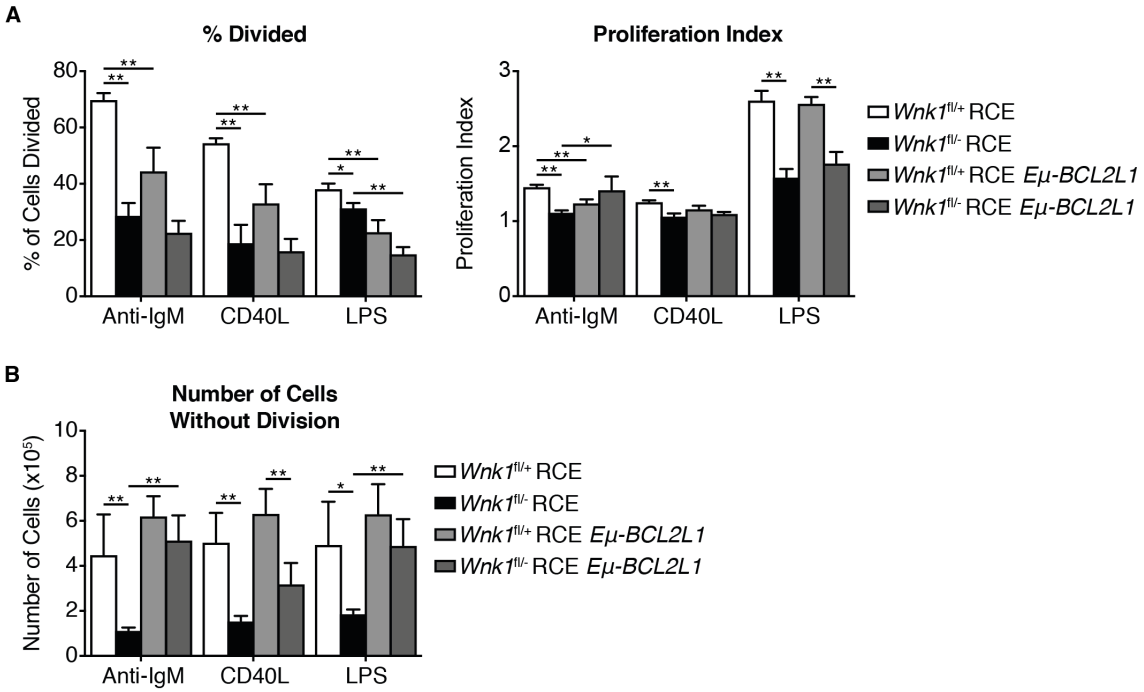

Figure 4.3 Overexpression of BCL- X_L does not Rescue Proliferation

(**A**) Bar graphs showing mean ± S.E.M. percentage of cells divided (left) and proliferation index (right) of *Wnk1*$^{fl/+}$ RCE, *Wnk1*$^{fl/-}$ RCE, *Wnk1*$^{fl/+}$ RCE *Eμ-BCL2L1* and *Wnk1*$^{fl/-}$ RCE *Eμ-BCL2L1* B cells stimulated with either anti-IgM F(ab)$_2$, recombinant murine CD40L or LPS (n=6). (**B**) Bar graph showing mean ± S.E.M. number of cells without division of *Wnk1*$^{fl/+}$ RCE, *Wnk1*$^{fl/-}$ RCE, *Wnk1*$^{fl/+}$ RCE *Eμ-BCL2L1*, *Wnk1*$^{fl/-}$ RCE *Eμ-BCL2L1* B cells stimulated with either anti-IgM F(ab)$_2$, recombinant murine CD40L or LPS (n=6). Statistical analysis was carried out using a Mann-Whitney U-test; * $p<0.05$, ** $p<0.01$.

4.1.3 Upregulation of MYC is not Affected by WNK1-Deficiency in B Cells

The transcription factor MYC regulates the expression of pro-proliferative genes and is upregulated upon stimulation with anti-IgM and CD40L (Leider and Melamed, 2003, Zarnegar *et al.*, 2004). I tested the upregulation of MYC in WNK1-deficient B cells downstream of BCR and CD40 stimulation. There was no difference in upregulation of MYC between *Wnk1*$^{fl/+}$ RCE B cells and *Wnk1*$^{fl/-}$ RCE B cells when stimulated with anti-IgM (Figure 4.4A) or CD40L (Figure 4.4B), except a slightly faster upregulation in anti-IgM stimulated WNK1-deficient B cells. Thus the decrease in proliferation of WNK1-deficient B cells is not due to a failure in upregulation of MYC protein levels.

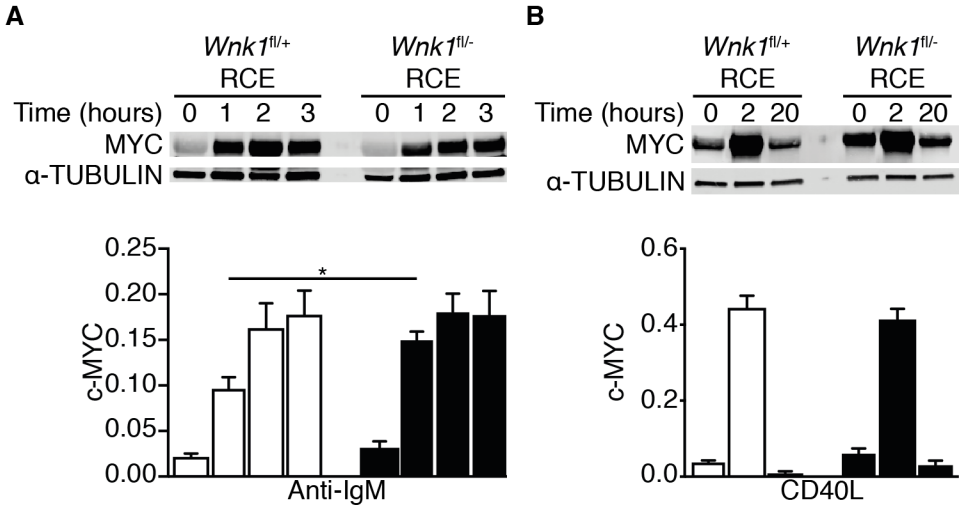

Figure 4.4 Upregulation of MYC is not Perturbed by Deletion of WNK1

(**A**) Representative immunoblots of B cells from either *Wnk1*$^{fl/+}$ RCE and *Wnk1*$^{fl/-}$ RCE mice stimulated with anti-IgM F(ab)$_2$ for the times shown and blotted with antibodies against MYC and α-TUBULIN. Below is a bar graph showing the mean ± S.E.M. relative signal of MYC normalised to α-TUBULIN at the different time points (n=6). (**B**) Representative immunoblots of B cells from either *Wnk1*$^{fl/+}$ RCE and *Wnk1*$^{fl/-}$ RCE mice stimulated with recombinant murine CD40L for the times shown and blotted with antibodies against MYC and α-TUBULIN. Below is a bar graph showing the mean ± S.E.M. relative signal of MYC normalised to α-TUBULIN at the different time points (n=6). Statistical analysis was carried out using a Mann-Whitney U-test; * $p<0.05$.

4.1.4 OXSR1 is Phosphorylated in a WNK1-Dependent Manner After Stimulation with CD40L but not LPS

Since deletion of *Wnk1* leads to defects in response to CD40L and LPS, I wanted to test whether WNK1 is activated by these stimuli. I stimulated B cells from WT mice with CD40L and measured phosphorylation of OXSR1 over a time course. Figure 4.5A shows that CD40L induces phosphorylation of OXSR1 to a similar extent as CXCL13 (~2.5-fold) but displays similar dynamics to anti-IgM with peak phosphorylation occurring at 10 minutes. To determine whether CD40L-induced phosphorylation of OXSR1 is dependent on WNK1, I stimulated B cells from *Wnk1*$^{fl/+}$ RCE and *Wnk1*$^{fl/-}$ RCE mice with CD40L. There was a decrease in phosphorylation of OXSR1 in WNK1-deficient B cells compared to the control B cells (Figure 4.5B). To demonstrate that CD40L driven OXSR1 phosphorylation is dependent on the kinase function of WNK1, I repeated the stimulation with either *Wnk1*$^{fl/D368A}$ RCE B cells or WT B cells incubated with WNK463. Again, there was a reduction in phosphorylation of OXSR1 before stimulation and no increase upon stimulation (Figure 4.5C and D), showing that kinase function of WNK1 is required for OXSR1 phosphorylation downstream of CD40 stimulation. I tested whether the phosphorylation of OXSR1 is dependent on PI3K and AKT by using the inhibitors PI-103 and MK2206. The CD40L-induced OXSR1 phosphorylation was partially reduced by MK2206 but not by PI-103 (Figure 4.5E). PI-103 and MK2206 were shown to actively inhibit PI3K and AKT respectively in this experiment as phosphorylation of AKT and PRAS40 were reduced in the presence of the inhibitors (Figure 4.5E). To determine if levels of CD40 on the surface remain the same after deletion of *Wnk1*, I used flow cytometry to measure CD40 levels on resting B cells from *Wnk1*$^{fl/+}$ RCE and *Wnk1*$^{fl/-}$ RCE mice. Figure 4.5F shows that loss of WNK1 in B cells has no effect on the levels of CD40 on the surface, indicating that the reduction in OXSR1 phosphorylation in WNK1-deficient B cells is not due to a reduction of CD40 expression.

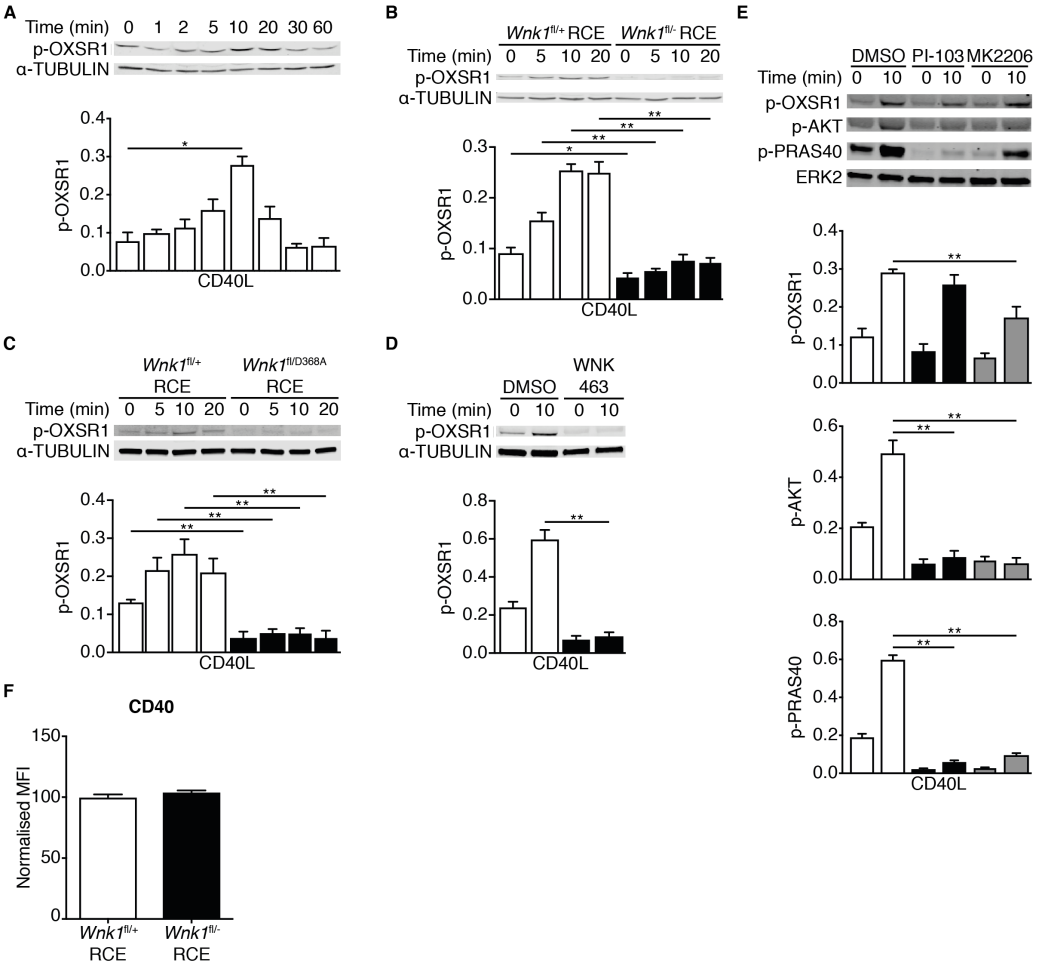

Figure 4.5 CD40L Stimulation Leads to OXSR1 Phosphorylation in a WNK1-Dependent Manner

(**A**) Representative immunoblot of WT B cells stimulated with recombinant murine CD40L for the times shown and blotted with antibodies against p-OXSR1 and α-TUBULIN. Below is a bar graph showing the mean ± S.E.M. relative signal of p-OXSR1 normalised to α-TUBULIN at the different time points (n=4). (**B**) Representative immunoblots of B cells from either *Wnk1*$^{fl/+}$ RCE and *Wnk1*$^{fl/-}$ RCE mice stimulated with recombinant murine CD40L for the times shown and blotted with antibodies against p-OXSR1 and α-TUBULIN. Below is a bar graph showing the mean ± S.E.M. relative signal of p-OXSR1 normalised to α-TUBULIN at the different time points (n=5). (**C**) Representative immunoblots of B cells from either *Wnk1*$^{fl/+}$ RCE and *Wnk1*$^{fl/D368A}$ RCE mice stimulated with recombinant murine CD40L for the times shown and blotted with antibodies against p-OXSR1 and α-TUBULIN. Below is a bar graph showing the mean ± S.E.M. relative signal of p-OXSR1 normalised to α-TUBULIN at the different time points (n=5). (**D**) Representative immunoblot of WT B cells incubated with 5μM WNK463 or vehicle alone (DMSO) and then stimulated with recombinant murine CD40L for 10 minutes and blotted with antibodies against p-OXSR1 and TUBULIN. Below is a bar graph showing mean ± S.E.M. relative signal of p-OXSR1 normalised to α-TUBULIN at the different time points (n=5). (**E**) Representative immunoblot of WT B cells incubated with either 1μM PI-103 or 2μM MK2206 or vehicle alone (DMSO) and then stimulated with recombinant murine CD40L for 10 minutes and blotted with antibodies against p-OXSR1, p-AKT, p-PRAS40 and TUBULIN. Below are bar graphs showing mean ± S.E.M. relative signal of p-OXSR1, pAKT and pPRAS40 (all normalised to ERK2) from cells incubated with the different inhibitors (n=6). (**F**) Bar graph showing mean ± S.E.M. of normalised MFI of CD40 on the surface of *Wnk1*$^{fl/+}$ RCE and *Wnk1*$^{fl/-}$ RCE B cells. MFI was normalised to the average MFI on *Wnk1*$^{fl/+}$ RCE B cells, which was set to 100 (n=7). Statistical analysis was carried out using a Mann-Whitney U-test; * $p<0.05$, ** $p<0.01$.

To test phosphorylation of OXSR1 downstream of LPS stimulation, I stimulated WT B cells with LPS over a range of time points and performed an immunoblot to detect phosphorylation of OXSR1. No increase in phosphorylation of OXSR1 was detected up to an hour after stimulation with LPS (Figure 4.6). Thus, TLR4 signalling does not activate the WNK1/OXSR1 pathway.

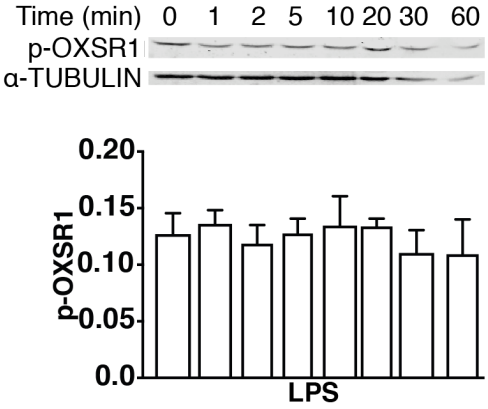

Figure 4.6 LPS Stimulation does not Induce Phosphorylation OXSR1

Representative immunoblot of WT B cells stimulated with LPS for the time points shown and blotted with antibodies against p-OXSR1 and α-TUBULIN. Below is a bar graph showing the mean $\pm$ S.E.M. relative signal of p-OXSR1 normalised to α-TUBULIN at the different time points (n=5). Statistical analysis was carried out using a Mann-Whitney U-test.

4.1.5 Upregulation of Activation Markers After Stimulation with Anti-IgM and CD40L is Regulated by WNK1

WNK1-deficient B cells have a defective response to activation signals, therefore I wanted to assess their ability to activate as indicated by upregulation of activation markers. *Wnk1*$^{fl/+}$ RCE and *Wnk1*$^{fl/-}$ RCE B cells were stimulated with anti-IgM over three days and the level of CD69, CD71, CD80, CD86, CD95 and MHC Class II were assessed by flow cytometry. Both WNK1-deficient B cells and control B cells upregulate all activation markers after stimulation with anti-IgM but WNK1-deficient B cells displayed differences in the levels of upregulation (Figure 4.7). There was an increase in CD80 at day 3 and CD95 at days 2 and 3 in WNK1-deficient B cells. Contrastingly, there was a decrease in levels of MHC Class II at days 2 and 3 in B cells lacking WNK1 compared to control B cells.

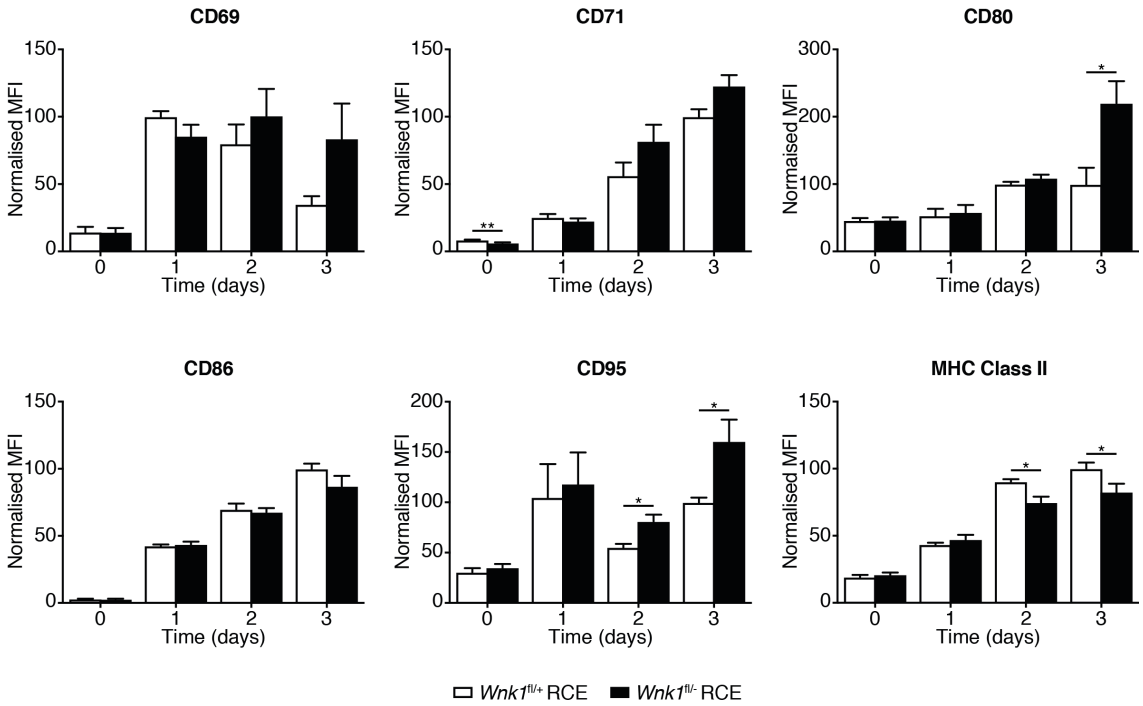

Figure 4.7 Upregulation of Activation Markers After Stimulation Through the BCR

Bar graphs showing mean ± S.E.M. normalised MFI of CD69, CD71, CD80, CD86, CD95 and MHC Class II on *Wnk1*$^{fl/+}$ RCE and *Wnk1*$^{fl/-}$ RCE B cells after stimulation with anti-IgM F(ab)$_2$ for 1, 2 and 3 days (n=5-6). MFI values were normalised to the peak response in *Wnk1*$^{fl/+}$ RCE B cells, which was set to 100. Statistical analysis was carried out using a Mann-Whitney U-test; * $p<0.05$, ** $p<0.01$.

To address how activation markers change upon T-cell help in B cells lacking WNK1, I assessed changes in B cell activation markers after stimulation with CD40L. Figure 4.8 shows that WNK1-deficient B cells upregulated surface levels of activation markers after stimulation with CD40L, but the levels of CD69, CD80, CD86, CD95 were higher in WNK1-deficient B cells compared to control B cells. In contrast, levels of ICOSL and MHC class II were lower in WNK1-deficient B cells than in control B cells. These data show that WNK1 is not required for upregulation of activation markers in response to stimulation with anti-IgM or CD40L. However, WNK1 does regulate the level of upregulation of these markers.

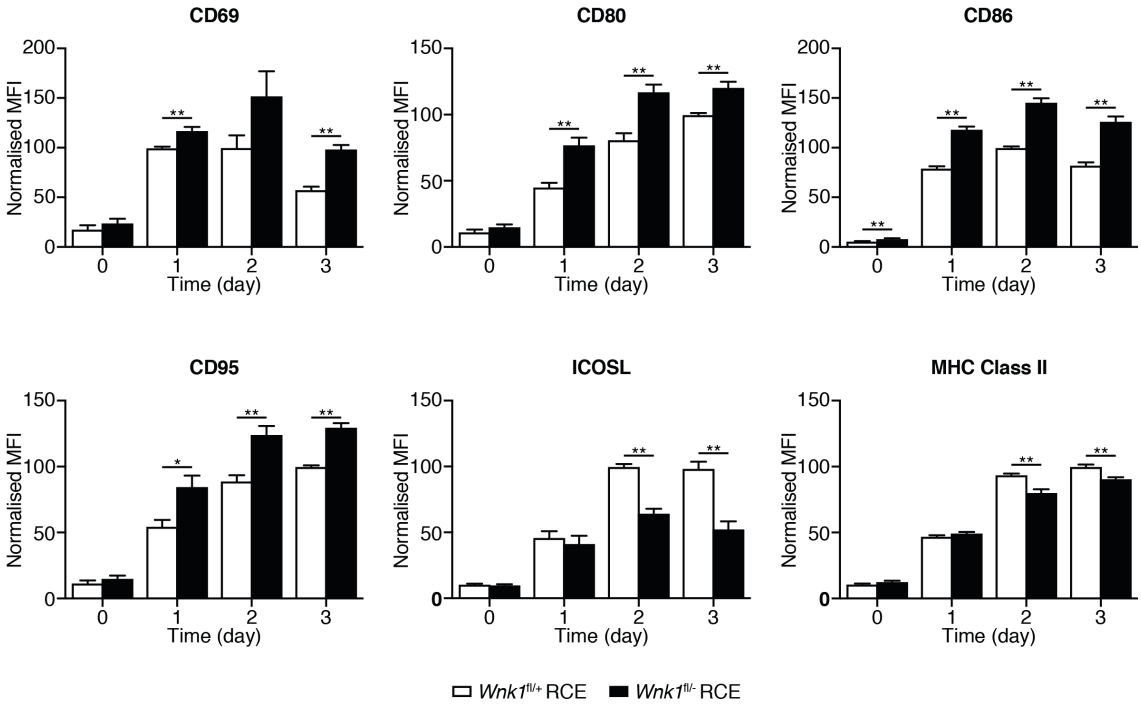

Figure 4.8 Upregulation of Activation Markers After Stimulation Through CD40

Bar graphs showing mean ± S.E.M. normalised MFI of CD69, CD80, CD86, CD95, ICOSL and MHC Class II on *Wnk1*$^{fl/+}$ RCE and *Wnk1*$^{fl/-}$ RCE B cells after stimulation with recombinant murine CD40L for 1, 2 and 3 days (n=6). MFI values were normalised to the peak response in *Wnk1*$^{fl/+}$ RCE B cells, which was set to 100. Statistical analysis was carried out using a Mann-Whitney U-test; * $p<0.05$, ** $p<0.01$.

4.1.6 Activated WNK1-Deficient B Cells Have Higher Forward Scatter Area After Stimulation with CD40L

Upon activation, B cells increase in size which can be detected using flow cytometry and measuring forward scatter (FSC) (Bondada *et al.*, 2003). I measured the FSC of *Wnk1*$^{fl/+}$ RCE and *Wnk1*$^{fl/-}$ RCE B cells after stimulation with anti-IgM or CD40L. WNK1-deficient B cells displayed increased FSC after stimulation with anti-IgM and CD40L, indicating that WNK1-deficient B cells are activated (Figure 4.9A and B). There was no difference in the FSC between WNK1-deficient and control cells after stimulation with anti-IgM (Figure 4.9A). However, there was an increase in FSC in WNK1-deficient B cells compared to control B cells after stimulation with CD40L (Figure 4.9B). This suggests that WNK1 may regulate cell volume after stimulation with CD40L but not with anti-IgM.

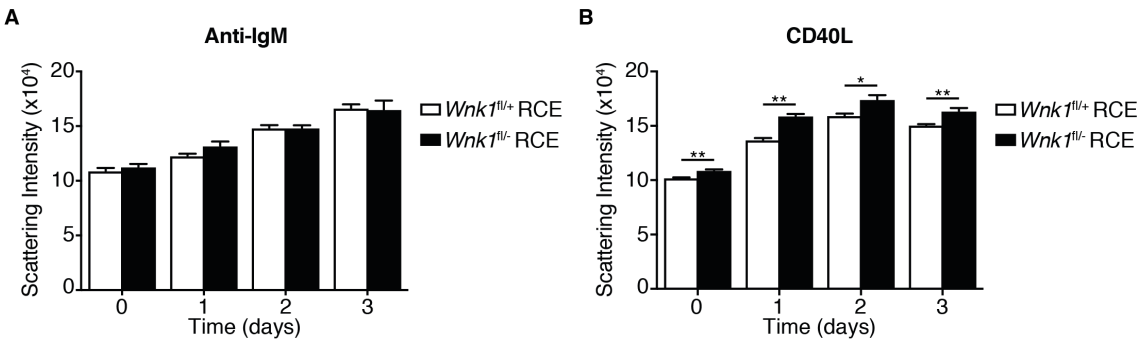

Figure 4.9 WNK1-Deficient B Cells Display Higher FSC After CD40L Stimulation

Bar graphs showing mean ± S.E.M. scattering index for forward scatter of *Wnk1*$^{fl/+}$ RCE and *Wnk1*$^{fl/-}$ RCE B cells stimulated with anti-IgM F(ab)$_2$ (**A**) or recombinant murine CD40L (**B**) for 1, 2 and 3 days (n=6). Statistical analysis was carried out using a Mann-Whitney U-test; * $p<0.05$, ** $p<0.01$.

4.1.7 WNK1 Regulates Cytokine Secretion in WNK1-Deficient B Cells After Anti-IgM Stimulation

B cells are able to secrete a subset of cytokines after activation and this is a further hallmark of their activation. Previous work by Harald Hartweger in our group showed that IL-6, IL-10, TNF-α and VEGF-A are secreted by B cells at detectable levels following *in vitro* stimulation with anti-IgM and CD40L (Hartweger *et al.*, 2014). I tested supernatants from either *Wnk1*$^{fl/+}$ RCE B cells or *Wnk1*$^{fl/-}$ RCE B cells stimulated with either medium alone, anti-IgM or CD40L for 3 days. There was no difference in secretion of IL-6, IL-10 and TNF-α and a trend for a decrease in VEGF-A when *Wnk1*$^{fl/-}$ RCE B cells were stimulated with CD40L when compared to *Wnk1*$^{fl/+}$ RCE B cells (Figure 4.10). In contrast, to when *Wnk1*$^{fl/-}$ RCE B cells were stimulated through the BCR as they secreted more IL-10 and TNF-α compared to *Wnk1*$^{fl/+}$ RCE B cells (Figure 4.10).

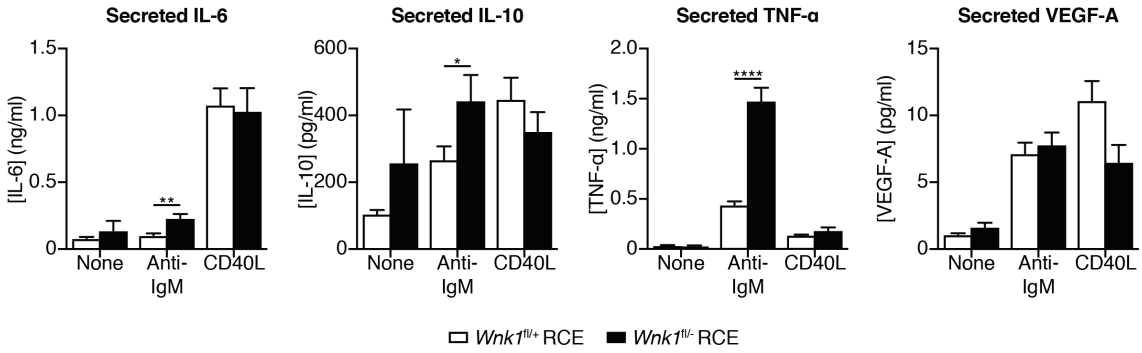

Figure 4.10 WNK1 Regulates Secretion of IL-10 and TNF-α

Bar graphs showing mean ± S.E.M. concentration of IL-6, IL-10, TNF-α and VEGF-A secreted by *Wnk1*$^{fl/+}$ RCE and *Wnk1*$^{fl/-}$ RCE B cells after 3-day stimulation *in vitro* with either medium alone, anti-IgM F(ab)$_2$ or recombinant murine CD40L (n=9-15). Statistical analysis was carried out using a Mann-Whitney U-test; * p<0.05, ** p<0.01, **** p<0.0001.

In summary, I have shown that WNK1-deficient B cells have defects in activation *in vitro*. These include a reduced ability to proliferate and to survive when stimulated through the BCR, CD40 and TLR4, as well changes in levels of activation markers and cytokine secretion. Signalling downstream of CD40, but not TLR4, induces a WNK1-dependent phosphorylation of OXSR1. However, WNK1-deficient B cells can undergo some aspects of activation, since stimulation induces secretion of cytokines and upregulation of activation markers. Taken together, these data suggest that WNK1 regulates activation of B cells stimulated with anti-IgM, CD40L and LPS.

4.2 Analysis of Antigen Processing and Presentation

4.2.1 WNK1-Deficient B Cells Have Defects in Antigen Presentation to CD4$^+$ T Cells

To further test whether WNK1 is required for other processes during B cell activation, I tested the ability of WNK1-deficient B cells to present antigen to CD4$^+$ T cells as this is crucial for a T-dependent antibody response. One method I used was testing the ability of B cells to present ovalbumin (OVA) peptides to OT-II CD4$^+$ T cells in an *in vitro* co-culture assay shown in Figure 4.11A. When OT-II CD4$^+$ T cells are co-cultured with *Wnk1*$^{fl/-}$ RCE B cells that have been loaded with OVA fewer entered division and those that divided underwent fewer divisions than cells cocultured with *Wnk1*$^{fl/+}$ RCE B cells (Figure 4.11B and C). This suggests a defect in antigen presentation, but, as shown previously, WNK1-deficient B cells have defects in survival and proliferation, which would lead to a decrease in number of antigen-presenting cells. Thus the reduced response of OT-II CD4$^+$ T cell to OVA-loaded WNK1-deficient B cells could be due to reduced numbers of B cells in the culture.

To circumvent these potentially confounding phenotypes, I measured presentation of Eα peptide on MHC class II in a short-term assay by delivering the peptide on fluorescent microspheres coated with anti-IgM (Figure 4.12A). As levels of MHC class II increase upon activation (Figure 4.12B), I normalised the MFI of Eα-MHC class II to the MFI of total MHC class II. As shown in Figure 4.12C *Wnk1*$^{fl/-}$ RCE B cells were able to present antigen on MHC class II as shown by the increase in Eα-MHC class II over time but they presented less antigen compared to *Wnk1*$^{fl/+}$ RCE B cells. This reduced presentation of peptides may contribute to the reduced proliferation seen in OT-II CD4$^+$ T cells co-cultured with WNK1-deficient B cells loaded with OVA.

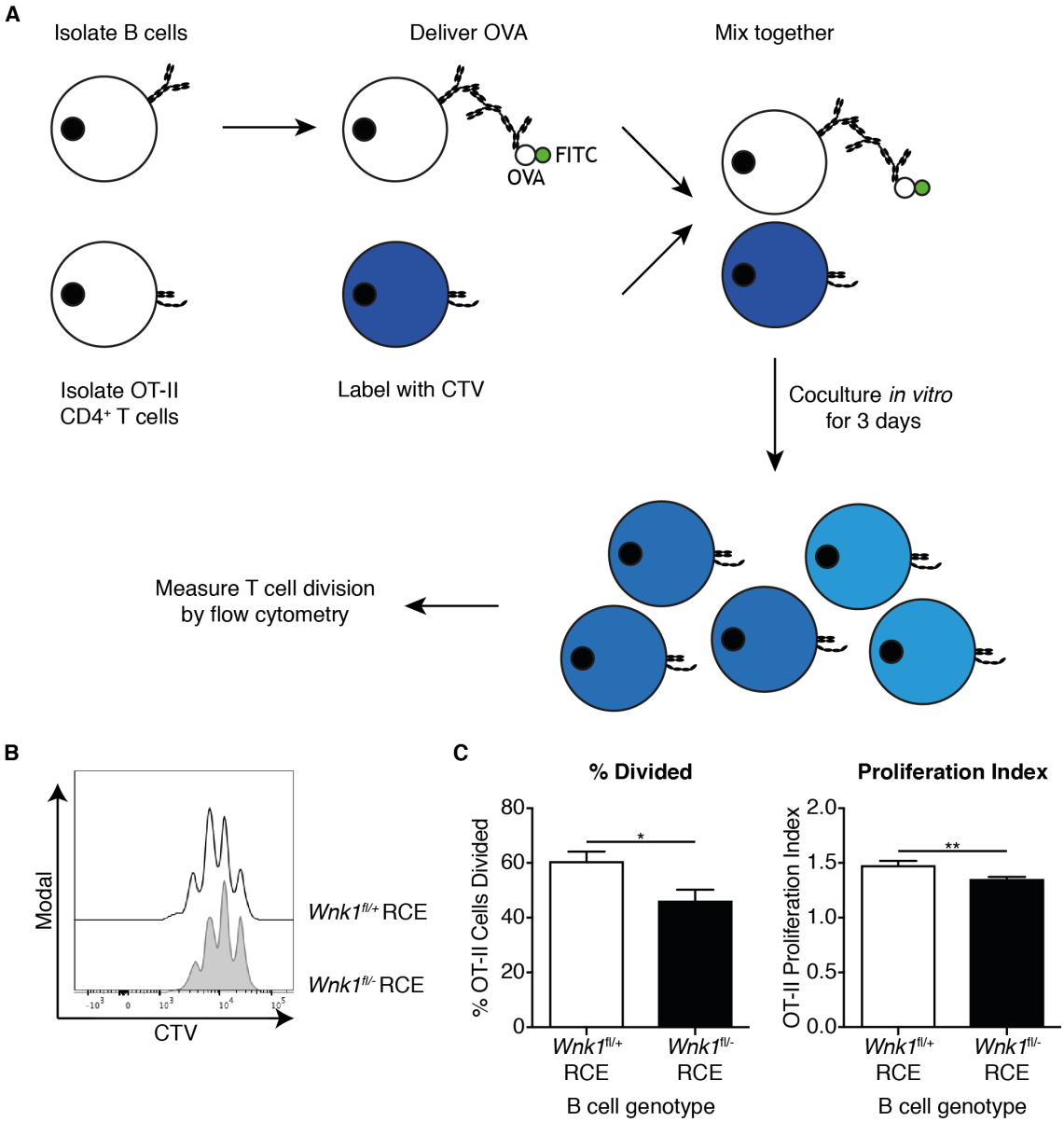

Figure 4.11 WNK1-Deficient B Cells Display Defects in Antigen Presentation to T Cells

(**A**) Schematic of antigen presentation to OT-II T cells. B cells were loaded with ovalbumin (OVA) by incubating the cells with biotinylated anti-IgM $F(ab)_2$ followed by anti-biotin antibody coupled to OVA and FITC. These B cells were then cocultured with CTV-labelled OT-II T cells for 3 days and division of the T cells was determined by flow cytometry. (**B**) Overlay of representative histograms of CTV fluorescence of OT-II T cells cocultured with either *Wnk1*$^{fl/+}$ RCE or *Wnk1*$^{fl/-}$ RCE B cells. (**C**) Bar graphs showing mean ± S.E.M. percentage of cells that had divided at least once and the proliferation index of OT-II T cells when cocultured with either *Wnk1*$^{fl/+}$ RCE or *Wnk1*$^{fl/-}$ RCE B cells (n=10). Statistical analysis was carried out using a Mann-Whitney U-test; * $p<0.05$, ** $p<0.01$.

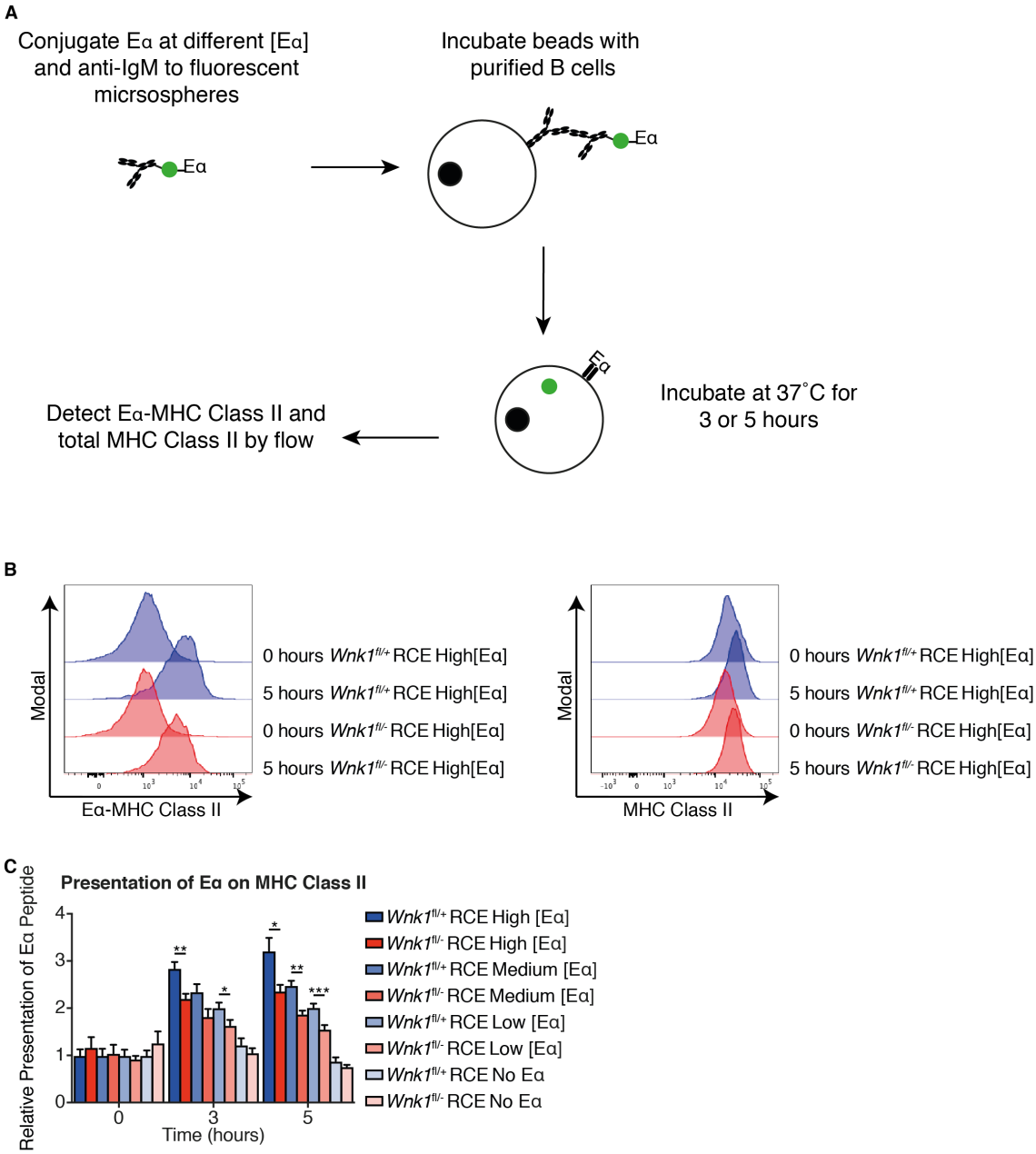

Figure 4.12 Presentation of Peptides is Impaired in B Cells Lacking WNK1

(**A**) Schematic of antigen presentation of Eα peptide on B cells. Purified B cells were loaded with fluorescent microspheres coated with biotinylated anti-IgM F(ab)$_2$ (1.38 μg/10^9 microspheres) and three doses of biotinylated Eα peptide (high: 2.76 μg/10^9 microspheres, medium: 1.38 μg/10^9 microspheres, and low: 0.08 μg/10^9 microspheres). Some B cells were loaded with fluorescent microspheres coated with biotinylated anti-IgM F(ab)$_2$ alone. Then they were incubated at 37°C for 0, 3 and 5 hours before fixation and detection of Eα on MHC class II and total MHC class II by flow cytometry. (**B**) Overlay of representative histograms of Eα on MHC class II (left) and total MHC class II (right) on *Wnk1*$^{fl/+}$ RCE and *Wnk1*$^{fl/-}$ RCE B cells after 0 and 5 hours of stimulation with a high concentration of Eα, gated on FITC$^+$B220$^+$ cells. (**C**) Bar graph showing mean ± S.E.M. normalised levels of Eα on MHC class II on *Wnk1*$^{fl/+}$ RCE and *Wnk1*$^{fl/-}$ RCE B cells incubated with microspheres coated with a range of Eα concentrations for the times shown (n=7). Statistical analysis was carried out using a Mann-Whitney U-test; * p<0.05, ** p<0.01, *** p<0.001.

4.2.2 WNK1-Deficient B Cells Internalise More Soluble Antigen

Since many cellular processes are involved in antigen presentation, I next tested one of the first to occur: antigen internalisation. I carried out a soluble antigen internalisation assay by using flow cytometry to determine changes in levels of biotin on the surface of B cells stimulated with biotinylated anti-kappa antibody (Figure 4.13A). I used the following formula to calculate percentage of antigen internalised at time x:

$$= \frac{\text{gMFI(Streptavidin at 0 minutes)} - \text{gMFI(Streptavidin at x minutes)}}{\text{gMFI(Streptavidin at 0 minutes)}} * 100$$

I measured the internalisation of antigen by B cells from *Wnk1*$^{fl/+}$ RCE and *Wnk1*$^{fl/-}$ RCE mice and found that WNK1-deficient B cells displayed a marginal increase in the percentage of antigen internalised (Figure 4.13B and C). This suggests that WNK1 possibly negatively regulates soluble antigen internalisation in B cells.

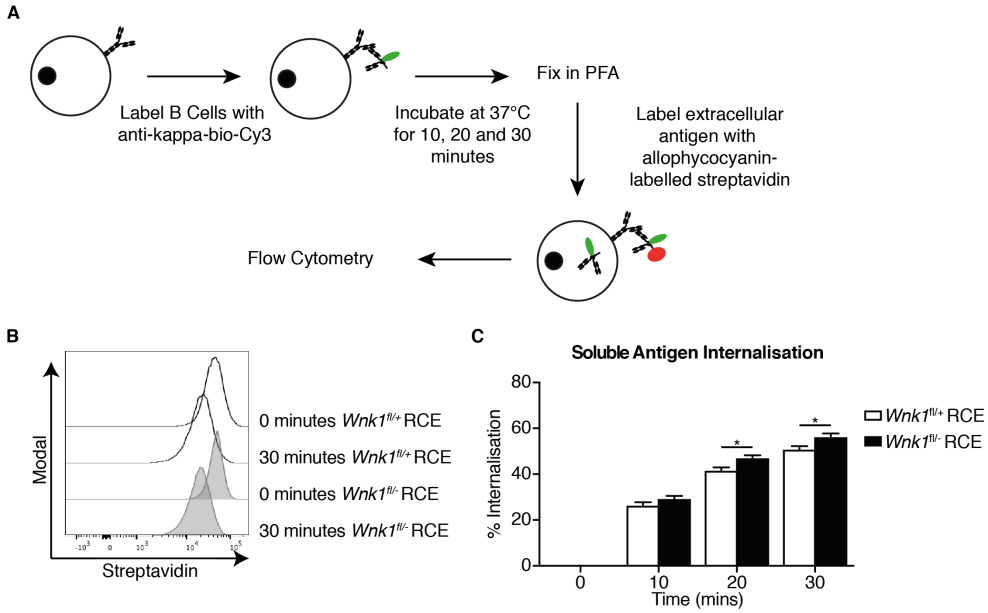

Figure 4.13 WNK1-Deficient B Cells Internalise Soluble Antigen

(**A**) Schematic of soluble antigen internalisation assay. B cells were stimulated with biotinylated anti-IgM F(ab)$_2$ labelled with Cy3 (green) for 0, 10, 20 or 30 minutes at 37°C before fixation with PFA. Streptavidin-allophycocyanin (red) labelling was used to measure levels of surface bound biotinylated anti-IgM F(ab)$_2$ by flow cytometry. (**B**) Overlay of representative histograms showing levels of streptavidin fluorescence in *Wnk1*$^{fl/+}$ RCE and *Wnk1*$^{fl/-}$ RCE B cells after 0 and 30 minutes of stimulation gated on Cy3$^+$B220$^+$ cells. (**C**) Bar graph showing mean ± S.E.M. percentage of antigen internalisation of *Wnk1*$^{fl/+}$ RCE and *Wnk1*$^{fl/-}$ RCE B cells at the times shown (n=8). Statistical analysis was carried out using a Mann-Whitney U-test; * p<0.05.

4.2.3 Antigen Degradation is not Regulated by WNK1

After B cells internalise antigen through their BCR, the antigen-containing endosomes are trafficked to the lysosome for degradation to take place. Figure 4.14A shows a schematic of the assay I used to measure antigen degradation. B cells were stimulated with biotinylated anti-IgM and immunoblotting techniques were used to measure amount of biotinylated IgH and IgL over time after stimulation. There was no difference between *Wnk1*$^{fl/+}$ RCE and *Wnk1*$^{fl/-}$ RCE B cells in their ability to degrade antigen in this set up (Figure 4.14B).

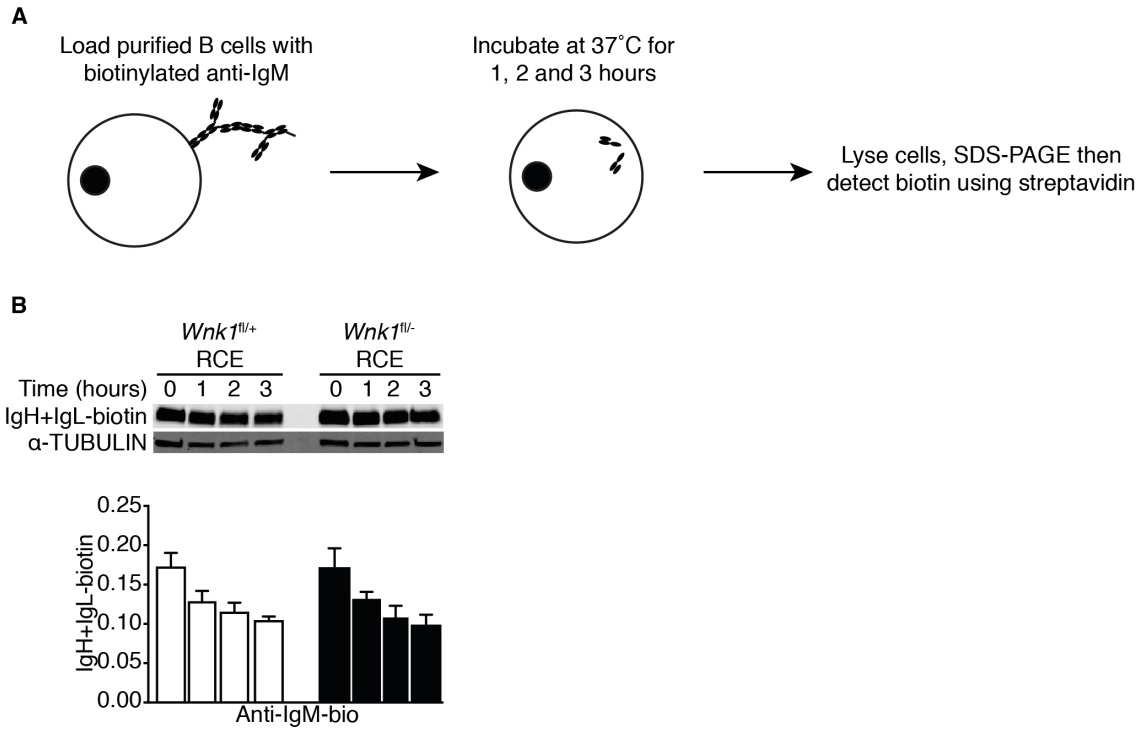

Figure 4.14 WNK1 Deficiency does not Affect Antigen Degradation

(**A**) Schematic of soluble antigen internalisation assay. B cells were stimulated with biotinylated anti-IgM F(ab)$_2$ for 0, 1, 2 or 3 hours at 37°C before lysing cells and assessing levels of biotinylated IgH and IgL by immunoblot with streptavidin. (**B**) Representative immunoblots of B cells from either *Wnk1*$^{fl/+}$ RCE and *Wnk1*$^{fl/-}$ RCE mice stimulated with biotinylated anti-IgM F(ab)$_2$ for the times shown and blotted with streptavidin and antibody against α-TUBULIN. Below is a bar graph showing the mean ± S.E.M. relative signal of IgH+IgL-biotin normalised to α-TUBULIN at the different time points (n=6). Statistical analysis was carried out using a Mann-Whitney U-test.

In summary, I have shown that WNK1 is a positive regulator of antigen presentation in B cells. This function of WNK1 is not through regulation of internalisation of soluble antigen or degradation since WNK1-deficient B cells internalise marginally more antigen than controls and display no difference in antigen degradation when compared to control B cells. Further investigation is required to determine how WNK1 regulates antigen presentation in B cells.

4.3 Discussion and Outstanding Questions

In this chapter I have shown that WNK1 is involved in processes during B cell activation; specifically in survival, proliferation and antigen presentation. Measurements of the ability of WNK1-deficient B cells to activate show that they exhibit some hallmarks of activation since they can secrete cytokines, increase FSC area, and upregulate activation markers after stimulation with either anti-IgM or CD40L. This shows that B cells lacking WNK1 retain the capability to respond to activation signals in spite of displaying defects in survival. There is dysregulation in secretion of cytokines when WNK1-deficient B cells are stimulated through their BCR but not when stimulated through CD40. Additionally, WNK1-deficient B cells display higher FSC compared to controls after stimulation with CD40L but not anti-IgM. These data highlight that WNK1 regulates signals from the BCR and CD40 differently and perhaps there are different signalling pathways stemming from WNK1 downstream of these two receptors. This is speculation as there is no data to support this statement but it would be interesting to compare the phosphoproteome of WNK1-deficient B cells to controls with both anti-IgM and CD40L stimulation in an attempt to unravel this difference further.

In addition, there is also moderate dysregulation of level of upregulation of activation markers. When stimulated with anti-IgM or CD40L, there is an increase in CD69, CD80, CD86 and CD95 levels and a reduction in ICOSL and MHC class II in WNK1-deficient B cells. These changes may not have a consequence in the cell biology of the B cells as they are not large changes but this remains to be tested. However, many of these proteins are involved in the communication of B and T cells suggesting that this communication could be impaired. This is further confirmed by the antigen presentation to OT-II T cells assay, where there is less T cell division when WNK1-deficient B cells are cocultured. The activation markers of the B and T cells were not tested in this experiment, nor the proliferation of the B cells in the setting of receiving signal 1 and 2. Therefore, it would be worthwhile investigating both the levels of activation markers on both B and T cells and B cell proliferation in this experimental setup.

The levels of CD80, CD86, ICOSL and MHC Class II may not be the only contributing factor in reduced T cell proliferation in the OT-II antigen presentation assay. The reduction in the number of B cells on day 3 after stimulation with anti-IgM

is a confounding factor. This means there are less cells to act at antigen presenting cells to the T cells, which could have an impact on the division of the T cells. Therefore, the direct measurement of antigen presentation using Eα peptide is a better approach to test antigen presentation in WNK1-deficient B cells. This revealed that there is a reduced capability to present peptides on MHC class II when B cells lack WNK1. This is not due to defects in antigen internalisation or degradation as these are comparable between WNK1-deficient and control B cells. The mechanism by which WNK1 regulates antigen presentation remains unknown. There are several processes that I have not tested that could be regulated by WNK1, such as fusion of the endolysosome with MHC class II containing vesicles, peptide loading on MHC class II by regulation of H2-M or similar regulatory proteins, and transport of MHC class II loaded with peptides to the plasma membrane.

As well as there being defects in signals derived from B cells to T cells, there are defects in signals B cells receive from T cells. This is shown by reduced cell recovery when WNK1-deficient B cells are stimulated with CD40L, and CD40L and IL-4. I showed that there was WNK1-dependent phosphorylation induced by CD40L stimulation. As WNK1 is activated by CD40L stimulation, the major signal from T cells providing help to B cells, it is possible that B cell responses to T cell help are impaired in an *in vivo* setting but this remains to be directly tested. Unlike the OXSR1 phosphorylation induced by anti-IgM and CXCL13, CD40L-induced phosphorylation of OXSR1 is not dependent on PI3K and only partially dependent on AKT. The signalling mediators downstream of CD40 signalling that activate WNK1 remain undetermined. As TRAFs (TRAF1, TRAF2, TRAF 3, TRAF5 and TRAF6) are known to be recruited to CD40, it could be that WNK1 is activated downstream of any of these signalling mediators. WNK1 is not known to associate with any TRAFs so it could be indirect activation through downstream signalling molecules. Further investigation is required to unravel the regulation of WNK1 downstream of CD40 stimulation.

The major function of WNK1 is positive regulation of proliferation after B cell activation, with the kinase function of WNK1 being critical for this role. WNK1 has previously been described to positively regulate proliferation in neural progenitor cells, although they did not measure survival of the cells in this study (Sun *et al.*, 2006). Additional work has shown that WNK1 is localised at spindles during metaphase and knock-down of WNK1 leads to defects in abscission in HeLa cells

(Tu *et al.*, 2011). In this chapter, I have shown that WNK1-deficient B cells or cells where WNK1 has been inhibited display a reduced capability to divide upon stimulation through the BCR or CD40. The defect in proliferation is not solely due to a defect in survival as survival can be rescued by overexpression of BCL-X_L but the defect in entry into cell division is not. It appears that overexpression of BCL-X_L leads to a decrease in percentage of cells dividing as there is a trend for fewer cells entering division in B cells overexpressing BCL-X_L. This is most likely due to more cells surviving without dividing, however it is possible that overexpression of BCL-X_L has an impact on cell division in B cells.

It remains to be shown whether the regulation of cell division by WNK1 is due to either regulation of entry into the cell cycle, regulation of the cell cycle as a whole or regulation of mitosis as would be suggested by work in HeLa cells and rat vascular smooth muscle cells (Tu *et al.*, 2011, Zhang *et al.*, 2018b). WNK1 has been implicated in the regulation of cyclins (Zhang *et al.*, 2018a). The regulation of cyclins could be mediated by WNK1 in B cells. MYC controls transcription of pro-proliferative genes, such as cyclins and ribosomal genes. However, upregulation of MYC is unaffected by the deletion of *Wnk1*, suggesting that transcription of cyclins may be unaffected in WNK1-deficient B cells, but this has not been directly shown. Cyclins are not only transcriptionally controlled; there is also translational regulation as well as post-translational modifications that regulate their activity. Thus, it is possible that WNK1 may regulate cell cycle progression through regulation of cyclins at either the translational or post-translational levels, but further work would be required to test these hypotheses.

The regulation of ion homeostasis by WNK1 through NKCC1 is not the mechanism by which it regulates proliferation in B cells, as shown by bumetanide not having an effect on cells entering division. This does not exclude ion movement from regulating cell division in B cells as NKCC1 may have a redundant role and other ion channels may compensate for the lack of transport through NKCC1. It remains unclear whether OXSR1 is involved in proliferation in B cells. Previous work indicates that OXSR1 is not localised to mitotic spindles and knock-down of OXSR1 leads to no defects in mitosis (Tu *et al.*, 2011). However, there is no quantification in this paper, so it remains unclear if there is a partial reduction in cell division or redundancy by expression of *Stk39* compensating for the lack of *Oxsr1* expression. To investigate whether OXSR1 is required for B cell division, a conditional knockout

of *Oxsr1* would need to be utilised due to the lack of mature B cells found in the *Oxsr1*$^{T185A/T185A}$ bone marrow chimeras. The *Oxsr1*^{fl} mice were not available during the time frame of this PhD project.

Chapter 5. Role of WNK1 in B Cells During an Immune Response

I have shown in the previous chapters that WNK1 regulates antigen presentation, proliferation, migration, survival and adhesion of B cells. In this chapter, I aimed to determine whether WNK1 has a function in B cells during an immune response, specifically a T-dependent antibody response. I explored this by using model antigen immunisations, transgenic mice with a fixed BCR and mice with Cre under the control of the *Aicda* promoter.

5.1 WNK1-Deficient B Cells Mount a Defective Antibody Response to NP-CGG

In order to assess the ability of WNK1-deficient B cells to partake in an immune response, I needed to restrict the deletion of *Wnk1* to B cells to eliminate potential effects of the *Wnk1* knockout in other cell types. $\mu MT^{-/-}$ mice have no mature B cells (Kitamura *et al.*, 1991) and their bone marrow can be mixed with mutant bone marrow to reconstitute irradiated $Rag1^{-/-}$ mice. In the resulting mixed chimeric mice all B cells carry the mutated allele. The majority of cells of other haematopoietic cell types do not carry the mutated allele and thus the mutation is expected to have little impact on these other cell types. Together with Harald Hartweger, $\mu MT^{-/-}$ mixed bone marrow chimeras were made with either $Wnk1^{fl/+}$ RCE or $Wnk1^{fl/-}$ RCE bone marrow. These chimeras are named $\mu MT^{-/-}$ + $Wnk1^{fl/+}$ RCE and $\mu MT^{-/-}$ + $Wnk1^{fl/-}$ RCE mice respectively. Seven days after initial injection of tamoxifen, the mice were immunised with the hapten NP coupled to chicken gamma globulin (CGG) (NP-CGG) in alum. I tracked the immune response by measuring NP-specific antibodies in the blood by ELISA and differentiation into germinal centre and plasma cells by flow cytometry (Figure 5.1A). When $\mu MT^{-/-}$ + $Wnk1^{fl/-}$ RCE mice were immunised, there was a failure of the B cells to differentiate into germinal centre cells as shown by reduced numbers of NP-specific germinal centre cells, including both unswitched IgM^+ and switched $IgG1^+$ germinal centre cells, in comparison to $\mu MT^{-/-}$ + $Wnk1^{fl/+}$ RCE mice up to day 14 post immunisation (Figure 5.1B). A similar result was observed in NP-specific plasma cells where $\mu MT^{-/-}$ + $Wnk1^{fl/-}$ RCE mice had fewer total NP-specific plasma

cells than $\mu MT^{-/-}$ + $Wnk1^{fl/+}$ RCE mice. No NP-specific $IgG1^+$ plasma cells were observed in $\mu MT^{-/-}$ + $Wnk1^{fl/-}$ RCE mice, in contrast to the increase seen in $\mu MT^{-/-}$ + $Wnk1^{fl/+}$ RCE mice after immunisation. From day 0 to day 7 post immunisation, there was a small increase in NP-specific plasma cells that were IgM^+ in both $\mu MT^{-/-}$ + $Wnk1^{fl/+}$ RCE and $\mu MT^{-/-}$ + $Wnk1^{fl/-}$ RCE mice (Figure 5.1B). However by day 14 there were many fewer WNK1-deficient IgM^+ plasma cell compared to controls.

Harald Hartweger performed an ELISA to measure NP-specific IgM and IgG1 antibodies in the serum of $\mu MT^{-/-}$ + $Wnk1^{fl/+}$ RCE mice and $\mu MT^{-/-}$ + $Wnk1^{fl/-}$ RCE mice before and after immunisation with NP-CGG in alum. As can be seen in Figure 5.1C, there was no detectable secretion of NP-specific IgM or IgG1 in $\mu MT^{-/-}$ + $Wnk1^{fl/-}$ RCE mice while there was an increase in concentration of serum NP-specific IgM and NP-specific $IgG1^+$ in $\mu MT^{-/-}$ + $Wnk1^{fl/+}$ RCE mice after immunisation. These data together show that WNK1 is required in B cells for their differentiation into germinal centre B cells and plasma cells, and for the secretion of antigen-specific antibodies.

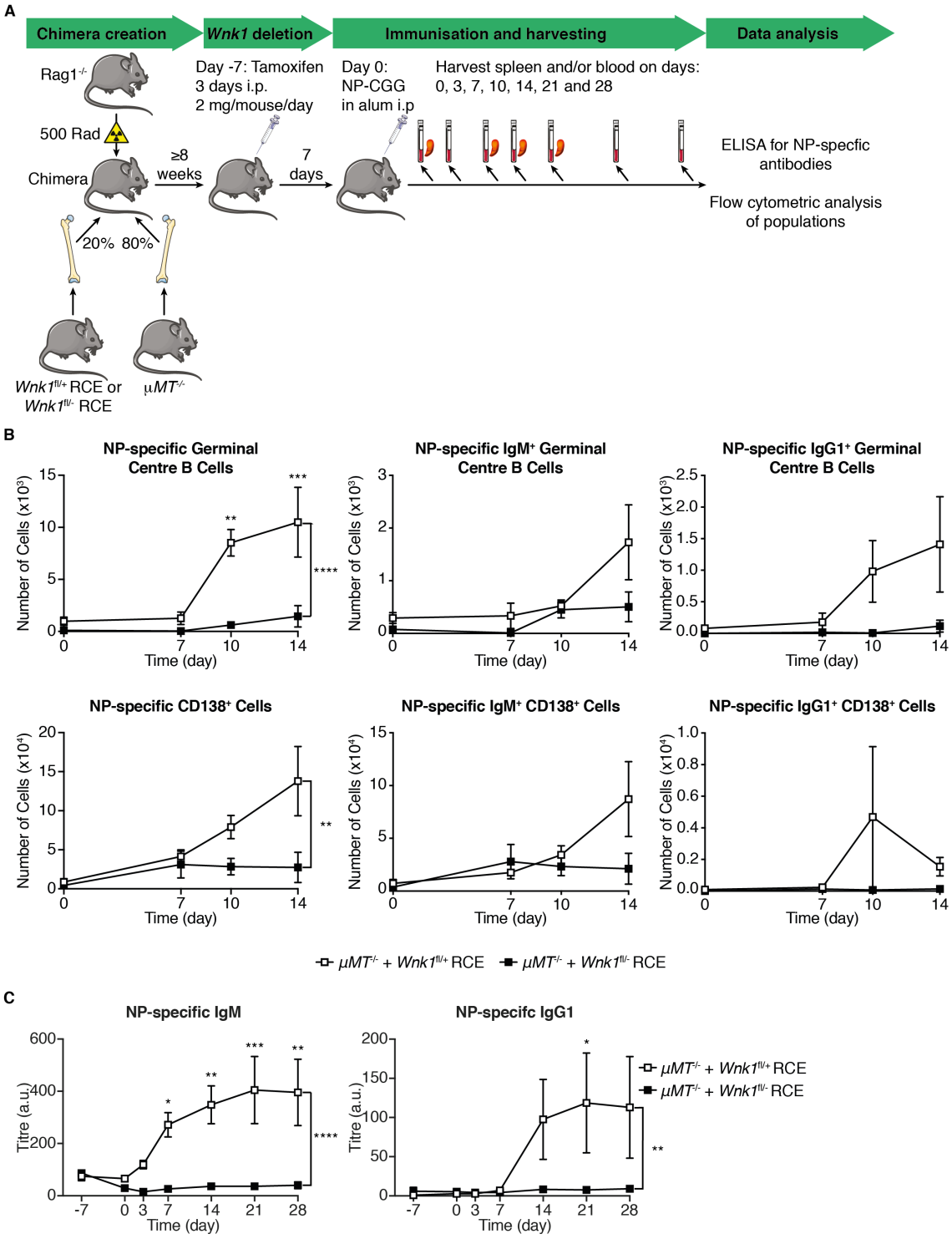

Figure 5.1 WNK1 is Required in B Cells for Antigen-Specific Antibody Responses and Differentiation

(**A**) Schematic of generation of *μMT*$^{-/-}$ mixed bone marrow chimeras and subsequent immunisation with NP-CGG in alum. Bone marrow chimeras were generated by reconstituting irradiated *Rag1*$^{-/-}$ mice with a mix of bone marrow cells from either *Wnk1*$^{fl/+}$ RCE or *Wnk1*$^{fl/-}$ RCE mice and *μMT*$^{-/-}$ mice at a 4:1 ratio. After reconstitution for ≥ 8 weeks, mice were injected with tamoxifen. Seven days later they were injected with NP-CGG in alum and at the indicated days spleens and/or blood were harvested. NP-specific antibodies were analysed by ELISA and B cell

populations were analysed by flow cytometry. (**B**) Line graphs showing mean ± S.E.M. number of NP-specific germinal centre cells ($B220^+$ $CD19^+$ Fas^+ $GL7^+$ NP^+), NP-specific IgM^+ germinal centre cells ($B220^+$ $CD19^+$ Fas^+ $GL7^+$ NP^+ IgM^+), NP-specific $IgG1^+$ germinal centre cells ($B220^+$ $CD19^+$ Fas^+ $GL7^+$ NP^+ $IgG1^+$), NP-specific $CD138^+$ cells ($B220^-$ $CD138^+$ NP^+), NP-specific IgM^+ $CD138^+$ cells ($B220^-$ $CD138^+$ NP^+ IgM^+) and NP-specific $IgG1^+$ $CD138^+$ cells ($B220^-$ $CD138^+$ NP^+ $IgG1^+$) in $\mu MT^{-/-}$ + $Wnk1^{fl/+}$ RCE and $\mu MT^{-/-}$ + $Wnk1^{fl/-}$ RCE mice immunised with NP-CGG in alum (n=3-4). (**C**) Work done by Harald Hartweger. Line graphs showing mean ± S.E.M. antibody titres of NP-specific IgM and NP-specific IgG1 as measured in arbitrary units (a.u.) in $\mu MT^{-/-}$ + $Wnk1^{fl/+}$ RCE and $\mu MT^{-/-}$ + $Wnk1^{fl/-}$ RCE mice immunised with NP-CGG in alum (n=4-5). Statistical analysis was carried out using a two-way ANOVA with multiple comparisons; * $p<0.05$, ** $p<0.01$, *** $p<0.001$, **** $p<0.0001$. Asterisks outside bracket indicate significant difference between genotypes from the two-way ANOVA analysis. Asterisks above points indicate significant difference using multiple comparisons from the two-way ANOVA analysis.

5.2 WNK1 is Required for Activation of B Cells *in vivo*

Since WNK1-deficient B cells fail to differentiate into germinal centre cells, I wanted to assess their ability to activate *in vivo* to determine if they fail to become germinal centre cells due to defective activation. In order to measure activation of WNK1-deficient B cells, I needed to generate control and knockout B cells that are specific for an antigen. Thus, I utilised MD4 transgenic mice, which have a fixed BCR specific for hen egg lysozyme (HEL) coupled to the inducible knock-out of *Wnk1*. MD4^{+} *Wnk1*$^{fl/+}$ RCE or MD4^{+} *Wnk1*$^{fl/-}$ RCE to use as donors for bone marrow chimeras. These chimeras were treated with tamoxifen and 7 days later I isolated B cells from these chimeras and labelled them with CMFDA before transferring them into congenically marked *Ptprc*$^{a/b}$ (CD45.1/CD45.2 F1) mice. I immunised these mice with either sheep red blood cells (SRBC) or HEL coupled to SRBC (HEL-SRBC) (Figure 5.2A). To assess the ability of MD4^{+} *Wnk1*$^{fl/+}$ RCE and MD4^{+} *Wnk1*$^{fl/-}$ RCE B cells to become activated, I analysed the levels of activation markers on transferred B cells 3 days after transfer and immunisation. I compared these between genotypes, and between those that received HEL and those that did not. Figure 5.2B shows that in response to HEL-SRBC, MD4^{+} *Wnk1*$^{fl/-}$ RCE B cells failed to upregulate CD69 and CD80 compared to MD4^{+} *Wnk1*$^{fl/+}$ RCE B cells and showed no increase compared to B cells from mice immunised with SRBC only. CD86 was upregulated on MD4^{+} *Wnk1*$^{fl/-}$ RCE B cells but to a lower extent than on MD4^{+} *Wnk1*$^{fl/+}$ RCE B cells, whereas there was no difference in the upregulation of MHC class II between the genotypes. I wanted to determine if there were differences in proliferation at this time point but unfortunately the CMFDA signal was insufficient for FlowJo to measure division. These data indicate that WNK1-deficient B cells are unable to become fully activated *in vivo* as they are unable to upregulate CD69 or CD80. However, they are able to be partially activated as they upregulate CD86 and MHC class II in an antigen-dependent manner.

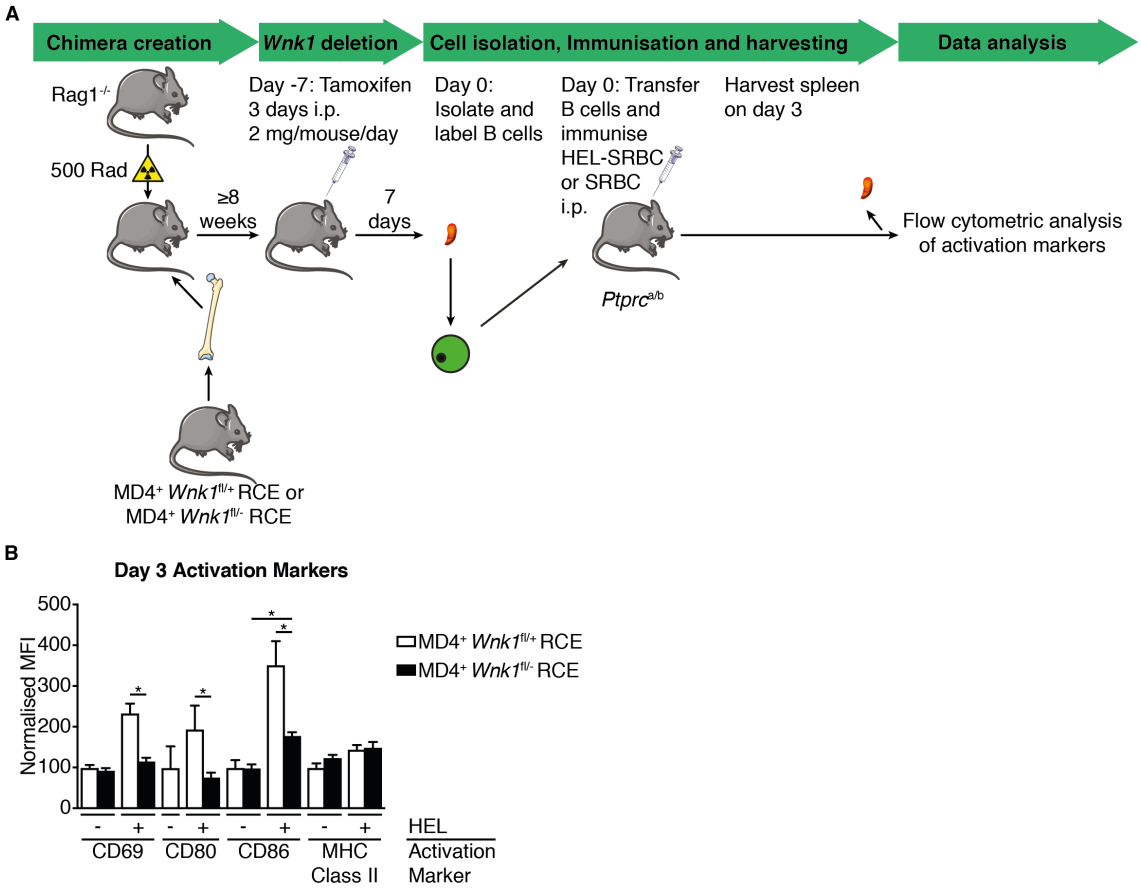

Figure 5.2 WNK1 is Required in B Cells for B Cell Activation *in vivo*

(**A**) Schematic of generation of MD4$^+$ *Wnk1*$^{fl/+}$ RCE and MD4$^+$ *Wnk1*$^{fl/-}$ RCE mice, subsequent transfer of isolated B cells and immunisation with HEL-SRBC. Bone marrow chimeras were generated by reconstituting irradiated *Rag1*$^{-/-}$ mice with a mix of bone marrow cells from either MD4$^+$ *Wnk1*$^{fl/+}$ RCE or MD4$^+$ *Wnk1*$^{fl/-}$ RCE mice. After reconstitution for ≥ 8 weeks, mice were injected with tamoxifen, and B cells were isolated 7 days later and labelled with CMFDA (green). These cells were transferred into *Ptprc*$^{a/b}$ mice intravenously and the recipients were immunised with either SRBC or HEL-SRBC. Three days later the mice were culled, spleens harvested and flow cytometry was used to measure activation markers. (**B**) Bar graph showing mean ± S.E.M. normalised MFI of CD69, CD80, CD86 and MHC class II on MD4$^+$ *Wnk1*$^{fl/+}$ RCE and MD4$^+$ *Wnk1*$^{fl/-}$ RCE B cells from mice that were immunised with either SRBC (-) or HEL-SRBC (+) (n=3-4). The MFI was normalised to the average MFI of each marker on MD4$^+$ *Wnk1*$^{fl/+}$ RCE B cells from mice that received SRBC only, which was set to 100. Statistical analysis was carried out using a Mann-Whitney U-test; * $p<0.05$.

5.3 NKCC1 is not Required in B Cells to Mount an Antibody Response to NP-CGG

WNK1 activates NKCC1 (SLC12A2) through phosphorylation of OXSR1, which in turn phosphorylates NKCC1. This phosphorylation event activates NKCC1 and opens the channel allowing sodium, potassium and chloride ions to enter the cell. To assess whether NKCC1 plays a role in the immune response of B cells, I generated mixed foetal liver chimeras with $\mu MT^{-/-}$ foetal liver and with either $Slc12a2^{+/+}$ or $Slc12a2^{-/-}$ foetal liver so that all the B cells were either $Slc12a2^{+/+}$ or $Slc12a2^{-/-}$ and the majority of other haematopoietic cells were WT. These mice are named $\mu MT^{-/-}$ + $Slc12a2^{+/+}$ and $\mu MT^{-/-}$ + $Slc12a2^{-/-}$ respectively. I immunised these mice with NP-CGG or CGG alone and then measured NP-specific antibodies in the serum and differentiated B cell populations at day 14 post-immunisation (Figure 5.3A). One caveat with the interpretation of these results is that there were NP-specific germinal centre cells in mice that only received CGG, indicating that there was either an issue with the staining or the immunisation. Despite this, there is no difference between total number of germinal centre cells, including IgM^+ and $IgG1^+$ germinal centre B cells, nor in the number of plasma cells (Figure 5.3B). Furthermore, there was no difference in the concentration of NP-specific IgM or NP-specific IgG1 in the serum (Figure 5.3C). Since this experiment is suboptimal, it will need to be repeated. Despite this, these data suggest that NKCC1 is not required in B cells to mount an antigen-specific antibody response nor for differentiation into germinal centre B cells or plasma cells.

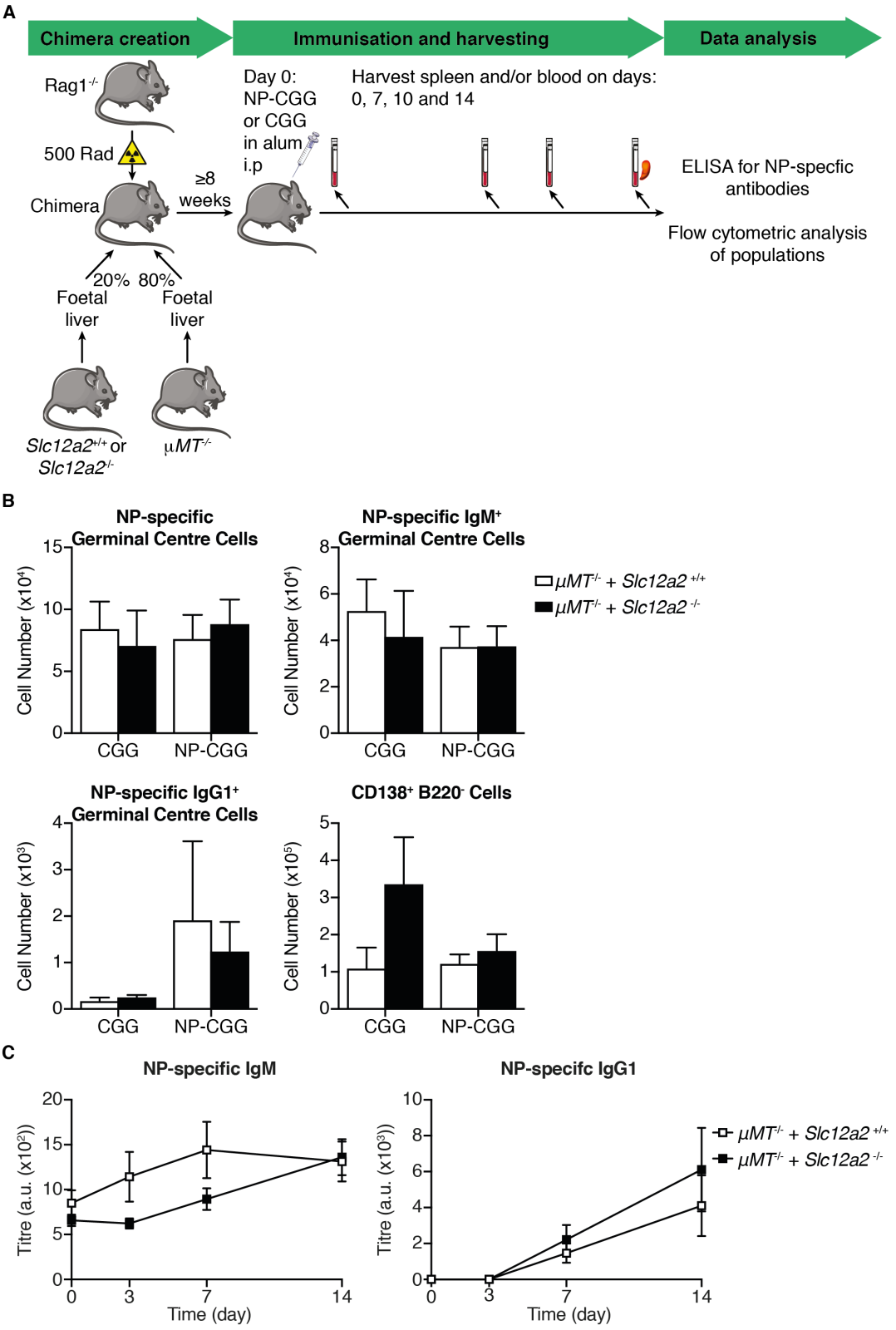

Figure 5.3 NKCC1 is not Required in B Cells for an Immune Response

(**A**) Schematic of generation of *μMT*$^{-/-}$ mixed foetal liver chimeras and subsequent immunisation with NP-CGG in alum. Foetal liver chimeras were generated by reconstituting irradiated *Rag1*$^{-/-}$ mice with a mix of foetal liver cells from either *Slc12a2*$^{+/+}$ or *Slc12a2*$^{-/-}$ mice and *μMT*$^{-/-}$ mice at a 4:1 ratio. After reconstitution for ≥ 8 weeks, mice were injected with NP-CGG or CGG alone in

alum and at the indicated days spleen and/or blood were harvested. NP-specific antibodies were analysed by ELISA and B cell populations were analysed by flow cytometry. (**B**) Bar graphs showing mean ± S.E.M. number of NP-specific germinal centre cells ($B220^+$ $CD19^+$ Fas^+ $GL7^+$ NP^+), NP-specific IgM^+ germinal centre cells ($B220^+$ $CD19^+$ Fas^+ $GL7^+$ NP^+ IgM^+), NP-specific $IgG1^+$ germinal centre cells ($B220^+$ $CD19^+$ Fas^+ $GL7^+$ NP^+I $gG1^+$) and total $CD138^+$ cells ($B220^-$ $CD138^+$) in $\mu MT^{-/-}$ + $Slc12a2^{+/+}$ and $\mu MT^{-/-}$ + $Slc12a2^{-/-}$ mice at day 14 post-immunisation with NP-CGG or CGG in alum (n=5-6). (**C**) Line graphs showing mean ± S.E.M. antibody titres of NP-specific IgM and NP-specific IgG1 as measured in arbitrary units (a.u.) in $\mu MT^{-/-}$ + $Slc12a2^{+/+}$ and $\mu MT^{-/-}$ + $Slc12a2^{-/-}$ mice immunised with NP-CGG or CGG in alum (n=6). Statistical analysis was carried out using a Mann-Whitney U-test (B) or a two-way ANOVA with multiple comparisons (C).

5.4 Analysis of Requirement of WNK1 After Activation in an Immune Response

The previous work has described the *in vivo* activation or differentiation of naïve B cells that lack expression of *Wnk1*. However, there are compounding factors in these experiments such as homing and survival. To circumvent these issues, I investigated the immune response in mice where the deletion of *Wnk1* is restricted to activated B cells using *Wnk1*$^{fl/+}$ *Aicda*^{Cre} and *Wnk1*$^{fl/-}$ *Aicda*^{Cre} mice. The *Aicda*^{Cre} allele is not expressed in naïve B cells, but is induced after B cells are activated. I immunised these mice with either NP-CGG or CGG in alum and assessed the ability of the B cells to differentiate into germinal centre cells or plasma cells, as well as evaluating NP-specific antibodies in the blood (Figure 5.4A). When *Wnk1* expression was lost following B cell activation, there was a reduction in the number of total germinal centre cells and there were no germinal centre cells in which Cre had been expressed, as measured by huCD2 on the surface (Figure 5.4B). Thus WNK1 is required for the differentiation of B cells into germinal centre B cells. However, there was no difference in the differentiation into IgM$^+$ or IgG1$^+$ plasma cells (Figure 5.4B). Despite this, there was a trend for more NP-specific IgM and less NP-specific IgG1 in the serum of *Wnk1*$^{fl/-}$ *Aicda*^{Cre} mice compared to *Wnk1*$^{fl/+}$ *Aicda*^{Cre} mice (Figure 5.4C). This shows that WNK1 is not required after activation of B cells for differentiation into plasma cells but there may be a requirement for WNK1 in the production of antigen-specific IgG1 antibodies.

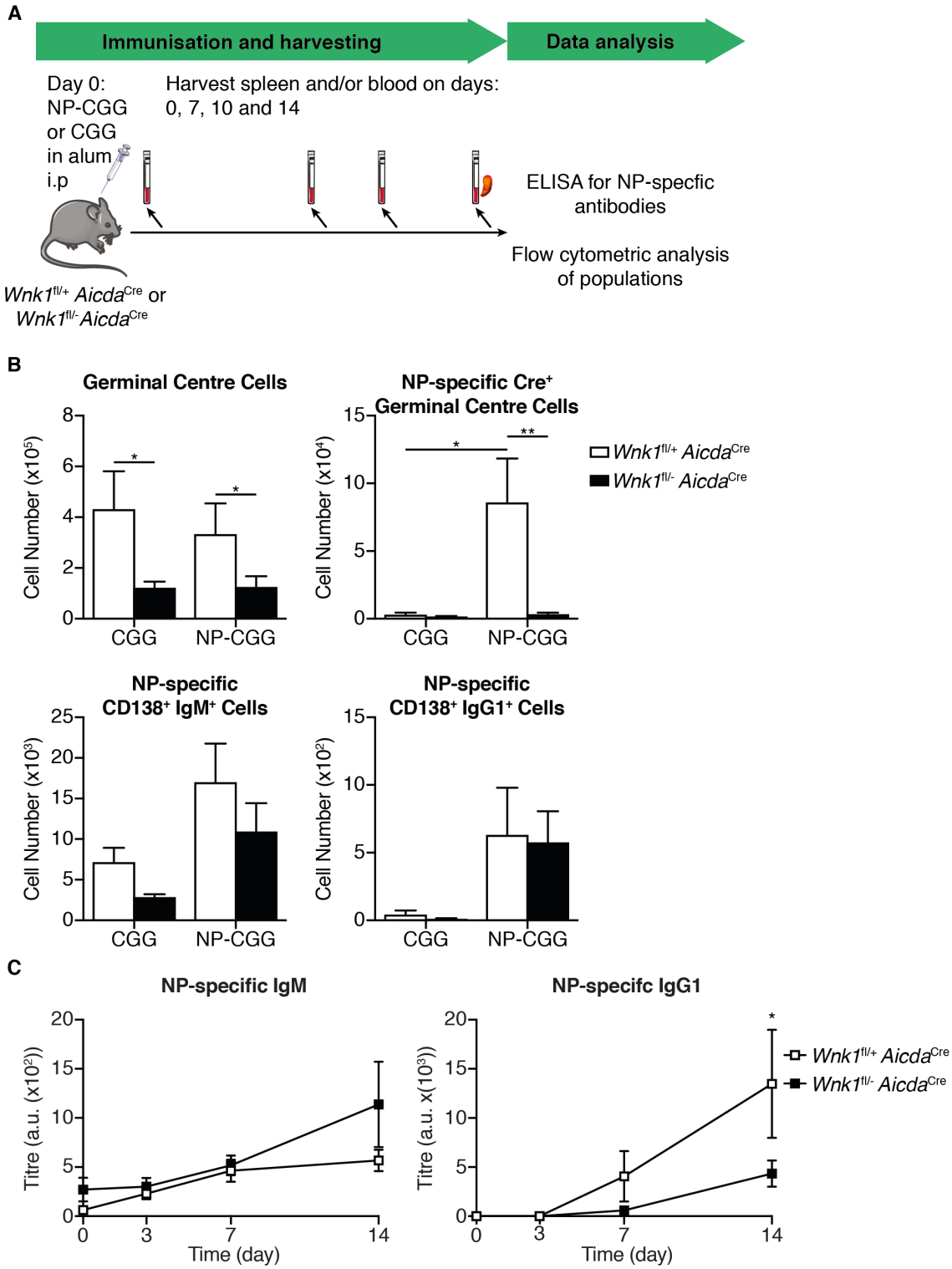

Figure 5.4 WNK1 Expression in Activated B Cells is Required for an Immune Response

(**A**) Schematic of immunisation of *Wnk1*$^{fl/+}$ *Aicda*^{Cre} or *Wnk1*$^{fl/-}$ *Aicda*^{Cre} mice with NP-CGG in alum. Mice were injected with NP-CGG or CGG alone in alum and at the indicated days spleen and/or blood were harvested. NP-specific antibodies were analysed by ELISA and B cell populations were analysed by flow cytometry. (**B**) Bar graphs showing mean ± S.E.M. number of total germinal centre cells (B220$^+$ CD19$^+$ Fas$^+$ GL7$^+$), NP-specific germinal centre cells with Cre expression

(B220^{+} CD19^{+} Fas^{+} GL7^{+} NP^{+} huCD2^{+}), NP-specific IgM^{+} CD138^{+} cells (B220^{-} CD138^{+} NP^{+} IgM^{+}) and NP-specific IgG1^{+} CD138^{+} cells (B220^{-} CD138^{+} NP^{+} IgG1^{+}) in *Wnk1*$^{fl/+}$ *Aicda*^{Cre} or *Wnk1*$^{fl/-}$ *Aicda*^{Cre} mice at day 14 post-immunisation with NP-CGG or CGG in alum (n=4-5). (**C**) Line graphs showing mean ± S.E.M. antibody titres of NP-specific IgM and NP-specific IgG1 as measured in arbitrary units (a.u.) in *Wnk1*$^{fl/+}$ *Aicda*^{Cre} or *Wnk1*$^{fl/-}$ *Aicda*^{Cre} mice immunised with NP-CGG or CGG in alum (n=4-5). Statistical analysis was carried out using a Mann-Whitney U-test (B) or a two-way ANOVA with multiple comparisons (C); * $p<0.05$, ** $p<0.01$. Asterisks above points indicate significant differences using multiple comparisons from the two-way ANOVA analysis.

5.5 Discussion and Outstanding Questions

In this chapter, I have shown for the first time that WNK1 plays a critical role in B cells during a T-dependent immune response. When *Wnk1* is knocked out in naïve B cells, there are defects in differentiation into germinal centre and plasma cells, accompanied by a lack of antigen-specific antibodies in the serum. In a T-dependent immune response, when B cells encounter cognate antigen they first migrate to the B-T border where they interact with cognate $CD4^+$ T cells. Upon successful interaction and receiving help, they migrate back into the follicle and differentiate into germinal centre cells, where they undergo further rounds of proliferation, somatic hypermutation and class switch recombination. It is possible that WNK1-deficient B cells fail to mount a T-dependent antibody response because of defects at many stages in this process. For example, they have defects in migration so they may not be able to localise to the B-T border correctly upon encounter of cognate antigen. If they are able to migrate to the B-T border, then they may not be able to transduce signals from T cells sufficiently due to defects in CD40 signalling or defects in signals delivered to T cells through defective antigen presentation or upregulation of CD80, CD86 and ICOSL. Furthermore, if the cells receive appropriate signals to differentiate into germinal centre cells, there could be defects in proliferation *in vivo* leading to a reduced ability to produce adequate numbers of germinal centre cells that can then further differentiate. On top of all of these contributing factors, there is the survival defect. This could hamper the development of a T-dependent immune response in two ways: reduction in precursor frequency (i.e. not enough cells specific for immunogen to drive an antibody response) or the B cells may continue to die throughout the immune response leading to a reduced antibody titre.

In the studies described, I have not shown that the kinase function of WNK1 is required for its critical role in B cells to mount a T-dependent antibody response. However, I would predict that B cells carrying a kinase-dead allele of *Wnk1* would display a similar defect in B cell immune responses. My studies of B cells *in vitro* showed that the kinase function of WNK1 is required for many of its functions, including survival and proliferation, which are potentially the major functions of WNK1 in B cells during an immune response. To test whether kinase activity of WNK1 is required in B cells for them to mount a T-dependent antibody response, mixed bone marrow chimeras could be generated using bone marrow from $\mu MT^{-/-}$ and either

Wnk1$^{fl/+}$ RCE or *Wnk1*$^{fl/D368A}$, which would then be immunised with NP-CGG. Additionally, *Wnk1*$^{+/D368A}$ mice could be bred to *Wnk1*$^{fl/fl}$ *Aicda*^{Cre}/ *Aicda*^{Cre} mice to generate progeny that could be immunised with NP-CGG to determine whether the kinase function of WNK1 is required following B cell activation.

One difference between the data generated from *in vitro* assays and from the *in vivo* immunisations is the ability to upregulate activation markers. WNK1-deficient B cells are unable to upregulate CD69 and CD80 three days after immunisation, whereas they are able to do so *in vitro*, indeed to a greater extent than control B cells. An explanation for this could be that in the *in vivo* experiment, the homing defect plays a role and the cells may be mis-localised. This mis-localisation could mean that they cannot encounter antigen or receive correct signals that drive upregulation of these markers, although there is upregulation of MHC class II and partial upregulation of CD86. This suggests that the WNK1-deficient B cells in this experiment are partially activated. To look at whether the cells are differentially localised, the labelled B cells could have been identified by histology and the ability of the knockout B cells to migrate to the B-T border of the follicles could have been determined. This would provide information about whether these cells are able to interact with $CD4^+$ T cells *in vivo*. Again, another complication of this experiment is the defect in survival in B cells lacking WNK1 adding to a further drop in precursor frequency.

It seems that NKCC1 is not required for B cell responses *in vivo* as NKCC1-deficient B cells are able to differentiate into germinal centre and plasma cells, as well as secrete antigen-specific IgM and IgG1 antibodies. This suggests that WNK1 regulation of ion homeostasis through NKCC1 is not required for the immune function of B cells. It does not rule out that ion homeostasis in general is not required for B cell immune responses since other ion channels may be compensating for the loss of NKCC1. To investigate this further *in vivo* a knockout mouse for multiple ion channel genes would need to be used. This may not be possible as disruption of ion homeostasis is likely to have a negative impact on many cell types and may not be viable. Indeed, this could be the mechanism by which WNK1 regulates B cell immune responses. It could be that B cells lacking WNK1 are unable to sense stresses in the environment efficiently, such as osmotic stress or intracellular chloride, causing the B cells to become unresponsive to external stimuli, although this is unsubstantiated at the current time.

When the effect of knocking out WNK1 in naïve B cells is circumvented by using a Cre that is expressed in activated B cells (*Aicda*^{Cre}), there is still a loss of germinal centre B cells. This suggests that despite maintenance of precursor frequency, localisation and normal initial activation, once WNK1 has been deleted there is an inability to form germinal centres. This could be due to defects in proliferation, survival or receipt of signals from CD4^{+} T cells to differentiate. Further investigation is required to determine whether there are any defects in these B cells in activation *in vitro* such as differentiation in an iGC culture or proliferation. Since the mice have the genotypes *Wnk1*$^{fl/+}$ *Aicda*^{Cre} and *Wnk1*$^{fl/-}$ *Aicda*^{Cre}, these mice could be used to assess whether *Wnk1* heterozygosity has an impact on localisation, adhesion and antigen presentation in naïve B cells.

Of note is the finding that there is no difference in numbers of plasma cells up to day 7 post immunisation between μ*MT*$^{-/-}$ + *Wnk1*$^{fl/+}$ RCE and μ*MT*$^{-/-}$ + *Wnk1*$^{fl/-}$ RCE mice or at day 14 post immunisation between *Wnk1*$^{fl/+}$ *Aicda*^{Cre} and *Wnk1*$^{fl/-}$ *Aicda*^{Cre} mice. Some plasma cell differentiation occurs in a GC-independent fashion, which could be unperturbed by deletion of *Wnk1*. In the experiment with μ*MT*$^{-/-}$ mixed chimeras, at day 7 there was no increase in NP-specific germinal centre cells yet suggesting that these NP-specific plasma cells have arisen independently of the germinal centre reaction and they are mostly unswitched indicating they may have arisen in a GC-independent fashion. In the experiment with *Wnk1*$^{fl/+}$ *Aicda*^{Cre} and *Wnk1*$^{fl/-}$ *Aicda*^{Cre} mice, the unchanged numbers of plasma cells could also be because of a GC-independent response, but another contributing factor could be that it takes several days for the Cre to be expressed, recombine the floxed allele, mRNA decay to occur, and eventually loss of WNK1 protein. During this time, the cells may have already committed to plasma cell differentiation. It appears that WNK1 is not required for the survival of plasma cells in the steady state, so it could be that after commitment to this fate, loss of WNK1 no longer has an effect on survival of the cells and they are able to persist and secrete antibody. My current work does not make it clear if there are defects in antibody secretion; immunisation of μ*MT*$^{-/-}$ + *Wnk1*$^{fl/-}$ RCE mice indicated that there was no secretion of antigen-specific IgM antibodies in the serum, no difference in number of antigen-specific IgM^{+} plasma cells up to day 7 post immunisation. Whereas immunisation of *Wnk1*$^{fl/-}$ *Aicda*^{Cre} mice suggest that antigen-specific antibodies can be secreted. Further work is required to unravel the function of WNK1 in plasma cells and whether it plays a role in antibody secretion or not.

Chapter 6. Discussion

The role of WNK1 has been previously defined most extensively in the kidney and in neurons where it regulates ion homeostasis via activation of NKCC1 and NCC1, and inhibition of KCC1, KCC2, KCC3 and KCC4 through OXSR1 and STK39 (Anselmo *et al.*, 2006, De Los Heros *et al.*, 2014, Friedel *et al.*, 2015, Inoue *et al.*, 2012, Moriguchi *et al.*, 2005, Vitari *et al.*, 2005). Other work has shown that WNK1 has a role in controlling cell cycle and mitosis in a variety of cell types, including neural progenitor cells, HeLa cells and rat vascular smooth muscle cells (Sun *et al.*, 2006, Tu *et al.*, 2011, Zhang *et al.*, 2018b). The migration of glioma and neural progenitor cells is also regulated by WNK1 (Sun *et al.*, 2006, Zhu *et al.*, 2014).

However, WNK1 has not been rigorously studied in the immune system. Work from our laboratory has revealed that WNK1 is a negative regulator of T cell adhesion through LFA-1 and a positive regulator of T cell migration. Phosphorylation of OXSR1 and expression of NKCC1 is required for T cell migration but not regulation of LFA-1 (Köchl *et al.*, 2016). Further unpublished work from our laboratory has shown that WNK1 is critical for T cell development, as WNK1-deficient thymocytes are blocked at the β-selection checkpoint in the thymus.

To further understand the role of WNK1 in the immune system, the work presented in this thesis set out to investigate the role of WNK1 in B cell biology. To briefly summarise the findings, I have shown that WNK1 regulates B cell adhesion, migration, survival, development, proliferation, antigen presentation to $CD4^+$ T cells and antibody responses to T-dependent antigens. Thus, WNK1 is a critical kinase that regulates many aspects of B cell biology and its expression is required in B cells to mount an adequate antibody response.

6.1 Key Findings

The role of WNK1 had not been previously studied in B cells. Thus, I have been able to show for the first time that it is a crucial kinase in a variety of processes in B cells. WNK1 is activated downstream of the BCR, CXCR5, BAFFR and CD40 leading to the phosphorylation of OXSR1. In the case of BCR, CXCR5 and BAFFR signalling, the activation of WNK1 is dependent on PI3K and AKT activity. However, signalling downstream of CD40 leading to activation of WNK1 is not dependent on PI3K, but has a partial dependency on AKT (Figure 6.1A).

I have also shown that WNK1 is required for the development of B cells, since the deletion of *Wnk1* resulted in a drastic decrease in the numbers of pre-B and immature B cells in the bone marrow. I have shown that WNK1 is a negative regulator of B cell adhesion through both LFA-1 and VLA-4, and this function is not dependent on NKCC1, similar to the pathway described in $CD4^+$ T cells (Köchl *et al.*, 2016). B cells that lacked the expression of *Wnk1* displayed a defect in migration both *in vitro* and *in vivo*, highlighting its role as a positive regulator of B cell migration. I have revealed that WNK1 plays a crucial role in B cell survival, as a week after inducing deletion of *Wnk1* the number of mature B cells plummeted to around a third the number observed in control mice, and the numbers continued to drop over time. I showed that WNK1 is required for B cell differentiation to germinal centre B cells, and to generate antibodies against T-dependent antigens. Similar to the previously described function of WNK1 in the regulation of cell cycle and mitosis (Sun *et al.*, 2006, Tu *et al.*, 2011, Zhang *et al.*, 2018b), WNK1 was observed to positively regulate proliferation of B cells after activation, which was independent of its role in regulation of survival. WNK1 is not critical for activation of B cells after stimulation through BCR or CD40 as activation markers were upregulated post-stimulation in WNK1-deficent B cells, albeit some markers are altered in the degree of upregulation. Additionally, I showed that WNK1 regulates the ability of B cells to communicate with $CD4^+$ T cells, WNK is required for normal presentation of peptides on MHC class II, for full responses to CD40 stimulation and for upregulation of ICOSL. All of these processes are important for the generation and maintenance of the germinal centre reaction, suggesting that failure of WNK1-deficient B cells to differentiate into germinal centre B cells and to generate a T-dependent antibody response may be the result of cellular defects at multiple levels (Figure 6.1B).

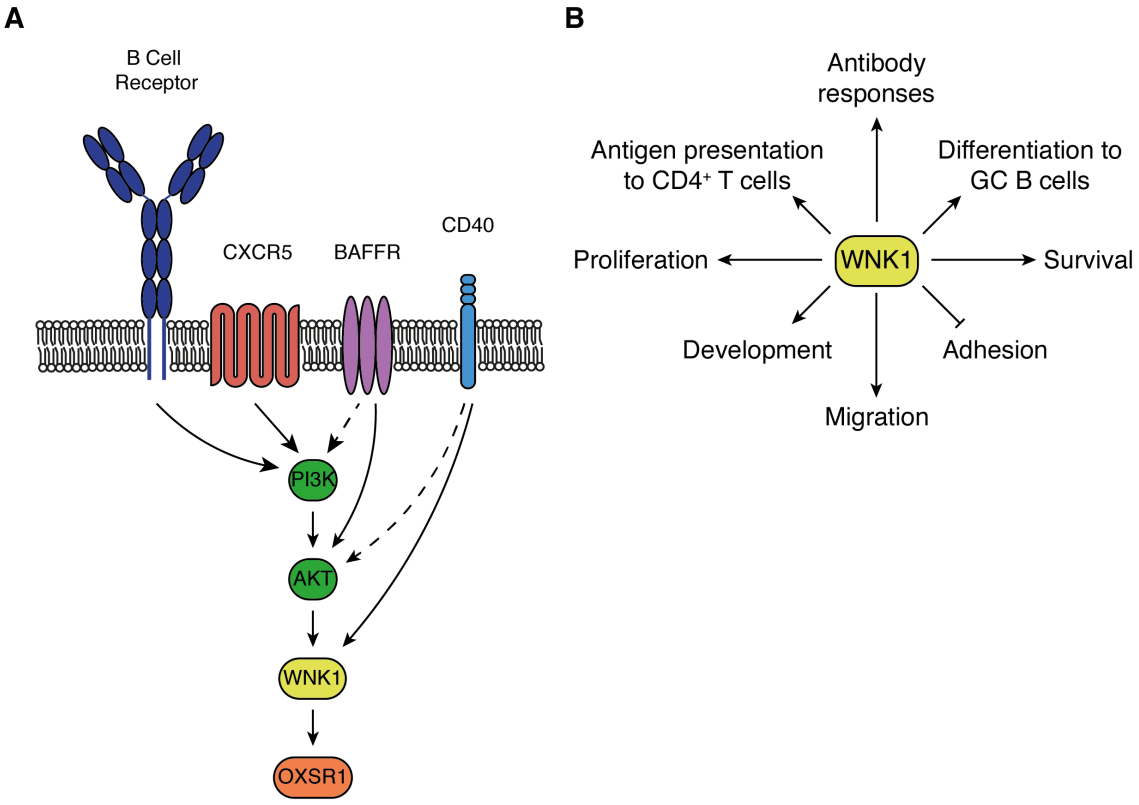

Figure 6.1 Summary of Key Findings

(**A**) Schematic of activation of WNK1 by BCR, CXCR5, BAFFR and CD40L. PI3K is activated downstream of BCR, CXCR5 and BAFFR stimulation, which leads to the activation of WNK1 via AKT and results in phosphorylation of OXSR1. CD40 stimulation leads to activation of WNK1 and phosphorylation of OXSR1 in a manner that is partially dependent on AKT but not on PI3K. (**B**) Schematic showing the processes in B cells that are regulated by WNK1. WNK1 is a negative regulator of adhesion through the integrins LFA-1 and VLA-4. WNK1 is a positive regulator of B cell survival, migration, development, proliferation, antigen presentation and differentiation to germinal centre B cells, and is required in B cells in order to mount an antibody response to T-dependent antigens.

6.2 Outstanding Questions

The outstanding questions for each part of this project have been discussed in the relevant chapters. The main unanswered question from this project is: what is the mechanism by which WNK1 regulates all of these processes in B cells? One explanation is that WNK1 could be required for maintenance of ion homeostasis in B cells. Furthermore, through regulation of ion fluxes in and out of cells, WNK1 may control the volume of B cells. In this scenario, the absence of WNK1 would lead to inactivation of NKCC1 and activation of KCC1, KCC3 and KCC4 (NKCC2, NCC and KCC2 are not expressed in B cells), resulting in a net efflux of K^+ and Cl^- ions out of the B cell. This would lead to cell shrinkage as intracellular tonicity is reduced causing water to move out of the cell across the plasma membrane via osmosis. It is conceivable that the inability of WNK1-deficient B cells to regulate their volume may cause the majority of phenotypes that I have observed in WNK1-deficient B cells.

When I measured FSC of B cells after stimulation with either anti-IgM or CD40L, WNK1-deficient B cells displayed increased FSC after stimulation with CD40L but not with anti-IgM compared to control B cells. Indeed, over time the WNK1-deficient B cells displayed increased in FSC signal. However, FSC is not a reliable measure of cell volume as it can also be affected by the refractive index of the cell, cell shape, cell size and membrane ruffling (personal communication with Flow Cytometry STP, Crick). Furthermore, work has shown that, although FSC does correlate with cell/particle size, it may not represent an accurate measure of cell size since smaller cells/particles can display similar or slightly higher FSC than larger cells (Salzman, 2001, Tzur *et al.*, 2011). Thus, to more accurately measure cell size, a Coulter Counter or microscopy should be used to measure cell volume. Indeed, when cell area of control and WNK1-deficient $CD4^+$ T cells was measured using microscopy, WNK1-deficient $CD4^+$ T cells displayed lower cell area compared to control $CD4^+$ T cells (Leon de Boer, unpublished data). This supports the notion that WNK1 regulates cell volume in lymphocytes possibly through NKCC1 and KCC-family proteins.

Regulation of cell volume and ion homeostasis are important for regulation of several cellular processes, such as migration, apoptosis and proliferation. In order for cells to migrate, they need to change volume in a regulated manner such that there are local increases in volume at the leading edge of migrating cells and

decreases in volume at the rear. The osmotic engine model suggests that 3D migration through the extracellular matrix is regulated by localised ion and water movements across the plasma membrane (Stroka *et al.*, 2014). For WNK1 to regulate B cell migration in this manner, WNK1 or WNK1 activity would have to be localised at the leading edge of the migrating cell resulting in activation of NKCC1 and inactivation of KCC-family proteins to drive localised increases in volume. At the rear of the cell, WNK1 or WNK1 activity would have to be decreased leading to activation of KCC-family proteins and inactivation of NKCC1, thus causing a localised reduction in volume.

Apoptosis is associated with a decrease in cell volume termed apoptotic volume decrease (AVD). Several studies show how regulation of cell size, and tonicity of both extracellular and intracellular areas are important for survival of cells. They indicate that decreases in cell volume are an early event in apoptosis, and in some cases a reduction in cell volume induces cell death (Bortner and Cidlowski, 1996, Hoffmann *et al.*, 2009, Hughes *et al.*, 1997, Maeno *et al.*, 2000, Nielsen *et al.*, 2008). AVD has been shown to proceed cytochrome c release and caspase activation, and that preventing AVD can rescue a cell from apoptosis (Maeno *et al.*, 2000). Hypertonic media, which induce cell shrinkage, have been shown to induce programmed cell death, and decreasing potassium concentration in cell extracts and cell nuclei leads to caspase 3 activation and DNA fragmentation (Bortner and Cidlowski, 1996, Hughes *et al.*, 1997). Furthermore, hypertonic medium has been shown to reduce the signalling downstream of platelet-derived growth factor receptor β, as measured by its delayed phosphorylation and a lack of phosphorylation of AKT upon stimulation in hypertonic medium compared to isotonic medium (Nielsen *et al.*, 2008). Thus, if loss of WNK1 causes a reduction in cell volume, which cannot be rescued by increasing cell volume through activation of ion channels, then apoptosis could be activated leading to the loss of B cells after deletion of *Wnk1*. Additionally, the shrinkage could lead to decreased BAFFR signalling and decreased phosphorylation of AKT similar to that observed in platelet-derived growth factor receptor. Both of these mechanisms could be responsible for the lower survival I observed in WNK1-deficient B cells, but further work is required to determine this.

In order for cells to divide, they must increase in volume so that the daughter cells are of appropriate volume and cells do not diminish in size over progressive rounds of division. Treatment of cells with hypertonic media has been shown to promote

longer S and G2/M phases of the cell cycle, suggesting that shrunken cells progress through the cell cycle at a slower rate (Michea *et al.*, 2000). Additionally, voltage-gated potassium channels have been implicated in proliferation as quinidine, an inhibitor of voltage-gated potassium channels, causes inhibition of division due to an arrest in G1, indicating that potassium transport is important for cell cycle progression (Wang *et al.*, 1998). B cells and T cells express the voltage-gated potassium channel $K_V1.3$, which when inhibited in T cells leads to reduced IL-2 secretion and proliferation (Chandy *et al.*, 1984, DeCoursey *et al.*, 1984, Koo *et al.*, 1999, Wulff *et al.*, 2004). Modelling and experimental data have shown that water movement affects cytokinesis (Li *et al.*, 2017). In this model, there is localised water movement out of the cell at the cleavage furrow and localised water movement into the cell at the poles. This water movement could be regulated by localised activation of ion transporters. Thus if WNK1 regulates ion transport and cell volume in B cells, the proliferation defect observed in WNK1-deficient B cells could be caused by a delays in cell cycle progression due to shrinkage or delays in cytokinesis due to dysregulated ion fluxes and subsequent water movement.

Control of ion homeostasis and cell volume by WNK1 may not contribute to the increased adhesion or decreased antigen presentation phenotypes observed in WNK1-deficient B cells. Work in $CD4^+$ T cells has shown that OXSR1 and NKCC1 do not regulate adhesion through LFA-1, instead WNK1 negatively regulates GTP-loading of RAP1 (Köchl *et al.*, 2016). This suggests that WNK1 activates signalling cascades other than OXSR1/NKCC1 that lead to the regulation of LFA-1. I have shown that NKCC1 was not required for the hyperadhesion phenotype observed in WNK1-deficient B cells. Thus, it is possible that GTP-loading of RAP1 is negatively regulated by WNK1 in B cells as well, but this has not been shown. Since WNK1 is a large protein with many SH3-binding motifs (PxxP), it is possible that it can act as a scaffolding protein for many different SH3 domain-containing proteins. Therefore, WNK1 may regulate the localisation and activation of different signalling proteins leading to regulation of different signalling cascades. It is possible that one of these signalling cascades is important for the regulation of peptide presentation in B cells, however, this has not been shown. Further investigation is required to determine the molecular mechanisms behind WNK1-regulated control of B cell adhesion and antigen presentation, as well as whether WNK1 controls cell volume in B cells.

6.3 Concluding Remarks

The analysis of WNK1-deficient B cells has shown for the first time that WNK1 is a critical kinase in B cells that regulates several aspects of B cell biology. I have shown that WNK1 is activated and phosphorylates OXSR1 downstream of stimulation of the BCR, CXCR5, BAFFR and CD40L. I have shown that WNK1 is a negative regulator of B cell adhesion and a positive regulator of migration, survival, development, proliferation and antigen presentation in B cells. Additionally, I have shown that B cells require *Wnk1* expression in order to mount a T-dependent antibody response. It is possible that WNK1 is required for control of cell volume by regulation of ion fluxes in B cells, and this may be responsible for several aspects of the phenotypes I observed in WNK1-deficient B cells. However, further investigation is required to determine the molecular mechanisms behind the regulation of these processes by WNK1.

Reference List

Adler, L. N., Jiang, W., Bhamidipati, K., Millican, M., Macaubas, C., Hung, S. & Mellins, E. D. 2017. The Other Functions: Class Ii-Restricted Antigen Presentation by B Cells. *Frontiers in Immunology,* 8**,** 1-14.

Alessi, D. R., James, S. R., Downes, P., Holmes, A. B., Gaffney, P. R. J., Reese, C. B. & Cohen, P. 1997. Characterisation of a 3-Phosphoinositide-Dependent Protein Kinase Which Phosphorylates and Activates Protein Kinase Balpha. *Current Biology,* 7**,** 261-269.

Allen, C. D. C., Okada, T. & Cyster, J. G. 2007a. Germinal-Center Organization and Cellular Dynamics. *Immunity,* 27**,** 190-202.

Allen, C. D. C., Okada, T., Tang, H. L. & Cyster, J. G. 2007b. Imaging of Germinal Center Selection Events During Affinity Maturation. *Science,* 315**,** 528-531.

Allie, S. R., Bradley, J. E., Mudunuru, U., Schultz, M. D., Graf, B. A., Lund, F. E. & Randall, T. D. 2019. The Establishment of Resident Memory B Cells in the Lung Requires Local Antigen Encounter. *Nat Immunol,* 20**,** 97-108.

Allman, D., Lindsley, R. C., Demuth, W., Rudd, K., Shinton, S. A. & Hardy, R. R. 2001. Resolution of Three Nonproliferative Immature Splenic B Cell Subsets Reveals Multiple Selection Points During Peripheral B Cell Maturation. *The Journal of Immunology,* 167**,** 6834-6840.

Aloulou, M., Carr, E. J., Gador, M., Bignon, A., Liblau, R. S., Fazilleau, N. & Linterman, M. A. 2016. Follicular Regulatory T Cells Can Be Specific for the Immunizing Antigen and Derive from Naive T Cells. *Nat Commun,* 7**,** 10579.

Amin, R. H. & Schlissel, M. S. 2008. Foxo1 Directly Regulates the Transcription of Recombination-Activating Genes During B Cell Development. *Nat Immunol,* 9**,** 613-22.

Andrew, D. P., Spellberg, J. P., Takimoto, H., Schmits, R., Mak, T. W. & Zukowski, M. M. 1998. Transendotheial Migration and Trafficking of Leukocytes in Lfa-1-Deficient Mice. *European Journal of Immunology,* 28**,** 1959-1969.

Angeli, V., Ginhoux, F., Llodrà, J., Quemeneur, L., Frenette, P. S., Skobe, M., Jessberger, R., Merad, M. & Randolph, G. J. 2006. B Cell-Driven Lymphangiogenesis in Inflamed Lymph Nodes Enhances Dendritic Cell Mobilization. *Immunity,* 24**,** 203-215.

Anselmo, A. N., Earnest, S., Chen, W., Juang, Y. C., Kim, S. C., Zhao, Y. & Cobb, M. H. 2006. Wnk1 and Osr1 Regulate the Na+, K+, 2cl- Cotransporter in Hela Cells. *Proc Natl Acad Sci U S A,* 103**,** 10883-8.

Arnon, T. I., Horton, R. M., Grigorova, I. L. & Cyster, J. G. 2013. Visualization of Splenic Marginal Zone B-Cell Shuttling and Follicular B-Cell Egress. *Nature,* 493**,** 684-8.

Arron, J. R., Vologodskaia, M., Wong, B. R., Naramura, M., Kim, N., Gu, H. & Choi, Y. 2001. A Positive Regulatory Role for Cbl Family Proteins in Tumor Necrosis Factor-Related Activation-Induced Cytokine (Trance) and Cd40l-Mediated Akt Activation. *J Biol Chem,* 276**,** 30011-7.

Bai, Z., Cai, L., Umemoto, E., Takeda, A., Tohya, K., Komai, Y., Veeraveedu, P. T., Hata, E., Sugiura, Y., Kubo, A., Suematsu, M., Hayasaka, H., Okudaira, S., Aoki, J., Tanaka, T., Albers, H. M., Ovaa, H. & Miyasaka, M. 2013. Constitutive Lymphocyte Transmigration across the Basal Lamina of High Endothelial Venules Is Regulated by the Autotaxin/Lysophosphatidic Acid Axis. *J Immunol,* 190**,** 2036-48.

Bankovich, A. J., Shiow, L. R. & Cyster, J. G. 2010. Cd69 Suppresses Sphingosine 1-Phosophate Receptor-1 (S1p1) Function through Interaction with Membrane Helix 4. *J Biol Chem,* 285**,** 22328-37.

Bao, X., Moseman, E. A., Saito, H., Petryniak, B., Thiriot, A., Hatakeyama, S., Ito, Y., Kawashima, H., Yamaguchi, Y., Lowe, J. B., Von Andrian, U. H. & Fukuda, M. 2010. Endothelial Heparan Sulfate Controls Chemokine Presentation in Recruitment of Lymphocytes and Dendritic Cells to Lymph Nodes. *Immunity,* 33**,** 817-29.

Barnden, M. J., Allison, J., Heath, W. R. & Carbone, F. R. 1998. Defective Tcr Expression in Transgenic Mice Constructed Using cDNA-Based A- and B-Chain Genes under the Control of Heterologous Regulatory Elements. *Immunology and Cell Biology,* 76**,** 34-40.

Bassing, C. H., Saw, W. & Alt, F. W. 2002. The Mechanism and Regulation of Chromosomal V(D)J Recombination. *Cell,* 109 Suppl**,** S45-S55.

Beals, C. R., Clipstone, N. A., Ho, S. N. & Crabtree, G. R. 1997. Nuclear Localization of Nf-Atc by a Calcineurin-Dependent, Cyclosporin-Sensitive Intramolecular Interaction. *Genes & Development,* 11**,** 824-834.

Bekeredjian-Ding, I. & Jego, G. 2009. Toll-Like Receptors - Sentries in the B-Cell Response. *Immunology,* 128**,** 311-323.

Benson, M. J., Dillon, S. R., Castigli, E., Geha, R. S., Xu, S., Lam, K. P. & Noelle, R. J. 2008. Cutting Edge: The Dependence of Plasma Cells and Independence of Memory B Cells on Baff and April. *The Journal of Immunology,* 180**,** 3655-3659.

Berek, C., Berger, A. & Apel, M. 1991. Maturation of the Immune Response in Germinal Centers. *Cell,* 67**,** 1121-1129.

Berlin-Rufenach, C., Otto, F., Mathies, M., Westermann, J., Owen, M. J., Hamann, A. & Hogg, N. 1999. Lymphocyte Migration in Lymphocyte Function-Associated Antigen (Lfa)-1–Deficient Mice. *The Journal of Experimental Medicine,* 189**,** 1467-1478.

Bondada, S., Troyer, A. & Chelvarajan, R. 2003. Early Events in B Lymphocyte Activation. *Current Protocols in Immunology,* 57**,** 3.9.1-3.9.14.

Bortner, C. D. & Cidlowski, J. A. 1996. Absence of Volume Regulatory Mechanisms Contributes to the Rapid Activation of Apoptosis in Thymocytes. *Am J Physiol,* 271**,** C950-61.

Bradl, H., Wittmann, J., Milius, D., Vettermann, C. & Jack, H. M. 2003. Interaction of Murine Precursor B Cell Receptor with Stroma Cells Is Controlled by the Unique Tail of 5 and Stroma Cell-Associated Heparan Sulfate. *The Journal of Immunology,* 171**,** 2338-2348.

Bransteitter, R., Pham, P., Scharff, M. D. & Goodman, M. F. 2003. Activation-Induced Cytidine Deaminase Deaminates Deoxycytidine on Single-Stranded DNA but Requires the Action of Rnase. *Proceedings of the National Academy of Sciences,* 100**,** 4102-4107.

Brazao, T. F., Johnson, J. S., Muller, J., Heger, A., Ponting, C. P. & Tybulewicz, V. L. J. 2016. Long Noncoding Rnas in B-Cell Development and Activation. *Blood,* 128**,** e10-e19.

Bretou, M., Jouannot, O., Fanget, I., Pierobon, P., Larochette, N., Gestraud, P., Guillon, M., Emiliani, V., Gasman, S., Desnos, C., Lennon-Duménil, A.-M., Darchen, F. & Bement, W. 2014. Cdc42 Controls the Dilation of the Exocytotic Fusion Pore by Regulating Membrane Tension. *Molecular Biology of the Cell,* 25**,** 3195-3209.

Bretou, M., Kumari, A., Malbec, O., Moreau, H. D., Obino, D., Pierobon, P., Randrian, V., Sáez, P. J. & Lennon-Dumenil, A. M. 2016. Dynamics of the Membrane-Cytoskeleton Interface in Mhc Class Ii-Restricted Antigen Presentation. *Immunological Reviews,* 272**,** 39-51.

Brightbill, H. D., Jackman, J. K., Suto, E., Kennedy, H., Jones, C., 3rd, Chalasani, S., Lin, Z., Tam, L., Roose-Girma, M., Balazs, M., Austin, C. D., Lee, W. P. & Wu, L. C. 2015. Conditional Deletion of Nf-Kappab-Inducing Kinase (Nik) in Adult Mice Disrupts Mature B Cell Survival and Activation. *J Immunol,* 195**,** 953-64.

Bross, L., Fukita, Y., Mcblane, F., Démollière, C., Rajewsky, K. & Jacobs, H. 2000. DNA Double-Strand Breaks in Immunoglobulin Genes Undergoing Somatic Hypermutation. *Immunity,* 13**,** 589-597.

Brunet, A., Bonni, A., Zigmond, M. J., Lin, M. Z., Juo, P., Hu, L. S., Anderson, M. J., Arden, K. C., Blenis, J. & Greenberg, M. E. 1999. Akt Promotes Cell Survival by Phosphorylating and Inhibiting a Forkhead Transcription Factor. *Cell,* 96**,** 857-868.

Burkhardt, A. L., Brunswick, M., Bolen, J. B. & Mond, J. J. 1991. Anti-Immunoglobulin Stimulation of B Lymphocytes Activates Src-Related Protein-Tyrosine Kinases. *Proceedings of the National Academy of Sciences of the United States of America,* 88**,** 7410-7414.

Cambier, J. C. 1995. New Nomenclature for the Reth Motif (or Arh1/Tam/Aram/Yxxl). *Immunology Today,* 16**,** 110.

Carrasco, Y. R. & Batista, F. D. 2007. B Cells Acquire Particulate Antigen in a Macrophage-Rich Area at the Boundary between the Follicle and the Subcapsular Sinus of the Lymph Node. *Immunity,* 27**,** 160-71.

Chandy, K. G., Decoursey, T. E., Cahalan, M. D., Mclaughlin, C. & Gupta, S. 1984. Voltage-Gated Potassium Channels Are Required for Human T Lymphocyte Activation. *J Exp Med,* 160**,** 369-85.

Chaudhuri, J., Tian, M., Khuong, C., Chua, K., Pinaud, E. & Alt, F. W. 2003. Transcription-Targeted DNA Deamination by the Aid Antibody Diversification Enzyme. *Nature,* 422**,** 726-730.

Cheng, C. J. & Huang, C. L. 2011. Activation of Pi3-Kinase Stimulates Endocytosis of Romk Via Akt1/Sgk1-Dependent Phosphorylation of Wnk1. *Journal of the American Society of Nephrology,* 22**,** 460-71.

Chiu, C. W., Dalton, M., Ishiai, M., Kurosaki, T. & Chan, A. C. 2002. Blnk: Molecular Scaffolding through 'Cis'-Mediated Organization of Signaling Proteins. *EMBO Journal,* 21**,** 6461-6472.

Chu, V. T., Fröhlich, A., Steinhauser, G., Scheel, T., Roch, T., Fillatreau, S., Lee, J. J., Löhning, M. & Berek, C. 2011. Eosinophils Are Required for the Maintenance of Plasma Cells in the Bone Marrow. *Nat Immunol,* 12**,** 151-159.

Chung, Y., Tanaka, S., Chu, F., Nurieva, R. I., Martinez, G. J., Rawal, S., Wang, Y. H., Lim, H., Reynolds, J. M., Zhou, X. H., Fan, H. M., Liu, Z. M., Neelapu, S. S. & Dong, C. 2011. Follicular Regulatory T Cells Expressing Foxp3 and Bcl-6 Suppress Germinal Center Reactions. *Nat Med,* 17**,** 983-8.

Cinamon, G., Matloubian, M., Lesneski, M. J., Xu, Y., Low, C., Lu, T., Proia, R. L. & Cyster, J. G. 2004. Sphingosine 1-Phosphate Receptor 1 Promotes B Cell Localization in the Splenic Marginal Zone. *Nat Immunol,* 5**,** 713-20.

Cinamon, G., Shinder, V. & Alon, R. 2001. Shear Forces Promotoe Lymphocyte Migration across Vascular Endothelium Bearing Apical Chemokines. *Nature Immunology,* 2**,** 515-522.

Cinamon, G., Zachariah, M. A., Lam, O. M., Foss, F. W., Jr. & Cyster, J. G. 2008. Follicular Shuttling of Marginal Zone B Cells Facilitates Antigen Transport. *Nat Immunol,* 9**,** 54-62.

Clark, M. R., Campbell, K. S., Kazlauskas, A., Johnson, S. A., Hertz, M., Potter, T. A., Pleimen, C. & Cambier, J. C. 1992. The B Cell Antigen Receptor Complex: Association of Ig-Alpha and Ig-Beta with Distinct Cytoplasmic Effectors. *Science,* 258**,** 123-126.

Constantinides, M. G., Mcdonald, B. D., Verhoef, P. A. & Bendelac, A. 2014. A Committed Precursor to Innate Lymphoid Cells. *Nature,* 508**,** 397-401.

Coughlin, J. J., Stang, S. L., Dower, N. A. & Stone, J. C. 2005. Rasgrp1 and Rasgrp3 Regulate B Cell Proliferation by Facilitating B Cell Receptor-Ras Signaling. *J Immunol,* 175**,** 7179-7184.

Craxton, A., Draves, K. E., Gruppi, A. & Clark, E. A. 2005. Baff Regulates B Cell Survival by Downregulating the Bh3-Only Family Member Bim Via the Erk Pathway. *J Exp Med,* 202**,** 1363-74.

Cremasco, V., Woodruff, M. C., Onder, L., Cupovic, J., Nieves-Bonilla, J. M., Schildberg, F. A., Chang, J., Cremasco, F., Harvey, C. J., Wucherpfennig, K., Ludewig, B., Carroll, M. C. & Turley, S. J. 2014. B Cell Homeostasis and Follicle Confines Are Governed by Fibroblastic Reticular Cells. *Nat Immunol,* 15**,** 973-81.

D'ambrosio, D., Hippen, K. L. & Cambier, J. C. 1996. Distinct Mechanisms Medate Shc Association with the Activated and Resting B Cell Antigen Receptor. *European Journal of Immunology,* 26**,** 1960-1965.

Dal Porto, J. M., Gauld, S. B., Merrell, K. T., Mills, D., Pugh-Bernard, A. E. & Cambier, J. 2004. B Cell Antigen Receptor Signaling 101. *Molecular Immunology,* 41**,** 599-613.

De Los Heros, P., Dario, Gourlay, R., David, Deak, M., Thomas, Kristopher & Zhang, J. 2014. The Wnk-Regulated Spak/Osr1 Kinases Directly Phosphorylate and Inhibit the K+–Cl−Co-Transporters. *Biochemical Journal,* 458**,** 559-573.

De Luca, C., Kowalski, T. J., Zhang, Y., Elmquist, J. K., Lee, C., Kilimann, M. W., Ludwig, T., Liu, S. M. & Chua, S. C., Jr. 2005. Complete Rescue of Obesity, Diabetes, and Infertility in Db/Db Mice by Neuron-Specific Lepr-B Transgenes. *J Clin Invest,* 115**,** 3484-93.

Decoursey, T. E., Chandy, K. G., Gupta, S. & Cahalan, M. D. 1984. Voltage-Gated K+ Channels in Human T Lymphocytes: A Role in Mitogenesis? *Nature,* 307**,** 465-468.

Degasperi, A., Birtwistle, M. R., Volinsky, N., Rauch, J., Kolch, W. & Kholodenko, B. N. 2014. Evaluating Strategies to Normalise Biological Replicates of Western Blot Data. *PLoS One,* 9**,** e87293.

Del Fresno, C., Iborra, S., Saz-Leal, P., Martínez-López, M. & Sancho, D. 2018. Flexible Signaling of Myeloid C-Type Lectin Receptors in Immunity and Inflammation. *Frontiers in Immunology,* 9**,** 804.

Delaloy, C., Lu, J., Houot, A. M., Disse-Nicodeme, S., Gasc, J. M., Corvol, P. & Jeunemaitre, X. 2003. Multiple Promoters in the Wnk1 Gene: One Controls Expression of a Kidney-Specific Kinase-Defective Isoform. *Molecular and Cellular Biology,* 23**,** 9208-9221.

Denzin, L. K. & Cresswell, P. 1995. Hla-Dm Induces Clip Dissociation from Mhc Class Ii Alphabeta Dimers and Facilitates Peptide Loading. *Cell,* 82**,** 155-165.

Dias, S., Silva, H., Jr., Cumano, A. & Vieira, P. 2005. Interleukin-7 Is Necessary to Maintain the B Cell Potential in Common Lymphoid Progenitors. *J Exp Med,* 201**,** 971-9.

Dickerson, S. K., Market, E., Besmer, E. & Papavasiliou, F. N. 2003. Aid Mediates Hypermutation by Deaminating Single Stranded DNA. *J Exp Med,* 197**,** 1291-1296.

Dingler, F. A., Kemmerich, K., Neuberger, M. S. & Rada, C. 2014. Uracil Excision by Endogenous Smug1 Glycosylase Promotes Efficient Ig Class Switching and Impacts on A:T Substitutions During Somatic Mutation. *European Journal of Immunology,* 44**,** 1925-1935.

Dolmetsch, R. E., Lewis, R. S., Goodnow, C. C. & Healy, J. I. 1997. Differential Activation of Trancription Factors Induced by Ca2+ Response Amplitude and Duration. *Nature,* 386**,** 855-858.

Doody, G. M., Bell, S. E., Vigorito, E., Clayton, E., Mcadam, S., Tooze, R., Fernandez, C., Lee, I. J. & Turner, M. 2001. Signal Transduction through Vav-2 Participates in Humoral Immune Responses and B Cell Maturation. *Nat Immunol,* 2**,** 542-7.

Ebisuno, Y., Tanaka, T., Kanemitsu, N., Kanda, H., Yamaguchi, K., Kaisho, T., Akira, S. & Miyasaka, M. 2003. Cutting Edge: The B Cell Chemokine Cxc Chemokine

Ligand 13/B Lymphocyte Chemoattractant Is Expressed in the High Endothelial Venules of Lymph Nodes and Peyer's Patches and Affects B Cell Trafficking across High Endothelial Venules. *The Journal of Immunology,* 171**,** 1642-1646.

Ehrhardt, A., David, M. D., Ehrhardt, G. R. & Schrader, J. W. 2004. Distinct Mechanisms Determine the Patterns of Differential Activation of H-Ras, N-Ras, K-Ras 4b, and M-Ras by Receptors for Growth Factors or Antigen. *Mol Cell Biol,* 24**,** 6311-23.

Ehrhardt, R. O., Strober, W. & Harriman, G. R. 1992. Effect of Transforming Growth Factor (Tgf)-Beta 1 on Iga Isotype Expression. Tgf-Beta 1 Induces a Small Increase in Siga+ B Cells Regardless of the Method of B Cell Activation. *Journal of Immunology,* 148**,** 3830-3836.

Embgenbroich, M. & Burgdorf, S. 2018. Current Concepts of Antigen Cross-Presentation. *Frontiers in Immunology,* 9**,** 1643.

Filippi, B. M., De Los Heros, P., Mehellou, Y., Navratilova, I., Gourlay, R., Deak, M., Plater, L., Toth, R., Zeqiraj, E. & Alessi, D. R. 2011. Mo25 Is a Master Regulator of Spak/Osr1 and Mst3/Mst4/Ysk1 Protein Kinases. *EMBO J,* 30**,** 1730-1741.

Flagella, M., Clarke, L. L., Miller, M. L., Erway, L. C., Giannella, R. A., Andringa, A., Gawenis, L. R., Kramer, J., Duffy, J. J., Doetschman, T., Lorenz, J. N., Yamoah, E. N., Cardell, E. L. & Shull, G. E. 1999. Mice Lacking the Basolateral Na-K-2cl Cotransporter Have Impaired Epitheial Chloride Secretion and Are Profoundly Deaf. *Journal of Biological Chemistry,* 274**,** 26945-26955.

Flaswinkel, H. & Reth, M. 1994. Dual Role of the Tyrosine Activation Motif of the Ig-Alpha Protein During Signal Transduction Via the B Cell Antigen Receptor. *EMBO Journal,* 13**,** 83-89.

Fonseca, V. R., Ribeiro, F. & Graca, L. 2019. T Follicular Regulatory (Tfr) Cells: Dissecting the Complexity of Tfr-Cell Compartments. *Immunol Rev,* 288**,** 112-127.

Forthal, D. N. 2014. Functions of Antibodies. *Microbiology Spectrum,* 2**,** 1-17.

Friedel, P., Kahle, K. T., Zhang, J., Hertz, N., Pisella, L. I., Buhler, E., Schaller, F., Duan, J., Khanna, A. R., Bishop, P. N., Shokat, K. M. & Medina, I. 2015. Wnk1-Regulated Inhibitory Phosphorylation of the Kcc2 Cotransporter Maintains the Depolarizing Action of Gaba in Immature Neurons. *Science Signaling,* 8**,** ra65-ra65.

Fu, C., Turck, C. W., Kurosaki, T. & Chan, A. C. 1998. Blnk: A Central Linker Protein in B Cell Activation. *Immunity,* 9**,** 93-103.

Fujimoto, M., Fujimoto, Y., Poe, J. C., Jansen, P. J., Lowell, C. A., Defranco, A. L. & Tedder, T. F. 2000. Cd19 Regulates Src Family Protein Tyrosine Kinase Activation in B Lympphocytes through Processive Amplification. *Immunity,* 13**,** 47-57.

Gallagher, E., Enzler, T., Matsuzawa, A., Anzelon-Mills, A., Otero, D., Holzer, R., Janssen, E., Gao, M. & Karin, M. 2007. Kinase Mekk1 Is Required for Cd40-Dependent Activation of the Kinases Jnk and P38, Germinal Center Formation, B Cell Proliferation and Antibody Production. *Nat Immunol,* 8**,** 57-63.

Gallolu Kankanamalage, S., Lee, A. Y., Wichaidit, C., Lorente-Rodriguez, A., Shah, A. M., Stippec, S., Whitehurst, A. W. & Cobb, M. H. 2016. Multistep Regulation of Autophagy by Wnk1. *Proceedings of the National Academy of Sciences,* 113**,** 14342-14347.

Galvez, A., Morales, M. P., Eltit, J. M., Ocaranza, P., Carrasco, L., Campos, X., Sapag-Hagar, M., Díaz-Araya, G. & Lavandero, S. 2001. A Rapid and Strong Apoptotic Process Is Triggered by Hyperosmotic Stress in Cultured Rat Cardiac Myocytes. *Cell and Tissue Research,* 304**,** 279-285.

Gascoigne, N. R. J., Rybakin, V., Acuto, O. & Brzostek, J. 2016. Tcr Signal Strength and T Cell Development. *Annu Rev Cell Dev Biol,* 32**,** 327-348.

Gauthier, L., Rossi, B., Roux, F., Termine, E. & Schiff, C. 2002. Galectin-1 Is a Stromal Cell Ligand of the Pre-B Cell Receptor (Bcr) Implicated in Synapse Formation between Pre-B and Stromal Cells and in Pre-Bcr Triggering. *Proc Natl Acad Sci U S A,* 99**,** 13014-13019.

Gerlach, B., Cordier, S. M., Schmukle, A. C., Emmerich, C. H., Rieser, E., Haas, T. L., Webb, A. I., Rickard, J. A., Anderton, H., Wong, W. W., Nachbur, U., Gangoda, L., Warnken, U., Purcell, A. W., Silke, J. & Walczak, H. 2011. Linear Ubiquitination Prevents Inflammation and Regulates Immune Signalling. *Nature,* 471**,** 591-6.

Gershon, R. K. & Kondo, K. 1970. Cell Interaction in the Induction of Tolerance: The Role of Thymic Lymphocytes. *Immunology,* 18**,** 723-737.

Ghandour, H., Cullere, X., Alvarez, A., Luscinskas, F. W. & Mayadas, T. N. 2007. Essential Role for Rap1 Gtpase and Its Guanine Exchange Factor Caldag-Gefi in Lfa-1 but Not Vla-4 Integrin-Mediated Human T-Cell Adhesion. *Blood,* 110**,** 3682-3690.

Gialeli, C., Gungor, B. & Blom, A. M. 2018. Novel Potential Inhibitors of Complement System and Their Roles in Complement Regulation and Beyond. *Molecular Immunology,* 102**,** 73-83.

Girard, J. P., Moussion, C. & Forster, R. 2012. Hevs, Lymphatics and Homeostatic Immune Cell Trafficking in Lymph Nodes. *Nat Rev Immunol,* 12**,** 762-73.

Goitsuka, R., Fujimura, Y., Mamada, H., Umeda, A., Morimura, T., Uetsuka, K., Doi, K., Tsuji, S. & Kitamura, D. 1998. Cutting Edge, Bash, a Novel Signaling Molecule Preferentially Expressed in B Cells of the Bursa of Fabricius. *Journal of Immunology,* 161**,** 5804-5808.

Goodnow, C. C., Crosbie, J., Adelstein, S., Lavoie, T. B., Smith-Gill, S. J., Brink, R. A., Pritchard-Briscoe, H., Wotherspoon, J. S., Loblay, R. H., Raphael, K., Trent, R. J. & Basten, A. 1988. Alter Immunoglobulin Expression and Functional Silencing of Self-Reactive B Lymphocytes in Transgenic Mice. *Nature,* 334**,** 676-682.

Grillot, D. A., Merino, R., Pena, J. C., Fanslow, W. C., Finkelan, F. D., Thompson, C. B. & Nunez, G. 1996. Bcl-X Exhibits Regulated Expression During B Cell Development and Activation and Modulates Lymphocyte Survival in Transgenic Mice. *Journal of Experimental Medicine,* 183**,** 381-391.

Gross, J. A., Dillon, S. R., Mudri, S., Johnston, J., Littau, A., Roque, R., Rixon, M., Schou, O., Foley, K. P., Haugen, H., Mcmillen, S., Waggie, K., Schreckhise, R. W., Shoemaker, K., Vu, T., Moore, M., Grossman, A. & Clegg, C. H. 2001. Taci-Ig Neutralizes Molecules Critical for B Cell Development and Autoimmune Disease: Impaired B Cell Maturation in Mice Lacking Blys. *Immunity,* 15**,** 289-302.

Guce, A. I., Mortimer, S. E., Yoon, T., Painter, C. A., Jiang, W., Mellins, E. D. & Stern, L. J. 2013. Hla-Do Acts as a Substrate Mimic to Inhibit Hla-Dm by a Competitive Mechanism. *Nat Struct Mol Biol,* 20**,** 90-8.

Gunn, M. D., Ngo, V. N., Ansel, K. M., Ekland, E. H., Cyster, J. G. & Williams, L. T. 1998. A B-Cell-Homing Chemokine Made in Lymphoid Follicles Activates Burkitt's Lymphoma Receptor-1. *Nature,* 391**,** 799-803.

Hahn, M., Macht, A., Waisman, A. & Hovelmeyer, N. 2016. Nf-Kappab-Inducing Kinase Is Essential for B-Cell Maintenance in Mice. *Eur J Immunol,* 46**,** 732-41.

Halle, S., Halle, O. & Förster, R. 2017. Mechanisms and Dynamics of T Cell-Mediated Cytotoxicity in Vivo. *Trends in Immunology,* 38**,** 432-443.

Hamel, K. M., Cao, Y., Olalekan, S. A. & Finnegan, A. 2014. B Cell-Specific Expression of Inducible Costimulator Ligand Is Necessary for the Induction of Arthritis in Mice. *Arthritis Rheumatol,* 66**,** 60-7.

Hamon, M. A. & Quintin, J. 2016. Innate Immune Memory in Mammals. *Seminars in Immunology,* 28**,** 351-358.

Han, J., Lim, C. J., Watanabe, N., Soriani, A., Ratnikov, B., Calderwood, D. A., Puzon-Mclaughlin, W., Lafuente, E. M., Boussiotis, V. A., Shattil, S. J. & Ginsberg, Mark h. 2006. Reconstructing and Deconstructing Agonist-Induced Activation of Integrin Aiibβ3. *Current Biology,* 16**,** 1796-1806.

Han, S., Hathcock, K., Zheng, B., Kepler, T. B., Hodes, R. & Kelsoe, G. 1995a. Cellular Interaction in Germinal Centers. Roles of Cd40 Ligand and B7-2 Established Germinal Centers. *Journal of Immunology,* 155**,** 556-567.

Han, S., Zheng, B., Dal Porto, J. & Kelsoe, G. 1995b. In Situ Studies of the Primary Immune Response to (4-Hydroxy-3- Nitrophenyl)Acetyl. Iv. Affinity-Dependent, Antigen-Driven B Cell Apoptosis in Germinal Centers as a Mechanism for Maintaining Self- Tolerance. *Journal of Experimental Medicine,* 182**,** 1635-1644.

Hao, Z. & Rajewsky, K. 2001. Homeostasis of Peripheral B Cells in the Absence of B Cell Influx from the Bone Marrow. *The Journal of Experimental Medicine,* 194**,** 1151-1164.

Hargreaves, D. C., Hyman, P. L., Lu, T. T., Ngo, V. N., Bidgol, A., Suzuki, G., Zou, Y.-R., Littman, D. R. & Cyster, J. G. 2001. A Coordinated Change in Chemokine Responsiveness Guides Plasma Cell Movements. *J Exp Med,* 194**,** 45-56.

Hartweger, H., Schweighoffer, E., Davidson, S., Peirce, M. J., Wack, A. & Tybulewicz, V. L. J. 2014. Themis2 Is Not Required for B Cell Development, Activation, and Antibody Responses. *J Immunol,* 193**,** 700-707.

Hashimoto, A., Okada, H., Jiang, A., Kurosaki, M., Greenberg, S., Clark, E. A. & Kurosaki, T. 1998. Involvement of Guanosine Triphosphatases and Phospholipase C-Γ2 in Extracellular Signal–Regulated Kinase, C-Jun Nh2-Terminal Kinase, and P38 Mitogen-Activated Protein Kinase Activation by the B Cell Antigen Receptor. *The Journal of Experimental Medicine,* 188**,** 1287-1295.

Hashimoto, S., Iwamatsu, A., Ishiai, M., Okawa, K., Yamadori, T., Matsushita, M., Baba, Y., Kishimoto, T., Kurosaki, T. & Tsukada, S. 1999. Identification of the Sh2 Domain Binding Protein of Bruton's Tyroosine Kinase as Blnk - Functional Significance of Btk-Sh2 Domain in B-Cell Antigen Receptor-Coupled Calcium Signaling. *Blood,* 94**,** 2357-2364.

Haswell, L. E., Glennie, M. J. & Al-Shamkhani, A. 2001. Analysis of the Oligomeric Requirement for Signaling by Cd40 Using Soluble Multimeric Forms of Its Ligand, Cd154. *European Journal of Immunology,* 31**,** 3094-3100.

Hauser, A. E., Junt, T., Mempel, T. R., Sneddon, M. W., Kleinstein, S. H., Henrickson, S. E., Von Andrian, U. H., Shlomchik, M. J. & Haberman, A. M. 2007. Definition of Germinal-Center B Cell Migration In vivo Reveals Predominant Intrazonal circulation patterns. *Immunity,* 26**,** 655-667.

Heubl, M., Zhang, J., Pressey, J. C., Al Awabdh, S., Renner, M., Gomez-Castro, F., Moutkine, I., Eugène, E., Russeau, M., Kahle, K. T., Poncer, J. C. & Lévi, S. 2017. Gabaa Receptor Dependent Synaptic Inhibition Rapidly Tunes Kcc2 Activity Via the Cl−-Sensitive Wnk1 Kinase. *Nature Communications,* 8**,** 1776.

Hobeika, E., Levit-Zerdoun, E., Anastasopoulou, V., Pohlmeyer, R., Altmeier, S., Alsadeq, A., Dobenecker, M. W., Pelanda, R. & Reth, M. 2015. Cd19 and Baff-R Can Signal to Promote B-Cell Survival in the Absence of Syk. *EMBO J,* 34**,** 925-39.

Hoffmann, E. K., Lambert, I. H. & Pedersen, S. F. 2009. Physiology of Cell Volume Regulation in Vertebrates. *Physiol Rev,* 89**,** 193-277.

Hoffmann, F. S., Kuhn, P. H., Laurent, S. A., Hauck, S. M., Berer, K., Wendlinger, S. A., Krumbholz, M., Khademi, M., Olsson, T., Dreyling, M., Pfister, H. W., Alexander, T., Hiepe, F., Kumpfel, T., Crawford, H. C., Wekerle, H., Hohlfeld, R., Lichtenthaler, S. F. & Meinl, E. 2015. The Immunoregulator Soluble Taci Is Released by Adam10 and Reflects B Cell Activation in Autoimmunity. *J Immunol,* 194**,** 542-52.

Hoogeboom, R., Natkanski, E. M., Nowosad, C. R., Malinova, D., Menon, R. P., Casal, A. & Tolar, P. 2018. Myosin Iia Promotes Antibody Responses by Regulating B Cell Activation, Acquisition of Antigen, and Proliferation. *Cell Rep,* 23**,** 2342-2353.

Hou, T. Z., Qureshi, O. S., Wang, C. J., Baker, J., Young, S. P., Walker, L. S. & Sansom, D. M. 2015. A Transendocytosis Model of Ctla-4 Function Predicts Its Suppressive Behavior on Regulatory T Cells. *J Immunol,* 194**,** 2148-59.

Hsu, B. L., Harless, S. M., Lindsley, R. C., Hilbert, D. M. & Cancro, M. P. 2002. Cutting Edge: Blys Enables Survival of Transitional and Mature B Cells through Distinct Mediators. *The Journal of Immunology,* 168**,** 5993-5996.

Hu, H., Wu, X., Jin, W., Chang, M., Cheng, X. & Sun, S. C. 2011. Noncanonical Nf-Kappab Regulates Inducible Costimulator (Icos) Ligand Expression and T Follicular Helper Cell Development. *Proc Natl Acad Sci U S A,* 108**,** 12827-32.

Hughes, F. M., Bortner, C. D., Purdy, G. D. & Cidlowski, J. A. 1997. Intracellular K+ Suppresses the Activation of Apoptosis in Lymphocytes. *J Biol Chem,* 272**,** 30567-30576.

Inoue, K., Furukawa, T., Kumada, T., Yamada, J., Wang, T., Inoue, R. & Fukuda, A. 2012. Taurine Inhibits K+-Cl−Cotransporter Kcc2 to Regulate Embryonic Cl−Homeostasis Via with-No-Lysine (Wnk) Protein Kinase Signaling Pathway. *Journal of Biological Chemistry,* 287**,** 20839-20850.

Iqbal, A. J., Fisher, E. A. & Greaves, D. R. 2016. Inflammation-a Critical Appreciation of the Role of Myeloid Cells. *Microbiol Spectr,* 4.

Ise, W., Fujii, K., Shiroguchi, K., Ito, A., Kometani, K., Takeda, K., Kawakami, E., Yamashita, K., Suzuki, K., Okada, T. & Kurosaki, T. 2018. T Follicular Helper Cell-Germinal Center B Cell Interaction Strength Regulates Entry into Plasma Cell or Recycling Germinal Center Cell Fate. *Immunity,* 48**,** 702-715 e4.

Ishiai, M., Kurosaki, M., Pappu, R., Okawa, K., Ronko, I., Fu, C., Shibata, M., Iwamatsu, A., Chan, A. C. & Kurosaki, T. 1999. Blnk Required for Coupling Syk to Plcgamma2 and Rac1-Jnk in B Cells. *Immunity,* 10**,** 117-125.

Iwasato, T., Shimizu, A., Honjo, T. & Yamagishi, H. 1990. Circular DNA Is Excised by Immunoglobulin Class Switch Recombination. *Cell,* 62**,** 143-149.

Jacob, J., Kassir, R. & Kelsoe, G. 1991. In Situ Studies of the Primary Immune Response to (4-Hydroxy-3- Nitrophenyl)Acetyl. I. The Architecture and Dynamics of Responding Cell Populations. *Journal of Experimental Medicine,* 173**,** 1165-1175.

Jacque, E., Schweighoffer, E., Tybulewicz, V. L. & Ley, S. C. 2015. Baff Activation of the Erk5 Map Kinase Pathway Regulates B Cell Survival. *J Exp Med,* 212**,** 883-92.

Jellusova, J., Miletic, Ana v., Cato, Matthew h., Lin, W.-W., Hu, Y., Bishop, Gail a., Shlomchik, Mark j. & Rickert, Robert c. 2013. Context-Specific Baff-R Signaling by the Nf-Kb and Pi3k Pathways. *Cell Reports,* 5**,** 1022-1035.

Jennings, M. L. & Al-Rohil, N. 1990. Kinetics of Activation and Inactivation of Swelling-Stimulated K+/Cl- Transport. The Volume-Sensitive Parameter Is the Rate Constant for Inactivation. *The Journal of General Physiology,* 95**,** 1021-1040.

Kabashima, K., Haynes, N. M., Xu, Y., Nutt, S. L., Allende, M. L., Proia, R. L. & Cyster, J. G. 2006. Plasma Cell S1p 1 Expression Determines Secondary Lymphoid Organ Retention Versus Bone Marrow Tropism. *J Exp Med,* 203**,** 2683-2690.

Kahle, K. T., Schmouth, J.-F., Lavastre, V., Latremoliere, A., Zhang, J., Andrews, N., Omura, T., Laganière, J., Rochefort, D., Hince, P., Castonguay, G., Gaudet, R., Mapplebeck, J. C. S., Sotocinal, S. G., Duan, J., Ward, C., Khanna, A. R., Mogil, J. S., Dion, P. A., Woolf, C. J., Inquimbert, P. & Rouleau, G. A. 2016. Inhibition of the Kinase Wnk1/Hsn2 Ameliorates Neuropathic Pain by Restoring Gaba Inhibition. *Science Signaling,* 9**,** ra32-ra32.

Kaisho, T., Takeda, K., Tsujimura, T., Kawai, T., Nomura, F., Terada, N. & Akira, S. 2001. Iκb Kinase A Is Essential for Mature B Cell Development and Function. *The Journal of Experimental Medicine,* 193**,** 417-426.

Kallies, A., Hasbold, J., Fairfax, K., Pridans, C., Emslie, D., Mckenzie, B. S., Lew, A. M., Corcoran, L. M., Hodgkin, P. D., Tarlinton, D. M. & Nutt, S. L. 2007. Initiation of Plasma-Cell Differentiation Is Independent of the Transcription Factor Blimp-1. *Immunity,* 26**,** 555-566.

Kallies, A., Hasbold, J., Tarlinton, D. M., Dietrich, W., Corcoran, L. M., Hodgkin, P. D. & Nutt, S. L. 2004. Plasma Cell Ontogeny Defined by Quantitative Changes in Blimp-1 Expression. *The Journal of Experimental Medicine,* 200**,** 967-977.

Karasuyama, H., Kudo, A. & Melchers, F. 1990. The Proteins Encoded by the Vpreb and Lambda 5 Pre-B Cell-Specific Genes Can Associate with Each Other and with Mu Heavy Chain. *Journal of Experimental Medicine,* 172**,** 969-972.

Katagiri, K., Maeda, A., Shimonaka, M. & Kinashi, T. 2003. Rapl, a Rap1-Binding Molecule That Mediates Rap1-Induced Adhesion through Spatial Regulation of Lfa-1. *Nature Immunology,* 4**,** 741-478.

Kitamura, D., Roes, J., Kühn, R. & Rajewsky, K. 1991. A B Cell-Deficient Mouse by Targeted Disruption of the Membrane Exon of the Immunoglobulin Mu Chain Gene. *Nature,* 350**,** 423-426.

Köchl, R., Thelen, F., Vanes, L., Brazão, T. F., Fountain, K., Xie, J., Huang, C.-L., Lyck, R., Stein, J. V. & Tybulewicz, V. L. J. 2016. Wnk1 Kinase Balances T Cell Adhesion Versus Migration in Vivo. *Nature Immunology,* 17**,** 1075-1083.

Kondo, M., Weissman, I. L. & Akashi, K. 1997. Identification of Clonogenic Common Lymphoid Progenitors in Mouse Bone Marrow. *Cell,* 91**,** 661-672.

Koo, G. C., Blake, J. T., Shah, K., Staruch, M. J., Dumont, F., Wunderler, D., Sanchez, M., Mcmanus, O. B., Sirotina-Meisher, A., Fischer, P., Boltz, R. C., Goetz, M. A., Baker, R., Bao, J., Kayser, F., Rupprecht, K. M., Parsons, W. H., Tong, X.-C., Ita, I. E., Pivnichny, J., Vincent, S., Cunningham, P., Hora, D., Feeney, W., Kaczorowski, G. & Springer, M. S. 1999. Correolide and Derivatives Are Novel Immunosuppressants Blocking the Lymphocyte Kv1.3 Potassium Channels. *Cell Immunol,* 197**,** 99-107.

Kovacina, K. S., Park, G. Y., Bae, S. S., Guzzetta, A. W., Schaefer, E., Birnbaum, M. J. & Roth, R. A. 2003. Identification of a Proline-Rich Akt Substrate as a 14-3-3 Binding Partner. *J Biol Chem,* 278**,** 10189-94.

Kraus, M., Alimzhanov, M. B., Rajewsky, N. & Rajewsky, K. 2004. Survival of Resting Mature B Lymphocytes Depends on Bcr Signaling Via the Igalpha/Beta Heterodimer. *Cell,* 117**,** 787-800.

Kräutler, N. J., Suan, D., Butt, D., Bourne, K., Hermes, J. R., Chan, T. D., Sundling, C., Kaplan, W., Schofield, P., Jackson, J., Basten, A., Christ, D. & Brink, R. 2017. Differentiation of Germinal Center B Cells into Plasma Cells Is Initiated by High-Affinity Antigen and Completed by Tfh Cells. *The Journal of Experimental Medicine,* 214**,** 1259-1267.

Kurosaki, T., Shinohara, H. & Baba, Y. 2010. B Cell Signaling and Fate Decision. *Annual Review of Immunology,* 28**,** 21-55.

Kwon, K., Hutter, C., Sun, Q., Bilic, I., Cobaleda, C., Malin, S. & Busslinger, M. 2008. Instructive Role of the Transcription Factor E2a in Early B Lymphopoiesis and Germinal Center B Cell Development. *Immunity,* 28**,** 751-62.

L., K. G. J. P., De Ruier, N. D., De Vries-Smits, A. M. M., Powel, D. R., Bos, J. L. & Burgering, B. M. T. 1999. Direct Control of the Forkhead Transcription Factor Afx by Protein Kinase B. *Nature,* 398**,** 630-634.

Lafrenière, R. G., Macdonald, M. L. E., Dubé, M.-P., Macfarlane, J., O'driscoll, M., Brais, B., Meilleur, S., Brinkman, R. R., Dadivas, O., Pape, T., Platon, C., Radomski, C., Risler, J., Thompson, J., Guerra-Escobio, A.-M., Davar, G., Breakefield, X. O., Pimstone, S. N., Green, R., Pryse-Phillips, W., Goldberg, Y. P., Younghusband, H. B., Hayden, M. R., Sherrington, R., Rouleau, G. A. & Samuels, M. E. 2004. Identification of a Novel Gene (Hsn2) Causing Hereditary Sensory

and Autonomic Neuropathy Type Ii through the Study of Canadian Genetic Isolates. *The American Journal of Human Genetics,* 74**,** 1064-1073.

Lam, K.-P., Kühn, R. & Rajewsky, K. 1997. In Vivo Ablation of Surface Immunoglobulin on Mature B Cells by Inducible Gene Targeting Results in Rapid Cell Death. *Cell,* 90**,** 1073-1083.

Lee, B.-H., Chen, W., Stippec, S. & Cobb, M. H. 2007. Biological Cross-Talk between Wnk1 and the Transforming Growth Factor B-Smad Signaling Pathway. *Journal of Biological Chemistry,* 282**,** 17985-17996.

Leider, N. & Melamed, D. 2003. Differential C-Myc Responsiveness to B Cell Receptor Ligation in B Cell-Negative Selection. *The Journal of Immunology,* 171**,** 2446-2452.

Lentz, V. M., Cancro, M. P., Nashold, F. E. & Hayes, C. E. 1996. *Bcmd* Governs Recruitment of New B Cells into the Stable Peripheral B Cell Pool in the a/Wysnj Mouse. *The Journal of Immunology,* 157**,** 598-606.

Li, Y., He, L., Gonzalez, N. a. P., Graham, J., Wolgemuth, C., Wirtz, D. & Sun, S. X. 2017. Going with the Flow: Water Flux and Cell Shape During Cytokinesis. *Biophys J,* 113**,** 2487-2495.

Liao, G., Zhang, M., Harhaj, E. W. & Sun, S. C. 2004. Regulation of the Nf-Kappab-Inducing Kinase by Tumor Necrosis Factor Receptor-Associated Factor 3-Induced Degradation. *J Biol Chem,* 279**,** 26243-50.

Lin, Y. C., Jhunjhunwala, S., Benner, C., Heinz, S., Welinder, E., Mansson, R., Sigvardsson, M., Hagman, J., Espinoza, C. A., Dutkowski, J., Ideker, T., Glass, C. K. & Murre, C. 2010. A Global Network of Transcription Factors, Involving E2a, Ebf1 and Foxo1, That Orchestrates B Cell Fate. *Nat Immunol,* 11**,** 635-43.

Ling, L., Cao, Z. & Goeddel, D. V. 1998. Nf-Kappa B-Inducing Kinase Activates Ikk-Alpha by Phosphorylation of Ser-176. *Proc Natl Acad Sci U S A,* 95**,** 3792-3797.

Linsley, P. S., Brady, W., Grosmaire, L., Aruffo, A., Damle, N. K. & Ledbetter, J. A. 1991. Binding of the B Cell Activation Antigen B7 to Cd28 Costimulates T Cell Proliferation and Interleukin 2 Mrna Accumulation. *Journal of Experimental Medicine,* 173**,** 721-730.

Linsley, P. S., Clark, E. A. & Ledbetter, J. A. 1990. T-Cell Antigen Cd28 Mediates Adhesion with B Cells by Interacting with Activation Antigen B7/Bb-1. *Proc Natl Acad Sci U S A,* 87**,** 5031-5035.

Linterman, M. A., Beaton, L., Yu, D., Ramiscal, R. R., Srivastava, M., Hogan, J. J., Verma, N. K., Smyth, M. J., Rigby, R. J. & Vinuesa, C. G. 2010. Il-21 Acts Directly on B Cells to Regulate Bcl-6 Expression and Germinal Center Responses. *J Exp Med,* 207**,** 353-363.

Linterman, M. A., Pierson, W., Lee, S. K., Kallies, A., Kawamoto, S., Rayner, T. F., Srivastava, M., Divekar, D. P., Beaton, L., Hogan, J. J., Fagarasan, S., Liston, A., Smith, K. G. & Vinuesa, C. G. 2011. Foxp3+ Follicular Regulatory T Cells Control the Germinal Center Response. *Nat Med,* 17**,** 975-82.

Liu, D., Xu, H., Shih, C., Wan, Z., Ma, X., Ma, W., Luo, D. & Qi, H. 2015. T-B-Cell Entanglement and Icosl-Driven Feed-Forward Regulation of Germinal Centre Reaction. *Nature,* 517**,** 214-8.

Loder, F., Mutschler, B., Ray, R. J., Paige, C. J., Sideras, P., Torres, R., Lamers, M. C. & Carsetti, R. 1999. B Cell Development in the Spleen Takes Place in Discrete Steps and Is Determined by the Quality of B Cell Receptor–Derived Signals. *The Journal of Experimental Medicine,* 190**,** 75-90.

Lu, T. T. & Cyster, J. G. 2002. Integrin-Mediated Long-Term B Cell Retention in the Splenic Marginal Zone. *Science,* 297**,** 409-412.

Lund, F. E., Garvy, B. A., Randall, T. D. & Harris, D. P. 2005. Regulatory Roles for Cytokine-Producing B Cells in Infection and Autoimmune Disease. *Curr Dir Autoimmun,* 8**,** 25-54.

Lutzker, S., Rothman, P., Pollock, R., Coffman, R. & Alt, F. W. 1988. Mitogen- and Il-4-Regulated Expression of Germ-Line Ig Γ2b Transcripts: Evidence for Directed Heavy Chain Class Switching. *Cell,* 53**,** 177-184.

Maceiras, A. R., Almeida, S. C. P., Mariotti-Ferrandiz, E., Chaara, W., Jebbawi, F., Six, A., Hori, S., Klatzmann, D., Faro, J. & Graca, L. 2017. T Follicular Helper and T Follicular Regulatory Cells Have Different Tcr Specificity. *Nat Commun,* 8**,** 15067.

Mackay, F., Woodcock, S. A., Lawton, P., Ambrose, C., Baetscher, M., Schneider, P., Tschopp, J. & Browning, J. L. 1999. Mice Transgenic for Baff Develop Lymphocytic Disorders Along with Autoimmune Manifestations. *The Journal of Experimental Medicine,* 190**,** 1697-1710.

Maclennan, I. C. M. 1994. Germinal Centers. *Annual Review of Immunology,* 12**,** 117-139.

Maeno, E., Ishizaki, Y., Kanaseki, T., Hazama, A. & Okada, Y. 2000. Normotonic Cell Shrinkage Because of Disordered Volume Regulation Is an Early Prerequisite to Apoptosis. *Proc Natl Acad Sci U S A,* 97**,** 9487-9492.

Manning, B. D. & Toker, A. 2017. Akt/Pkb Signaling: Navigating the Network. *Cell,* 169**,** 381-405.

Mårtensson, I.-L., Almqvist, N., Grimsholm, O. & Bernardi, A. I. 2010. The Pre-B Cell Receptor Checkpoint. *FEBS Letters,* 584**,** 2572-9.

Martin, F., Oliver, A. M. & Kearney, J. F. 2001. Marginal Zone and B1 B Cells Unite in the Early Response against T-Independent Blood-Borne Particulate Antigens. *Immunity,* 14**,** 617-629.

Matioubian, M., Lo, C. G., Cinamon, G., Lesneski, M. J., Xu, Y., Brinkmann, V., Allende, M. L., Proia, R. L. & Cyster, J. G. 2004. Lymphocyte Egress from Thymus and Peripheral Lymphoid Organs Is Dependent on S1p Receptor 1. *Nature,* 427**,** 355-360.

Matsuoka, M., Yoshida, K., Maeda, T., Usuda, S. & Sakano, H. 1990. Switch Circular DNA Formed in Cytokine-Treated Mouse Splenocytes: Evidence for Intramolecular DNA Deletion in Immunoglobulin Class Switching. *Cell,* 62**,** 135-142.

Matthews, A. J., Zheng, S., Dimenna, L. J. & Chaudhuri, J. 2014. Regulation of Immunoglobulin Class-Switch Recombination. Elsevier.

Mcblane, J. F., Van Gent, D. C., Ramsden, D. A., Romeo, C., Cuomo, C. A., Gellert, M. & Oettinger, M. A. 1995. Cleavage at a V(D)J Recombination Signal Requires Only Rag1 and Rag2 Proteins and Occurs in Two Steps. *Cell,* 83**,** 387-395.

Mebius, R. E. & Kraal, G. 2005. Structure and Function of the Spleen. *Nat Rev Immunol,* 5**,** 606-16.

Methot, S. P. & Di Noia, J. M. 2017. Molecular Mechanisms of Somatic Hypermutation and Class Switch Recombination. Elsevier.

Michea, L., Ferguson, D. R., Peters, E. M., Andrews, P. M., Kirby, M. R. & Burg, M. B. 2000. Cell Cycle Delay and Apoptosis Are Induced by High Salt and Urea in Renal Medullary Cells. *Am J Physiol Renal Physiol,* 278**,** F209-18.

Min, X., Lee, B. H., Cobb, M. H. & Goldsmith, E. J. 2004. Crystal Structure of the Kinase Domain of Wnk1, a Kinase That Causes a Hereditary Form of Hypertension. *Structure,* 12**,** 1303-11.

Moalli, F., Cupovic, J., Thelen, F., Halbherr, P., Fukui, Y., Narumiya, S., Ludewig, B. & Stein, J. V. 2014. Thromboxane A2 Acts as Tonic Immunoregulator by Preferential Disruption of Low-Avidity Cd4+T Cell–Dendritic Cell Interactions. *The Journal of Experimental Medicine,* 211**,** 2507-2517.

Mombaerts, P., Iacomini, J., Johnson, R. S., Herrup, K., Tonegawa, S. & Papaioannou, V. E. 1992. Rag-1-Deficient Mice Have N Mature B and T Lymphocytes. *Cell,* 68**,** 869-877.

Monaco, G., Decrock, E., Arbel, N., Van Vliet, A. R., La Rovere, R. M., De Smedt, H., Parys, J. B., Agostinis, P., Leybaert, L., Shoshan-Barmatz, V. & Bultynck, G. 2015. The Bh4 Domain of Anti-Apoptotic Bcl-Xl, but Not That of the Related Bcl-2, Limits the Voltage-Dependent Anion Channel 1 (Vdac1)-Mediated Transfer of Pro-Apoptotic Ca2+ Signals to Mitochondria. *J Biol Chem,* 290**,** 9150-61.

Mond, J. J., Lees, A. & Snapper, C. M. 1995. T Cell-Independent Antigens Type 2. *Annual Review of Immunology,* 13**,** 655-692.

Moon, T. M., Correa, F., Kinch, L. N., Piala, A. T., Gardner, K. H. & Goldsmith, E. J. 2013. Solution Structure of the Wnk1 Autoinhibitory Domain, a Wnk-Specific Pf2 Domain. *J Mol Biol,* 425**,** 1245-52.

Moore, K. W., Rogers, J., Hunkapiller, T., Early, P., Nottenburg, C., Weissman, I., Bazin, H., Wall, R. & Hood, L. E. 1981. Expression of Igd May Use Both DNA Rearrangement and Rna Splicing Mechanisms. *Proceedings of the National Academy of Sciences,* 78**,** 1800-1804.

Moriguchi, T., Urushiyama, S., Hisamoto, N., Iemura, S., Uchida, S., Natsume, T., Matsumoto, K. & Shibuya, H. 2005. Wnk1 Regulates Phosphorylation of Cation-Chloride-Coupled Cotransporters Via the Ste20-Related Kinases, Spak and Osr1. *J Biol Chem,* 280**,** 42685-93.

Morrison, M. D., Reiley, W., Zhang, M. & Sun, S. C. 2005. An Atypical Tumor Necrosis Factor (Tnf) Receptor-Associated Factor-Binding Motif of B Cell-Activating Factor Belonging to the Tnf Family (Baff) Receptor Mediates Induction of the Noncanonical Nf-Kappab Signaling Pathway. *J Biol Chem,* 280**,** 10018-24.

Mosier, D. E., Mond, J. J. & Goldings, E. A. 1977. The Ontogeny of Thymic Independent Antibody Response in Vitro in Normal Mice and Mice with an X-Linked B Cell Defect. *Journal of Immunology,* 119**,** 1874-1878.

Muramatsu, M., Kinoshita, K., Fagarasan, S., Yamada, S., Shinkai, Y. & Honjo, T. 2000. Class Switch Recombination and Hypermutation Require Activation-Induced Cytidine Deaminase (Aid), a Potential Rna Editing Enzyme. *Cell,* 102**,** 553-563.

Nagai, K., Takata, M., Yamamura, H. & Kurosaki, T. 1995. Tyrosine Phosphorylation of Shc Is Mediated Throught Lyn and Syk in B Cell Receptor Signalling. *Journal of Biological Chemistry,* 270**,** 6824-6829.

Nagaoka, H., Takahashi, Y., Hayashi, R., Nakamura, T., Ishii, K., Matsuda, J., Ogura, A., Shirakata, Y., Karasuyama, H., Sudo, T., Nishikawa, S.-I., Tsubata, T., Mizuochi, T., Asano, T., Sakano, H. & Takemori, T. 2000. Ras Mediates Effector Pathways Responsible for Pre-B Cell Survival, Which Is Essential for the Developmental Progression to the Late Pre-B Cell Stage. *The Journal of Experimental Medicine,* 192**,** 171-182.

Nardelli, B., Belvedere, O., Roschke, V., Moore, P. A., Olsen, H. S., Migone, T. S., Sosnovtseva, S., Carrell, J. A., Feng, P., Giri, J. G. & Hilbert, D. M. 2001. Synthesis and Release of B-Lymphocyte Stimulator from Myeloid Cells. *Blood,* 97**,** 198-204.

Natkanski, E., Lee, W.-Y., Mistry, B., Casal, A., Molloy, J. E. & Tolar, P. 2013. B Cells Use Mechanical Energy to Discriminate Antigen Affinities. *Science,* 340**,** 1587-1590.

Nechanitzky, R., Akbas, D., Scherer, S., Gyory, I., Hoyler, T., Ramamoorthy, S., Diefenbach, A. & Grosschedl, R. 2013. Transcription Factor Ebf1 Is Essential for the Maintenance of B Cell Identity and Prevention of Alternative Fates in Committed Cells. *Nat Immunol,* 14**,** 867-75.

Nemazee, D. 2017. Mechanisms of Central Tolerance for B Cells. *Nat Rev Immunol,* 17**,** 281-294.

Nielsen, M. B., Christensen, S. T. & Hoffmann, E. K. 2008. Effects of Osmotic Stress on the Activity of Mapks and Pdgfr- -Mediated Signal Transduction in Nih-3t3 Fibroblasts. *Am J Physiol Cell Physiol,* 294**,** C1046-C1055.

Nieuwenhuis, P. & Opstelten, D. 1984. Functional Anatomy of Germinal Centers. *American Journal of Anatomy,* 170**,** 421-435.

Nowosad, C. R., Spillane, K. M. & Tolar, P. 2016. Germinal Center B Cells Recognize Antigen through a Specialized Immune Synapse Architecture. *Nat Immunol,* 17**,** 870-7.

O'connor, B. P., Raman, V. S., Erickson, L. D., Cook, W. J., Weaver, L. K., Ahonen, C., Lin, L. L., Mantchev, G. T., Bram, R. J. & Noelle, R. J. 2004. Bcma Is Essential for the Survival of Long-Lived Bone Marrow Plasma Cells. *J Exp Med,* 199**,** 91-8.

O'reilly, M. 2003. Wnk1, a Gene within a Novel Blood Pressure Control Pathway, Tissue-Specifically Generates Radically Different Isoforms with and without a Kinase Domain. *Journal of the American Society of Nephrology,* 14**,** 2447-2456.

O'riordan, M. & Grosschedl, R. 1999. Coordinate Regulation of B Cell Differentiation by the Transcription Factors Ebf and E2a. *Immunity,* 11**,** 21-31.

Oh-Hora, M., Johmura, S., Hashimoto, A., Hikida, M. & Kurosaki, T. 2003. Requirement for Ras Guanine Nucleotide Releasing Protein 3 in Coupling Phospholipase C-Γ2 to Ras in B Cell Receptor Signaling. *The Journal of Experimental Medicine,* 198**,** 1841-1851.

Okada, T., Miller, M. J., Parker, I., Krummel, M. F., Neighbors, M., Hartley, S. B., O'garra, A., Cahalan, M. D. & Cyster, J. G. 2005. Antigen-Engaged B Cells Undergo Chemotaxis toward the T Zone and Form Motile Conjugates with Helper T Cells. *PLoS Biol,* 3**,** e150.

Okada, T., Ngo, V. N., Ekland, E. H., Forster, R., Lipp, M., Littman, D. R. & Cyster, J. G. 2002. Chemokine Requirements for B Cell Entry to Lymph Nodes and Peyer's Patches. *Journal of Experimental Medicine,* 196**,** 65-75.

Ori, D., Murase, M. & Kawai, T. 2017. Cytosolic Nucleic Acid Sensors and Innate Immune Regulation. *Int Rev Immunol,* 36**,** 74-88.

Papavasiliou, F. N. & Schatz, D. G. 2000. Cell-Cycle-Regulates DNA Double-Strand Breaks in Somatic Hypermutation of Immunoglobulin Genes. *Nature,* 408**,** 2-6-221.

Park, C., Hwang, I. Y., Sinha, R. K., Kamenyeva, O., Davis, M. D. & Kehrl, J. H. 2012. Lymph Node B Lymphocyte Trafficking Is Constrained by Anatomy and Highly Dependent Upon Chemoattractant Desensitization. *Blood,* 119**,** 978-89.

Pelanda, R., Braun, U., Hobeika, E., Nussenzweig, M. C. & Reth, M. 2002. B Cell Progenitors Are Arrested in Maturation but Have Intact Vdj Recombination in the Absence of Ig- and Ig- *The Journal of Immunology,* 169**,** 865-872.

Perkins, N. D. 2007. Integrating Cell-Signalling Pathways with Nf-Kb and Ikk Function. *Nat Rev Mol Cell Biol,* 8**,** 49-62.

Petiot, A., Ogier-Denis, E., Blommaart, E. F. C., Meijer, A. J. & Codogno, P. 2000. Distinct Classes of Phosphatidylinositol 3'-Kinases Are Involved in Signaling Pathways That Control Macroautophagy in Ht-29 Cells. *Journal of Biological Chemistry,* 275**,** 992-998.

Pham, T. H., Baluk, P., Xu, Y., Grigorova, I., Bankovich, A. J., Pappu, R., Coughlin, S. R., Mcdonald, D. M., Schwab, S. R. & Cyster, J. G. 2010. Lymphatic Endothelial Cell Sphingosine Kinase Activity Is Required for Lymphocyte Egress and Lymphatic Patterning. *J Exp Med,* 207**,** 17-27.

Phan, T. G., Grigorova, I., Okada, T. & Cyster, J. G. 2007. Subcapsular Encounter and Complement-Dependent Transport of Immune Complexes by Lymph Node B Cells. *Nat Immunol,* 8**,** 992-1000.

Piala, A. T., Moon, T. M., Akella, R., He, H., Cobb, M. H. & Goldsmith, E. J. 2014. Chloride Sensing by Wnk1 Involves Inhibition of Autophosphorylation. *Science Signaling,* 7**,** ra41-ra41.

Piechotta, K., Lu, J. & Delpire, E. 2002. Cation Chloride Cotransporters Interact with the Stress-Related Kinases Ste20-Related Proline-Alanine-Rich Kinase (Spak) and Oxidative Stress Response 1 (Osr1). *Journal of Biological Chemistry,* 277**,** 50812-50819.

Puga, I., Cols, M., Barra, C. M., He, B., Cassis, L., Gentile, M., Comerma, L., Chorny, A., Shan, M., Xu, W., Magri, G., Knowles, D. M., Tam, W., Chiu, A., Bussel, J. B., Serrano, S., Lorente, J. A., Bellosillo, B., Lloreta, J., Juanpere, N., Alameda, F., Baró, T., De Heredia, C. D., Torán, N., Català, A., Torrebadell, M., Fortuny, C., Cusí, V., Carreras, C., Diaz, G. A., Blander, J. M., Farber, C.-M., Silvestri, G., Cunningham-Rundles, C., Calvillo, M., Dufour, C., Notarangelo, L. D., Lougaris, V., Plebani, A., Casanova, J.-L., Ganal, S. C., Diefenbach, A., Aróstegui, J. I., Juan, M., Yagüe, J., Mahlaoui, N., Donadieu, J., Chen, K. & Cerutti, A. 2011. B Cell–Helper Neutrophils Stimulate the Diversification and Production of Immunoglobulin in the Marginal Zone of the Spleen. *Nat Immunol,* 13**,** 170-180.

Pullen, S. S., Dang, T. T. A., Crute, J. J. & Kehry, M. R. 1999a. Cd40 Signaling through Tumor Necrosis Factor Receptor-Associated Factors (Trafs). Binding Site Specificity and Activation of Downstream Pathways by Distinct Trafs. *Journal of Biological Chemistry,* 274**,** 14246-14254.

Pullen, S. S., Labadia, M. E., Ingraham, R. H., Mcwhirter, S. M., Everdeen, D. S., Alber, T., Crute, J. J. & Kehry, M. R. 1999b. High-Affinity Interactions of Tumor Necrosis Factor Receptor-Associated Factors (Trafs) and Cd40 Require Traf Trimerization and Cd40 Multimerization. *Biochemistry,* 38**,** 10168-10177.

Pullen, S. S., Miller, H. G., Everdeen, D. S., Dang, T. T. A., Crute, J. J. & Kehry, M. R. 1998. Cd40−Tumor Necrosis Factor Receptor-Associated Factor (Traf) Interactions: Regulation of Cd40 Signaling through Multiple Traf Binding Sites and Traf Hetero-Oligomerization. *Biochemistry,* 37**,** 11836-11845.

Qi, H., Cannons, J. L., Klauschen, F., Schwartzberg, P. L. & Germain, R. N. 2008. Sap-Controlled T-B Cell Interactions Underlie Germinal Centre Formation. *Nature,* 455**,** 764-9.

Qi, H., Egen, J. G., Huang, A. Y. C. & Germain, R. N. 2006. Extrafollicular Activation of Lymph Node B Cells by Antigen-Bearing Dendritic Cells. *Science,* 312**,** 1672-1676.

Qureshi, O. S., Zheng, Y., Nakamura, K., Attridge, K., Manzotti, C., Schmidt, E. M., Baker, J., Jeffery, L. E., Kaur, S., Briggs, Z., Hou, T. Z., Futter, C. E., Anderson, G., Walker, L. S. & Sansom, D. M. 2011. Trans-Endocytosis of Cd80 and Cd86: A Molecular Basis for the Cell-Extrinsic Function of Ctla-4. *Science,* 332**,** 600-3.

Rada, C., Williams, G. T., Nilsen, H., Barnes, D. E., Lindahl, T. & Neuberger, M. S. 2002. Immunoglobulin Isotype Switching Is Inhibited and Somatic Hypermutation Perturbed in Ung-Deficient Mice. *Current Biology,* 12**,** 1748-1755.

Rafiqi, F. H., Zuber, A. M., Glover, M., Richardson, C., Fleming, S., Jovanovic, S., Jovanovic, A., O'shaughnessy, K. M. & Alessi, D. R. 2010. Role of the Wnk-Activated Spak Kinase in Regulating Blood Pressure. *EMBO Mol Med,* 2**,** 63-75.

Rauch, M., Tussiwand, R., Bosco, N. & Rolink, A. G. 2009. Crucial Role for Baff-Baff-R Signaling in the Survival and Maintenance of Mature B Cells. *PLoS One,* 4**,** e5456.

Rawlings, D. J., Scharenberg, A. M., Park, H., Wahl, M. I., Lin, S., Kato, R. M., Fluckiger, A.-C., Witte, O. N. & Kinet, J.-P. 1996. Activation of Btk by a Phosphorylation Mechanism Initiated by Src Family Kinases. *Science,* 271**,** 822-825.

Reaban, M. E. & Griffin, J. A. 1990. Induction of Rna-Stabilized DNA Conformers by Transcription of an Immunoglobulin Switch Region. *Nature,* 348**,** 342-344.

Reth, M. 1989. Antigen Receptor Tail Clue. *Nature,* 338**,** 383-384.

Revy, P., Muto, T., Levy, Y., Geissmann, F., Plebani, A., Sanal, O., Catalan, N., Forveille, M., Dufourcq-Lagelouse, R., Gennery, A., Tezcan, I., Ersoy, F., Kayserili, H., Ugazio, A. G., Brousse, N., Muramatsu, M., Notarangelo, L. D., Kinoshita, K.,

Honjo, T., Fischer, A. & Durandy, A. 2000. Activation-Induced Cytidine Deaminase (Aid) Deficiency Causes the Autosomal Recessive Form of the Hyper-Igm Syndrome (Higm2). *Cell,* 102**,** 565-575.

Richardson, C., Sakamoto, K., De Los Heros, P., Deak, M., Campbell, D. G., Prescott, A. R. & Alessi, D. R. 2011. Regulation of the Nkcc2 Ion Cotransporter by Spak-Osr1-Dependent and -Independent Pathways. *J Cell Sci,* 124**,** 789-800.

Rogozin, I. B., Pavlov, Y. I., Bebenek, K., Matsuda, T. & Kunkel, T. A. 2001. Somatic Mutation Hotspots Correlate with DNA Polymerase Eta Error Spectrum. *Nature Immunology,* 2**,** 530-536.

Rooney, S., Chaudhuri, J. & Alt, F. W. 2004. The Role of the Non-Homologous End-Joining Pathway in Lymphocyte Development. *Immunological Reviews,* 200**,** 115-131.

Roozendaal, R., Mempel, T. R., Pitcher, L. A., Gonzalez, S. F., Verschoor, A., Mebius, R. E., Von Andrian, U. H. & Carroll, M. C. 2009. Conduits Mediate Transport of Low-Molecular-Weight Antigen to Lymph Node Follicles. *Immunity,* 30**,** 264-76.

Rosen, S. D. 2004. Ligands for L-Selectin: Homing, Inflammation, and Beyond. *Annu Rev Immunol,* 22**,** 129-56.

Rosenbaek, L. L., Kortenoeven, M. L., Aroankins, T. S. & Fenton, R. A. 2014. Phosphorylation Decreases Ubiquitylation of the Thiazide-Sensitive Cotransporter Ncc and Subsequent Clathrin-Mediated Endocytosis. *J Biol Chem,* 289**,** 13347-61.

Rothman, P., Lutzker, S., Cook, W., Coffman, R. & Alt, F. W. 1988. Mitogen Plus Interleukin 4 Induction of C Epsilon Transcripts in B Lymphoid Cells. *Journal of Experimental Medicine,* 168**,** 2385-2389.

Rowley, R. B., Burkhardt, A. L., Chao, H.-G., Matsueda, G. R. & Bolen, J. B. 1995. Syk Protein-Tyrosine Kinase Is Regulated by Tyrosine-Phosphorylated Igalpha/Igbeta Immunoreceptor Tyrosine Activation Motif Binding and Autophosphorylation. *Journal of Biological Chemistry,* 270**,** 11590-11594.

Saccani, S., Pantano, S. & Natoli, G. 2003. Modulation of Nf-Kb Activity by Exchange of Dimers. *Molecular Cell,* 11**,** 1563-1574.

Sage, Peter t., Paterson, Alison m., Lovitch, Scott b. & Sharpe, Arlene h. 2014. The Coinhibitory Receptor Ctla-4 Controls B Cell Responses by Modulating T Follicular Helper, T Follicular Regulatory, and T Regulatory Cells. *Immunity,* 41**,** 1026-1039.

Sage, P. T., Ron-Harel, N., Juneja, V. R., Sen, D. R., Maleri, S., Sungnak, W., Kuchroo, V. K., Haining, W. N., Chevrier, N., Haigis, M. & Sharpe, A. H. 2016. Suppression by Tfr Cells Leads to Durable and Selective Inhibition of B Cell Effector Function. *Nat Immunol,* 17**,** 1436-1446.

Saijo, K., Mecklenbräuker, I., Santana, A., Leitger, M., Schmedt, C. & Tarakhovsky, A. 2002. Protein Kinase C B Controls Nuclear Factor Kb Activation in B Cells through Selective Regulation of the Iκb Kinase A. *The Journal of Experimental Medicine,* 195**,** 1647-1652.

Saito, K., Scharenberg, A. M. & Kinet, J. P. 2001. Interaction between the Btk Ph Domain and Phosphatidylinositol-3,4,5-Trisphosphate Directly Regulates Btk. *J Biol Chem,* 276**,** 16201-6.

Salzman, G. C. 2001. Light Scatter: Detection and Usage. *Curr Protoc Cytom,* Chapter 1**,** Unit 1 13.

Sasaki, Y., Casola, S., Kutok, J. L., Rajewsky, K. & Schmidt-Supprian, M. 2004. Tnf Family Member B Cell-Activating Factor (Baff) Receptor-Dependent and -Independent Roles for Baff in B Cell Physiology. *The Journal of Immunology,* 173**,** 2245-2252.

Schebesta, A., Mcmanus, S., Salvagiotto, G., Delogu, A., Busslinger, G. A. & Busslinger, M. 2007. Transcription Factor Pax5 Activates the Chromatin of Key Genes

Involved in B Cell Signaling, Adhesion, Migration, and Immune Function. *Immunity,* 27**,** 49-63.

Schiemann, B., Gommerman, J. L., Vora, K., Cachero, T. G., Shulga-Morskaya, S., Dobles, M., Frew, E. & Scott, M. L. 2001. An Essential Role for Baff in the Normal Development of B Cells through a Bcma-Independent Pathway. *Science,* 293**,** 2111-2114.

Schindelin, J., Arganda-Carreras, I., Frise, E., Kaynig, V., Longair, M., Pietzsch, T., Preibisch, S., Rueden, C., Saalfeld, S., Schmid, B., Tinevez, J. Y., White, D. J., Hartenstein, V., Eliceiri, K., Tomancak, P. & Cardona, A. 2012. Fiji: An Open-Source Platform for Biological-Image Analysis. *Nat Methods,* 9**,** 676-82.

Schneider, P., Mackay, F., Steiner, V., Hofmann, K., Bodmer, J.-L., Holler, N., Ambrose, C., Lawton, P., Bixler, S., Acha-Orbea, H., Valmori, D., Romero, P., Werner-Favre, C., Zubler, R. H., Browning, J. L. & Tschopp, J. 1999. Baff, a Novel Ligand of the Tumor Necrosis Factor Family, Stimulates B Cell Growth. *The Journal of Experimental Medicine,* 189**,** 1747-1756.

Schnyder, T., Castello, A., Feest, C., Harwood, N. E., Oellerich, T., Urlaub, H., Engelke, M., Wienands, J., Bruckbauer, A. & Batista, F. D. 2011. B Cell Receptor-Mediated Antigen Gathering Requires Ubiquitin Ligase Cbl and Adaptors Grb2 and Dok-3 to Recruit Dynein to the Signaling Microcluster. *Immunity,* 34**,** 905-18.

Schrader, C. E., Guikema, J. E., Wu, X. & Stavnezer, J. 2009. The Roles of Ape1, Ape2, DNA Polymerase Beta and Mismatch Repair in Creating S Region DNA Breaks During Antibody Class Switch. *Philos Trans R Soc Lond B Biol Sci,* 364**,** 645-52.

Schweighoffer, E. & Tybulewicz, V. L. J. 2018. Signalling for B Cell Survival. *Current Opinion in Cell Biology,* 51**,** 8-14.

Schweighoffer, E., Vanes, L., Mathiot, A., Nakamura, T. & Tybulewicz, V. L. 2003. Unexpected Requirement for Zap-70 in Pre-B Cell Development and Allelic Exclusion. *Immunity,* 18**,** 523-533.

Schweighoffer, E., Vanes, L., Nys, J., Cantrell, D., Mccleary, S., Smithers, N. & Tybulewicz, V. L. 2013. The Baff Receptor Transduces Survival Signals by Co-Opting the B Cell Receptor Signaling Pathway. *Immunity,* 38**,** 475-88.

Schwickert, T. A., Lindquist, R. L., Shakhar, G., Livshits, G., Skokos, D., Kosco-Vilbois, M. H., Dustin, M. L. & Nussenzweig, M. C. 2007. In Vivo Imaging of Germinal Centres Reveals a Dynamic Open Structure. *Nature,* 446**,** 83-87.

Sciammas, R., Li, Y., Warmflash, A., Song, Y., Dinner, A. R. & Singh, H. 2011. An Incoherent Regulatory Network Architecture That Orchestrates B Cell Diversification in Response to Antigen Signaling. *Molecular Systems Biology,* 7**,** 495-495.

Sciammas, R., Shaffer, A. L., Schatz, J. H., Zhao, H., Staudt, L. M. & Singh, H. 2006. Graded Expression of Interferon Regulatory Factor-4 Coordinates Isotype Switching with Plasma Cell Differentiation. *Immunity,* 25**,** 225-236.

Senftleben, U., Cao, X., Xiao, G., Greten, F. R., Krähn, G., Bonizzi, G., Chen, Y., Hu, Y., Fong, A., Sun, S.-C. & Karin, M. 2001. Activation by Ikkalpha of a Second, Evolutionary Conserved, Nf-Kappa B Signaling Pathway. *Science,* 293**,** 1495-1499.

Seshasayee, D., Valdez, P., Yan, M., Dixit, V. M., Tumas, D. & Grewal, I. S. 2003. Loss of Tci Causes Fatal Lymphoproliferation and Autoimmunity, Establishing Taci as an Inhibitory Blys Receptor. *Immunity,* 18**,** 279-288.

Shaffer, A. L., Lin, K. I., Kuo, T. C., Yu, X., Hurt, E. M., Rosenwald, A., Giltnane, J. M., Yang, L., Zhao, H., Calame, K. & Staudt, L. M. 2002. Blimp-1 Orchestrates Plasma Cell Differentiation by Extinguishing the Mature B Cell Gene Expression Program. *Immunity,* 17**,** 51-62.

Shaw, P. J., Qu, B., Hoth, M. & Feske, S. 2013. Molecular Regulation of Crac Channels and Their Role in Lymphocyte Function. *Cell Mol Life Sci,* 70**,** 2637-56.

Shekarabi, M., Girard, N., Rivière, J.-B., Dion, P., Houle, M., Toulouse, A., Lafrenière, R. G., Vercauteren, F., Hince, P., Laganiere, J., Rochefort, D., Faivre, L., Samuels, M. & Rouleau, G. A. 2008. Mutations in the Nervous System–Specific Hsn2 Exon of Wnk1 Cause Hereditary Sensory Neuropathy Type Ii. *Journal of Clinical Investigation,* 118**,** 2496-505.

Shekarabi, M., Zhang, J., Khanna, A. R., Ellison, D. H., Delpire, E. & Kahle, K. T. 2017. Wnk Kinase Signaling in Ion Homeostasis and Human Disease. *Cell Metab,* 25**,** 285-299.

Shinkai, Y., Rathbun, G., Lam, K.-P., Oltz, E. M., Stewart, V., Mendelsohn, M., Charron, J., Datta, M., Young, F., Stall, A. M. & Alt, F. W. 1992. Rag-2-Deficient Mice Lack Mature Lymphocytes Owing to Inability to Initiate V(D)J Recombination. *Cell,* 68**,** 855-867.

Shinkura, R., Tian, M., Smith, M., Chua, K., Fujiwara, Y. & Alt, F. W. 2003. The Influence of Transcriptional Orientation on Endogenous Switch Region Function. *Nature Immunology,* 4**,** 435-441.

Shinnakasu, R., Inoue, T., Kometani, K., Moriyama, S., Adachi, Y., Nakayama, M., Takahashi, Y., Fukuyama, H., Okada, T. & Kurosaki, T. 2016. Regulated Selection of Germinal-Center Cells into the Memory B Cell Compartment. *Nat Immunol,* 17**,** 861-869.

Shinohara, H., Yasuda, T., Aiba, Y., Sanjo, H., Hamadate, M., Watarai, H., Sakurai, H. & Kurosaki, T. 2005. Pkcβ Regulates Bcr-Mediated Ikk Activation by Facilitating the Interaction between Tak1 and Carma1. *J Exp Med,* 202**,** 1423-1431.

Silva, R. D., Sotoca, R., Johansson, B., Ludovico, P., Sansonetty, F., Silva, M. T., Peinado, J. M. & Corte-Real, M. 2005. Hyperosmotic Stress Induces Metacaspase- and Mitochondria-Dependent Apoptosis in Saccharomyces Cerevisiae. *Mol Microbiol,* 58**,** 824-34.

Sindhava, V. J., Scholz, J. L., Stohl, W. & Cancro, M. P. 2014. April Mediates Peritoneal B-1 Cell Homeostasis. *Immunol Lett,* 160**,** 120-7.

Sinha, R. K., Park, C., Hwang, I. Y., Davis, M. D. & Kehrl, J. H. 2009. B Lymphocytes Exit Lymph Nodes through Cortical Lymphatic Sinusoids by a Mechanism Independent of Sphingosine-1-Phosphate-Mediated Chemotaxis. *Immunity,* 30**,** 434-46.

Sitnicka, E., Brakebusch, C., Martensson, I. L., Svensson, M., Agace, W. W., Sigvardsson, M., Buza-Vidas, N., Bryder, D., Cilio, C. M., Ahlenius, H., Maraskovsky, E., Peschon, J. J. & Jacobsen, S. E. 2003. Complementary Signaling through Flt3 and Interleukin-7 Receptor Alpha Is Indispensable for Fetal and Adult B Cell Genesis. *J Exp Med,* 198**,** 1495-506.

Sitnicka, E., Bryder, D., Theilgaard-Mönch, K., Buza-Vidas, N., Adolfsson, J. & Jaobsen, S. E. W. 2002. Key Role of Flt3 Ligand in Regulation of the Common Lyphoid Progenitor but Not in Maintenance of the Hematopoietic Stem Cell Pool. *Immunity,* 17**,** 463-472.

Stavnezer, J., Radcliffe, G., Lin, Y. C., Nietupski, J., Berggren, L., Sitia, R. & Severinson, E. 1988. Immunoglobulin Heavy-Chain Switching May Be Directed by Prior Induction of Transcripts from Constant-Region Genes. *Proceedings of the National Academy of Sciences,* 85**,** 7704-7708.

Stokoe, D., Stephens, L. R., Copeland, T., Gaffney, P. R. J., Reese, C. B., Painter, G. F., Holmes, A. B., Mccormick, F. & Hawkins, P. T. 1997. Dual Role of Phosphatidylinositol-3,4,5-Trisphosphate in the Activation of Protein Kinase B. *Science,* 277**,** 567-570.

Stroka, K. M., Jiang, H., Chen, S. H., Tong, Z., Wirtz, D., Sun, S. X. & Konstantopoulos, K. 2014. Water Permeation Drives Tumor Cell Migration in Confined Microenvironments. *Cell,* 157**,** 611-23.

Sugawara, H., Kurosaki, M., Takata, M. & Kurosaki, T. 1997. Genetic Evidence for Involvement of Type 1, Type 2 and Type 3 Inositol 1,4,5-Trisphosphate Receptors in Signal Transduction through the B-Cell Antigen Receptor. *EMBO Journal,* 16**,** 3078-3088.

Sun, X., Gao, L., Yu, R. K. & Zeng, G. 2006. Down-Regulation of Wnk1 Protein Kinase in Neural Progenitor Cells Suppresses Cell Proliferation and Migration. *J Neurochem,* 99**,** 1114-21.

Suzuki, K., Grigorova, I., Phan, T. G., Kelly, L. M. & Cyster, J. G. 2009. Visualizing B Cell Capture of Cognate Antigen from Follicular Dendritic Cells. *J Exp Med,* 206**,** 1485-93.

Tadokoro, S., Shattil, S. J., Eto, K., Tai, V., Liddington, R. C., De Pereda, J. M., Ginsberg, M. H. & Calderwood, D. A. 2003. Talin Binding to Integrin Beta Tails: A Final Common Step in Integrin Activation. *Science,* 302**,** 103-106.

Taher, T. E., Bystrom, J., Ong, V. H., Isenberg, D. A., Renaudineau, Y., Abraham, D. J. & Mageed, R. A. 2017. Intracellular B Lymphocyte Signalling and the Regulation of Humoral Immunity and Autoimmunity. *Clin Rev Allergy Immunol,* 53**,** 237-264.

Takeuchi, O. & Akira, S. 2010. Pattern Recognition Receptors and Inflammation. *Cell,* 140**,** 805-820.

Tamma, R. & Ribatti, D. 2017. Bone Niches, Hematopoietic Stem Cells, and Vessel Formation. *Int J Mol Sci,* 18.

Teague, B. N., Pan, Y., Mudd, P. A., Nakken, B., Zhang, Q., Szodoray, P., Kim-Howard, X., Wilson, P. C. & Farris, A. D. 2007. Cutting Edge: Transitional T3 B Cells Do Not Give Rise to Mature B Cells, Have Undergone Selection, and Are Reduced in Murine Lupus. *The Journal of Immunology,* 178**,** 7511-7515.

Tedford, K., Nitschke, L., Girkontaite, I., Charlesworth, A., Chan, G., Sakk, V., Barbacid, M. & Fischer, K. D. 2001. Compensation between Vav-1 and Vav-2 in B Cell Development and Antigen Receptor Signaling. *Nat Immunol,* 2**,** 548-55.

Teixeira, C., Stang, S. L., Zheng, Y., Beswick, N. S. & Stone, J. C. 2003. Integration of Dag Signaling Systems Mediated by Pkc-Dependent Phosphorylation of Rasgrp3. *Blood,* 102**,** 1414-20.

Thompson, J. S., Bixler, S. A., Qian, F., Vora, K., Scott, M. L., Cachero, T. G., Hession, C., Schneider, P., Sizing, I. D., Mullen, C., Strauch, K., Zafari, M., Benjamin, C. D., Tschopp, J., Browning, J. L. & Ambrose, C. 2001. Baff-R, a Newly Identified Tnf Receptor That Specifically Interacts with Baff. *Science,* 293**,** 2108-2111.

Tinevez, J.-Y., Perry, N., Schindelin, J., Hoopes, G. M., Reynolds, G. D., Laplantine, E., Bednarek, S. Y., Shorte, S. L. & Eliceiri, K. W. 2017. Trackmate: An Open and Extensible Platform for Single-Particle Tracking. *Methods,* 115**,** 80-90.

Tock, M. R. & Dryden, D. T. 2005. The Biology of Restriction and Anti-Restriction. *Current Opinion in Microbiology,* 8**,** 466-472.

Tokoyoda, K., Egawa, T., Sugiyama, T., Choi, B.-I. & Nagasawa, T. 2004. Cellular Niches Controlling B Lymphocyte Behavior within Bone Marrow During Development. *Immunity,* 20**,** 707-718.

Tolar, P. 2017. Cytoskeletal Control of B Cell Responses to Antigens. *Nat Rev Immunol,* 17**,** 621-634.

Tolar, P. & Spillane, K. M. 2014. Force Generation in B-Cell Synapses: Mechanisms Coupling B-Cell Receptor Binding to Antigen Internalization and Affinity Discrimination. *Adv Immunol,* 123**,** 69-100.

Tomayko, M. M., Steinel, N. C., Anderson, S. M. & Shlomchik, M. J. 2010. Cutting Edge: Hierarchy of Maturity of Murine Memory B Cell Subsets. *J Immunol,* 185**,** 7146-50.

Trushin, S. A., Pennington, K. N., Algeciras-Schimnich, A. & Paya, C. V. 1999. Protein Kinase C and Calcineurin Synergize to Activate Ikappab Kinase and Nf-Kappab in T Lymphocytes. *Journal of Biological Chemistry,* 274**,** 22932-22931.

Tsubata, T. & Reth, M. 1990. The Products of Pre-B Cell-Specific Genes (Lambda 5 and Vpreb) and the Immunoglobulin Mu Chain Form a Complex That Is Transported onto the Cell Surface. *Journal of Experimental Medicine,* 172**,** 973-976.

Tu, S. W., Bugde, A., Luby-Phelps, K. & Cobb, M. H. 2011. Wnk1 Is Required for Mitosis and Abscission. *Proc Natl Acad Sci U S A,* 108**,** 1385-90.

Turner, C. A., Mack, D. H. & Davis, M. M. 1994. Blimp-1, a Novel Zinc Finger-Containing Protein That Can Drive the Maturation of B Lymphocytes into Immunoglobulin-Secreting Cells. *Cell,* 77**,** 297-306.

Tuveson, D. A., Carter, R. H., Soltoff, A. P. & Fearon, D. T. 1993. Cd19 of B Cells as a Surrogate Kinase Insert Region to Bind Phosphatidylinositol 3-Kinase. *Science,* 260**,** 986-989.

Tybulewicz, V. L. & Henderson, R. B. 2009. Rho Family Gtpases and Their Regulators in Lymphocytes. *Nat Rev Immunol,* 9**,** 630-44.

Tzur, A., Moore, J. K., Jorgensen, P., Shapiro, H. M. & Kirschner, M. W. 2011. Optimizing Optical Flow Cytometry for Cell Volume-Based Sorting and Analysis. *PLoS One,* 6**,** e16053.

Van De Weijer, M. L., Luteijn, R. D. & Wiertz, E. J. H. J. 2015. Viral Immune Evasion: Lessons in Mhc Class I Antigen Presentation. *Semin Immunol,* 27**,** 125-137.

Van Vlasselaer, P., Punnonen, J. & De Vries, J. E. 1992. Transforming Growth Factor-Beta Directs Iga Switching in Human B Cells. *Journal of Immunology,* 148**,** 2062-2067.

Varfolomeev, E., Kischkel, F., Martin, F., Seshasayee, D., Wang, H., Lawrence, D., Olsson, C., Tom, L., Erickson, S., French, D., Schow, P., Grewal, I. S. & Ashkenazi, A. 2004. April-Deficient Mice Have Normal Immune System Development. *Molecular and Cellular Biology,* 24**,** 997-1006.

Vénéreau, E., Ceriotti, C. & Bianchi, M. E. 2015. Damps from Cell Death to New Life. *Frontiers in Immunology,* 6**,** 422.

Verissimo, F. & Jordan, P. 2001. Wnk Kinases, a Novel Protien Kinase Subfamily in Multi-Cellular Organisms. *Oncogene,* 20**,** 5562-5569.

Vettermann, C., Herrmann, K., Albert, C., Roth, E., Bosl, M. R. & Jack, H. M. 2008. A Unique Role for the 5 Nonimmunoglobulin Tail in Early B Lymphocyte Development. *The Journal of Immunology,* 181**,** 3232-3242.

Victora, G. D. & Nussenzweig, M. C. 2012. Germinal Centers. *Annual Review of Immunology,* 30**,** 429-57.

Victora, G. D., Schwickert, T. A., Fooksman, D. R., Kamphorst, A. O., Meyer-Hermann, M., Dustin, M. L. & Nussenzweig, M. C. 2010. Germinal Center Dynamics Revealed by Multiphoton Microscopy with a Photoactivatable Fluorescent Reporter. *Cell,* 143**,** 592-605.

Vinuesa, C. G. & Chang, P.-P. 2013. Innate B Cell Helpers Reveal Novel Types of Antibody Responses. *Nat Immunol,* 14**,** 119-126.

Vissers, J. L. M., Hartgers, F. C., Lindhout, E., Figdor, C. G. & Adema, G. J. 2001. Blc (Cxcl13) S Expressed by Different Dendritic Cell Subsets in Vitro and in Vivo. *European Journal of Immunology,* 31**,** 1544-1549.

Vitari, A. C., Deak, M., Morrice, N. A. & Alessi, D. R. 2005. The Wnk1 and Wnk4 Protein Kinases That Are Mutated in Gordon's Hypertension Syndrome Phosphorylate and Activate Spak and Osr1 Protein Kinases. *Biochem J,* 391**,** 17-24.

Vladymyrov, M., Abe, J., Moalli, F., Stein, J. V. & Ariga, A. 2016. Real-Time Tissue Offset Correction System for Intravital Multiphoton Microscopy. *J Immunol Methods,* 438**,** 35-41.

Von Andrian, U. H. 1996. Intravital Microscopy of the Peripheral Lymph Node Microcirculation in Mice. *Microcirculation,* 3**,** 287-300.

Von Bülow, G.-U., Van Deursen, J. M. & Bram, R. J. 2001. Regulation of the T-Independent Humoral Response by Taci. *Immunity,* 14**,** 573-582.

Walker, L. S. & Sansom, D. M. 2011. The Emerging Role of Ctla4 as a Cell-Extrinsic Regulator of T Cell Responses. *Nat Rev Immunol,* 11**,** 852-63.

Walker, L. S. K. & Sansom, D. M. 2015. Confusing Signals: Recent Progress in Ctla-4 Biology. *Trends in Immunology,* 36**,** 63-70.

Wang, C. J., Heuts, F., Ovcinnikovs, V., Wardzinski, L., Bowers, C., Schmidt, E. M., Kogimtzis, A., Kenefeck, R., Sansom, D. M. & Walker, L. S. 2015. Ctla-4 Controls Follicular Helper T-Cell Differentiation by Regulating the Strength of Cd28 Engagement. *Proc Natl Acad Sci U S A,* 112**,** 524-9.

Wang, S., Melkoumian, Z., Woodfork, K. A., Cather, C., Davidson, A. G., Wonderlin, W. F. & Stobl, J. S. 1998. Evidence for an Early G1 Ionic Event Necessary for Cell Cycle Progression and Survival in the Mcf-7 Human Breast Carcinoma Cell Line. *Journal of Cellular Physiology,* 176**,** 456-464.

Warnock, R. A., Askari, S., Butcher, E. C. & Von Andrian, U. H. 1998. Molecular Mechanisms of Lymphocyte Homing to Peripheral Lymph Nodes. *The Journal of Experimental Medicine,* 187**,** 205-216.

Wienands, J., Schweikert, J., Wollscheid, B., Jumaa, H., Nielsen, P. J. & Reth, M. 1998. Slp-65: A New Signaling Component in B Lymphocytes Which Requires Expression of the Antigen Receptor for Phosphorylation. *The Journal of Experimental Medicine,* 188**,** 791-795.

Wilson, F. H., Disse-Nicodeme, S., Choate, K. A., Ishikawa, K., Nelson-Williams, C., Desitter, I., Gunel, M., Milford, D. V., Lipkin, G. W., Achard, J. M., Feely, M. P., Dussol, B., Berland, Y., Unwin, R. J., Mayan, H., Simon, D. B., Farfel, Z., Jeunemaitre, X. & Lifton, R. P. 2001. Human Hypertension Caused by Mutations in Wnk Kinases. *Science,* 293**,** 1107-1112.

Wollenberg, I., Agua-Doce, A., Hernandez, A., Almeida, C., Oliveira, V. G., Faro, J. & Graca, L. 2011. Regulation of the Germinal Center Reaction by Foxp3+ Follicular Regulatory T Cells. *J Immunol,* 187**,** 4553-60.

Woodland, R. T., Fox, C. J., Schmidt, M. R., Hammerman, P. S., Opferman, J. T., Korsmeyer, S. J., Hilbert, D. M. & Thompson, C. B. 2008. Multiple Signaling Pathways Promote B Lymphocyte Stimulator Dependent B-Cell Growth and Survival. *Blood,* 111**,** 750-60.

Wulff, H., Knaus, H. G., Pennington, M. & Chandy, K. G. 2004. K+ Channel Expression During B Cell Differentiation: Implications for Immunomodulation and Autoimmunity. *The Journal of Immunology,* 173**,** 776-786.

Xiao, G., Harhaj, E. W. & Sun, S.-C. 2001. Nf-Kappa B-Inducing Kinase Regulates the Procesing of Kf-Kappa B2 P100. *Molecular Cell,* 7**,** 401-409.

Xie, J., Wu, T., Xu, K., Huang, I. K., Cleaver, O. & Huang, C. L. 2009. Endothelial-Specific Expression of Wnk1 Kinase Is Essential for Angiogenesis and Heart Development in Mice. *Am J Pathol,* 175**,** 1315-27.

Xie, J., Yoon, J., Yang, S.-S., Lin, S.-H. & Huang, C.-L. 2013. Wnk1 Protein Kinase Regulates Embryonic Cardiovascular Development through the Osr1 Signaling Cascade. *Journal of Biological Chemistry,* 288**,** 8566-8574.

Xu, B.-E., Stippec, S., Lenertz, L., Lee, B.-H., Zhang, W., Lee, Y.-K. & Cobb, M. H. 2004. Wnk1 Activates Erk5 by an Mekk2/3-Dependent Mechanism. *Journal of Biological Chemistry,* 279**,** 7826-7831.

Xu, B. E., English, J. M., Wilsbacher, J. L., Stippec, S., Goldsmith, E. J. & Cobb, M. H. 2000. Wnk1, a Novel Mammalian Serine/Threonine Protein Kinase Lacking the Catalytic Lysine in Subdomain Ii. *Journal of Biological Chemistry,* 275**,** 16795-16801.

Xu, B. E., Min, X., Stippec, S., Lee, B. H., Goldsmith, E. J. & Cobb, M. H. 2002. Regulation of Wnk1 by an Autoinhibitory Domain and Autophosphorylation. *J Biol Chem,* 277**,** 48456-62.

Xu, B. E., Stippec, S., Chu, P.-Y., Lazrak, A., Li, X.-J., Lee, B. H., English, J. M., Ortega, B., Huang, C. L. & Cobb, M. H. 2005a. Wnk1 Activates Sgk1 to Regulate the Epithelial Sodium Channel. *Proc Natl Acad Sci U S A,* 102**,** 10315-103-20.

Xu, B. E., Stippec, S., Lazrak, A., Huang, C. L. & Cobb, M. H. 2005b. Wnk1 Activates Sgk1 by a Phosphatidylinositol 3-Kinase-Dependent and Non-Catalytic Mechanism. *J Biol Chem,* 280**,** 34218-23.

Yamada, K., Park, H.-M., Rigel, D. F., Dipetrillo, K., Whalen, E. J., Anisowicz, A., Beil, M., Berstler, J., Brocklehurst, C. E., Burdick, D. A., Caplan, S. L., Capparelli, M. P., Chen, G., Chen, W., Dale, B., Deng, L., Fu, F., Hamamatsu, N., Harasaki, K., Herr, T., Hoffmann, P., Hu, Q.-Y., Huang, W.-J., Idamakanti, N., Imase, H., Iwaki, Y., Jain, M., Jeyaseelan, J., Kato, M., Kaushik, V. K., Kohls, D., Kunjathoor, V., Lasala, D., Lee, J., Liu, J., Luo, Y., Ma, F., Mo, R., Mowbray, S., Mogi, M., Ossola, F., Pandey, P., Patel, S. J., Raghavan, S., Salem, B., Shanado, Y. H., Trakshel, G. M., Turner, G., Wakai, H., Wang, C., Weldon, S., Wielicki, J. B., Xie, X., Xu, L., Yagi, Y. I., Yasoshima, K., Yin, J., Yowe, D., Zhang, J.-H., Zheng, G. & Monovich, L. 2016. Small-Molecule Wnk Inhibition Regulates Cardiovascular and Renal Function. *Nat Chem Biol,* 12**,** 896-898.

Yan, M., Brady, J. R., Chan, B., Lee, W. P., Hsu, B., Harless, S., Michael, C., Grewal, I. S. & Dixit, V. M. 2001. Identification of a Novel Receptor for B Lymphocyte Stimulator That Is Mutated in a Mouse Strain with Severe B Cell Deficiency. *Current Biology,* 11**,** 1547-1552.

Yang, Q., Saenz, S. A., Zlotoff, D. A., Artis, D. & Bhandoola, A. 2011. Cutting Edge: Natural Helper Cells Derive from Lymphoid Progenitors. *J Immunol,* 187**,** 5505-9.

Yeh, C. H., Nojima, T., Kuraoka, M. & Kelsoe, G. 2018. Germinal Center Entry Not Selection of B Cells Is Controlled by Peptide-Mhcii Complex Density. *Nat Commun,* 9**,** 928.

Youle, R. J. & Strasser, A. 2008. The Bcl-2 Protein Family: Opposing Activities That Mediate Cell Death. *Nat Rev Mol Cell Biol,* 9**,** 47-59.

Yuseff, M. I., Reversat, A., Lankar, D., Diaz, J., Fanget, I., Pierobon, P., Randrian, V., Larochette, N., Vascotto, F., Desdouets, C., Jauffred, B., Bellaiche, Y., Gasman, S., Darchen, F., Desnos, C. & Lennon-Dumenil, A. M. 2011. Polarized Secretion of Lysosomes at the B Cell Synapse Couples Antigen Extraction to Processing and Presentation. *Immunity,* 35**,** 361-74.

Zandi, S., Mansson, R., Tsapogas, P., Zetterblad, J., Bryder, D. & Sigvardsson, M. 2008. Ebf1 Is Essential for B-Lineage Priming and Establishment of a Transcription Factor Network in Common Lymphoid Progenitors. *The Journal of Immunology,* 181**,** 3364-3372.

Zarnegar, B., He, J. Q., Oganesyan, G., Hoffmann, A., Baltimore, D. & Cheng, G. 2004. Unique Cd40-Mediated Biological Program in B Cell Activation Requires Both Type 1 and Type 2 Nf- b Activation Pathways. *Proc Natl Acad Sci U S A,* 101**,** 8108-8113.

Zeng, X., Winter, D. B., Kasmer, C., Kraemer, K. H., Lehmann, A. R. & Gearhart, P. J. 2001. DNA Polymerase Eta Is an a-T Mutator in Somatic Hypermutation of Immunoglobulin Variable Genes. *Nature Immunology,* 2**,** 537-541.

Zhang, Y., Tech, L., George, L. A., Acs, A., Durrett, R. E., Hess, H., Walker, L. S. K., Tarlinton, D. M., Fletcher, A. L., Hauser, A. E. & Toellner, K. M. 2018a. Plasma Cell Output from Germinal Centers Is Regulated by Signals from Tfh and Stromal Cells. *J Exp Med,* 215**,** 1227-1243.

Zhang, Y.-J., Zheng, H.-Q., Chen, B.-Y., Sun, L., Ma, M.-M., Wang, G.-L. & Guan, Y.-Y. 2018b. Wnk1 Is Required for Proliferation Induced by Hypotonic Challenge in Rat Vascular Smooth Muscle Cells. *Acta Pharmacologica Sinica,* 39**,** 35-47.

Zhou, R., Patel, S. V. & Snyder, P. M. 2007. Nedd4-2 Catalyzes Ubiquitination and Degradation of Cell Surface Enac. *J Biol Chem,* 282**,** 20207-20212.

Zhu, J. 2018. T Helper Cell Differentiation, Heterogeneity, and Plasticity. *Cold Spring Harb Perspect Biol,* 10.

Zhu, W., Begum, G., Pointer, K., Clark, P. A., Yang, S.-S., Lin, S.-H., Kahle, K. T., Kuo, J. S. & Sun, D. 2014. Wnk1-Osr1 Kinase-Mediated Phospho-Activation of Na+-K+-2cl- Cotransporter Facilitates Glioma Migration. *Molecular Cancer,* 13**,** 31.

Zuccarino-Catania, G. V., Sadanand, S., Weisel, F. J., Tomayko, M. M., Meng, H., Kleinstein, S. H., Good-Jacobson, K. L. & Shlomchik, M. J. 2014. Cd80 and Pd-L2 Define Functionally Distinct Memory B Cell Subsets That Are Independent of Antibody Isotype. *Nat Immunol,* 15**,** 631-7.